Titre: Title:	Novel Polymer Blends with Thermoplastic Starch
Auteur: Author:	Ata Taghizadeh
Date:	2012
Type:	Mémoire ou thèse / Dissertation or Thesis
Référence: Citation:	Taghizadeh, A. (2012). Novel Polymer Blends with Thermoplastic Starch [Thèse de doctorat, École Polytechnique de Montréal]. PolyPublie. https://publications.polymtl.ca/1041/

URL de PolyPublie: PolyPublie URL:	https://publications.polymtl.ca/1041/
Directeurs de recherche: Advisors:	Basil D. Favis
Programme: Program:	Génie chimique

UNIVERSITÉ DE MONTRÉAL

NOVEL POLYMER BLENDS WITH THERMOPLASTIC STARCH

ATA TAGHIZADEH

DÉPARTEMENT DE GÉNIE CHIMIQUE

ÉCOLE POLYTECHNIQUE DE MONTRÉAL

THÈSE PRÉSENTÉE EN VUE DE L'OBTENTION

DU DIPLÔME DE PHILOSOPHIAE DOCTOR

(GÉNIE CHIMIQUE)

DÉCEMBRE 2012

UNIVERSITÉ DE MONTRÉAL

ÉCOLE POLYTECHNIQUE DE MONTRÉAL

Cette thèse intitulée::

NOVEL POLYMER BLENDS WITH THERMOPLASTIC STARCH

présentée par: TAGHIZADEH Ata

en vue de l'obtention du diplôme de : Philosophiae Doctor

a été dûment acceptée par le jury d'examen constitué de :

M. DUBOIS Charles, Ph.D., président

M. FAVIS Basil, Ph.D., membre et directeur de recherche

Mme HEUZEY Marie-Claude, Ph.D., membre

M. LIU Qiang, Ph.D., membre

DEDICATIONS

To My Family

ACKNOWLEDGEMENTS

My family always comes first. I would like to express my endless gratitude to my father, mother, sister, brother-in-law (and my beautiful niece, Elena), who have been always there for me in every situation. Words are unable to reflect what I feel in my heart towards them.

Professor Basil Favis is someone I will remember to the end of my life as the most understanding, cool, knowledgeable, hard-working and wise professor I have ever met. It was a pleasure to work with him, and he taught me a lot, much more than what is written in this thesis, lessons that will help me in all aspects of my life.

Thanks to Prof. Charles Dubois, Prof. Marie-Claude HEUZEY and Prof. Qiang Liu for taking part in my thesis committee.

Dr. Pierre Sarazin, who co-supervised a part of my thesis, has helped me a lot over the years, and I consider him a great friend for me. The support of our research group was also crucial to this work, so I'd to thank all of them.

The world has little meaning if you are alone. One of the most beautiful aspects of life are true friends who understand you, calm you down and are always there for you. I have a list of great people to include here: Mohammad T, Mohammad G, Saman, Ebrahim, Mohsen, Reza, Pejman, Javad, Jean-Claude, Majid, Parisa, Helia, Arash, Sina, Sarah, Hamed, Eve, Amin, Milad, Hesam, Amirhossein, Farhad, and all my friends, who are now like my family, in "SAVALAN Cultural Group".

Dr. Pierre Sarazin, who co-supervised a part of my thesis, has helped me a lot over the years, and I consider him a great friend for me. The support of our research group was also crucial to this work, so I'd to thank all of them.

The technicians in the department of chemical engineering have been of great help during my experiments: Guillaume, Martine, Gino, Robert, and Jean. My special thanks also go to Melina Hamdine and Weavkamol Leelapornpisit, who have been patiently there for me with a smile on their faces.

The administrative staff of our department had a significant role in helping us and providing us with a calm atmosphere in order to advance our projects, namely: Evelyne Rousseau, Jose Rivest, Lyne Henley and Louise Beaudry-Parent.

RÉSUMÉ

De nos jours, il ne fait aucun doute que le développement de l'industrie plastique est directement lié à son adaptation face aux nouvelles préoccupations écologiques. De nouveaux polymères, les bioplastiques, sont apparus sur le marché et se développent très rapidement. Ils regroupent les polymères biosourcés et / ou biodégradables tels que le bio-polyéthylène (bio-PE), le bio-polypropylène (bio-PP), le polycaprolactone (PCL), le poly(butylène adipate-co-téréphtalate) (PBAT) ainsi que le polylactide (PLA) et les polysaccharides. Parmi ces polymères, l'amidon présente des caractéristiques très intéressantes. Il peut être obtenu à partir de multiples ressources et se dégrade naturellement dans l'environnement. L'amidon peut être plastifié, on le nomme alors amidon thermoplastique (TPS) et il possède l'avantage de pouvoir ensuite être mis en œuvre comme n'importe quel polymère thermoplastique. En raison de son faible coût et de sa grande disponibilité, l'amidon thermoplastique peut être ajouté dans d'autres résines.

Cependant, l'amidon thermoplastique (TPS) ne possède pas de très bonnes propriétés mécaniques et ses propriétés fluctuent en fonction de l'environnement, en raison de sa nature hygroscopique. Aussi, il est difficile d'utiliser le TPS tel quel : il doit être mélangé avec d'autres plastiques. Les applications pour les mélanges avec TPS se limitent principalement aux matériaux non-durables, tels que les sacs, les ustensiles et les articles de vaisselle. Si la résistance à l'humidité et / ou les propriétés mécaniques pouvaient être améliorées, la gamme d'application pourrait inclure des produits semi-durables et durables. Dans notre étude, deux options seront examinées: 1) la modification de la structure interne de l'amidon thermoplastique, 2) l'incorporation de nano-charges dans la structure du TPS.

La gélatinisation de l'amidon s'effectue avec l'aide de plastifiants qui ont des effets significatifs à la fois sur le procédé de plastification et sur les propriétés finales du TPS. Quatre plastifiants ont été sélectionnés : le glycérol, le sorbitol, qui sont déjà souvent utilisés, et le diglycérol et le polyglycérol, qui ont été étudiés pour la première fois dans ce procédé. Deux méthodes de caractérisation ont été mises en œuvre. L'analyse calorimétrique par DSC (Differential Scanning Calorimetry) associée à la microscopie optique est une méthode 'statique' où aucun cisaillement n'est appliqué. Comme la gélatinisation est une transition du premier ordre, on observe un pic endothermique en analyse calorimétrique. La gélatinisation correspond à la disparition de cristallinité des granules d'amidon et sous un microscope optique en lumière polarisée, on peut

suivre celle-ci par la perte de biréfringence. La gélatinisation de l'amidon en condition statique a été examinée pour les 4 plastifiants, en préparant une large gamme de composition amidon/eau/plastifiant. Le glycérol a servi de référence car il est connu pour être le plus largement utilisé pour obtenir de l'amidon thermoplastique. L'intervalle en température pour la gélatinisation avec du glycérol et du sorbitol s'est révélé être assez similaire, tandis que les échantillons contenant du diglycerol et du polyglycérol étaient caractérisés par des températures de transition significativement plus élevées. Cette transition était observée à des températures plus élevées pour le polyglycérol que pour le diglycérol, en raison de son plus haut poids moléculaire et de sa viscosité. Cet effet a été attribué à l'augmentation du poids moléculaire et de la viscosité des deux nouveaux plastifiants, combinée aussi à leur plus faible solubilité dans l'eau. Pour une quantité constante d'amidon dans tous les essais, il a été montré que le rapport eau/plastifiant avait un effet évident sur les températures de gélatinisation. Pour une proportion constante de plastifiant, l'augmentation de la quantité d'eau permettait de diminuer la température de gélatinisation pour tous les plastifiants. Par ailleurs, quand la quantité d'eau était constante et que l'on augmentait la quantité de plastifiant, la température de gélatinisation augmentait pour le glycérol, le sorbitol et le diglycérol, mais diminuait pour le polyglycérol. La variation de la température de gélatinisation pour les trois premiers plastifiants indique que l'eau a un rôle prépondérant dans le phénomène de plastification en faisant gonfler les granules d'amidon. En raison de son haut poids moléculaire et de sa viscosité, ainsi que de sa faible densité en groupe hydroxyle (environ un –OH par deux carbones) et de sa solubilité plus faible dans l'eau, le polyglycérol ne bénéficie pas de l'aide de l'eau qui favorise la pénétration du plastifiant dans l'amidon. Ainsi il a été proposé que, pour les plastifiants de faible solubilité dans l'eau, la température de gélatinisation est déterminée principalement par la quantité totale de plastifiant et d'eau, plutôt que le rapport eau/plastifiant. On peut dire que chaque élément dans le procédé agit séparément et est indépendant l'un de l'autre. L'augmentation de la miscibilité du polyglycérol dans l'eau en augmentant la température de la suspension initiale, se traduit par un retour du système à la dépendance thermique de gélatinisation typique à "plastifiant / eau" ratio.

Deuxièmement, la gélatinisation de l'amidon sous 'condition dynamique' est étudié. Dans ce cas-ci un cisaillement constant est appliqué sur la suspension, et la gélatinisation est induite en augmentant la température. Il s'agit en fait d'une technique rhéologique qui convient bien à l'étude de l'amidon thermoplastique. Le TPS est produit par des procédés d'extrusion impliquant

du cisaillement, mais il n'y a pas d'études approfondies sur l'effet du cisaillement sur la gélatinisation, à ce jour. Dans notre étude, le glycérol, le diglycérol et le sorbitol ont été soumis à différents traitements de gélatinisation dynamiques dans un système d'écoulement Couette et les résultats ont été comparés avec ceux de la gélatinisation statique. Le cisaillement n'a montré pratiquement aucun effet sur la température initiale de gélatinisation, alors que la température finale a été remarquablement réduite (jusqu'à 21˚C) en présence de cisaillement. On a pu conclure que la température finale était plus dépendante de la cinétique et qu'une gélatinisation complète pouvait être obtenue dans des délais plus courts sous cisaillement. De plus, il a été observé que la structure du plastifiant n'avait aucun effet sur la manière dont le cisaillement influence la gélatinisation.

Nous avons ensuite étudié l'efficacité des plastifiants dans des mélanges. Les bioplastiques sont les meilleurs candidats pour être mélangé avec du TPS. Le polyéthylène, l'un des plastiques les plus utilisés, peut être aujourd'hui produit à partir de la biomasse et par conséquent il existe des bio-polyéthylènes (bio-PE), quand même s'il reste non biodégradable. Ces facteurs soulignent l'intérêt de préparer de nouvelles formulations de TPS avec du bio-PE et d'étudier la relation structure morphologique / propriétés mécaniques de ces mélanges.

Dans la deuxième partie de cette étude, les formulations de TPS à partir des quatre plastifiants mentionnés, que nous nommerons glycérol-TPS, sorbitol-TPS, diglycérol-TPS et polyglycérol-TPS par la suite, ont été caractérisées par deux essais préliminaires : l'absorption d'humidité dans une chambre environnementale et la stabilité en température mesurée par analyse thermogravimétrique (TGA). L'essai à 80% d'humidité relative et 25˚C a révélé que le polyglycérol-TPS présentait l'absorption d'humidité la plus faible (15% d'augmentation en masse) par rapport au glycérol-TPS (40%). Ainsi, les fluctuations des propriétés mécaniques induites par l'humidité devraient être moins prononcées pour le polyglycérol-TPS, suivi par le diglycérol-TPS et le sorbitol-TPS. Le test de stabilité en température a également révélé le potentiel d'applications nouvelles pour le polyglycérol-TPS. L'analyse thermogravimétrique a montré qu'à 156°C, 5% du plastifiant de l'échantillon glycérol-TPS avaient été volatilisés. Cette température est très faible considérant que la majorité des polymères ont une température de mise en œuvre souvent supérieure à 150°C. La température pour une perte de masse du plastifiant de 5% était de 235°C, 225°C et 203°C, respectivement pour le sorbitol-TPS, le polyglycérol-TPS et le diglycérol-TPS. En tenant compte de leur nature moins hygroscopique, ces plastifiants pourraient

accroître le champ d'application de l'amidon thermoplastique. Suite à ces essais, les mélanges de polyéthylène haute densité (HDPE) / TPS 80/20 (% massique) ont été préparés par un procédé breveté de ce laboratoire. Les résultats de la microscopie électronique à balayage (SEM) sur des échantillons préparés par extrusion, ont démontré qu'en dépit de la viscosité élevée de ces nouveaux plastifiants, la taille des gouttelettes de TPS dans la matrice PE était du même ordre de grandeur que celle obtenue avec du TPS plastifié avec du glycérol. Un copolymère (polyéthylène greffé anhydride maléique, PE-g-MA) a été en outre ajouté aux mélanges à différents taux pour obtenir les courbes d'émulsification. Ces courbes montrent que la taille des gouttelettes (caractérisée par le diamètre moyen en volume, d_v et le diamètre moyen en nombre, d_n) diminue lorsqu'on augmente la quantité du PE-g-MA jusqu'à atteindre un plateau pour 9% en masse de PE-g-MA pour le glycérol-TPS et le sorbitol-TPS. Les résultats sont différents pour le diglycérol-TPS et le polyglycérol-TPS : la concentration critique pour la saturation de l'interface est aussi à 9% en masse pour le d_v mais est à 1% pour le d_n. En incorporant seulement 1% de copolymère, un nombre considérable de très petites gouttelettes apparaissent qui maintiennent la même taille jusqu'à des concentrations plus élevées de copolymère. Ce comportement inhabituel pour le diglycérol-TPS et le polyglycérol-TPS peut indiquer que le mécanisme de formation des gouttelettes s'effectue par érosion, favorisant le départ de fragments de TPS à la surface extérieure des gouttelettes. Le TPS, qui est un mélange partiellement miscible d'amidon et de plastifiant, présente deux pics de transition dans les analyses dynamiques mécaniques (DMA). On a observé que les températures de transition vitreuse du diglycérol et du polyglycérol dans le TPS ont considérablement été déplacées (~ 45 ˚C) vers les températures de transition des molécules d'amidon. Ces changements sont de 50% supérieur à ceux observés pour les molécules de glycérol dans le TPS. Par conséquent, on peut considérer que le diglycérol-TPS et le polyglycérol-TPS ont une meilleure miscibilité (moins de séparation de phase) par rapport au glycérol-TPS. Cette homogénéité renforcée permet au processus d'érosion d'être observé à plus faible concentration de copolymère pour le diglycérol-TPS et le polyglycérol-TPS. L'effet est probablement masqué dans le glycérol-TPS en raison de la formation d'une couche intermédiaire de glycérol à la surface extérieure de la gouttelette. Les propriétés mécaniques présentent un comportement global identique pour toutes les formulations sauf pour le sorbitol-TPS dont la ductilité n'était pas améliorée en présence du compatibilisant, probablement en raison de la cristallisation du sorbitol à température ambiante.

Les nanotubes de carbone (CNT) peuvent être ajoutés aux bioplastiques pour cibler des applications de haute performance. En raison de la disponibilité du TPS et du nombre croissant de mélanges TPS sur le marché, il est intéressant d'incorporer des nanotubes dans les mélanges TPS. Pour cette partie, nous avons choisi le mélange de Polycaprolactone (PCL) / TPS. Le PCL a une rigidité très faible et l'ajout de nanotubes pourrait permettre de nouvelles applications pour les mélanges avec PCL. Le PCL peut être facilement dissous dans le tétrahydrofurane (THF) à température ambiante qui est un bon solvant pour les nanotubes de carbone. La température de fusion du PCL est très faible (65˚C) et le mélange peut être fait à basse température, sans dégrader le TPS. Enfin, il y a une vaste connaissance dans ce laboratoire sur la relation structure-morphologie dans les mélanges PCL/TPS.

Les propriétés mécaniques, optiques et électriques dans les mélanges de polymères chargés dépendent fortement de la localisation des charges et de leur niveau de la dispersion. Afin d'obtenir une très bonne dispersion, un produit concentré (une ‘masterbach’) de PCL/CNT a été préparé par la méthode de solution. Cette formulation a été ensuite mélangée avec du PCL et du TPS par deux procédés. Dans la première méthode, une extrudeuse bi-vis (TSE) a été utilisée pour mélanger le TPS et le PCL. Il a été observé qu’en utilisant la TSE et en alimentant les nanotubes avec le PCL, la majorité des nanotubes de carbone sont situés dans la phase dispersée et aussi en partie à l'interface. Ceci est un résultat très intéressant car le temps de séjour dans la TSE était de moins de deux minutes. Cette localisation restait stable même après une longue durée de recuit à l’état fondu. En utilisant le modèle de Young afin de déterminer l'état thermodynamiquement préférée de dispersion, conduit à la localisation des nanotubes à l'interface mais pas au sein de la phase TPS. Afin d'étudier le niveau d'interaction entre TPS et les nanotubes, X-ray spectroscopie de photoélectrons (XPS) a été utilisé sur les échantillons qui ont été extraites de la TSE en plusieurs étapes. Il a été démontré que les nanotubes sont toujours encapsulés par les molécules d'amidon. La capacité de l'amidon de rester sur la surface du nanotube de carbone, même après plusieurs extractions et deux semaines de solubilisation est un indice important de formation d'une liaison covalente entre les groupes acide carboxylique sur la surface du nanotube et du TPS. Alors, il a été conclu qu'une fois que les nanotubes de carbone ont été poussés à l'interface, afin de réduire l'énergie libre totale du système, la réaction survient à l'interface entre les groupes carboxyliques des nanotubes de carbone et les groupes hydroxyles des molécules d'amidon. À la suite de cette réaction et la formation d'une couche d'encapsulation

TPS autour du nanotube, les nanotubes de carbone sont attirés dans la phase dispersée de l'amidon thermoplastique.

Paramètres de traitement se sont révélées à influer profondément sur le phénomène de localisation. Autrement dit, l'équilibre thermodynamique ne peut être atteint que si les paramètres cinétiques de fournir les conditions requises. Afin d'évaluer l'influence de la technique de traitement différent sur la localisation des nanotubes de carbone, un mélangeur interne a été utilisé. Étant donné que le mélangeur interne impose un champ d'écoulement principalement de cisaillement, son influence sur le processus de localisation sera intéressante à examiner. Afin d'évaluer la performance du mélangeur interne (IM) dans la préparation de ce nanocomposite, nous avons répété une approche similaire à celle pour le processus de TSE. Les échantillons obtenus uniquement avec le mélangeur interne ont montré une localisation tout à fait différente : les nanotubes restaient dans la phase PCL et aussi à l'interface. Mais ils n'ont pas entré dans la phase dispersée dans toutes les conditions. Considérant le modèle mentionné ci-dessus à propos de l'état d'équilibre thermodynamique, la différence dans la localisation a été attribuée aux effets cinétiques. Les essais rhéologiques ont révélé un fort comportement rhéofluidifiant naturel du TPS. La comparaison des taux de cisaillement et de la contrainte de cisaillement dans les deux procédés, TSE et IM, ont montré que le TPS avait des viscosités très différentes. En raison des conditions de taux de cisaillement / contrainte de cisaillement élevés dans l'extrusion, la viscosité du TPS est remarquablement réduit, permettant aux nanotubes réagi de pénétrer dans la phase TPS. À l'opposé, la viscosité élevée du TPS dans le procédé IM ne permet pas aux nanotubes de se déplacer dans la phase TPS. Par conséquent, comme cela n'est pas l'état d'équilibre de la dispersion, la localisation est instable et très probablement il sera soumis à modification par le retraitement sous les paramètres de traitement différents. La morphologie du TPS dans le PCL a été étudiée plus en détail. En extrusion, les nanotubes n'ont pas montré de différence sur la taille des gouttelettes de TPS. Mais dans le précédé IM, en raison de l'augmentation de la viscosité du PCL et de la localisation des nanotubes dans l'interface, avec 0,5% massique de nanotubes la taille des gouttelettes chute de moitié.

En raison de l'interaction au niveau moléculaire entre les nanotubes et les chaînes polymères, il est prévu que l'ajout de nanotubes aux polymères affectera les propriétés physiques des polymères. La structure supramoléculaire du PCL a également été modifiée par l'ajout des nanotubes comme l'ont révélé les essais de DSC non isothermes. Il a été montré que les

nanotubes pouvaient effectivement agir comme des agents de nucléation en augmentant les températures de cristallisation tandis que le taux de cristallinité diminuait en raison des imperfections plus importantes dans les sphérolites de PCL en croissance. Un autre effet était sur les températures de transition de la phase de TPS chargé avec les nanotubes. Dans les échantillons extrudés, il a été observé que l'ajout de 0,5% en masse de nanotubes au mélange diminuait considérablement la température de la transition α des molécules d'amidon (~ 26 ˚ C). Ceci a été attribué aux effets causés par la facilité du glissement des chaînes d'amidon autour de la surface solide en raison d'une plus faible densité d'enchevêtrement et orientation imposée.

ABSTRACT

A new class of polymers known as “bioplastics” has emerged and is expanding rapidly. This class consists of polymers that are either bio-based or biodegradable, or both. Among these, polysaccharides, namely starch, are of great interest for several reasons. By gelatinizing starch via plasticizers, it can be processed in the same way as thermoplastic polymers with conventional processing equipment. Hence, these bio-based and biodegradable plastics, with their low source and refinery costs, as well as relatively easy processability, have made them ideal candidates for incorporation into various current plastic products.

However, thermoplastic starch (TPS) does have two major drawbacks: first, its low intrinsic mechanical properties, and second, its hygroscopic nature, which results in the fluctuation of its properties in different environments. Thus, it is difficult to use TPS as it is, and it must be blended with other plastics. Due to these reasons, the majority of TPS-blend applications are in the category of non-durable materials, such as grocery bags, cutlery, bowls and cups. If the moisture-resistance and/or mechanical properties of TPS are enhanced, however, its scope of application could be broadened to include semi-durable and durable products. To achieve this, two options will be examined: 1) altering the internal structure of thermoplastic starch, and 2) incorporating nanofillers into the structure of TPS.

Four different plasticizers have been chosen here for gelatinization of TPS: glycerol, sorbitol, diglycerol and polyglycerol, with the latter two being used for the first time in such a process. Two methodological categories are used. The first involves a calorimetric method (Differential Scanning Calorimetry) as well as optical microscopy; these are “static” methods where no shear is applied A wide range of starch/water/plasticizer compositions were prepared to explore the gelatinization regime for each plasticizer.. The onset and conclusion gelatinization temperatures for sorbitol and glycerol were found to be in the same vicinity, while diglycerol and polyglycerol showed significantly higher transition temperatures. The higher molecular weight and viscosity of polyglycerol allow this transition to occur at an even higher temperature than with diglycerol. This is due to the increase in molecular weight and viscosity of the two new plasticizers, as well as their significant decrease in water solubility. It is demonstrated that the water/plasticizer ratio has a pronounced effect on gelatinization temperatures. When plasticizer content was held constant and water content was increased, it was found that the gelatinization temperature

decreased for all the plasticizers. Meanwhile, when the water content was held constant and the plasticizer content was increased, the gelatinization temperature increased for glycerol, sorbitol and diglycerol, but it moved in the opposite direction in the case of polyglycerol. The gelatinization temperature variation for glycerol, sorbitol and diglycerol caused by changing water and plasticizer content indicates that water is the primary agent causing granular swell and plasticization in the gelatinization process. Due to the high molecular weight and viscosity, as well as the low hydroxyl group density (~ one –OH per two carbon) and borderline solubility of polyglycerol in water, it is believed that water-aided penetration of the plasticizer among the crystalline structure of starch molecules is significantly decelerated. So it is proposed that in the case of low-water solubility of the plasticizers, gelatinization temperature is determined more by the total amount of the plasticizer and water, rather than the water/plasticizer ratio. Increasing the miscibility of polyglycerol in water by increasing the temperature of the initial slurry, results in a return of the system to the typical thermal dependence of gelatinization with plasticizer/water ratio.

Secondly, the gelatinization of starch under "dynamic conditions" was studied. In this case, a constant shear is applied to the slurry, along with a temperature ramp to induce gelatinization. This is, in fact, a rheological technique that heats up the slurry, while a mechanical shear is applied throughout. The reason for using this method is that in the plastic industry, thermoplastic starch is produced via processes involving shear such as extrusion, but, to date, there has not yet been a thorough study on the effect of pure shear on the gelatinization process. Glycerol, diglycerol and sorbitol were subjected to different dynamic gelatinization treatments in a couette flow system, and the results were compared with static gelatinization. Applying shear showed virtually no effect on the onset gelatinization temperature. However, the conclusion temperature was remarkably reduced with the presence of shear. So it can be stated that the conclusion temperature is more kinetically driven (i.e. by applying high shear), so that complete gelatinization can be achieved in a shorter time-frame.

Bioplastics are the most obvious choice to be incorporated in TPS blends. Polyethylene, one of the most commonly used plastics, can also be currently produced from biomass and hence considered as a bioplastic, though it remains non-biodegradable. These factors underline the interest to incorporate the new TPS formulations in bio-PE products and study their structural, morphological and mechanical properties.

In this part of the work, all formulations of TPS—i.e. glycerol-TPS, sorbitol-TPS, diglycerol-TPS and polyglycerol-TPS—were subjected to two preliminary tests, examining moisture uptake level and temperature stability. Polyglycerol-TPS showed the least moisture uptake (15%), compared to glycerol-TPS (40%) at 25˚C and 80% humidity. So the above-mentioned humidity-induced fluctuations in the mechanical properties are less pronounced for polyglycerol-TPS, followed by diglycerol-TPS and sorbitol-TPS. The heat stability measurements also revealed new potential applications for polyglycerol-TPS. It was shown that the 5% plasticizer weight loss temperature for glycerol-TPS is 156˚C, which, considering the high processing temperature of the majority of commodity plastics (>150˚C), it is expected that high evaporation rates of the plasticizers would be observed during the process. Interestingly, it was found that the 5% plasticizer weight loss temperatures for sorbitol-TPS, polyglycerol-TPS and diglycerol-TPS are 235˚C, 225˚C and 203˚C, respectively, which, combined with their less hygroscopic nature, opens a wide range of applications for thermoplastic starch. In order to evaluate the performance of the new plasticizers in the TPS blends, blends of HDPE/TPS:80/20wt% were prepared through a patented process in the laboratory. Scanning electron microscopy results, demonstrated that despite the high viscosity of the new plasticizers, the droplet size of the TPS in PE matrix falls into the same region as glycerol-TPS. A copolymer (PE-g-Maleic Anhydride) was further added to the blends in various compositions. The emulsification curves show that the volume average droplet size (d_v) and number average droplet size (d_n), diminish accordingly by increasing compatibilizer content and reaches a plateau at 9wt% PE-g-MA for glycerol-TPS and sorbitol-TPS. But diglycerol-TPS and polyglycerol-TPS demonstrated different trends for the volume and number average diameters. For them, the critical concentration for saturation of the interface is at 1 wt% based on d_n, but at 9 wt% based on d_v. This means that for these latter two plasticizers, by incorporating only a 1% copolymer a significant number of very small droplets appear which maintain the same size throughout the whole copolymer composition range. This is demonstrated by droplet size-frequency histograms for diglycerol-TPS. The unusual behaviour exhibited by diglycerol-TPS and polyglycerol-TPS provides insight into their droplet formation mechanism and is indicative of an erosion-type mechanism where fragments of TPS break off of the outer envelope of the droplet. TPS as a partially miscible mixture of plasticizer and starch shows two transition peaks in dynamic mechanical analysis (DMA). It was observed that the transition temperatures of diglycerol and polyglycerol in TPS significantly shifted (~45˚C) towards the transition

temperatures of starch molecules. This shift was found to be 50% more than the same observed shifts for glycerol molecules in TPS. Consequently, diglycerol-TPS and polyglycerol-TPS appear to demonstrate an enhanced miscibility (less phase separation) as compared to glycerol-TPS. This enhanced TPS homogeneity allows the erosion process for diglycerol-TPS and polyglycerol-TPS to be observed at low interfacial modifier concentrations. The effect is likely masked in glycerol-TPS due to the formation of a glycerol interlayer at the outer boundary of the droplet. Mechanical properties show overall the same behaviour for all the formulations except for sorbitol-TPS, which did not show any improvement in ductility with the addition of a compatibilizer. This is most likely due to its re-crystallization at room temperature. Hence, the new TPS formulations display a similar performance to glycerol-TPS blends, but with enhanced moisture-resistance and thermal stability.

The addition of carbon nanotubes (CNTs) to bioplastics is a route towards developing new applications for them as high-performance materials. For this part, we chose Polycaprolactone/TPS blends for several reasons: PCL has a very low rigidity, so the addition of nanotubes will introduce new properties to its blends; PCL can be easily dissolved in THF (Tetrahydrofuran) at room temperature which is a good solvent for carbon nanotubes; its melting temperature is low (65˚C), so blending can be done at low temperatures which ensures that TPS will be stable under those conditions; and finally there is significant knowledge in this laboratory about the structure-morphology relationship of PCL/TPS blends.

One of the most important issues concerning the filled polymer blends which controls all their mechanical, optical and electrical properties is the localization of the fillers. Despite this importance, there is very little work in the literature on the stable localization of the nanotubes in multiphase polymers. The masterbatch of PCL/CNT was prepared using a solution casting technique. This masterbatch was then blended with virgin PCL and 20 wt% TPS via twin screw extrusion (TSE). Microscopic investigations revealed that while using the TSE, the carbon nanotubes were located majorly in the TPS bulk and also partly at the interface, while they were fed within the PCL phase. This gets more interesting, considering the fact that the residence time in TSE is less than 2 minute. This localization was found to be stable even after annealing for long durations. Using Young's model to determine the thermodynamically preferred state of dispersion, results in a prediction of interfacial localization for the nanotubes, not localization within the TPS phase. In order to investigate the level of interaction between TPS and nanotubes,

X-ray photoelectron spectroscopy (XPS) was used on the TSE. It was demonstrated that the nanotubes are still encapsulated by the starch molecules. The ability of starch to remain on the carbon nanotube surface even after multiple extractions and two weeks of solubilisation is strongly indicative of the formation of a covalent bond between the carboxylic acid groups on the nanotube surface and the TPS. So it was concluded that once the carbon nanotubes were driven to the interface in order to reduce the overall free energy of the system, an interface reaction occurs between carboxylic groups of CNTs and hydroxyl groups of starch molecules. Following this reaction and the formation of a TPS encapsulating layer around the nanotube, the carbon nanotubes are drawn into the thermoplastic starch dispersed phase.

Thermodynamic equilibrium can be achieved only if the kinetics parameters provide the required conditions. In order to assess the influence of a different processing technique on carbon nanotube localization, an internal mixer was used. Since the internal mixer imposes a predominantly shear flow field, its influence on the localization process will be interesting to examine. In this process, completely different localization was observed; all the nanotubes remained in the PCL phase and at the interface. But they did not enter the dispersed phase under any conditions. Considering the above-mentioned model about the thermodynamic equilibrium state, the difference in localization was attributed to the kinetic effects. Rheological tests revealed the high shear thinning nature of TPS. The comparison of the shear rate and shear stress between TSE and IM showed that TPS would have significantly different viscosities in both processes. Due to high shear rate/shear stress conditions present in TSE, the viscosity of TPS in TSE reduces remarkably, allowing the reacted nanotubes to penetrate into TPS phase; meanwhile, the high viscosity of TPS in IM would not allow this penetration to proceed. Hence, since this is not the equilibrium state of dispersion, localization is unstable and most likely it will be subjected to change by reprocessing under different processing parameters. In addition, the morphology of TPS in PCL was studied. In IM, due to the increased viscosity of filled PCL and interface localization of the nanotubes, with the addition of 0.5 wt% of the nanotubes in the system, the droplet size drops to the half.

Due to the molecular level interaction between nanofillers and the polymer chains, it is expected that the addition of nanofillers to the polymers will affect the physical properties of the polymers. The supramolecular structure of PCL was subjected to change by the addition of nanotubes, as revealed by non-isothermal DSC and DMA tests.

TABLE OF CONTENTS

LIST OF TABLES

LIST OF FIGURES

NOMENCLATURE

English letters

Ca	capillary number
Ca_{crit}	critical capillary number
C_h	chiral vector
D	diameter
Da	dalton (atomic mass unit)
G’	storage modulus
G”	loss modulus
L	length
M_w	molecular weight
p	droplet viscosity/matrix viscosity
T_c	conclusion gelatinziation temperature
T_g	glass transition temperature
T_o	onset gelatinziation temperature
T_p	peak gelatinization temperature
T_{sec}	secondary transition temperature
T_α	alpha transition temperature
T_β	beta transition temperature

V_i molar volume of the component i

V_M total volume of the mixture

Wa work of adhesion

W_t sample mass at time t

Greek letters

γ shear rate

γ_i surface tension of component i

γ_i^d dispersive component of surface tension

γ_{ij} interfacial tension of component i and j

γ_i^p polar component of surface tension

δ solubility parameter

Δ moisture uptake percentage

ΔE the energy of vaporization to a gas at zero pressure

ΔG_m Gibb's free energy of mixing

ΔH_m enthalpy of mixing

ΔS_m entropy of mixing

η^* complex viscosity

η_m matrix viscosity

ν_i volume fraction of the component i

σ	interfacial tension.
τ	shear stress
Φ	interaction parameter
ω	frequency
ω_s	*wetting coefficient*

List of Abbreviations

TPS	Themoplastic starch
ABS	Acrylonitrile butadiene styrene
CNT	Carbon Nanotubes
DTPS	Diglycerol plasticized starch
EVA	Ethylene vinyl acetate
GMA	Glycidyl MethAcrylate
GTPS	Glycerol plasticized starch
HDPE	High density polyethylene
LDPE	Low density polyethylene
LLDPE	Linear low density polyethylene
MA	Maleic anhydride
MWNT	Multiwall carbon nanotubes
PA	Polyamide

PC	Polycarbonate
PCL	Polycaprolactone
PE	Polyethyelene
PE-g-MA	Polyethyelene-grafted-maleic anhydride
PHA	Polyhydroxyalcakoate
PLA	Polylactic Acid
PMMA	Poly(methyl methacrylate)
PP	Polypropylene
PS	Polystyrene
PTPS	Polyglycerol plasticized starch
PVA	Polyvinyl Alcohol
STPS	Sorbitol plasticized starch
SWNT	Single wall carbon nanotubes
TSE	Twin screw extruder

Chapitre 1 **INTRODUCTION AND OBJECTIVES**

1.1 **Introduction**

Nowadays, the plastics industry is drifting more and more towards the production of bioplastics. According to "Europeen Bioplastics," bioplastics are described as all the plastics that are either biodegradable or bio-based, or both (Queiroz & Collares-Queiroz, 2009). Environmental concerns such as limiting the amount of petroleum and increasing the biodegradability of products are at the core of this growing trend towards bioplastics.

Among bio-based materials, starch is the most abundant, naturally occurring homopolymer present in a variety of botanical sources, such as maize, potato, rice and wheat. However, due to two major drawbacks, starch alone cannot be used in plastics: namely, high moisture sensitivity and poor mechanical properties. Hence, it needs to be blended with other polymers. Starch/plastic composites with or without interfacial modifiers have been extensively studied in the literature (Avella, Errico, Laurienzo, Martuscelli, Raimo & Rimedio, 2000; Averous, Moro, Dole & Fringant, 2000; Wu, 2003). The outcomes, however, show poor mechanical properties of the final products due to the high interfacial tension in the starch/polymer matrix. The crystalline structure of starch can be disrupted in by presence of a plasticizer plus heat/shear (Averous, 2004; Otey, Westhoff & Doane, 1980b). This results in a decrystallized starch/plasticizer mixture, which is referred to as "Thermoplastic Starch" (TPS). TPS is able to flow at high temperatures and be processed using conventional polymer-processing equipment. But due to its high hydrophilicity and weak mechanical properties, it must be blended with other polymers. Melt blending of starch/plastics is a one-step process during which starch is mixed with a plasticizer, decrystallized, homogenized and blended with other polymer(s) in the time frame of extrusion (1-2 min). The majority of TPS-blend applications are for non-durable products, due to the aforementioned problems of TPS. In order to upgrade TPS applications to semi-durable and durable products, we will adopt two strategies: enhancing the internal structure of TPS and incorporating nanofillers.

As mentioned, TPS is a partially miscible mixture of starch and a plasticizer. The structure of the plasticizer can influence TPS in two aspects. The first is through the gelatinization phenomenon that occurs during TPS preparation. It is demonstrated that various plasticizers such as glycerol,

glucose, sorbitol, ethylene glycol, and amides can show different gelatinization properties such as raised/lowered gelatinization temperature or enthalpy (Habeych, Guo, van Soest, der Goot & Boom, 2009; Li, Sarazin & Favis, 2008; Perry & Donald, 2000; van Soest, Bezemer, de Wit & Vliegenthart, 1996). The second is seen in the final TPS properties in blends with other materials. Molecular weight and chemical structure of the plasticizers are known to have a great impact on the molecular mobility and interfacial properties of TPS. Hence, the morphological, mechanical, electrical and optical properties of the blends are subjected to change by the type of plasticizer used. Glycerol is the most commonly used plasticizer, both in the industry and the literature (Kaseem, Hamad & Deri, 2012) due to its low cost and high efficacy in plasticization. But its low molecular weight and low boiling point makes glycerol evaporate at high temperatures or migrate to the interface/surface in high-temperature melt processes, such as TPS/PE or TPS/PLA blends. So using higher molecular weight plasticizers, which can gelatinize starch and stay bonded with starch molecules via strong hydrogen bonding and also possess high temperature stability, is of great interest for scientific and industrial work.

The major roadblock to the development of most bioplastics are the shortcomings found in mechanical and electrical properties, thermal stability, permeability, shelf life and aging (Haugaard, Udsen, Mortensen, Hoegh, Petersen & Monahan, 2001). One of the ways to overcome these disadvantages is the incorporation of nanofillers. In recent years, carbon nanotubes have been successfully added to polymer blends because of their superior mechanical, electrical, magnetic, optical and thermal properties (Potschke, Bhattacharyya & Janke, 2004; Wu et al., 2011; Wu & Shaw, 2004). Carbon nanotubes offer the potential to generate novel materials when mixed with a polymer resin; however, the mechanical properties of the solid, particle-filled materials are highly dependent on their localization (Baudouin, Devaux & Bailly, 2010; Laredo, Grimau, Bello, Wu, Zhang & Lin, 2010; Meincke, Kaempfer, Weickmann, Friedrich, Vathauer & Warth, 2004). There are two major factors influencing localization: thermodynamics and kinetics. In ideal equilibrium conditions, the carbon nanotubes will tend to minimize the free energy of the system by migrating to a phase where they generate the lowest interfacial tension (thermodynamic tendency). However, this migration can be controlled somewhat by altering processing effects such as composition, viscosity or feeding sequence (kinetic effect). Hence, in order to tailor any improvement in blend properties, we must be able to control the level of

dispersion and localization of the nanoinclusions. Considering the above-mentioned considerations, the main objectives of this work are stated in the following section.

1.2 **Objectives**

The main objective of the project is *to obtain high performance thermoplastic starch (TPS) blends with bioplastics*. Two general strategies are employed: Enhancing the internal structure of TPS via the incorporation of new, high molecular weight plasticizers; and incorporating carbon nanotubes. Due to the growing interest in bioplastics, as well as their wide variety, two types were chosen for our purposes: Polyethylene (which can be a bio-PE) and a biodegradable polyester (Polycaprolactone). Due to the high usage of polyethylene in the packaging industry and its well-known biodegradation problems, it would be highly significant to introduce a biodegradable portion to these products by blending PE with new high performance TPS. First, the structure of TPS and the new plasticizers will be investigated, before moving on to a study of the blends.

The incorporation of carbon nanotubes in a polymer matrix may deliver huge improvements to several mechanical, electrical, and optical properties. This may open new fields of applications for bioplastics and TPS blends if carbon nanotubes can be successfully added to the blends. Among the promising category of biodegradable polyesters, PCL is of great importance in packaging and biomedical applications, but due to some drawbacks such as its slow degradation rate and low stiffness, its wider application has been limited. However, by introducing nanotubes in PCL/TPS blends, it is possible to obtain a more rigid product with increased biodegradation rates. But this is only possible with effective dispersion and targeted localization of nanotubes.

Thus, our specific objectives are:

- Understanding the effect of high molecular weight plasticizers on the gelatinization of starch, as well as the efficacy and role of the water/plasticizer ratio on gelatinization in static (no shear) and dynamic (shear) conditions.
- Investigating the influence of high molecular weight plasticizers containing thermoplastic starch on the structure, morphology and mechanical properties of TPS/Polyethylene.

- Investigating the addition of carbon nanotubes on the physics, structure and morphology of TPS/Polycaprolactone blends. Controlling the localization of nanoparticles will be given special attention.

Chapitre 2 **LITERATURE REVIEW**

2.1 **Bioplastics**

In recent years, waste production is one of the major problems interfering with the development of applications in the plastics industry. The incorporation of biodegradable polymers is the most efficient way to overcome this problem, so their development has been a recent focus (Davis & Song, 2006). According to ASTM (D6400-99), a degradable plastic is a plastic designed to undergo a significant change in its chemical structure under specific environmental conditions resulting in the loss of some properties that may vary, as measured by standard test methods appropriate to the plastic and the application over a period of time that determines its classification. Biodegradation is a sort of degradation in which the act of disintegration of the polymer is made by biological activity under specific conditions (Nayak, 1999). Therefore, it may be aerobic (soil, compost, aquatic) or anaerobic (landfill); composting is currently the mostly commonly available method (Davis & Song, 2006). The family of biodegradable materials include two major subcategories (Averous, 2004):

a) Agro-polymers such as starch or cellulose, and

b) Biodegradable polyesters synthesized via various methods (agro-based, microbial production and chemical synthesis) such as PLA, PHA and PCL.

Another issue surrounding commodity plastics is the possibility of running out of oil in a few decades, a threat that has been hovering around in society for years, and which would force many industries to move towards oil-independency in many respects. However, due to recent discoveries, it is now known that there will be abundant oil and gas for at least a few more decades. Still, fluctuations in the price of oil, as well as the geopolitical issues surrounding its extraction and transport, along with ever-present CO_2 emission problems, have kept the pressure on the plastics industry to increase research and development of renewable resources. Recently, the industry discovered how to synthesize conventional polymers from biological resources, such as bio-based PE, PP or PET.

Thus, bioplastics are defined as polymeric materials that can be moulded with the help of heat and pressure, and satisfy one or both of the following criteria (www. european-bioplastics.org). They are either:

- Completely or partially driven from renewable resources, or
- Biodegradable.

This is demonstrated in Figure 2-1.

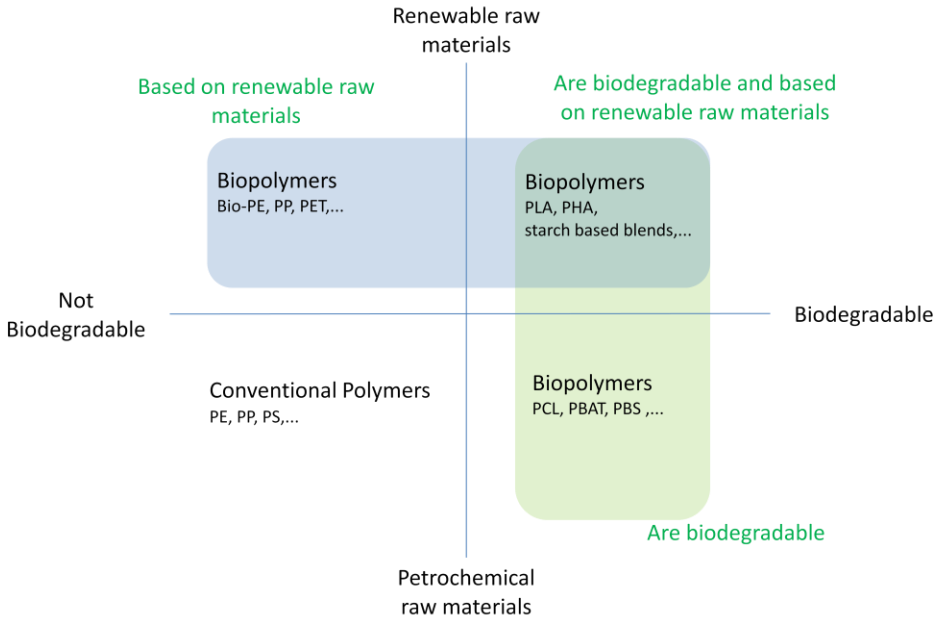

Figure 2-1. Material Coordinate System for Bioplastics (Source: University of Applied Science, Hanover, Germany).

Bioplastics are now used in a wide array of applications, such as packaging and electronics, in the automotive and agricultural industries, etc. The increasing demand for sustainable solutions has been the main reason for developing new markets. A predicted comparison between world-wide bioplastics production in 2010 and 2015 reveal an increase of 25-30% in production capacity per year (Figure 2-2). With the help of emerging technologies in the area of green polymers on one hand, and the demand for sustainability on the other, capacity is only expected to increase in the mid- to long-term. Among these bioplastics, one of the materials which satisfies both above

mentioned criteria and is considered the most abundant naturally occurring carbohydrate polymer is starch and its derivatives, which will be discussed in detail in section 2.2.

As it is observed in Figure 2-2, bio-PE is the mostly commonly used bioplastic (~28% of the market) and will likely hold this distinction in the future due to its broad range of applications.

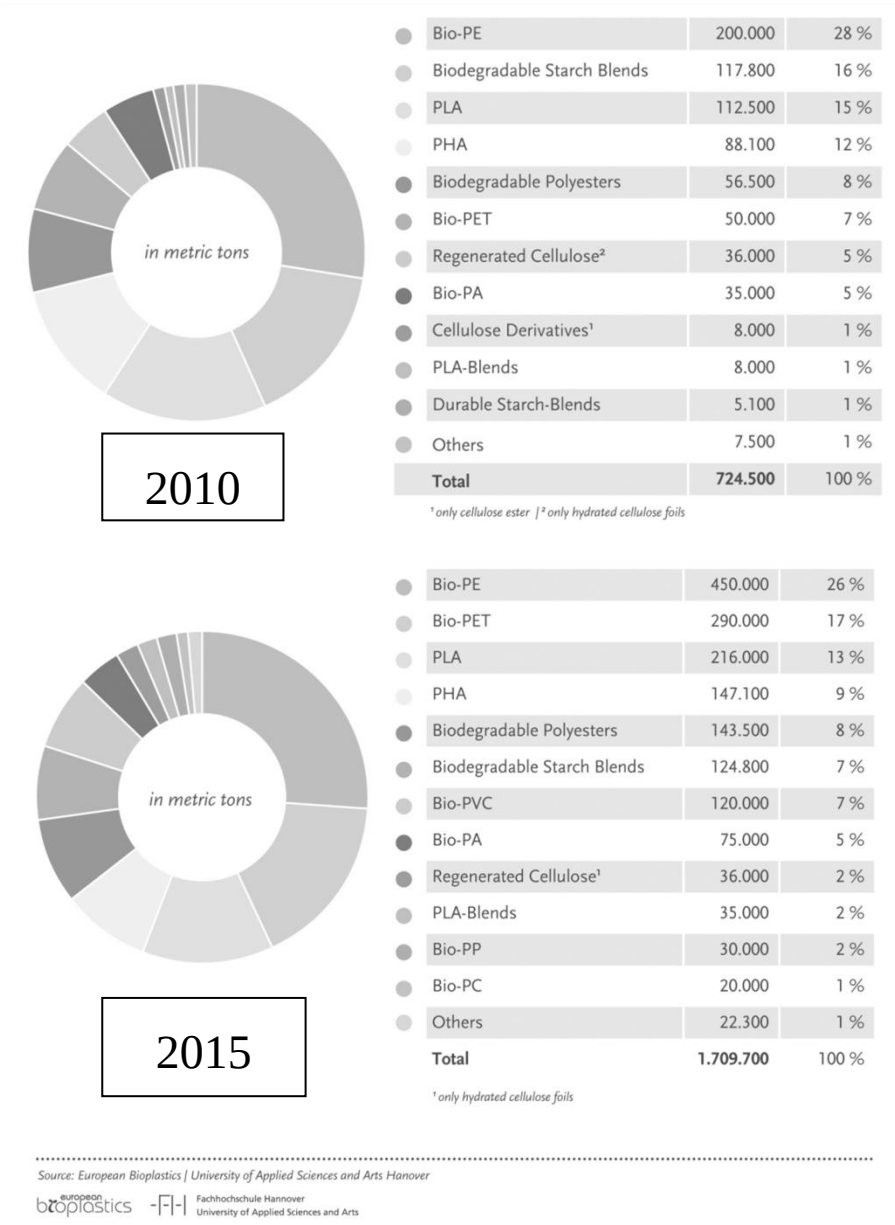

Figure 2-2 Bioplastics Production Capacity for 2010 and the prediction for 2015.

2.1.1.1 Polyethylene (PE)

Polyethylene is one of the most commonly used thermoplastics in the industry. Its production was over 80 million metric tons in 2008 and this is expected to increase by a rate of ~4-5% until 2015 (Piringer & Baner, 2008). Although a huge proportion of PE is fossil-fuel based, an increasing portion of it is now being produced from sugar cane (http://www.braskem.com/) and this makes bio-PE considered a bioplastic.

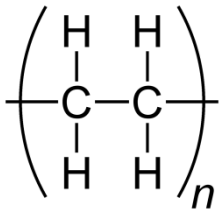

Figure 2-3 Polyethylene chemical structure.

The huge market for polyethylene is due to its low price, excellent chemical resistance, easy processability, high elongation at break and electrical insulation, as well its as heat resistance. The basic formula of PE is shown in Figure 2-3, but due to different molecular weights and architecture, it has several sub-categories, such as LLDPE (linear low-density polyethylene), LDPE (low-density polyethylene, highly branched), HDPE (high-density polyethylene, linear structure) and UHMWPE (ultra high molecular weight polyethylene)—each of which possesses different mechanical properties making it suitable for different applications. Due to the low degree of branching, HDPE has strong intermolecular forces and a consequently higher tensile strength. It is mostly used in hard packaging and products such as toys. Depending on the molecular weight and crystallinity, a melting temperature of 120–130˚C may be observed. Crystalline polyethylene can not be dissolved at room temperature, but at high temperatures some aromatic hydrocarbons such as xylene can dissolve PE.

The major problem with PE is that it is not biodegradable. So if a part of PE is replaced with a biodegradable polymer such as thermoplastic starch, it will essentially reduce the environmental impact of PE-based products.

2.1.1.2 Polycaprolactone (PCL)

Polycaprolactone (PCL) is a biodegradable aliphatic polyester produced through the ring-opening polymerization of ε-Caprolactone. It has a low melting point of around 60˚C and a glass

transition temperature of -60 ˚C. It is a linear and partially crystalline polymer with a crystallinity of around 40-50%.

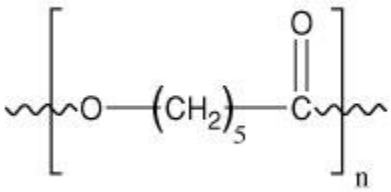

Figure 2-4 Polycaprolactone chemical structure.

Due to its high ductility and compatibility with a variety of materials it has been blended with materials such as starch, PLA, PVA, PVC, etc. (Biresaw & Carriere, 2004; Broz, VanderHart & Washburn, 2003; De Kesel, Lefevre, Nagy & David, 1999; Lim, Kim & Yoon, 2003; Singh, Pandey, Rutot, Degee & Dubois, 2003; Tsuji & Ishizaka, 2001; Wu, 2003). Since the biodegradation rate of PCL is low, it is used in long-term biomedical applications, such as implants (Williams et al., 2005). In order to use PCL in a wider range of products and replace polyolefins in some applications, its degradation rate must be increased. Another roadblock is its high price compared to other polymers. Thus, blending with a lower-priced, highly biodegradable polymer such as TPS is a way to develop new markets for PCL.

2.2 **Starch and Thermoplastic Starch (TPS)**

2.2.1 Starch Structure

Starch is the most abundant naturally occurring reserve carbohydrate that can be isolated from various botanical sources such as wheat, maize, rice, and cassava. The size of native starch granules might vary between 0.5 to 175μm, depending on the source (Averous, 2004) (Figure 2-5). Normally the starch granules absorb around 10-12% moisture in standard conditions (Tester, Karkalas & Qi, 2004). Like most other polymers, starch demonstrates a molecular weight distribution as well. It’s polydispersity depends on botanical source and method of extraction (Buléon, Colonna, Planchot & Ball, 1998; Ring, L'Anson & Morris, 1985).

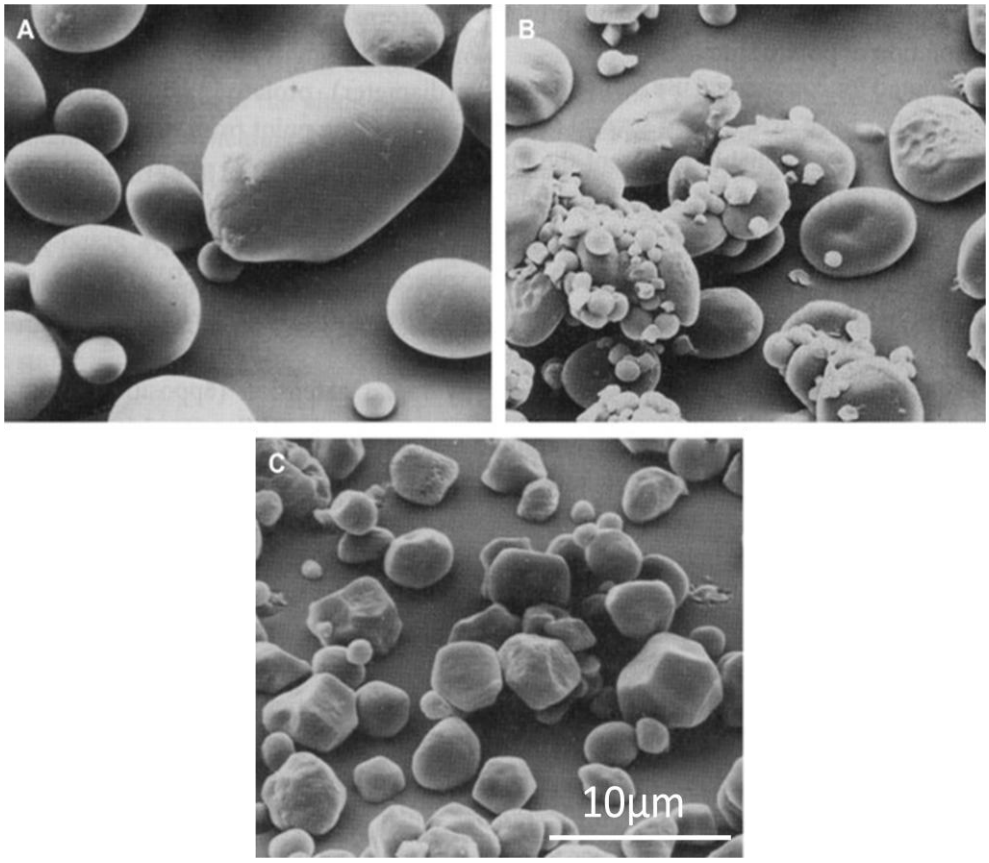

Figure 2-5 Scanning electron micrographs of starch granules from (A) potato, (B) wheat, (C) maize (Lehmann & Robin, 2007).

Starch is a homopolymer of two different structural α-D-glucose units. One is amylose, which is the linear or rarely branched part with a molecular weight of 10^5-10^6, which is bonded through α(1-4) bonds and a few occasional α(1-6) bonds resulting in long chain branches (Figure 2-6a) (Buléon, Colonna, Planchot & Ball, 1998; Mua & Jackson, 1997). Amylose content might vary from less than 15% for waxy starches to more than 40% for high-amylose starches.

The second unit, amylopectin, is heavily branched and the more crystalline part with a molecular weight of 10^7-10^9 and is linked together via α(1-4) bonds and α(1-6) bonds in the branching points (Figure 2-6b). Unlike amylose, the amylopectine side chains are relatively short, on average between 18-25 units long (Buléon, Colonna, Planchot & Ball, 1998; Hoover, 2001). The branching occurs every 20-70 glucose units.

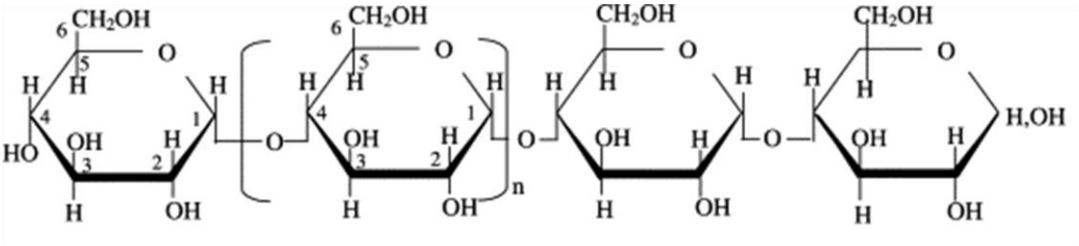

(a)

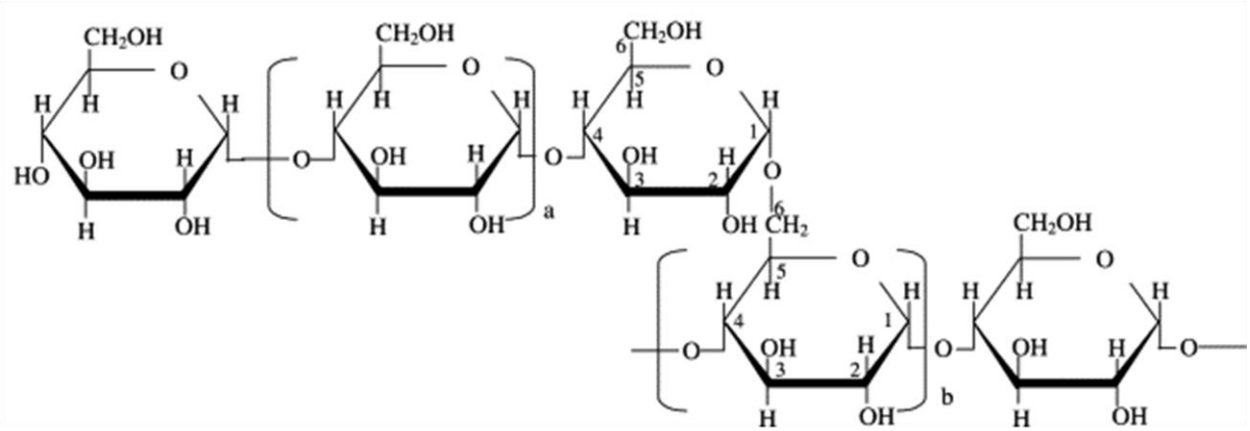

(b)

Figure 2-6 (a) Structure of amylose, n= ca. 1000, (b) structure of amylopectin, outer chains: a= ca. 12-23, for inner chains: b= ca. 20-30, a and b are subjected to change according to the botanical source (Tester, Karkalas & Qi, 2004).

2.2.1.1 Granular Structure (nano to micro scale)

The majority of native starch granules demonstrate Maltese cross pattern under polarized light, indicating their crystalline structure (Zobel, 1988). The crystallinity level in different starches may vary between 15% and 45%. The crystalline pattern of starch consists of alternating amorphous and crystalline layers (100-400 nm thick). It is believed that the crystallinity of starch is based on the ordered amylopectin side chains made of double helices (Tester, Karkalas & Qi, 2004). They all together form the "crystalline lamellae" (Figure 2-7). The majority of amylose chains and the branching points in amylopectin form the amorphous regions in the starch granules. The crystalline part of the starch is mostly comprised of the side chain double helices of amylopectin, and some co-crystallised amylose single helices (Angles & Dufresne, 2000). X-ray

diffractions reveal a periodicity of 9-10nm inside the starch granules, which is due to the crystalline and amorphous regions (Pérez, Baldwin & Gallant, 2009).

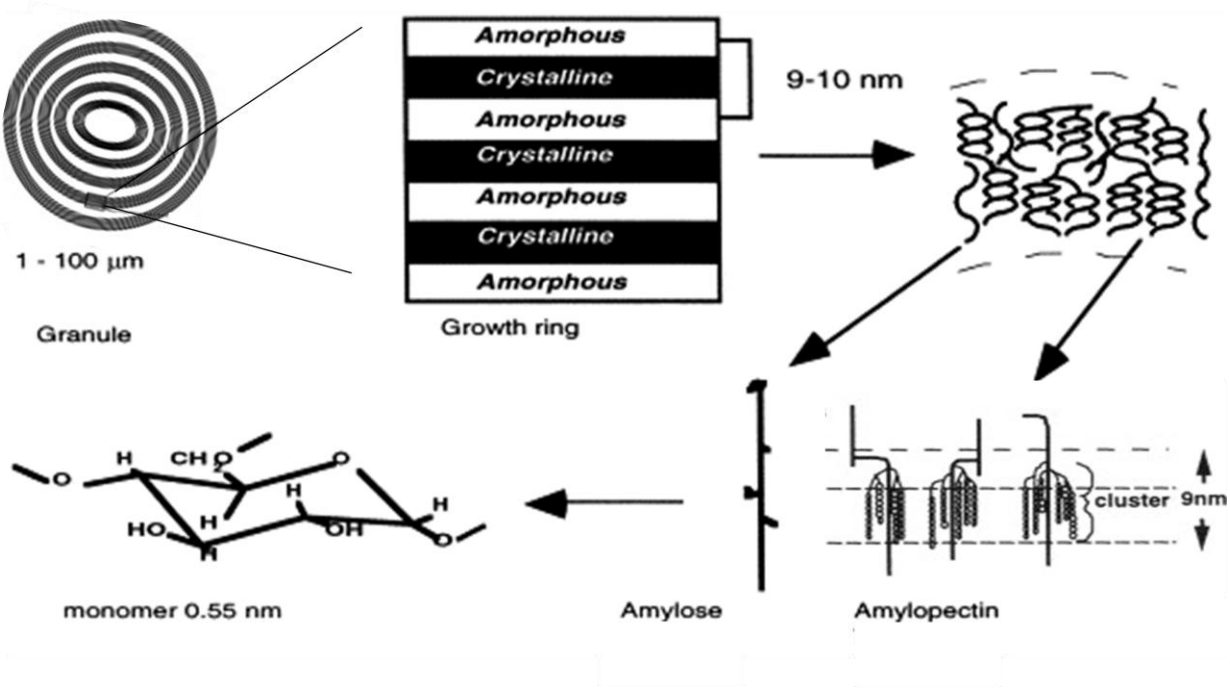

Figure 2-7 Schematic representation of the starch granule structure (Buléon, Colonna, Planchot & Ball, 1998; Tester, Karkalas & Qi, 2004; Vandeputte & Delcour, 2004).

Different patterns of crystallization can be found based on the different types of starch, namely A-, B- and C-types. The A- and B-types of the crystals are related to the orientation and the method of lamellar packing of the amylopectin chains, which may exhibit an orthogonal or hexagonal pattern in A-type and B-type, respectively (see Figure 2-8 below).

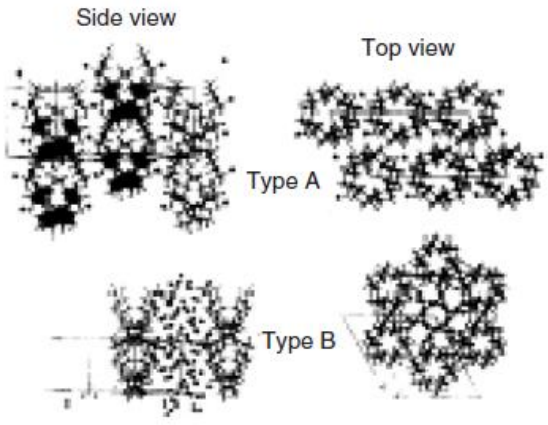

Figure 2-8 Crystalline packing of double helices in A-type (A) and B-type (B) amylose.

C-type is known to be a combination of A- and B-types (Biliaderis, 1992). A and B are observed more commonly in the native starches. A-type is normally associated with cereal starches, whereas B-type is observed in high-amylose or tuber starches (Swatloski, Spear, Holbrey & Rogers, 2002). Figure 2-9 demonstrates the X-ray diffraction patterns for A-type (corn), B-type (potato) and C-type (cassava) starch. A-type starch has shown to be more dense and less hydrated than B-type.

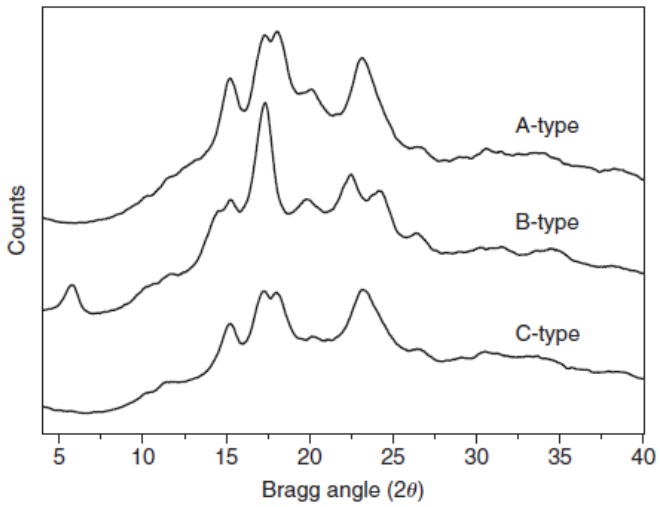

Figure 2-9 X -ray diffraction patterns of A-type (corn), B-type (potato) and C-type (cassava) starches (Carvalho, 2008)

At a larger scale of around 0.1-0.5μm (Figure 2-7), optical microscopy reveals that growth rings are composed of alternating amorphous-crystalline growth rings, as in crystalline lamellae (Jenkins & Donald, 1995). Small-Angle-X-ray Scattering (SAXS) was used to study the thickness of these layers, and their thickness was found to be in the same range (Cameron & Donald, 1992). The starch source greatly affects the size and number of these growth rings.

As observed in Figure 2-7, the growth rings form the shape of the final starch granules, and different botanical sources result in different granular shapes and sizes (Figure 2-5), e.g. maize (polygonal or round, 10–15μm) or wheat (oval, 15–100μm). Most of them have unimodal size distribution, but some, such as Triticicae-based starches, demonstrate a bimodal distribution of 10-35μm (large) and 1-8μm (small) granules (Stoddard, 1999; Vandeputte & Delcour, 2004).

2.2.1.2 Applications of Native Starch

Starch has been incorporated in polymer matrices primarily for two reasons: to increase the biodegradable portion of commodity polymeric products and to decrease the final cost. Due to the crystallinity and highly packed structure of starch granules, the melting temperature for starch is higher than its decomposition temperature. And due to the existence of an enormous number of hydroxyl groups in starch structure, it exhibits a very high hydrophilicity. Starch has been used as fillers or fibres in the plastic industry for polymers like PE or PP (Drummond, Hopewell & Shanks, 2000; Kim & Lee, 2002; Lawrence, Walia, Felker & Willett, 2004; Nawang, Danjaji, Ishiaku, Ismail & Ishak, 2001; Raghavan & Emekalam, 2001; Shah, Bandopadhyay & Bellare, 1995). However, it is generally shown that these composites result in very poor mechanical properties due to the incompatibility between starch and the polymers, and the consequent poor interfacial adhesion. For example, it was shown that by incorporating 0.5 vol% of starch in polyethylene, the strain at break drops to less than 10%. Hence, because of these drawbacks, native granular starch is not suitable for use in the polymer industry as a solid filler (see Figure 2-10 below).

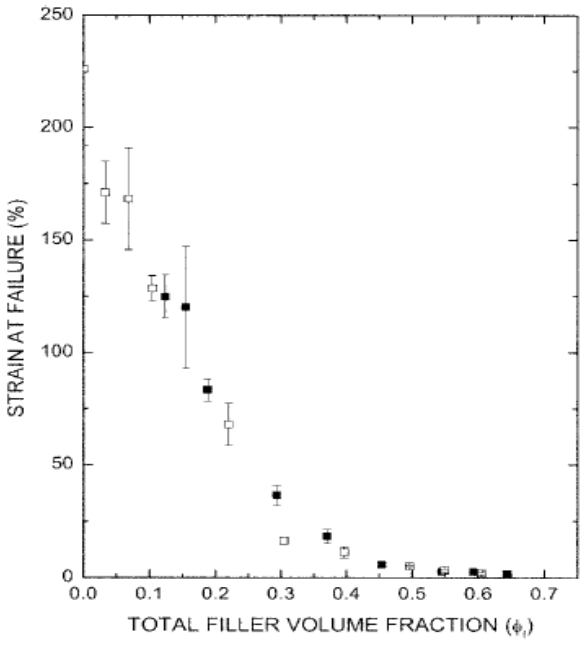

Figure 2-10 Strain at break vs. filler content in starch filled PE. Open symbols Starch/PE and filled symbols for Starch/PE/PHEE (Lawrence, Walia, Felker & Willett, 2004).

2.2.2 Thermoplastic Starch (TPS)

The crystalline structure of starch will be disrupted at high temperatures in the presence of excess water or any other plasticizer able to form hydrogen bonding with starch hydroxyl groups. During this process starch undergoes an irreversible order-disorder process during which the crystalline structure of amylopectine and amylose chains is disrupted irreversibly. The process of starch decrystallization is called "gelatinization," which is associated with the loss of double helices together with the loss of the lamellar and long-range structure of starch. This requires sufficient chain mobility, which can be provided by heat and/or mechanical energy in the presence of a plasticizer. Otey et al. (Otey, Mark, Mehltretter & Russell, 1974) demonstrated that gelatinization can be achieved through the processing of starch in presence of glycerol and water through conventional polymer processing equipment. Averous (Averous, 2004) has schematically described this process, showing the different stages of extrusion (Figure 2-11). The crystalline starch structure disappears at temperatures higher than 70–90˚C in the presence of plasticizers such as water, glycerol, formamide, sorbitol and liquid ammonia (Carvalho, 2008). The harder it is for the plasticizer to get into the starch structure, which is affected by plasticizer size as well as type, the higher the temperature and/or mechanical energy must be for the starch chains to acquire the sufficient mobility to break down the crystal structure.

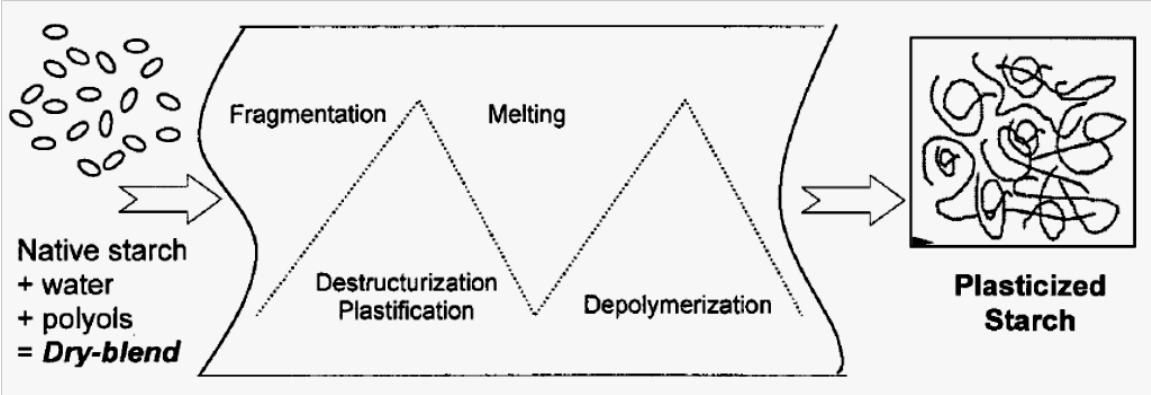

Figure 2-11 Different stages in extrusion processing of thermoplastic starch. (Averous, 2004)

Thus the degree of disruption and melting of the crystalline structure depends on the type of plasticizer and the processing parameters, which is explained in detail in the following section (Kim & Kim, 2006). To track this process, calorimteric techniques such as differential scanning calorimetry (DSC) (Baks, Ngene, van Soest, Janssen & Boom, 2007; Li, Sarazin & Favis, 2008), as well as optical microscopy (Hickman, Janaswamy & Yao, 2008; Palav & Seetharaman, 2006)

can be used. In case of enough plasticizer, it has been shown that the gelatinization phenomenon demonstrates one endothermic peak (Donovan, 1979). But in the case of a low or intermediate amount of plasticizer, another peak in higher temperatures is observed. This is attributed to the uneven distribution of the plasticizer in starch granule, hence, partial gelatinization is achieved in low temperatures, followed by recrystallization and re-melting of other parts (Biliaderis, Page, Maurice & Juliano, 1986; Donovan, 1979). A typical DSC thermogram is demonstrated in Figure 2-12 below. "Onset gelatinization temperature" is the temperature where the outer layer crystals start to decrystallize, and "conclusion temperature" is the temperature at which the majority of crystals have been broken apart. In optical microscopy, under polarized light, native starch granules will show birefringence, and this will be gradually lost over the course of the gelatinization process (Li, Sarazin & Favis, 2008).

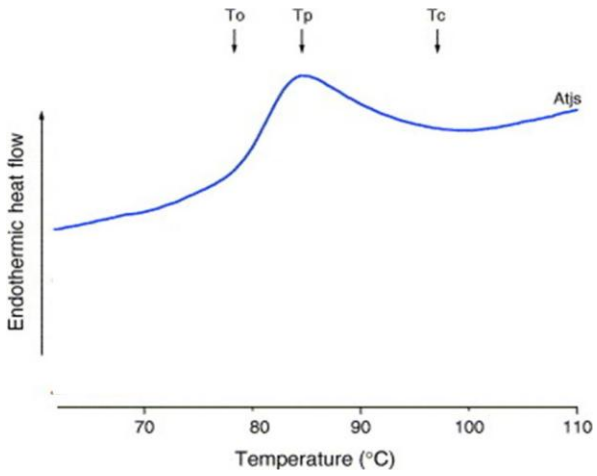

Figure 2-12 Typical DSC gelatinization thermograms of starch. T_o onset temperature; T_p peak temperature; T_c conclusion temperature (Lawal & Adebowale, 2005).

In addition to the above-mentioned techniques, several other methods can be used to visualize gelatinization, such as X-ray scattering, NMR spectroscopy, thermomechanical analysis or small angle X-ray analysis (SAXS) (Jenkins & Donald, 1998).

2.2.2.1 Factors Influencing the Gelatinization Phenomenon

In order to determine the influencing factors on starch gelatinization, the mechanism of the gelatinization should be better understood first. Waigh et al. (Waigh, Gidley, Komanshek & Donald, 2000), have described the crystalline structure of starch as double helices of amylopectine side-chains packed tightly together, forming a smectic liquid of crystalline

structures in dry starch which are linked together by amorphous amylopectine spacers and a backbone. This approach has been further investigated by Perry et al. (Perry & Donald, 2000, 2002), who proposed that gelatinization is comprised of two distinct steps independent of the type of plasticizer used (Figure 2-13).

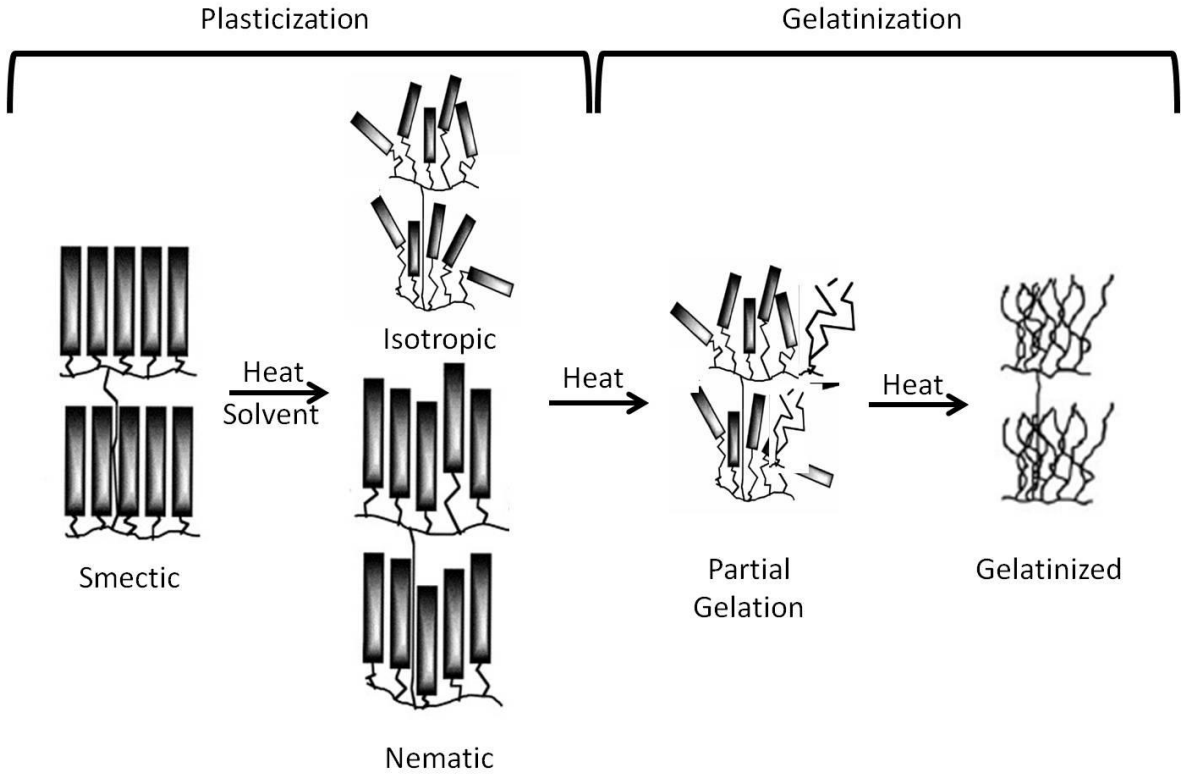

Figure 2-13 Schematic of starch gelatinization process based on liquid crystalline approach. (Perry & Donald, 2002; Waigh, Gidley, Komanshek & Donald, 2000)

The first step is the plasticization of amorphous regions through which the smectic/nematic side chains become isotropic. This step corresponds to the long-range order-disorder transition of helix-helix periodicity, which is reversible. The tightly packed structure of crystals ensures this transition continues until temperatures are very close to the gelatinization peak temperature (Donald, Kato, Perry & Weigh, 2001). Plasticization is mainly controlled by the ingress and diffusion of the plasticizer into amorphous parts of the complex starch granule structure (Antonio J.F, 2008). Independent of the type of plasticizer used, this step has been shown to be an essential precondition for gelatinization to begin (Perry & Donald, 2002; Tan, Wee, Sopade & Halley,

2004). During this step the amorphous parts of the starch gain a certain degree of freedom and molecular activity, i.e. they become plasticized. This mobility has a maximum limit after which the helix-coils begin their irreversible transition and the crystalline structure begins to melt. This is the second step, gelatinization, during which starch-starch hydrogen bonds are disrupted and at the same time starch-solvent hydrogen bonding occurs (Antonio J.F, 2008; Tan, Wee, Sopade & Halley, 2004).

During plasticization, there are several factors that influence transition dynamics, and gelatinization temperatures are thus subjected to change as well. Considering the above-mentioned explanation and the fact that the most important structural element building the starch crystalline structure is starch-starch hydrogen bonding (Antonio J.F, 2008), by increasing the hydrogen bonding capacity of the plasticizers, lamellar plasticization can be reached at lower temperatures (Perry & Donald, 2000; Waigh, Gidley, Komanshek & Donald, 2000). Tan et al (Tan, Wee, Sopade & Halley, 2004) recently showed that in addition to the hydrogen bonding ability of plasticizers, the solvent transport ability in granules of starch is of great importance in determining the gelatinization temperature. This is determined by parameters like molecular weight, viscosity and diffusion rate, as well, of course, as the starch source (Perry & Donald, 2000; Tan, Wee, Sopade & Halley, 2004; Ternstrom, Sjostrand, Aly & Jernqvist, 1996). It has been demonstrated that potato starch has a higher gelatinization temperature than waxy maize starch (Figure 2-14). It is proposed that as the solvent first enters the starch granule in order to initiate lammellar assembly, its structure and level of permeability to the solvents are the parameters determining the required energy to initiate gelatinization. The amount of energy or molecular mobility which a certain type of plasticizer can give to starch is another factor. Figure 2-14 compares the effect of glycerol and ethylene glycerol on potato starch gelatinization. It is shown that polyols cannot introduce the same degree of freedom that water can give to polysaccharides (Kilburn, Claude, Schweizer, Alam & Ubbink, 2005), therefore even if the ingression has reached higher levels (e.g. by extended time solution conditioning), the amount of energy needed for amorphous parts to reach the max level of mobility is increased in presence of plasticizers (Perry & Donald, 2002).

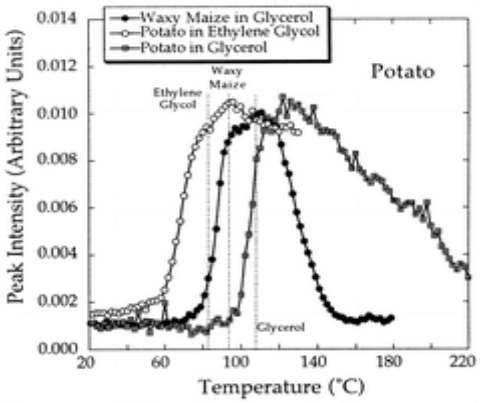

Figure 2-14 Variation of SAXS peak intensity upon heating (2 °C/min) a range of starch−solvent mixtures (1:3 starch−solvent). Waxy maize in glycerol and potato in glycerol and ethylene glyceol (Perry & Donald, 2000).

However, water activity can be retarded in the presence of polyols due to their high affinity with water such that given a certain plasticizer/water ratio, the plasticizers compete with starch in bonding with water molecules (Godbillot, Dole, Joly, Roge & Mathlouthi, 2006; Mali, Sakanaka, Yamashita & Grossmann, 2005). This increases the gelatinization temperature (Figure 2-15). It is also shown that the ingress rate of plasticizers in polysaccharides is greatly dependent on the molecular weight of plasticizers (Smits, Kruiskamp, van Soest & Vliegenthart, 2003) and the water concentration in water/polyol mixtures (Ternstrom, Sjostrand, Aly & Jernqvist, 1996). Thus, the gelatinization temperature, or in other words the thermal energy required to surpass mobility limits, is determined by a compromise between the above-mentioned parameters.

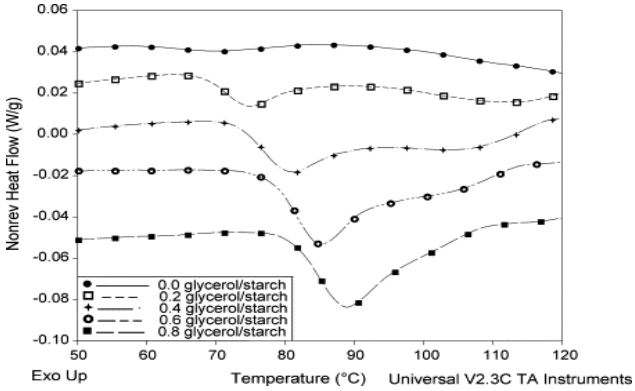

Figure 2-15 DSC gelatinization thermograms for maize starch at 0.4g water/g dry starch with varying glycerol content (Tan, Wee, Sopade & Halley, 2004).

Different plasticizers with various characteristics have been studied in the literature so far. Each shows different gelatinization temperatures and/or enthalpies. Figure 2-16, for example, compares different plasticizers used in the literature using glycerol as the reference material (Kaseem, Hamad & Deri, 2012).

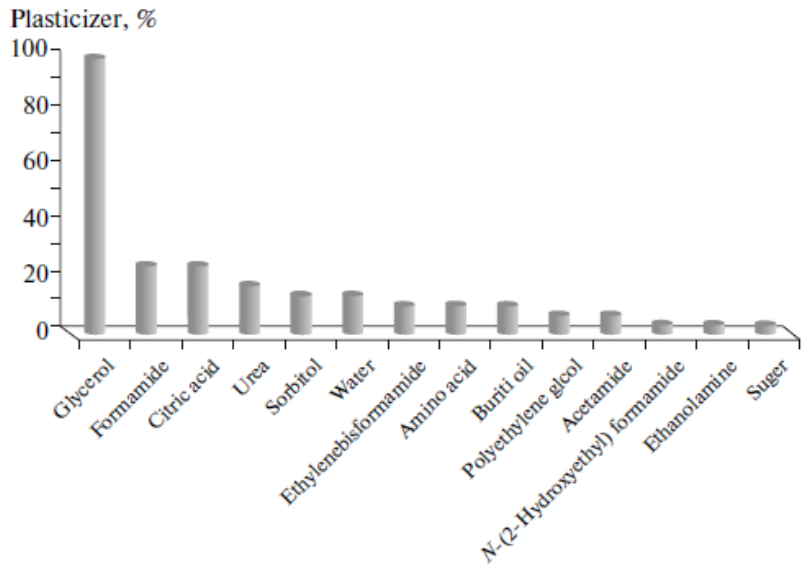

Figure 2-16 Comparison of plasticizers based on glycerol usage. (Kaseem, Hamad & Deri, 2012)

Although water is the most efficient plasticizer, due to process and application restrictions such as the high process temperatures of polymers (above 100˚C), surface evaporation during shelf life or service time, it cannot be used as the only plasticizer in the TPS structure. Instead, glycerol is the most commonly used plasticizer, due to its low cost, availability and efficacy in gelatinization. It does, however, have its own limitations, such as low temperature stability or surface migration, as well as its hygroscopic nature. The ideal plasticizer would be able to gelatinize starch in the required time frame, requires less water for gelatinization, be thermally stable, have low moisture uptake, and result in a homogeneous TPS structure. Hence, there is a need in the literature/industry to introduce more efficacy, less hygroscopy and higher temperature stability to thermoplastic starch formulations.

2.2.2.2 Thermoplastic Starch Properties

Thermoplastic starch is known as a partially miscible mixture of gelatinized starch and plasticizer(s). There are several methods of producing thermoplastic starch: namely, the static method, in which only a heat ramp is applied to starch and starch is gelatinized; and the dynamic

method in which mechanical shear is involved in the process. But irrespective of the applied process, the final thermoplastic starch shows some unique properties.

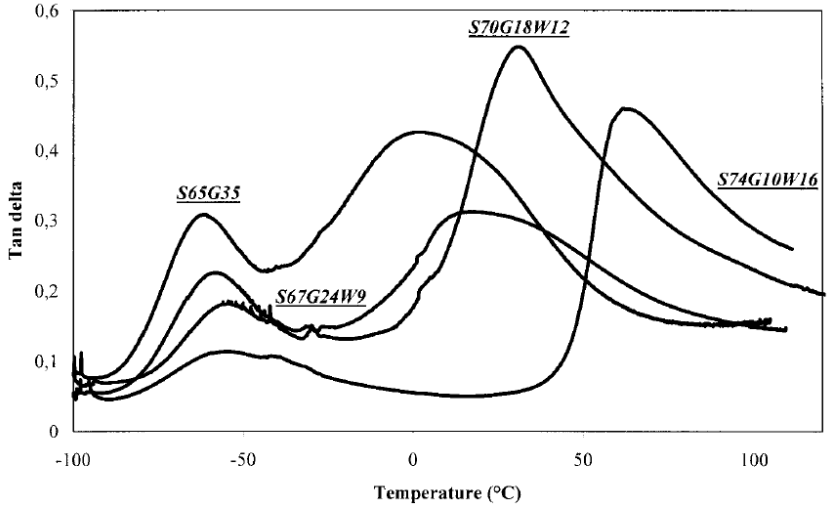

Figure 2-17 Tan δ curves for TPS formulations (DMTA): the coding shows the Starch/Glycerol /Water weight percentages in initial TPS.(Averous, Moro, Dole & Fringant, 2000)

Granular starch demonstrates only one transition peak (T_β), depending on the humidity level at high temperatures of around 100˚C (Bizot, LeBail, Leroux, Davy, Roger & Buleon, 1997). Thermomechanical analysis clearly demonstrates that TPS is a two-phase material (Figure 2-17), though the two transitions reveal some heterogeneity in its structure. High temperature transition is associated with the glass transition of the starch-rich phase (T_α (DMTA), T_g (DSC)), which depending on the starch source, plasticizer type and amount and gelatinization process could be around -20 to 120˚C (Myllarinen, Buleon, Lahtinen & Forssell, 2002). On the other hand, there is a secondary transition (T_β (DMTA) or T_{sec} (DSC)) at low temperatures, which is attributed to the glass transition of the plasticizer-rich phase (Curvelo, de Carvalho & Agnelli, 2001). This temperature is directly related to plasticizer properties as well as starch/plasticizer interaction.

Rheological properties of TPS are also subjected to change through various material and processing parameters (Li & Favis, 2010; Redl, Morel, Bonicel, Guilbert & Vergnes, 1999; Rodriguez-Gonzalez, Ramsay & Favis, 2004; Willett, Jasberg & Swanson, 1995). But overall, TPS generally demonstrates a power law behaviour in the frequency ranges of 0.1 to 1000 s^{-1} (e.g. Figure 2-18). TPS, at high plasticizer contents, demonstrates gel-like behaviour by larger numbers of G' (storage modulus) than G" (loss modulus) over the whole frequency range.

Various parameters affect the rheological properties of TPS, such as higher temperatures or moisture content that decreases viscosity and increases the power law index. Rheology is also an efficient method to determine the heat stability of TPS in longer time processes. It is shown that in case of plasticizers such as glycerol or water, TPS demonstrates very poor heat stability over time, which is mainly attributed to plasticizer evaporation (Della Valle, Buleon, Carreau, Lavoie & Vergnes, 1998).

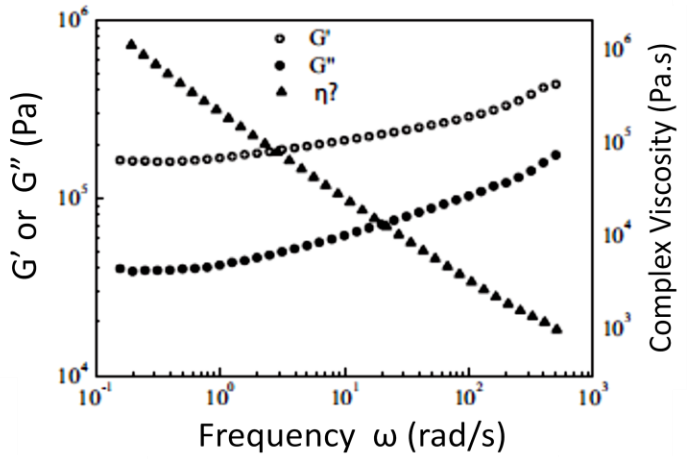

Figure 2-18 Rheological properties of TPS (36 wt% glycerol) at 110˚C. (Li & Favis, 2010)

The crystallinity of starch is completely disrupted in thermoplastic starch, but there are some parameters which make recrystallization possible in the TPS structure (Carvalho, 2008), such as a high mobility of starch molecules, plasticizer migration, or evaporation over time. Amorphous starch shows very ductile behaviour in tensile tests due to the high molecular weight of amylopectine and the ease of slipping on each other. The recrystallisation of starch molecules, which is called “retrogradation,” can deteriorate the mechanical properties of TPS and result in a brittle material (Van Soest, De Wit & Vliegenthart, 1996).

Another parameter which is important in determining the properties of TPS is the extent of molecular weight degradation during processing. The applied mechanical energy, processing temperature and plasticizer type and content seem to be the most important factors in determining the degradation of starch chains (Carvalho, 2008; Willett, Millard & Jasberg, 1997). It is shown that the amylose chains are not susceptible to chain scission under shear conditions due to their linear structure; howerver, high molecular weight, high branching density and low degree of freedom results in a significant drop in the molecular weight of amylopectine molecules

(Bindzus, Livings, Gloria-Hernandez, Fayard, van Lengerich & Meuser, 2002; Liu, Halley & Gilbert, 2010) (Figure 2-19).

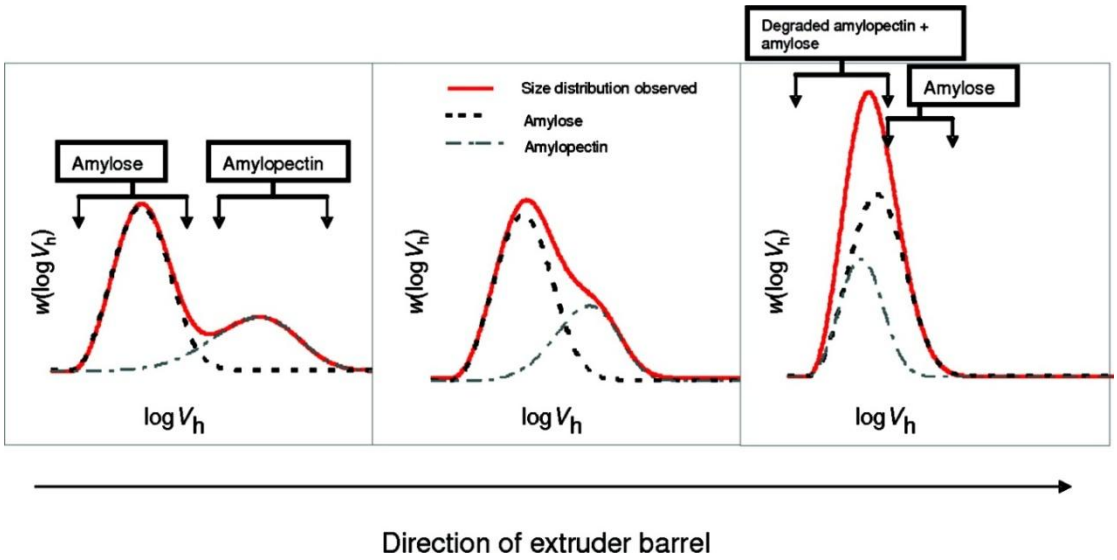

Figure 2-19 Qualitative presentation of the evolution of molecular weight of the amylose and amylopectin components and the superposition of the two components throughout the extrusion barrel by size exclusion chromatography, V_h:hydrodynamic volume, glycerol content: 31% (Liu, Halley & Gilbert, 2010).

Therefore, all thermal, rheological and mechanical properties of TPS are influenced by the type of plasticizer used, the level of its interaction with starch, as well as the processing parameters and starch source. The best properties are achieved through the optimal adjustment of above-mentioned parameters.

2.3 Melt Blending of Polymers

2.3.1 Overview

By emerging advanced technologies, the required properties of polymer materials have been more specific and targeted. Due to the high cost and difficulty of synthesizing new polymers, blending of polymers to achieve optimal properties has been the most appropriate road to take. By blending different polymers, a combination of different mechanical, electrical and physical properties can be introduced and tailored in the final products. Some other advantages of polymer blends are optimizing the final cost, as well as increasing the biodegration rate or biodegradable

portion of the polymeric products such as PHAs/TPS or PE/TPS. But due to the high molecular weight of polymers, there is frequently a lack of sufficient interaction among different macromolecules, hence, it seems ambitious to achieve the aforementioned tailored properties. Polymer blends are thus divided into two main categories, namely “miscible” and “immiscible,” which are further explained in the following sections.

If polymer A and B are able to be combined on a submolecular scale (segmental) they are classified as miscible polymers. The miscibility of polymer pairs can be translated into thermodynamic language. If a polymer pair fulfills the following condition, they can be called a “miscible pair”:

$$\Delta G_m = \Delta H_m - T\Delta S_m < 0$$

where ΔG_m is Gibb’s free energy of mixing, ΔH_m the enthalpy of mixing, and ΔS_m the entropy of mixing at temperature T. The value of $T\Delta S_m$ is essentially positive, since in mixing there is always an increase in entropy; however, based on the lattice theory of Flory-Huggins (Sperling, 2006), this increase in macromolecules is not as high as low molecular weight materials. So the value of ΔG_m depends mainly on the magnitude of enthalpy of mixing. The enthalpy of mixing is normally positive unless the two materials have attractive forces towards each other, for example through hydrogen-bonding or if they are an acid and a base. Thus, according to Hildebrand and Scott, the formula for regular solutions is:

$$\Delta H_M = V_M \left[\left(\frac{\Delta E_1}{V_1} \right)^{1/2} - \left(\frac{\Delta E_2}{V_2} \right)^{1/2} \right]^2 \nu_1 \nu_2$$

where V_M is the total volume of the mixture, ΔE the energy of vaporization to a gas at zero pressure, V_i the molar volume of the components, and ν_i the volume fraction of the components. The term $\Delta E/V$ (the energy of vaporization per unit volume) represents cohesive energy density, and is a direct measure of van der Waals force of a substance. If the intermolecular forces of two substances are alike, they can be effectively miscible. But if one has a sufficiently different attraction, the stronger attached molecules will adhere to each other, resulting in immiscibility. The square root of cohesive energy density is called the “solubility parameter”:

$$\delta = \left(\frac{\Delta E}{V} \right)^{1/2}$$

So the enthalpy of mixing is directly related to $(\delta_1 - \delta_2)^2$.

For a stable system of two miscible polymers at composition φ, temperature T and pressure p , the following equation should be satisfied as well:

$$\left(\frac{\partial^2 \Delta G_m}{\partial\, \phi^2}\right)_{p,T} > 0$$

Less than ~10% of all the polymer pairs experimentally studied were shown to be miscible, such as the blend of Polystyrene/PolyPropyleneOxide.

2.3.2 Immiscible Polymer Blends

The majority of polymer blends are immiscible. The molecular weight, structure and architecture of each polymer phase, as well as processing conditions, all influence the morphology of the blend. These parameters are normally categorized into kinetics and thermodynamic parameters. Kinetics include processing parameters such as temperature, mixing conditions, etc., as well as rheological properties such as the viscosity and elasticity of the materials. Thermodynamics basically considers the interfacial tension of the polymers (Reignier & Favis, 2000). Before introducing the effective parameters and their role in determining the morphology of polymer blends, it is essential to explain morphology development in the polymer blending process.

2.3.2.1 Morphology Development in Droplet-matrix Systems

Droplet deformation and break-up of a newtonian drop in a newtonian matrix was first investigated by Taylor (Taylor, 1932, 1934). In a steady shear flow, Taylor showed that droplet deformation is controlled by the viscosity ratio *p* (droplet viscosity/matrix viscosity), shear field and capillary number. Capillary number, *Ca*, is defined as the ratio of viscous to interfacial forces:

$$Ca = \frac{\eta_m \dot{\gamma}}{\sigma / R}$$

where η_m is the matrix viscosity, $\dot{\gamma}$ the shear rate, R the droplet radius, and σ the interfacial tension. A small capillary number represents high interfacial forces compared to viscous forces, which results in the deformation of the droplet into a steady-state ellipsoidal shape, with the major axis oriented in angle Θ. In case of increasing the viscous forces, the capillary number will

reach a critical value, Ca_{crit}, at which the droplet will deform to a sigmoidal shape with a thinning and stretching central part. Then the droplet breaks up into small daughter droplets. Taylor derived the following expression for Ca_{crit} in a simple shear flow:

$$Ca_{crit} = {}^{1}/_{2}\,((16\,p + 16)/(19\,p + 16))$$

Other researchers followed Taylor's work and proposed different models for break-up of droplets in shear flows based on viscosity ratios, e.g. Rumscheidt and Mason (Rumscheidt & Mason, 1961) who mention that in low viscosity ratios (p<0.1), the droplet experiences higher viscous forces and does not break up but rather elongates and very small fragments of the droplet phase release its sharp tips (Figure 2-20). If 0.1<p<2 the droplets break-up will be as explained with Ca_{crit} (daughter droplets), and in case of high viscosity ratios (p>4) the droplets will deform to ellipsoids but will not break up (Figure 2-20). The other values reported in the literature (Karam & Bellinger, 1968; Reignier & Favis, 2000) are almost similar to the above-mentioned values.

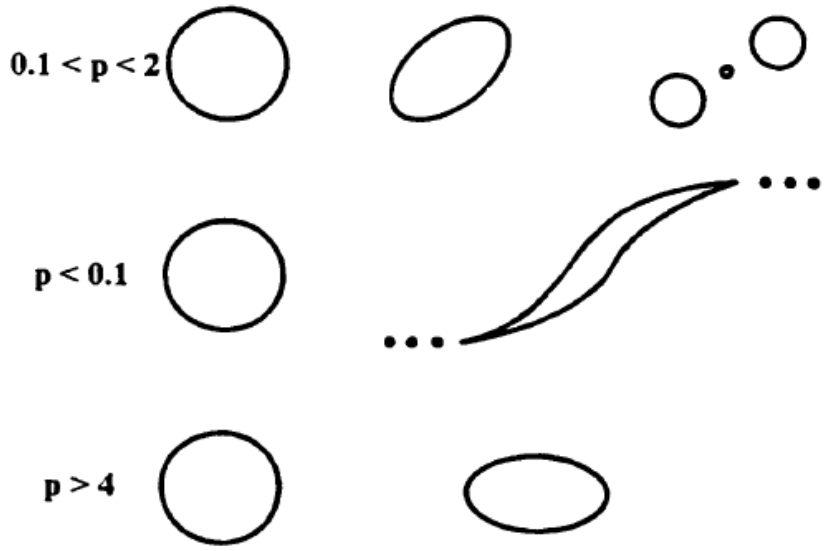

Figure 2-20 Models of droplet deformation and break-up based on the viscosity ratio (p: droplet viscosity/matrix viscosity) (Rumscheidt & Mason, 1961).

Taylor's theory was further developed into time dependant systems and the systems with viscoelastic properties (Cox, 1969; Flumerfelt, 1980). But one of the most outstanding extensions of this work is done by Grace (Grace, 1982), who studied the effect of the viscosity ratio on droplet break-up for simple shear and elongational flow fields. It was demonstrated that in simple shear flows, the droplet break-up is only possible at p< 4. But in an elongational flow field, the

viscosity ratio does not limit the flow field ability in breaking up the droplets (Figure 2-21). The mechanism of droplet break-up and dispersion through capillary instability is reported elsewhere (Janssen & Meijer, 1993).

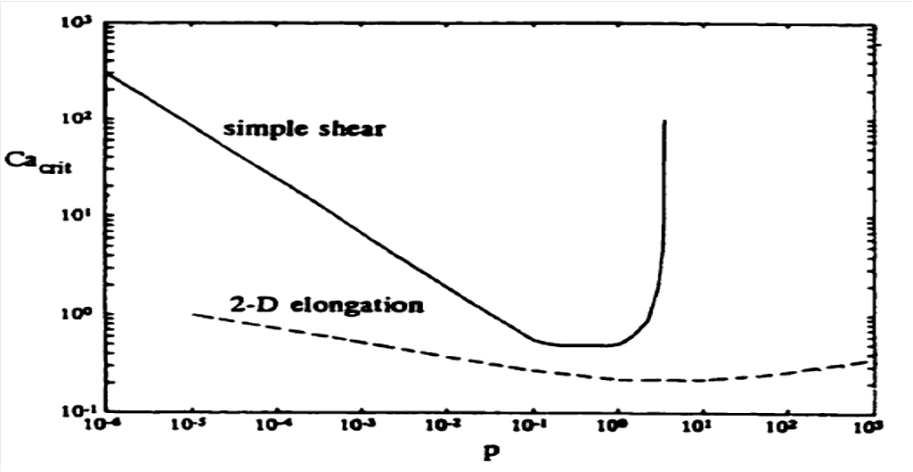

Figure 2-21 The diagram of viscosity ratio vs. critical capillary number in shear and elongational flow fields (Grace, 1982).

Following these works, the dependence of polymer blend morphology on the viscosity ratio has been studied as well (Favis & Chalifoux, 1987; Serpe, Jarrin & Dawans, 1990; Wu, 1987a). The results show strong a dependence of droplet diameter to the viscosity ratio in shear fields. Using rubber-polyamide blends, Wu (Wu, 1987a) showed that as the viscosity ratio drifts away from 1(higher or lower), the particle size becomes larger. Favis et al. (Favis & Chalifoux, 1987) further studied the effect of viscosity ratio on the morphology of polypropylene/polycarbonate blends. They reported that by increasing the torque ratio (≈ viscosity ratio) between 2 and 13, droplet diameter increased up to three to four times. Various authors have reported levels of increase or decrease, but most of the reports qualitatively confirm the above-mentioned trend (Everaert, Aerts & Groeninckx, 1999; Wildes, Keskkula & Paul, 1999; Yang, Lee & Oh, 1999)(Figure 2-22).

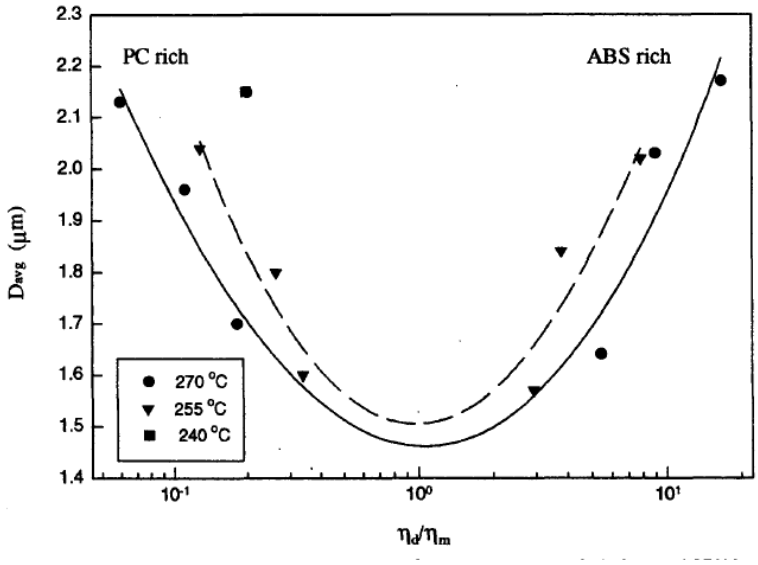

Figure 2-22 The effect of torque ratio (viscosity ratio) on the particle size in blends of PC/ABS in different compositions (Yang, Lee & Oh, 1999)

In a follow-up study (Favis & Therrien, 1991), Favis and Therrien showed that, similar to the Newtonian systems, droplet break-up is less sensitive to viscosity ratio in elongational flow fields (using a twin screw extruder) than in shear flow fields (using an internal mixer).

In addition to the viscosity ratio, several other parameters can influence the morphology of polymer blends, such as composition, elasticity, shear stress, interfacial tension or processing method. The following two sections study two of these parameters, namely interfacial modification and processing methods.

2.3.2.2 Interfacial Modification of Polymer Blends

As mentioned above, there are two categories of parameters that influence the morphology of polymer blends: kinetics and thermodynamics. It is generally believed that polymer blends can achieve stable morphology only if the system is in thermodynamic equilibrium, i.e. minimal free energy of the system (Favis, 2000b; Wu, 1978). Despite this, it is unfeasible to directly measure the interfacial tension of all polymer pairs due to various intrinsic properties or empirical difficulties, such as temperature sensitivity (e.g. PHB, PVA), or if one of the phases contains additives such as plasticizers (e.g. TPS). Statistical mechanical theories have helped to calculate the interfacial data based on the surface characteristics of each component. The surface tension of a material is the amount of energy required to produce a unit area of a given material. In addition

to the chemical structure and functionalities of the polymer chains, several other factors influence this property, such as temperature, molecular weight, chain structure (block or random copolymer) and additives (Wu, 1978).

There are several methods to theoretically calculate the interfacial tension based on the surface tension of each component, namely Antonoff's rule (Antonoff, 1942), the theory of Good and Girifalco (Girifalco & Good, 1957; Good & Girifalco, 1960; Good, Girifalco & Kraus, 1958), the theory of fractional polarity (Wu, 1971; Wu, 1978), and the harmonic mean equation. Due to the assumptions made for Antonoff's rule, i.e. the zero contact angle between polymer pairs, it cannot be used for polymers. It is important to note that the required energy to separate the interface of two materials is called the work of adhesion, which is calculated as:

$$W_a = \gamma_1 + \gamma_2 - \gamma_{12}$$

Where $\gamma_1, \gamma_2, \gamma_{12}$ are the surface tension of component 1, the surface tension of component 2, and the interfacial tension between component 1 and 2, respectively. Different theories have tried to express W_a as a function of surface tensions. For example, Good and Girifalco developed this equation:

$$\gamma_{12} = \gamma_1 + \gamma_2 - 2\emptyset(\gamma_1\gamma_2)^{1/2}$$

Where $\emptyset$ is the interaction parameter related to the molar volume, polarizability, ionization potential and dipole moment of the polymers. But because of the lack of data on these parameters concerning polymers and their accuracy, this theory is not often used.

The most commonly used method in calculating the interfacial tension of polymer pairs is the harmonic mean equation. In this theory, surface tension is divided into two components, namely polar and dispersive

$$\gamma_i = \gamma_i^d + \gamma_i^p$$

γ_i^d, γ_i^p dispersive and polar components, respectively. And based on this the harmonic mean equation is expressed as:

$$\gamma_{12} = \gamma_1 + \gamma_2 - \frac{4\gamma_1^d\gamma_2^d}{\gamma_1^d + \gamma_2^d} - \frac{4\gamma_1^p\gamma_2^p}{\gamma_1^p + \gamma_2^p}$$

In cases of low surface energies, this equation has been shown to be valid (Ravati, 2010). But in cases of incorporating a higher surface energy material in a low surface energy, the geometric mean equation has been shown to be more reliable (Wu, 1982):

$$\gamma_{12} = \gamma_1 + \gamma_2 - 2\left(\gamma_1^d \gamma_2^d\right)^{1/2} - 2\left(\gamma_1^p \gamma_2^p\right)^{1/2}$$

Based on the calculated interfacial tension data, it is possible to predict the morphology of multiphase polymers (Virgilio & Favis, 2011). As with surface tension, interfacial tension is also affected by several factors, such as temperature, polarity and the molecular weight of the components.

One of the methods used to decrease interfacial tension is the use of interfacial modifiers. These may include plasticizers, block copolymers, graft copolymers, etc. They can be added to the blends as a pre-made material, or generated *in situ* during a process called reactive compatbilization. In both cases, the goal is to decrease the interfacial tension between the phases by improving the adhesion between the two phases, impeding coalescence, and consequently reducing and homogenizing the phase sizes (figure below 2-23). In fact, efficient compatibilizer will pale into insignificance the dependency of the droplet size on the disperse phase composition, up to the co-continuity region (Willis, Caldas & Favis, 1991). Due to the high production cost of such materials, it is necessary to use the minimum amount, so optimizing the processing conditions as well as choosing the right structure is of great importance.

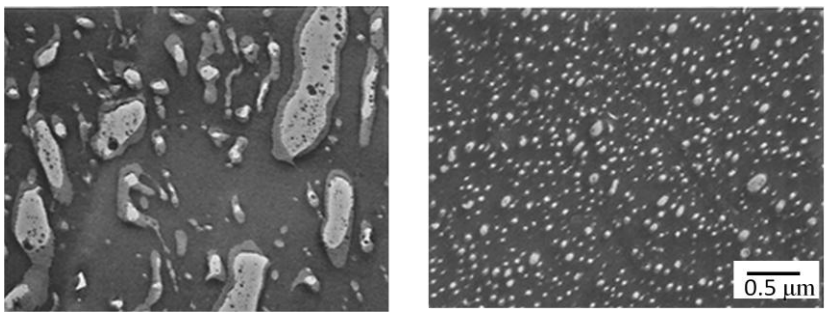

Figure 2-23 Effect of block copolymer on the morphology of PS/PMMA 70/30 wt% with 5wt% block copolymer (Macosko, Guegan, Khandpur, Nakayama, Marechal & Inoue, 1996).

Several factors can influence the efficacy of the compatibilizers: the molecular weight and structure of the compatibilizer, the molecular weight of the main polymers, the visoelastic

properties of materials, as well as the processing method (Macosko, Guegan, Khandpur, Nakayama, Marechal & Inoue, 1996; Sundararaj & Macosko, 1995). Normally, their chemical structure consists of two parts, one having a high interaction with phase 1 and the other a high interaction with phase 2. This can be either a simple block copolymer of the two homopolymers or a functional group consisting of side chains, each having an affinity with either of the phases. In a blend of polymer A and B, the graft copolymers of A-g-B are added to the blend. By migrating to the interface, the grafts make hydrogen or covalent bonds with phase B, while the backbone is already the same as phase A (Figure 2-24a).

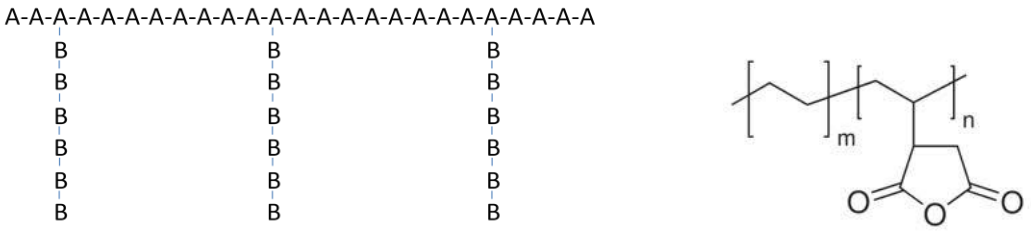

(a) (b)

Figure 2-24 Schematic representation of (a) graft copolymer; (b) Polyethylene-g-Maleic Anhydride.

Examples of graft copolymers as interfacial modifiers are numerous in the literature (Aravind, Albert, Ranganathaiah, Kurian & Thomas, 2004; Cho, Park & Kim, 1997; Elemans, Janssen & Meijer, 1990; Kum et al., 2007; Sailaja, Reddy & Chanda, 2001; Torres, Robin & Boutevin, 2001; Zhang, Feng, Gu, Hoppe & Hu, 2007). On the other hand, another class of graft copolymers is formed by the introduction of functional groups to the backbone of polymers such as PE or PP. One of the classic examples of this is maleic anhydride (MA) grafted copolymers, e.g. PE-g-MA (Figure 2-24b). Due to the lack of functional groups in polyethylene structure, the introduction of MA on the backbone can form *in situ* covalent bonds or hydrogen bonding with polar phases in TPS, polyamides or PET (Jiang, Filippi & Magagnini, 2003; Koulouri, Georgaki & Kallitsis, 1997; Martinez, Benavides & Guerrer, 2008; Taguet, Huneault & Favis, 2009). The expected interfacial reaction in blends of PE and TPS with addition of PE-g-MA is discussed further in section 2.3.5.

Interfacial modification is a dominant factor on the morphology, in that compatibilization may neutralize some other factors, such as viscosity ratio or composition (Lee, Ryu & Kim, 1997;

Wildes, Keskkula & Paul, 1999). For instance, it is observed in the figure below that the viscosity ratio may not have an effect on the droplet size of PA6 in the matrix of ABS.

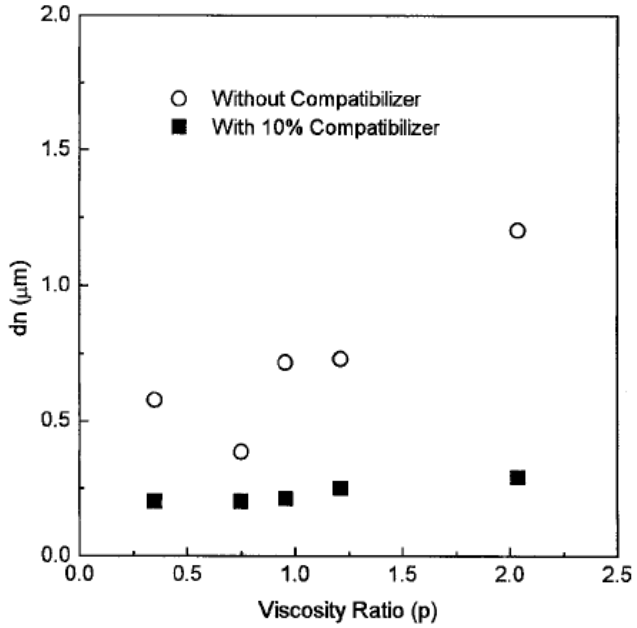

Figure 2-25 Droplet diameter vs. viscosity ratio in PA6/ABS (20/80 wt%) with and without compatibilizer (Lee, Ryu & Kim, 1997).

2.3.2.3 Processing methods

There are several types of polymer processing equipment on the market, e.g. extruders (single or twin), injection molders or internal mixers. Differences in the type of the flow field, shear rate or shear stress (torque), and processing residence times may result in different morphologies (Reignier & Favis, 2000; Utracki & Shi, 2002).

Internal mixers are very useful tools for studying the blends of various rubbers or thermoplastics because the time and temperature of mixing can be effectively controlled, the torque can be monitored, and it is possible to blend in small quantities. So in addition to the rubber industry (which mostly uses internal mixers for blending), this apparatus is used for experiments in a lot of scientific papers reviewed here.

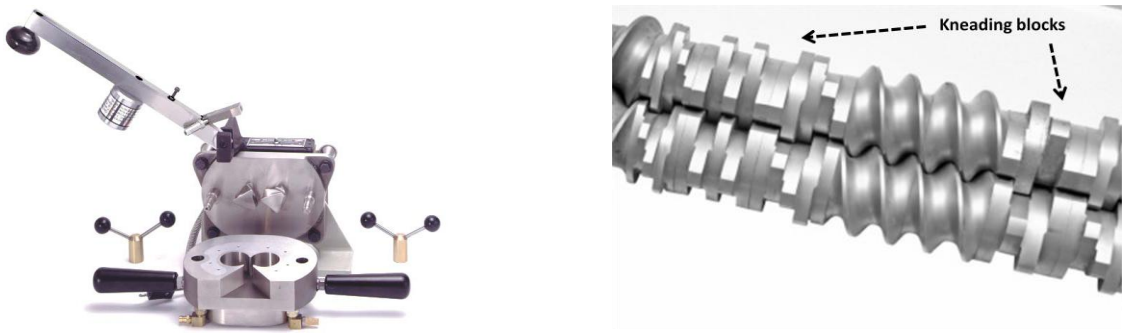

Figure 2-26 Internal mixer (Brabender Plasticorder) in the left and Twin screw extruder with several kneading blocks in the right.

It consists of a chamber in which two counterrotating rotors rotate at different rpm (Figure 2-26). Various studies have been conducted on the different controllable parameters in the internal mixer, and Favis (Favis, 1990) studied different viscosity ratios of PC/PP blends using the device. It was found that the main deformation and dispersion of droplets takes place during the first two minutes of mixing; further mixing (up to 20 minutes) does not have a significant effect on morphology, nor did changes in rotor speed. But, as expected from a mixer generating essentially shear flow fields, changes in viscosity ratio showed marked effects on morphology.

On the other hand, twin screw extruders (TSE) are among the most efficient industrial scale mixers used to blend thermoplastics. They are composed of two screws, whether intermeshing or not, which may co- or counter-rotate. Both screws have one (or more) kneading sections. The design of the screws can be fitted to perform special applications (such as high shear) by using more kneading blocks (Figure 2-26). They have several advantages over single screw extruders, such as lower residence times, narrower residence time distribution, self-wiping, scale-up ability, and large output (up to more than 60 ton/h) (Utracki & Shi, 2002).

It was shown that in LDPE/PS blends, the resulting droplet size in a twin screw extruder is smaller than with an internal mixer (Plochocki, Dagli, Starita & Curry, 1986). The enhanced morphology of polymer blends in twin screw extruders compared to the internal mixer was further corroborated by Favis et al. (Favis & Therrien, 1991) for PP/PC blends. They also reported significantly improved particle size distribution for these blends using twin screw extruders. There have been some models proposed for the morphology evolution in TSE (Huneault, Shi & Utracki, 1995; Shi & Utracki, 1992), which, taking into account the role of

coalescence in the screw line, seem to show promise and correspond well with the experimental data.

Lee and Han (Lee & Han, 1999, 2000) have investigated the evolution of the morphology using both an internal mixer and twin screw extruder. They showed that although the different shear field and intensity or other processing parameters might result in different domain sizes, qualitatively comparing the two processes, the screw axis in the extruder corresponds to the mixing time in the internal mixer.

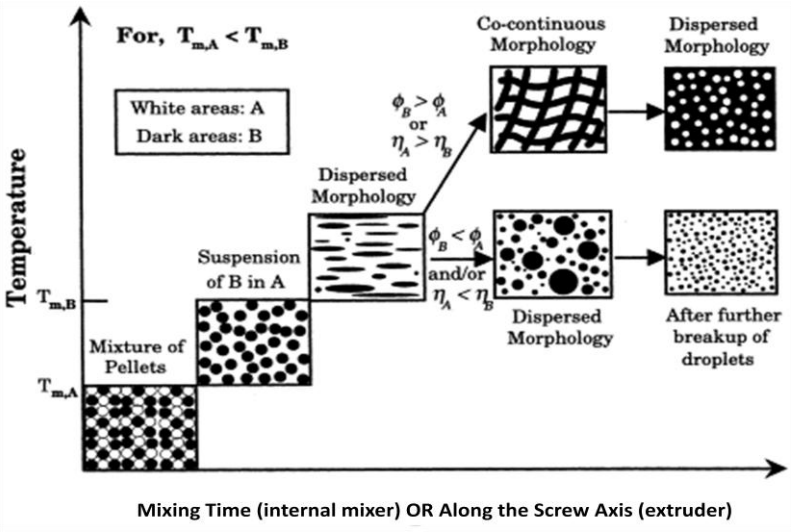

Figure 2-27 Qualitative evolution of the morphology during mixing of two immiscible blends with mixing time (internal mixer); or along the screw axis (twin screw extruder) (Lee & Han, 1999, 2000).

2.3.3 TPS blends with Bioplastics

2.3.3.1 Overview

Thermoplastic Starch (TPS) by itself is unsuitable for use in the plastics industry because of various disadvantages, including:

a. The hydrophilic nature of starch and its poor moisture resistance,

b. The deterioration of mechanical properties upon exposure to different environmental conditions like humidity, and

c. The soft and weak nature of starch in the presence of plasticizers.

Thus, TPS needs to be blended with other polymers to eliminate these disadvantages.

TPS is an economically and environmentally favourable material that not only enhances biodegradability, but also reduces the final cost. Blending TPS with other biodegradable polymers such as biodegradable polyesters may be an excellent way to provide a renewable, fully biodegradable and cost-effective material. We will first examine the work that has already been done on TPS blending with two types of polymers: biodegradable polyesters and biobased polyolefines.

2.3.3.2 TPS/Polyethylene

TPS/Polyolefines systems have been investigated by different authors (Bikiaris & Panayiotou, 1998; Bikiaris et al., 1998; Girija & Sailaja, 2006; Rodriguez-Gonzalez, Ramsay & Favis, 2003; Wang, Qu, Fan, Hu & Shen, 2002). Polyethylene is one of the most commonly used polyolefines and there is a lot of potential for it to be blended with TPS. One of the important markets of PE is the food packaging industry, however, its most significant drawback is the non-biodegradability of packaging films such as shopping bags. Therefore, it would be very interesting if TPS/PE with acceptable mechanical properties could be produced with more biodegradable TPS content inside the blend.

One of the pioneering works on TPS/PE was done by St. Pierre et al. (StPierre, Favis, Ramsay, Ramsay & Verhoogt, 1997). LDPE and LLDPE were blended with TPS in various compositions, and it was demonstrated that the elongation at break remained at values of 22% and 39% TPS in LDPE and LLDPE, respectively. In another work (Bikiaris & Panayiotou, 1998), LDPE-g-Maleic Anhydride was used as the compatibilizer in different MA contents (0.4 and 0.8 mol%) and compared with an uncompatibilized system. It was shown that the compatibilizer could successfully suppress the coalescence and maintain the droplet size independent of TPS content. But the elongation at breaks showed only marginal improvements in compatibilized systems. On the other hand, the compatibilizer showed a very limited effect on the biodegradability of the blends. Jang et al. (Jang, Huh, Jang & Bae, 2001) used Glycidyl Methacrylate (GMA) to compatibilize HDPE/TPS. This compatibilizer introduced a level of improvement to the elongation at break of the blends but still it remained low (maximum ~100% for PE/TPS 70/30 wt%), though morphology was improved by increasing the compatibilizer content. Sailaja and Chanda (Sailaja & Chanda, 2001) reported better elongation at break and tensile properties by

just adding 5% HDPE-g-Maleic Anhydride(MA) to HDPE/TPS blends with various TPS content. They also blended LDPE/TPS in presence of PE-g-MA as the compatibilizer, in a another article (Sailaja, Reddy & Chanda, 2001), though unlike Jang et al., they showed a significant improvement in elongation at break. Another compatibilizer was polyethylene-co-vinyl alcohol, which resulted in a higher impact strength of LDPE/TPS (Sailaja & Chanda, 2002) even at a high TPS content of 50 wt%. Without using a compatibilizer and by optimizing the processing parameters, Rodriguez-Gonzalez et al. (Rodriguez-Gonzalez, Ramsay & Favis, 2003, 2004; Rodriguez-Gonzalez, Virgilio, Ramsay & Favis, 2003) were able to get acceptable results. They also used a one- step process (Favis, Rodriguez & Ramsay, 2003; Tchomakov, Favis, Huneault, Champagne & Tofan, 2005) to blend LDPE and TPS, and highly elongated morphologies were produced. The elongated morphology resulted in improved elongation at break compared to spherical morphologies. Obviously by increasing the TPS content, the tensile properties of the blend would diminish, though they could still maintain 96% of the elongation at break with a 71/29 PE/TPS blend. The exceptional mechanical properties were attributed to the effective control of the morphology. Similar effects were reported by Wang et al. (Wang, Yu & Yu, 2004). Several authors have demonstrated the esterification reaction of maleic anhydride with hydroxyl groups (Bayram, Yilmazer, Xanthos & Patel, 2002; Kalambur & Rizvi, 2006; Wang, Jiugao & Jinglin, 2005), and it is believed that improvements to the blend properties occured through the esterification reactions, as well as the hydrogen bonding of MA with several alcohol groups of starch and glycerol (Figure 2-28).

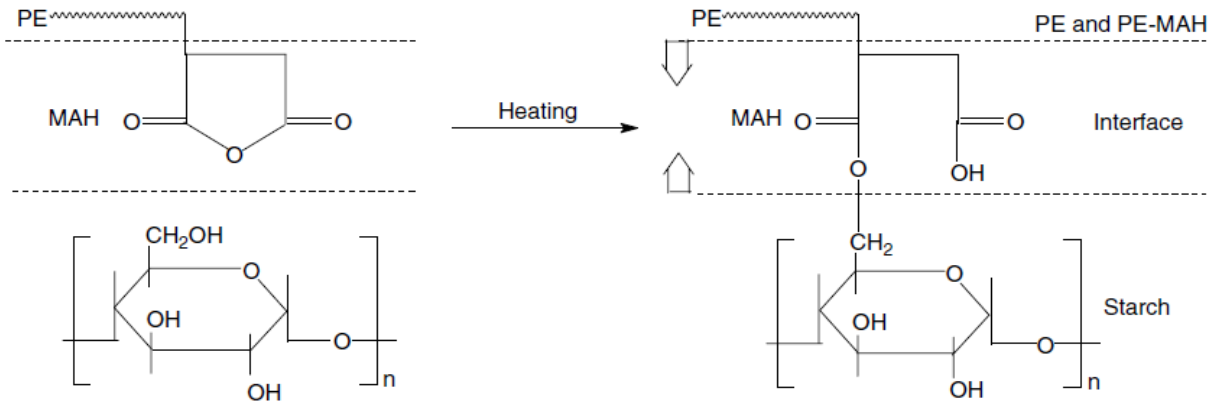

Figure 2-28 The reaction between starch and PE-g-Maleic Anhydride (Wang, Yu & Yu, 2005a).

Girija (Girija & Sailaja, 2006) used PE-g-dibutyl maleate as an alternative compatibilizer to maleic anhydride. Similarly, it could act as a compatibilizer and improve the morphological-mechanical properties of LDPE/TPS blends. More recently, Taguet et al. (Taguet, Huneault & Favis, 2009) studied the comaptibilzation of HDPE/TPS with their patented TPS preparation procedure (Favis, Rodriguez & Ramsay, 2003; Tchomakov, Favis, Huneault, Champagne & Tofan, 2005). They studied the interface-morphology-mechanical properties relationship in a blend of HDPE/TPS 80/20 wt% with different amounts of PE-g-MA. The compatibilizer demonstrated the classic effect of compatibilized systems by decreasing the droplet size via increasing the PE-g-MA content, reaching a plateau in high modifier contents.

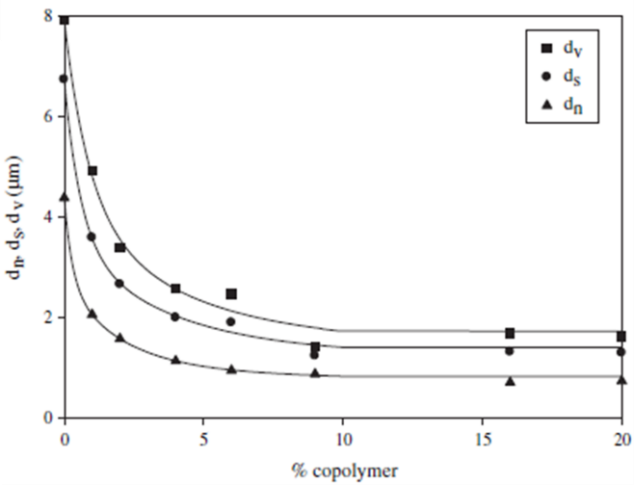

Figure 2-29 Droplet size of HDPE/TPS (80/20 wt%) vs. copolymer content; dn: number average; ds: surface average; dv: volume average droplet size (Taguet, Huneault & Favis, 2009)

In the same study, it was proposed that due to plasticizer migration to the interface, there is a nano-scale plasticizer layer at the interface, which helps decrease interfacial tension between phases in HDPE/TPS blends.

Other than compatibilizer and TPS content in all the above-mentioned blends, there are also some hidden variables missing in the review articles, such as starch source, plasticizer type and content, and TPS preparation process. Thus, further investigation is required to better understand the compatibilization mechanism.

The degradation of PE/TPS blends has been the subject of a few studies. Wang et al. (Wang, Yu & Yu, 2006) showed that LLDPE/TPS films exposed to air experience a higher level of degradation than samples in soil. Moist soil was shown to be a proper environment for

biodegradation of the samples, but the rate of air-exposed samples was higher. Senna et al. (Senna, Yossef, Hossam & El-Naggar, 2007) studied electron beam irradiated systems of LDPE/TPS and reported that foamed samples show higher degree of degradation.

A gap in the literature is the effect of TPS structure on the interface-morphology-mechanical properties of PE/TPS blends. Concerning the heterogeneous structure of TPS and the significant amount of plasticizer normally incorporated into it (above 20 wt%), this issue is expected to have an large impact on the interface and morphology of TPS blends.

2.3.3.2.1 Mechanical Properties

The mechanical properties of the blends are directly related to the state of the interface. This dependency is more pronounced for some properties such as elongation at break or fracture mechanism, since they are more dependent on the interface characteristics because the interface is extremely involved in the process. Obviously the intrinsic properties of the components are of great importance.

TPS as a two phase material has been shown to have a variety of properties based on the type of the starch source, plasticizer type, plasticizer content and water content (Rodriguez Gonzalez, 2002). On the other hand, the processing conditions are of great concern here, due to the fact that there is not one standard TPS preparation process, and similar to the various TPS morphologies obtained by different research groups (even in the same blends), mechanical properties will thus also fluctuate (Kaseem, Hamad & Deri, 2012).

The incorporation of TPS in PE generally increases the tensile modulus and strength of the blend, while the elongation at break decays as TPS content increases. Jang et al. (Jang, Huh, Jang & Bae, 2001) reported a 20% increase in tensile modulus by incorporating 30 wt% TPS in a HDPE matrix, while ductility significantly decreased, with elongation at break measurements of lower than 50% (Figure 2-30). Subsequently, they then demonstrated that by increasing compatibilizer content, both tensile strength and elongation at break show significant improvement.

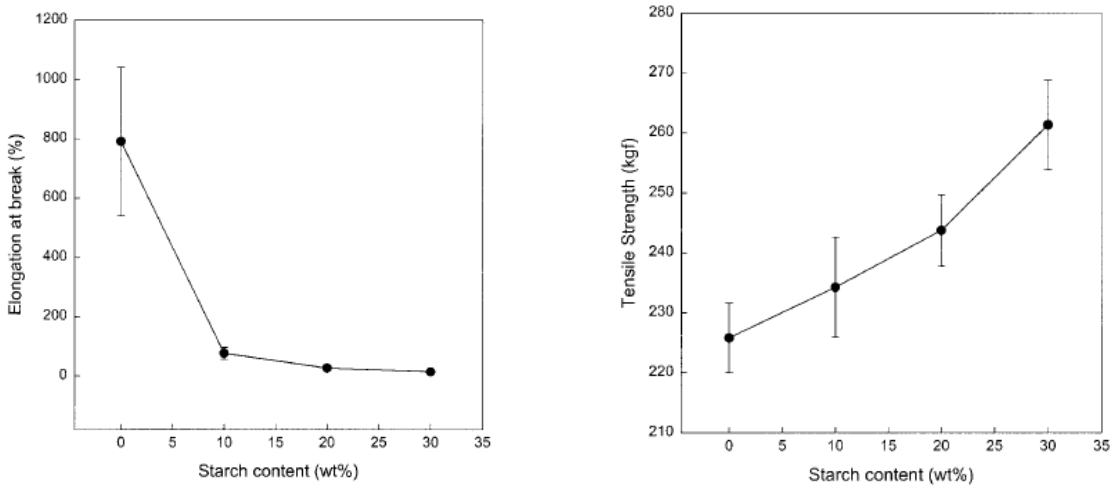

Figure 2-30 Elongation at Break and Tensile Strength of blends of HDPE/(GMA-g-PE) 90/10 wt% with TPS(40% glycerol) vs. TPS content (Jang, Huh, Jang & Bae, 2001).

Sailaja and Chanda (Sailaja & Chanda, 2001) reported similar results, and the incorporation of PE-g-MA as a compatibilizer improved the results similar to Wang et al. (Wang, Yu & Yu, 2005b). But, as mentioned above, one of the most promising factors determining the mechanical properties of TPS materials is the processing method. With an optimal process that can efficiently gelatinize starch molecules, homogenize the TPS phase and provide high enough mixing efficacy in the processing time frame, it is possible to achieve much better mechanical properties even without using a compatibilizer. Rodriguez et al. (Rodriguez-Gonzalez, Ramsay & Favis, 2003) processed TPS/PE blends in a one-step process (Favis, Rodriguez & Ramsay, 2003; Favis, Rodriguez & Ramsay, 2005) and reported that 96% of the elongation at break of PE/TPS (~70/30 wt%) could be maintained when TPS contained 36 wt% glycerol as a plasticizer (Figure 2-31).

In a follow-up study, Taguet et al. (Taguet, Huneault & Favis, 2009) added PE-g-MA to HDPE/TPS blends and observed that further addition of the compatibilizer could significantly improve their tensile properties. Taguet also reported that a certain level of plasticizer is needed to effectively plasticize wheat starch, which was determined to be ~30 wt%.

Overall, there are more than 150 articles on TPS/PE blends (based on Web of Science). Various grades of PE, different processes and numerous number of compatibilizers have been used to improve the properties of the blend. One of the issues that has not been dealt with thoroughly is

the internal structure of TPS with different plasticizers and its effect on the final properties of the blends.

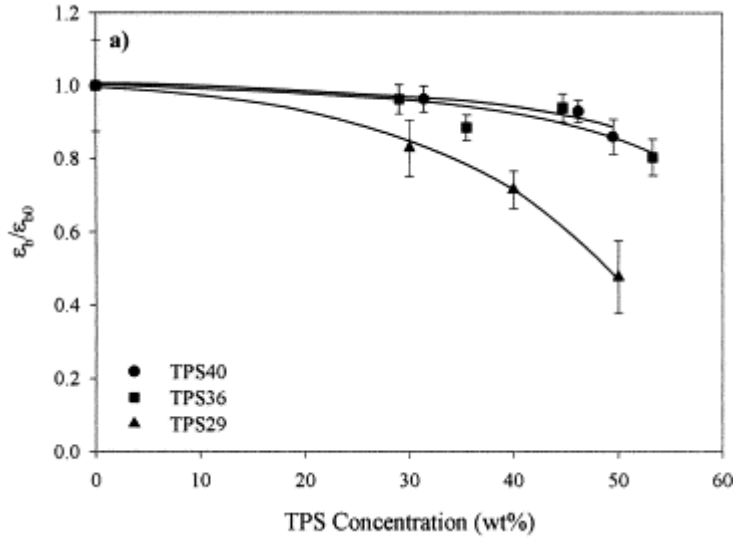

Figure 2-31 Relative elongation at break vs. TPS concentration in blends of LDPE/TPS; the term with subscript 0 refers to pure LDPE; Numbers in TPSXX denotes the glycerol content of TPS (Rodriguez-Gonzalez, Ramsay & Favis, 2003) .

2.3.3.3 TPS/Polycaprolactone

Biodegradable polyesters have shown to be interesting materials in different applications from packaging to biomedical uses. But they alternatively show acceptable properties i.e. they do not cover the whole range of mechanical properties demonstrated by other commodity polymers. PLA or PHAs exhibit high modulus and strength but are very brittle, while on the other hand PCL shows high elongation at break but has a very low modulus. So they need to be blended in order to cover a broader range of mechanical properties and develop their application range. However, they generally have high production costs, so the first step in developing their application range would be to blend it with a lower-priced bioplastic in order to justify the price.

The reported research on PCL/TPS blends appears relatively recently in the literature. Vikman et al. (Vikman, Hulleman, Van der Zee, Myllarinen & Feil, 1999) studied a homogeneous 50/50 blend of PCL/TPS with accelerated enzymatic hydrolyses in milled samples. Averous et al. (Averous, Moro, Dole & Fringant, 2000) performed a detailed investigation of various PCL/TPS

blends prepared by extrusion and injection molding. Marginal shifts in characteristic temperatures of the components demonstrated completely immiscible polymer pairs (Figure 2-32).

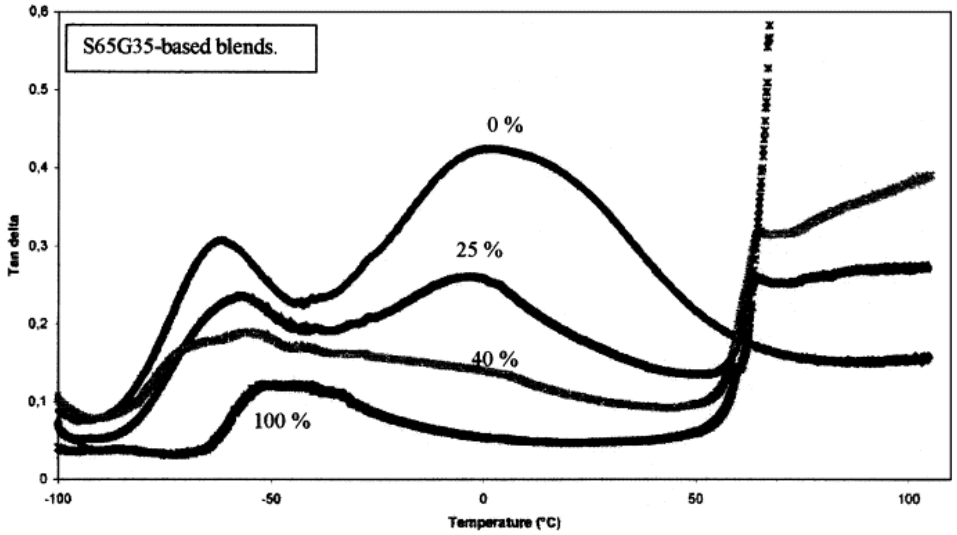

Figure 2-32 Tan δ curves for the blends of TPS/PCL with various PCL concentrations; TPS consists of 65/35 % of starch/glycerol (Averous, Moro, Dole & Fringant, 2000).

The prepared blends showed high hydrophobicity due to the presence of PCL, which is an advantage for TPS materials due to the very high hydrophilicity of TPS. The elongation at break decreased significantly with increasing TPS content due to the above-mentioned phase separation. In another work (Matzinos, Tserki, Gianikouris, Pavlidou & Panayiotou, 2002), LDPE/TPS/PCL blends were investigated, the morphology and mechanical properties of which were shown to be deeply affected by the PCL content and processing condition .

Similarly, Shin et al. (Shin, Lee, Shin, Balakrishnan & Narayan, 2004a) studied a wide range of PCL/TPS blends of 10 to 70% of TPS content. Again, the thermal properties indicated complete immiscibility, but the morphology of the blends implied a high level of compatibility due to hydrogen bonding between hydroxyl groups of the TPS and ester carbonyl groups of the PCL. In a follow-up work (Shin, Narayan, Lee & Lee, 2008b), starch was modified with maleic anhydride (MA). Here, it was shown that the hydroxyl groups of the modified TPS made hydrogen bonds with PCL macromolecules, but no significant improvement in the mechanical properties or morphologies was reported for the modified systems. The comparison of the tensile values can be

observed in the table below (Table 2-1). It was observed that modification of starch has been able to improve the elongation properties to some extent.

Table 2-1 Tensile properties for PCL/TPS in different concentrations; TPS contains 20% glycerol; MTPS: modified TPS (Shin, Lee, Shin, Balakrishnan & Narayan, 2004a; Shin, Narayan, Lee & Lee, 2008b).

	Modulus (Mpa)	Elongation at Break (%)
PCL	93	1090
PCL/TPS :90/10	117	860
PCL/MTPS :90/10	121	1030
PCL/TPS :70/30	136	560
PCL/MPS :70/30	150	800
PCL/TPS :50/50	176	18
PCL/MTPS :50/50	180	49

Sarazin et al. (Sarazin, Li, Orts & Favis, 2008) investigated blends of PLA/TPS/PCL, and it was demonstrated that addition of PCL significantly enhanced the ductility of the final material. In a more recent comprehensive work, Li et al. (Li & Favis, 2010) studied an extensive composition range of PCL/TPS blends using a twin screw extruder. The very high elongation at break of PCL was maintained up to 50% TPS content, though the modulus continuously diminished with increasing TPS content (Table 2-2). Comparing the ratio of elongation at break reduction with regard to TPS incorporation in Table 2-1 and 2-2, it can be seen that the method of TPS preparation has a significant effect on the performance of the final blends. On the other hand, the annealing property showed no significant coarsening over time in the morphologies of 70/30 and 50/50 compositions. Unlike PE/TPS blends, PCL/TPS blends do not demonstrate a compatibilizer incorporated system, most likely due to the reported high compatibility of TPS and PCL (Figure 2-33). Thus, as there already exists a high level of compatibility between TPS

and PCL phases, the major issue would be increasing the tensile strength and modulus of PCL/TPS blends in order to widen the application range of this blend.

Table 2-2 Tensile Properties for PCL/TPS blends in different compositions; TPS contains 36 wt% glycerol (Li & Favis, 2010).

	Modulus (Mpa)	Elongation at Break (%)		Modulus (Mpa)	Elongation at Break (%)
PCL	190	>1000	PCL/TPS :60/40	93	>1000
PCL/TPS :90/10	162	>1000	PCL/TPS :50/50	73	>1000
PCL/TPS :80/20	134	>1000	PCL/TPS :40/60	42	836
PCL/TPS :70/30	118	>1000	PCL/TPS :30/70	31	790

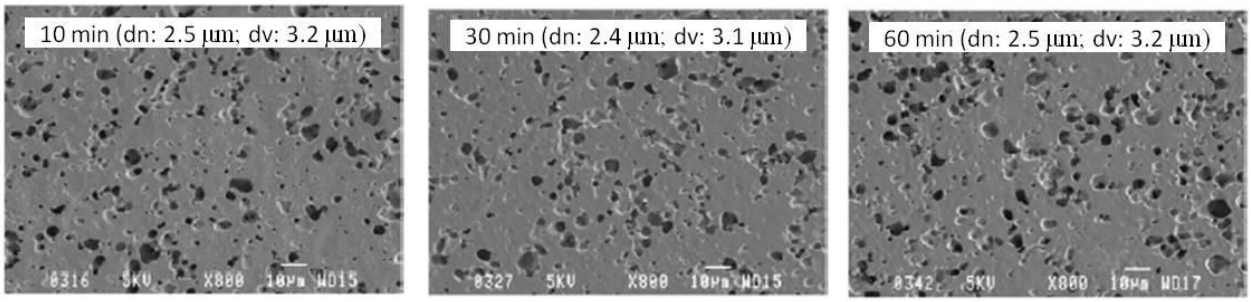

Figure 2-33 Morphology of PCL/TPS (70/30 wt%) after annealing at 150˚C (Li & Favis, 2010).

2.4 Nanotechnology and Nanocomposites

2.4.1 Overview

Nanotechnology is a name used for any modern technology that deals with the nanoscale (atomic or molecular scale) dimensions of materials (< 100 nm), which exist in different areas of application such as electronics, mechanics, biomedical, etc. Materials in gas, solid or liquid form may demonstrate unusual chemical, physical and biological properties on a nanoscale, dissimilar in important aspects to the regular scalar properties of the material. For example, some materials

might have different magnetic properties, or show better heat and electricity conductivity, be more chemically reactive, or even have different a colour by altering the size or structure. To be able to imagine how small "nano" is in the international system of units, it is defined as one-billionth of a metre. For a visual sense, some nanoscale materials are shown compared with other, normal-size materials in Figure 2-34.

Figure 2-34 The comparative scale of some materials (www.nano.gov/nanotech-101/what/nano-size).

Nanotechnology is used in many commercial applications today, including sunscreen and cosmetics, sporting equipment, automotive parts, chemical manufacturing (as catalysts), nanoceramics in dental healthcare, the new generation of transistors in electronics, etc. It is estimated that technology has a current value of $251 billion worldwide, and is predicted to reach $2.4 trillion by 2015, as indicated in the figure below.

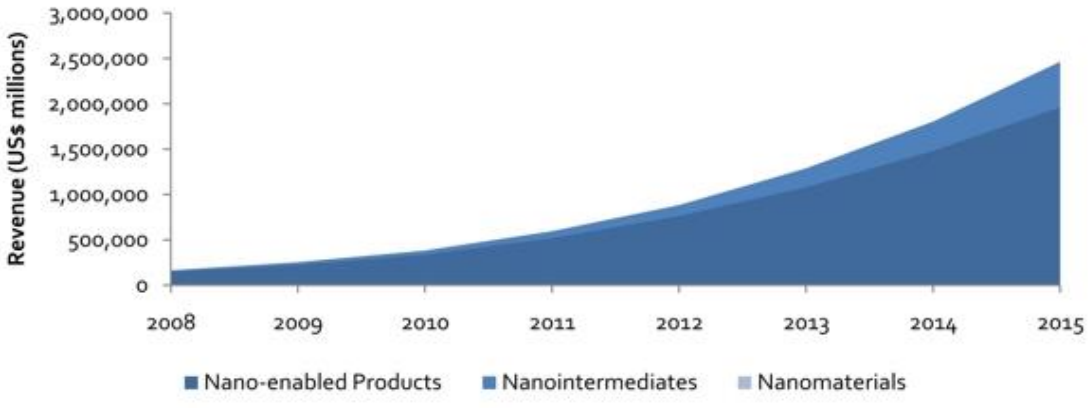

Value chain stage	2008	2009	2010	2011	2012	2013	2014	2015
Nano-enabled products	$145,291	$223,785	$336,062	$519,425	$762,204	$1,081,025	$1,480,928	$1,962,950
Nanointermediates	$18,353	$28,839	$45,592	$75,712	$120,206	$206,823	$322,691	$498,023
Nanomaterials	$812	$1,074	$1,309	$1,540	$1,798	$2,098	$2,462	$2,916
Total	$164,457	$253,699	$382,963	$596,677	$884,208	$1,289,947	$1,806,081	$2,463,890

Source: Lux Research, Inc.
www.luxresearchinc.com

Figure 2-35 Total and segmented revenue of global nanotechnology.

2.4.2 Polymer Nanocomposites

Polymer nanocomposites are a new class of materials containing solid nanoinclusions in the forms of nanotubes, nanoparticles, nanofibres or nanoclays in a single or multiphase polymer matrix. Compared to their conventional polymer composite counterparts, they possess some unique and outstanding functional and mechanical properties, such as dimensional stability, scratch resistance, enhanced processing properties, thermal stability and impact resistance, etc. They are now even replacing certain metal parts in the automobile industry. The first commercial polymer nanocomposites emerged in 1991 when Toyota Motor Co. introduced the Nylon6/clay nanocomposites for timing belt covers for its Camry model. The automobile industry has followed Toyota and introduced a wide variety of nanocomposites. Nanoclays have been the most frequently used in commercial products, accounting for around 80 percent. Another important product is the carbon nanotube which is rapidly expanding its application range owing to a reduction in price and improved performance/cost characteristics. Based on a study

conducted by Frost & Sullivan Co., carbon nanotubes will continue to expand in the automobile industry by an annual gain of 3.6%. The global market for carbon nanotubes in 2008 was estimated to be worth $18.79 billion, divided among the sectors observed in the figure below (Frost & Sullivan, 2011).

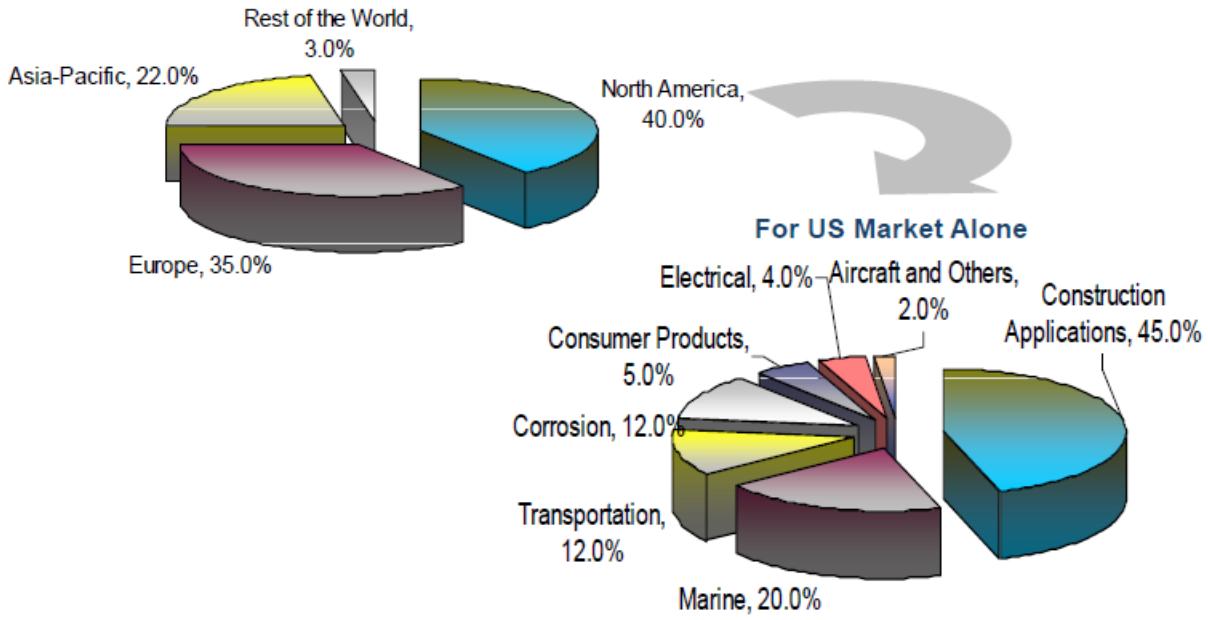

Figure 2-36 Global addressable market share for carbon nanotube based nanocomposites (Forst & Sullivan, 2011).

It is believed that the superiority of nanofillers is due to their molecular interaction and high interfacial are with the polymer matrix.

2.4.3 Carbon Nanotubes (CNT) and their properties

Carbon nanotubes (CNT) were first highlighted in 1991 by Ijima (Ijima, 1991). CNTs are made of carbon sheets with thickness of 1 atom, shaped in the form of seamless cylinder. The special properties of nanotubes, such as their high Young's modulus and good tensile strength, as well as their low weight, high stability and processability due to their carbonaceous nature, have motivated researchers to further investigate these materials in the last few years.

As mentioned, they actually resemble rolled up graphite layers in a form of seamless cylinders. This rolling up process can result in three different structures for single-walled carbon nanotubes,

determined by a vector C_h(chiral vector) and a chiral angle, which is the angle between C_h and vector a_1. C_h is determined as:

$$C_h = ma_1 + na_2$$

a_1 and a_2 are unit vectors in the two-dimensional hexagonal lattice and m,n are integers (OA in the figure below).

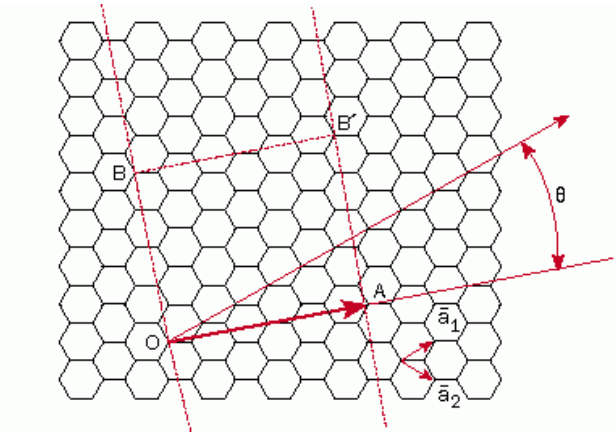

Figure 2-37 Schematic of two dimensional graphite sheet and the roll up vectors (Saito, Dresselhaus & Dresselhaus, 1998).

As seen in Figure 2-37, we can determine three different structures based on C_h and Θ. If n=m and the chiral angle is Θ= 30˚, an armchair structure is formed. If either n or m are zero and Θ= 0, then a zigzag structure is seen. The other structures are called chiral. These geometries determine its mechanical as well as electrical properties.

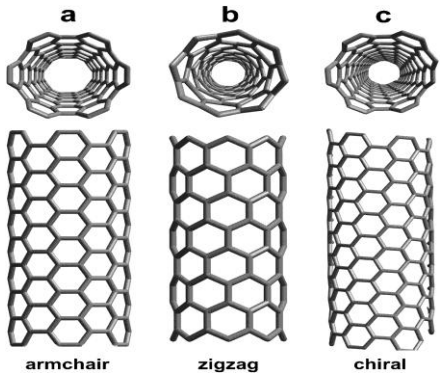

Figure 2-38 Models of different single wall nanotubes.

If n–m is a multiple of 3, then the nanotube is metallic, otherwise the nanotube is semiconductor, so the armchair structure is metallic. Theoretically, metallic nanotubes can reach an electrical current density of more than 1,000 times those of metals such as silver and copper.

SWNTs (Single Wall NanoTubes) have superior mechanical and electrical properties, but their production is costly and stabilizing their properties with polymers during the process is difficult. Besides, the commercial availability of MWNTs (Multi Wall NanoTubes) has led scientists develop CNT technology, and we can now see some commercialized CNT products.

One of the disadvantages of MWNTs is their weaker mechanical strength because of weaker bonds between their concentric cylinders; however, the application of CNTs in polymers is due to their heat and electrical conductivity rather than mechanical properties, and the techniques used for the production of SWNTs are not efficient yet enough to result in pure products, which may cause defects in their structure. Thus MWNTs are currently widely used in science and technology.

σ bonding is the strongest covalent bond in nature. So, nanotubes with σ bonds throughout their whole structure should have the highest strength. The mechanical properties of CNTs are observed in Table 2-3.

Table 2-3 Mechanical properties of Nanotubes (Meyyappan, 2005).

Material	Young's modulus (GPa)	Tensile Strength (GPa)	Density (g/cm^3)
MWNT	1200	~150	2.6
SWNT	1054	75	1.3
SWNT bundle	563	~150	1.3
Graphite (in-plane)	350	2.5	2.6
Steel	208	0.4	7.8

As we can see, their stiffness (Young's modulus) is around 1 TP, which is five times that of steel. These results have been proven both theoretically and experimentally. Young's modulus depends on the diameter of nanotube—the bigger the diameter, the lower the modulus. In MWNTs, the ultimate modulus will be one of SWNTs inside plus intertubular van der Waals forces, so this values is usually higher for MWNTs.

Nanotubes can be conductive or semiconductive according to the method used to roll the grapheme sheets. Thus some of them have very high conductivities ((m-n) mod 3=0) and others are semiconductive. Because of some defects in structure and the different chirality of the SWNTs inside MWNT, the electrical conductivity has some barriers on their ways (Meyyappan, 2005).

Experimental measurements show a thermal conductivity range of 200-6000 w/mk for CNTs, while heat conductivity is similar to electrical measurement, and is one dimensional for CNTs. This broad range shows the effects of tubes' quality and alignments, i.e. in the tube axis, they are conductive, and in the transverse axis are insulators (Meyyappan, 2005). These are all dependent on the quality of the sample, i.e. surface defects and purity, because defects have a considerable effect on CNT properties. Carbon Nanotubes/Polymer blends

2.4.3.1 Overview

Since the invention of carbon nanotubes (Ijima, 1991), there have been many efforts made to incorporate nanotubes with polymers to combine exceptional properties of nanotubes themselves those of another type of material like polymers. In fact, blending nanotubes with polymers can result in unique properties such as enhanced strength with increased viscoelasticity that other types of materials would never have. Thus, considering this potential, the polymer industry has moved towards nanotubes. In the following section, we will review what has been done in the literature in this area.

2.4.3.2 Surface Modification of Carbon Nanotubes

The superior mechanical, electrical, magnetic, optical and thermal properties of CNTs combined with the exceptional properties of polymers may result in a very high performance material indeed. The combination of high aspect ratio and high flexibility increases the ability of CNTs to entangle in bundles, with inter-tubular Van der Waals forces of around 500 eV/μm of CNTs

surface. Various efforts have been done to incorporate CNTs into the polymer matrix, which has resulted in big changes in the properties of the polymers (Anand, Agarwal & Joseph, 2006; Buffa, Abraham, Grady & Resasco, 2007; Chen et al., 2006; Dondero & Gorga, 2006; Du, Fischer & Winey, 2003; Fisher, Eitan, Andrews, Schadler & Brinson, 2004; Grady, Pompeo, Shambaugh & Resasco, 2002; Kim & Kim, 2006; Kymakis & Amaratunga, 2006; Li, Luo, Wei & Huang, 2006; Lin, Sundararaj & Potschke, 2006; Ounaies, Park, Wise, Siochi & Harrison, 2003; Shi, Hudson, Spicer, Tour, Krishnamoorti & Mikos, 2005; Tchoul et al., 2008; Velasco-Santos, Martinez-Hernandez, Fisher, Ruoff & Castano, 2003; Wu, Ma, Yang, Kuan, Yang & Chiang, 2006; Wu & Shaw, 2006; Zhang, Kandadai, Cech, Roth & Curran, 2006; Zhang, Lippits & Rastogi, 2006). Mostly they achieved results far below theoretical predictions (Xie, Mai & Zhou, 2005). The main reason for this is the level of dispersion of CNTs, since if they stay in bundles, they deteriorate the composite mechanical properties by the generated defects in the matrix, and mechanical failures usually start from the interfacial area of CNT/polymers. Thus, one of the most important factors in determining the performance of the nanotubes is the level of dispersion in polymer matrix.

One of the methods used to improve the dispersion level, along with mechanical properties of the nanocomposites, is the functionalization of the nanotubes (Bose, Bhattacharyya, Bondre, Kulkarni & Potschke, 2008; Chen, Hu, Zhou, Li, Yang & Wang, 2008; Dumitrescu, Wilson & Macpherson, 2007; Dyke & Tour, 2004b; Shaffer, Fan & Windle, 1998; Shaffer & Windle, 1999; Wu, Zhang, Zhang & Yu, 2009). The goal here is to create chemical affinity between the polymer and CNT walls in order to debundle the nanotubes and achieve a high degree of interaction between the tubes and the matrix. Interaction and dispersion are the keys to attaining optimum properties. Generally there are two types of surface modifications: covalent and non-covalent. Non-covalent modification includes using surfactants or coating nanotubes with other materials, such as ionic liquids (Kavan & Dunsch, 2003) or polymers (Carrillo et al., 2003; O'Connell et al., 2001). Covalent modification consists of introducing a functional group on the sidewalls or the end caps of the nanotubes through oxidative treatments. This leads to reactive couplings between the nanotubes' surface and the functional groups of the polymer matrix. Due to the harsh reaction conditions of functionalization, this type of modification shows some drawbacks in the final properties of the nanotubes, such as a loss of primary electrical conductivity (Song, 2006; Srivastava, Banerjee, Jehnichen, Voit & Boehme, 2009). It has been proposed that covalent

bonding enhances the debundling of CNTs (Dyke & Tour, 2004a), as well as their solubility in common solvents. The introduced functional groups on the CNT walls improve adhesion to the polymer matrix, which results in significant improvements in the mechanical properties and dispersion level of nanotubes (Bose, Khare & Moldenaers, 2010). Obviously, various types of functionalizations will result in different levels of phase adhesion and consequently different levels of property enhancement. For instance, in Figure 2-39 it is observed that the Diamine functionalization of the nanotubes results in better dispersion and adhesion levels in PA matrix, which is reflected in a higher storage modulus (Meng, Sui, Fang & Yang, 2008).

But as mentioned above, although the functionalization may introduce significant improvements to the mechanical properties, it may deteriorate the electrical conductivity of the nanotubes through defects on the walls, lower L/D or encapsulation or wrapping of the nanotubes due to covalent bonding with polymer matrix (Figure 2-40).

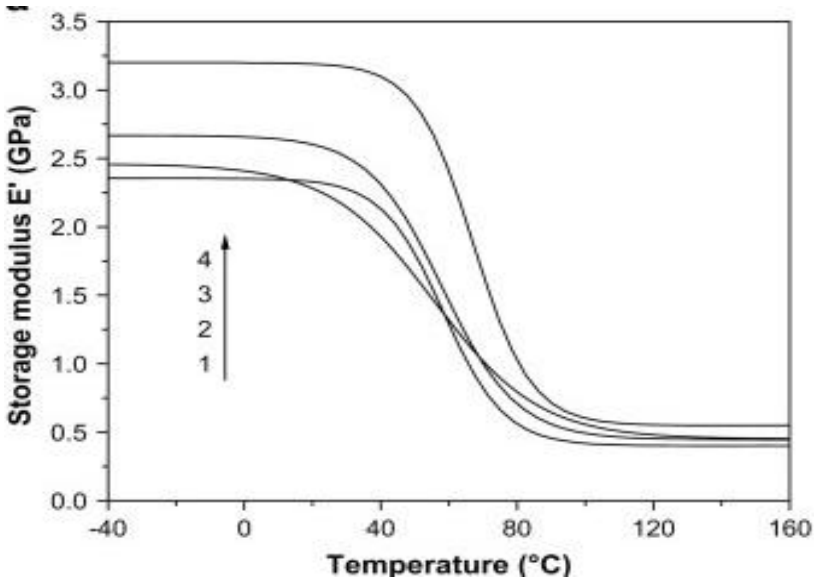

Figure 2-39 Storage Modulus for (1) PA6, (2) PA6/MWNT, (3) PA6/A-MWNT (acid modified) and (4) PA6/D-MWNT (diamine modified) (Meng, Sui, Fang & Yang, 2008)

Potschke et al. (Bose, Bhattacharyya, Bondre, Kulkarni & Potschke, 2008) have investigated co-continuous PA6/ABS blends with CNTs, comparing functionalized and pristine CNTs in terms of rheological and phase behaviour domains. The aspect ratio that is higher in non-functionalized

MWNTs (Figure 2-40), is a dominant factor in controlling the flow behaviour of the blends, i.e. with non-functionalized CNTs that have higher L/D and fewer defects, we'll see the electrical and rheological percolation thresholds in lower CNT content than with functionalized ones (Figure 2-41).

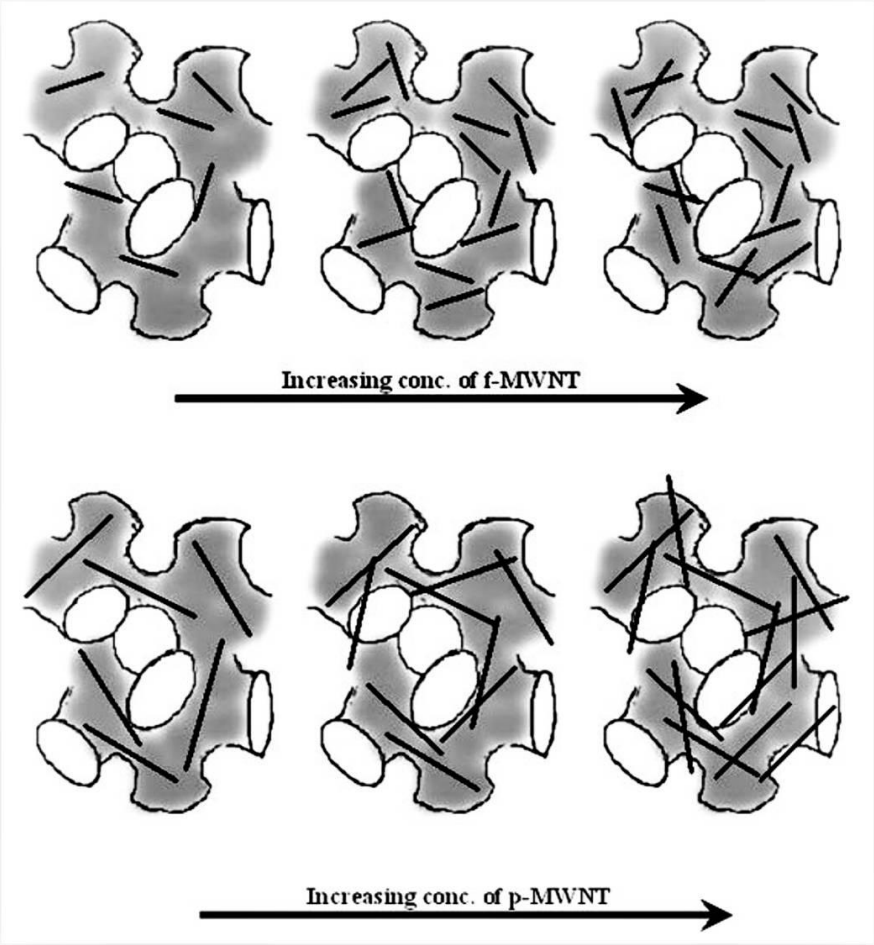

Figure 2-40 Schematic of the effect of L/D on the state of dispersion for functionalized-MWNT (upper image) and pristine-MWNT in the blends (lower image) (Bose, Bhattacharyya, Bondre, Kulkarni & Potschke, 2008).

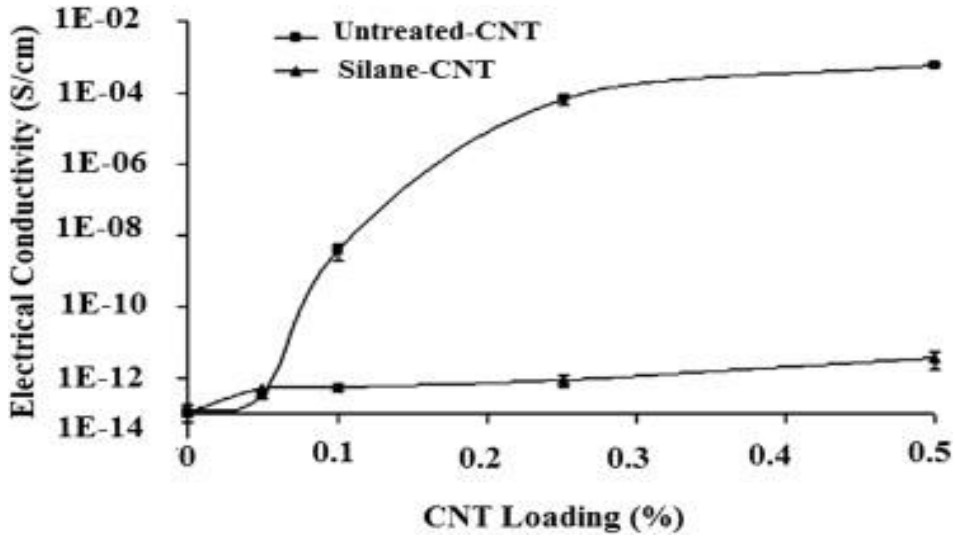

Figure 2-41 Electrical conductivity of nanocomposites of Epoxy/MWNT for untreated and silane-treated carbon nanotubes (Ma, Kim & Tang, 2007).

Thus, where electrical properties of the composites are not crucial in the final product, functionalization is an appropriate way to improve the dispersion and mechanical properties of the blends.

2.4.3.3 Processing methods

There are several methods for dispersing nanotubes in polymer blends. Depending on the materials used, the efficacy of these methods might be different for each system. The diagram briefly explaining these methods (Grady, 2011) can be seen in Figure 2-42. Among these, melt mixing is the method which has the most applicability in industrial processes. On the other hand, the solution method (Dissolution-Dispersion-Precipitation) is the methods that best disperses nanotubes in the polymer matrix.

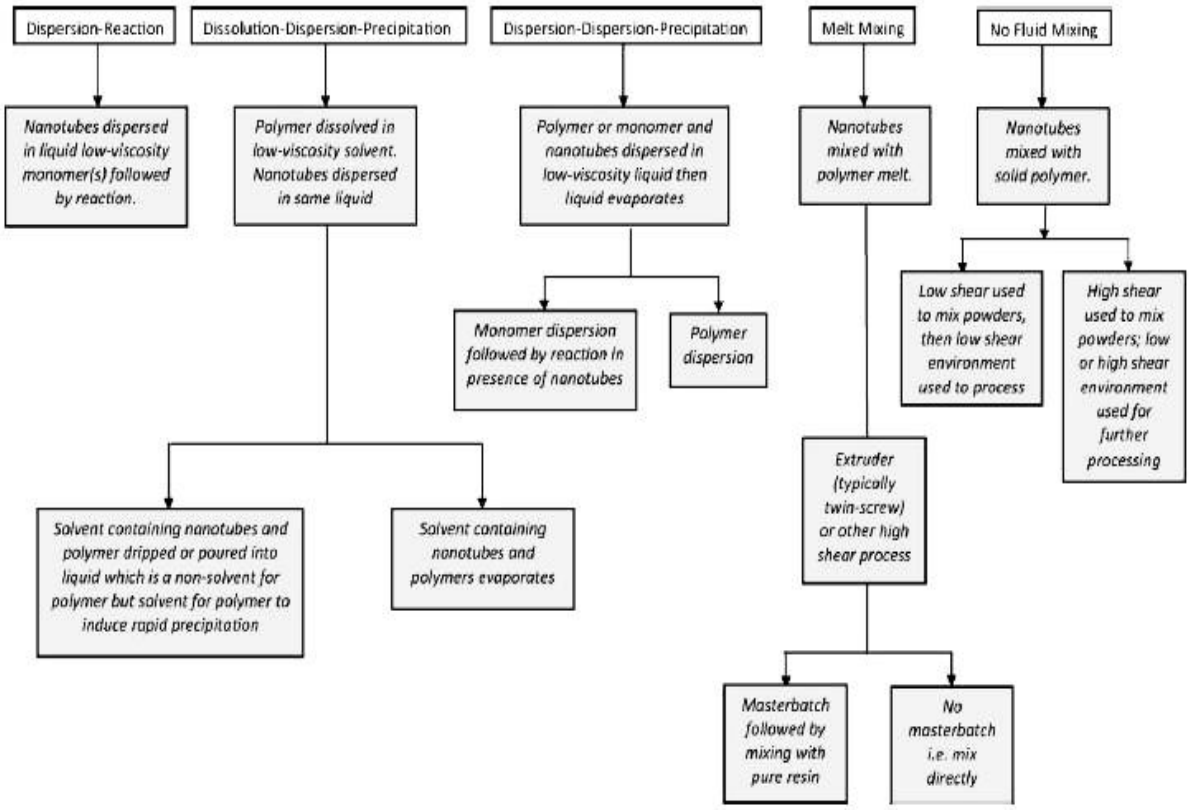

Figure 2-42 Methods used to disperse nanotubes in polymer matrix (Grady, 2011) .

2.4.3.3.1 Solution method

Solution mixing involves using a solvent to solubilise the polymer and using the same solvent to disperse the CNT, then mixing the two solutions and evaporating the solvent to get the film of composite (Buffa, Abraham, Grady & Resasco, 2007; Chen et al., 2006; Du, Fischer & Winey, 2003; Fisher, Eitan, Andrews, Schadler & Brinson, 2004; Grady, Pompeo, Shambaugh & Resasco, 2002; Kymakis & Amaratunga, 2006; Ounaies, Park, Wise, Siochi & Harrison, 2003; Shi, Hudson, Spicer, Tour, Krishnamoorti & Mikos, 2005; Tchoul et al., 2008b; Velasco-Santos, Martinez-Hernandez, Fisher, Ruoff & Castano, 2003; Wu, Ma, Yang, Kuan, Yang & Chiang, 2006; Zhang, Kandadai, Cech, Roth & Curran, 2006). Due to the possibility of complete dispersion of the nanotubes in low viscosity liquids, it is expected that high dispersion levels will be obtained using this method. This is mostly related to the rate of evaporation, i.e. how fast the film of polymer-nanotube can be made in order to prevent the nanotubes from re-aggregating (Bergin et al., 2008; Higginbotham et al., 2008). In order to improve the evaporation rate, this

process should either be done under higher temperatures (Chang, Kisliuk, Rhodes, Brittain & Sokolov, 2006; Singh, Pei, Miller & Sundararajan, 2003) or an anti-solvent should be used. This leads to the precipitation of the polymer chains and the entrapment of carbon nanotubes in between the chains (Tchoul et al., 2008a). Another way is to use supercritical fluids as a solvent, which has resulted in some interesting structures (Yue, Wang, Huang, Pfeffer & Iqbal, 2007; Yue, Xu, Zhang & Chen, 2007; Zhang, Feng, Zhao, Huang, Hoppe & Hu, 2008). This is the most obvious lab-scale process available to disperse nanotubes, though there are some drawbacks with this method. One is the use of significant amounts of the solvent, which is not industrially interesting, nor is it environmentally friendly. Water is available as a solvent, although it is obviously unable to solubilise a wide range of polymers. In order to be able to efficiently disperse the nanotubes in the solutions at either the first or second step, it seems necessary to use sonication. This can then be used as masterbatch (Barrera, 2000) and diluted with virgin polymers of the same type or blend it with other polymers.

2.4.3.3.2 Melt mixing

The most simple and straightforward way to mix the CNTs into the polymers is through melt mixing, a technique used for dispersing nanotubes in the polymer melt using high-shear processes such as twin screw extrusion. With this method, we don't need special equipment for mixing as in other methods. On the other hand, since there is normally no solvents nor surfactants involved that would need further purification, the material is ready to use immediately after the process. However, the dispersion level is normally below that of the previous method. This may be due to the lack of small molecular weight materials, which improve the exfoliation of nanotubes (Grady, 2010). Similar to the previous method, the level of dispersion depends highly on the type of nanotube (SWNT, MWNT) and the polymer characteristics, which may result in high/low levels of dispersion (Anand, Agarwal & Joseph, 2006; Valentini, Biagiotti, Kenny & Manchado, 2003). This issue is more pronounced in non-functionalized CNTs, so we should use high a shear rate or high mixing times to have better dispersion. But in that case, we will decrease the L/D ratio of the CNTs, which has a direct effect on the electrical and mechanical properties of the composite (Bose, Bhattacharyya, Bondre, Kulkarni & Potschke, 2008). Due to the high amount of exerted shear on the materials in corotating twin screw extruders, it has been mostly used in the melt processing of polymer-CNT composites. Due to the commercial interest in this method, there has been a huge number of articles written on improving the dispersion efficacy in melt mixing,

dealing with such topics as using ultrasonication in the melt extrusion lines (Villmow, Pötschke, Pegel, Häussler & Kretzschmar, 2008) and the functionalization of nanotubes walls (Prashantha, Soulestin, Lacrampe, Claes, Dupin & Krawczak, 2008; Wu, Sun & Zhang, 2009). This method is preferred when a masterbatch is commercially available (e.g. for PS, PC, EVA, HDPE, PE, PA). In these masterbatches, the CNTs are almost completely dispersed, so after dilution it can achieve high degrees of dispersion and distribution in the final product.

2.4.3.4 Localization of Nanotubes in Immiscible Polymer Blends

Generally speaking, all the phenomena regarding the morphology of polymer blends are governed by thermodynamics and/or kinetic effects, as well as the localization of nanoparticles. Localization is in fact the most important parameter in determining all the subsequent changes that the addition of nanofillers can bring about in polymer blends. Knowing this, it seems necessary to discuss the controlling parameters of localization.

2.4.3.4.1 Thermodynamics Effect

The term "thermodynamics" is based on the minimization of the free energy of the system which is achieved by balancing the interactions of nanotubes surface and blends components. Due to the fact that the surface properties of the components in immiscible blends are quite different (the reason for being immiscible), it is expected that the nanotubes distribute unequally in the blend systems. According to Young's equation, and in order to get the minimal interfacial free energy of the system, ΔG, a term named *wetting coefficient*, is introduced:

$$\omega_s = \cos\theta = \frac{\gamma_{S2} - \gamma_{S1}}{\gamma_{12}}$$

The involved terms are schematically shown in the figure below. γ_{S2} is the interfacial tension between the solid surface and polymer 2; γ_{S1} the interfacial tension between the solid surface and polymer 1; and γ_{21} the interfacial tension between polymer 1 and polymer 2.

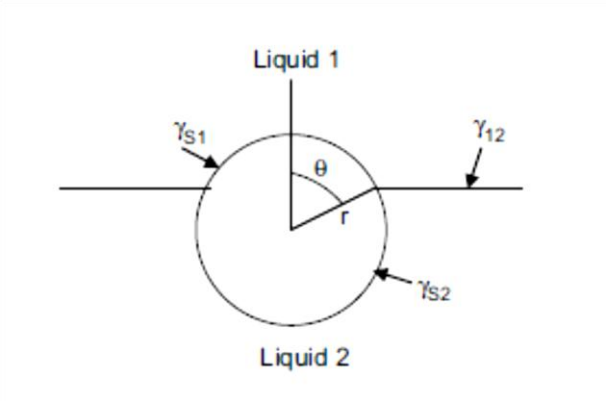

Figure 2-43 Schematic representation of the interfacial components in solid particles/polymer blends interface.

If $0< \Theta < 180^{\circ}$ i.e. $-1< \omega_s <1$, then the particles will localize at the interface, otherwise they will migrate to either of the phases: $\omega_s>1$ the nanotubes will prefer phase 1; and if $\omega_s<1$ they will migrate to phase 2. Although the experimental interfacial tension data exists for a broad range of polymers in different temperatures, the data is virtually absent in the literature on polymer-filler interfaces. This should be calculated via the interfacial tension equations (explained in section 2.3.2.2.). It is important to point out that these calculations should be done at melt temperature, not room temperatures, as some authors have done (Asai, Sakata, Sumita & Miyasaka, 1992; Elias, Fenouillot, Majeste & Cassagnau, 2007; Ibarra-Gomez, Marquez, Valle & Rodriguez-Fernandez, 2003; Sumita, Sakata, Asai, Miyasaka & Nakagawa, 1991b). It is very difficult to handle a single nanotube, so the problem with the surface tension data of the nanotubes is that each type of nanotube (functionalized or virgin) has a different surface tension value for every grade of commercially made nanotube. The existing data in the literature is thus mainly based on limited existing values for some grades of nanotube.

The results of wetting coefficient is then related to the surface properties of the nanotubes, which may be subject to change by functionalization, oxidation or other impurities, as well as the surface chemical structure of the polymer components. The results show some discrepancies, though some authors have successfully been able to predict localization by using this concept (Baudouin, Bailly & Devaux, 2010; Goeldel, Kasaliwal & Poetschke, 2009; Poetschke, Pegel, Claes & Bonduel, 2008; Sun, Guo & Yu, 2010; Wu & Shaw, 2004; Zhang, Wan & Zhang, 2009), e.g. using a twin screw extruder, when the nanotubes were fed in PP phase, the nanotubes could not migrate to their thermodynamically favourable phase, i.e. EVA, in the time frame of the

process (Liu, Wang, Xiang, Li, Han & Zhou, 2009). But in SAN/PC blends, the nanotubes migrated to their favourable phase within 5 minutes (Goeldel, Kasaliwal & Poetschke, 2009). Hence, it is not always possible to predict correctly either due to errors in interfacial tension data calculations or kinetic effects (Fenouillot, Cassagnau & Majeste, 2009).

In a recent study (Tao et al., 2011), low M_w PMMA was grafted onto the surface of the nanotubes. It was observed that functionalized CNTs were able to migrate to the interface of PA/EVA, while virgin nanotubes were only dispersed in PA phase. But on the other hand, when the CNTs were coated only with PMMA (no covalent bond), they acted like the pristine nanotubes.

2.4.3.4.2 Kinetic Effects

Kinetic effects involve altering parameters affecting the rate of mixing in order to achieve a thermodynamic equilibrium state. Due to the high viscosity of the polymer melts and relatively short processing times, any parameter affecting this rate will change the final morphology of the polymer blend, as well as the localization of the nanofillers.

One of these parameters is feeding sequence. In melt mixing, after adding the components, some time is required for the solids to melt down before the actual blending process begins. One of the ways to do this is to add all the components together in the mixing process. In the case of a high melting point difference between polymer pairs, the one that melts earlier, will most probably encapsulate the nanofillers, and may remain in that phase due to the mixing conditions, even if a thermodynamically stable localization has not occurred. Another method of addition involves the incorporation of the fillers in one phase (such as a masterbatch) and then addition of the other phase—the first phase would/would not be the thermodynamically preferential phase. Zaikin et al. (Zaikin, Zharinova & Bikmullin, 2007; Zaikin, Karimov & Arkhireev, 2001) have reported that conductivity was improved where carbon blacks were fed into the phase with less affinity and they had to cross the interface. Elias et al. (Elias, Fenouillot, Majeste & Cassagnau, 2007) reported that with PP/PS/silica particles, this transfer is achievable after a few minutes of mixing. Also, an interesting phenomenon of nanofillers gradually migrating during the process was shown by the electrical resistivity of the blends vs. mixing time. Gubbels et al. (Gubbels et al., 1994) found that using co-continuous blends of PE/PS (45/55wt%) filled with 1% carbon black, and by monitoring the electrical resistivity during the process, the localization of the nanofillers

can be determined during the mixing process. As observed, the minimum value of electrical resistivity corresponds to the interface localization of the nanotubes (see Figure 2-44). It is possible to use this approach to freeze localization at any point by means of controlling processing time; however, it may not be at the thermodynamically optimal state.

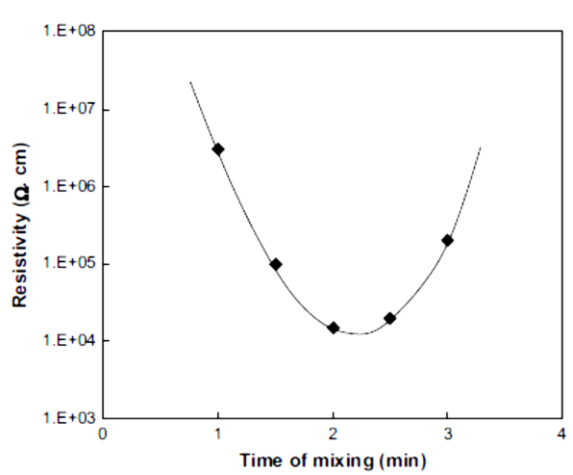

Figure 2-44 Electrical resistivity/mixing time graph in co-continuous blends of PE/PS (45/55wt%) filled with 1% carbon black (Gubbels et al., 1994).

Another factor that has been frequently dealt with in the literature is viscosity. One obvious issue is that according to basic mass transfer laws, the high viscosity of the polymers will diminish the transfer rate of the fillers. So if the fillers are first fed in a less thermodynamically favourable phase, in case of high viscosity of that phase, the diffusion rate will be lower or may even stop. The literature is full of reports on viscosity or the viscosity ratio effect on the localisation of the nanofillers (Clarke & Harris, 2001; Feng, Chan & Li, 2003; Gubbels, Jerome, Vanlathem, Deltour, Blacher & Brouers, 1998; Ibarra-Gomez, Marquez, Valle & Rodriguez-Fernandez, 2003; Persson & Bertilsson, 1998; Yuan, Yao, Sylvestre & Bai, 2011). It has also been shown that viscosity can play a controlling role in determining the localization of nanofillers in polymer blends. Yuan et al. (Yuan, Yao, Sylvestre & Bai, 2011) demonstrated that even though the wetting coefficient data indicates that nanotubes have more affinity with PVDF than LDPE, throughout the whole composition range, nanotubes disperse only in the LDPE phase (Figure 2-45). Since LDPE melts in lower temperatures than PVDF, it first encapsulates the nanotubes; however, they remain in LDPE even after a long processing time. This is attributed to the high

viscosity ratio of PVDF/LDPE, which inhibits nanotube migration to the thermodynamically optimal phase.

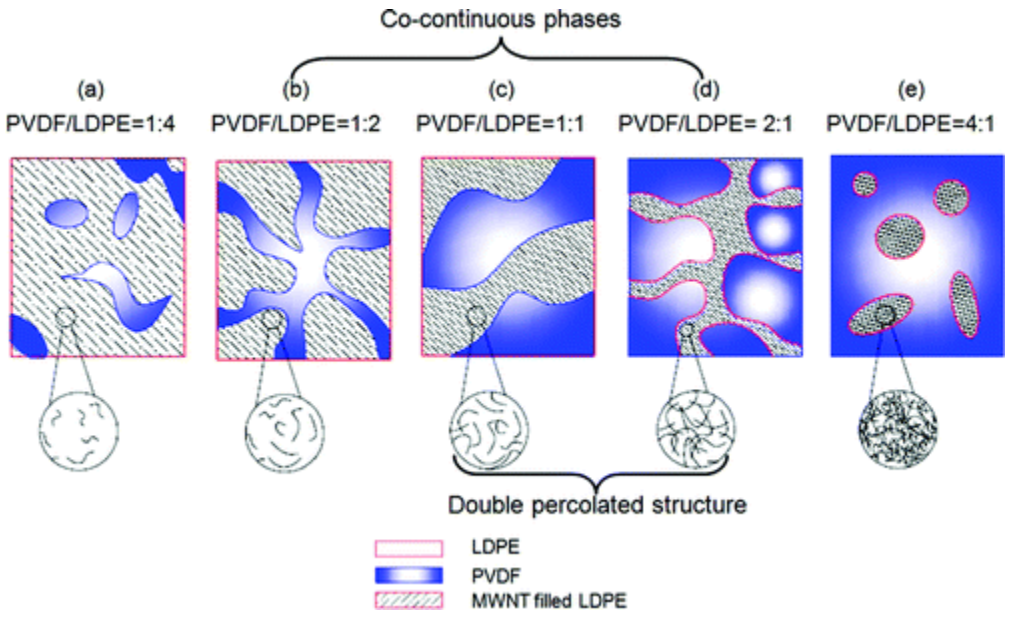

Figure 2-45 Illustration of the microstructure evolution for blends of PVDF/LDPE/MWNT in different volume ratios (Yuan, Yao, Sylvestre & Bai, 2011).

What is generally understood is that if nanofillers are fed into a high viscosity medium, it will be difficult for them to migrate to thermodynamically favourable phase. In addition to the diffusion issue explained above, the system also has the tendency to decrease the dissipative energy of the system by localizing the fillers in more viscous phase (Fenouillot, Cassagnau & Majeste, 2009). In the opposite case where less favourable phase viscosity is low, and the more favourable phase viscosity is high, the nanofillers would only be able to accumulate at the interface and thus unable to migrate to the destined phase (Feng, Chan & Li, 2003). Conflicting data has also been reported, however (Goeldel, Marmur, Kasaliwal, Poetschke & Heinrich, 2011; Mamunya, 2001; Wu et al., 2011). A recent study shows that the shape of the nanoparticle has a pronounced effect on the localization of nanoparticles (Goeldel, Marmur, Kasaliwal, Poetschke & Heinrich, 2011). in this study, it was also shown that the aspect ratio of the nanoparticles is of great importance to their localization, such that high aspect ratio particles are unlikely to locate at the interface, even though it is thermodynamically preferable.

Although it is believed that thermodynamicss is the most influential factor under normal processing conditions, it seems that thermodynamics and kinetics are too complicated and interconnected to be gauged independently.

2.4.3.5 Effects of Carbon Nanotubes in Polymer Blends Properties

2.4.3.5.1 Polymer Physics

Most of the changes that nanoinclusions impose on the polymer matrix are based on their size. The small dimensions of the nanotubes generate an enormous increase in the interfacial area between tubes and polymer. Hence, the number of the polymer chains that experience configurational (conformational) changes will increase accordingly. This effect will be amplified if there is a level of interaction/covalent bond between the functional/end groups of the polymer chains with the surface of nanotubes, which may or may not be functionalized. The existence of polar groups at the surface of the tubes will lead to a significant rise in surface energy, and consequently in the interfacial energy of the nanotube/polymer matrix. This will result in more adhesion of the bulk of the polymer to the surface.

2.4.3.5.1.1 Glass Transition Temperature (T_g)

Through surface area interactions, nanotubes can dramatically affect the dynamics of polymer chain mobility, and the boldest measure of polymer chain dynamics is glass transition temperature, T_g. The effect of carbon nanotubes on glass transition temperatures can either be an enhanced chain mobility (where T_g decreases) (e.g. Figure 2-46), or a restriction in the chain mobility (where T_g increases) (Grady, 2011). The existence of a solid surface in the vicinity of polymer chain will change the movement of the chains along the surface, compared to that at the interface. But there is no consistency in the results observed in the literature for different materials. In two studies conducted by Grohens et al. (Grohens, Brogly, Labbe, David & Schultz, 1998; Grohens, Hamon, Reiter, Soldera & Holl, 2002) on the films of PMMA-CNT, it was observed that for syndiotactic PMMA, T_g decreases with the addition of nanotubes, while for isotactic PMMA of the same Mw, glass transition increases. Considering the fact that stoichiometric alteration would not affect the interaction between polymer chains and the nanotubes, it is not understood why changes in T_g behaviour is even changing the trend.

However, the number of the papers reporting a decrease in T_g is greater than those reporting a T_g increase.

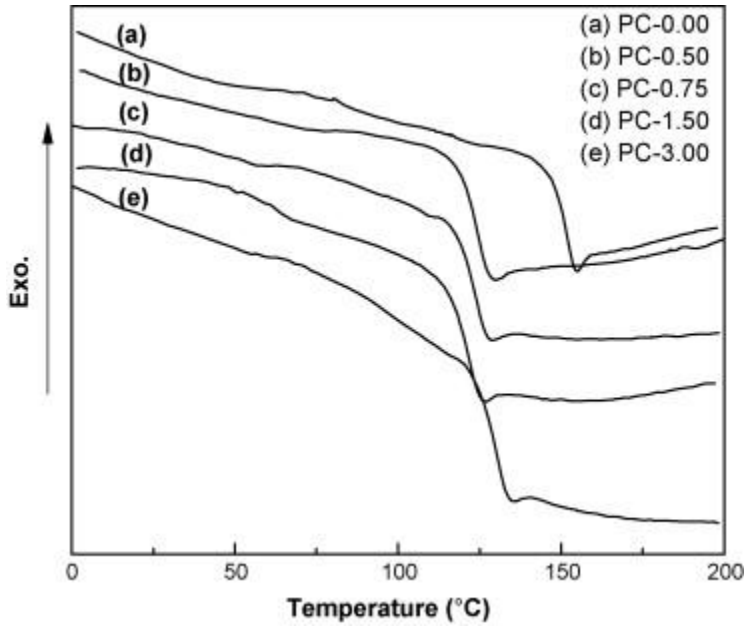

Figure 2-46 DSC curves for PC/MWNT nanocomposites (Jin, Choi & Lee, 2008).

But the majority of studies on T_g behaviour with nanotube content do reach one common conclusion: increases and decreases in glass transition temperature followed by a plateau after a certain CNT content (Grady, 2012). While this is not consistent with the theories of surface interaction proposed by the authors for the T_g change (Grossiord, Miltner, Loos, Meuldijk, Van Mele & Koning, 2007), the plateau is observed in a wide range of CNT content, from 0.3% (Jin, Kang, Kim, Park & Lee, 2008) to 10% (Jin & Lee, 2008), though mostly below 2 wt% (Cui, Tarte & Woo, 2009; Grady, Paul, Peters & Ford, 2009; Grossiord, Miltner, Loos, Meuldijk, Van Mele & Koning, 2007; Xia & Song, 2006). The observed plateau is most likely due to the saturation of polymer-nanotube available interfacial area after a certain amount of nanotubes due to the agglomeration of nanotubes in plateau contents (Grady, 2011). However, this remains a hypothesis as no experimental work has been done on this.

2.4.3.5.1.2 Crystalline Structure

The incorporation of solid fillers such as carbon nanotubes definitely alters the crystallization phenomenon in semicrystalline polymers in several aspects. The fact that carbon nanotubes are

able to nucleate the crystallinity has been well established in the literature (Grady, 2012), which has shown that they alter crystalline structure on both lamellar and shpherolite scales. Two types of nucleation morphology have been shown: “shish-kebab” and transcrystallinity. In the former type, nanotubes are simply acting like a long skewer, and the growing lamellae, perpendicular to the axis of the nanotubes, is like kebab meat (Figure 2-47). In transcrystallinity, the lamellae growth direction is similar to shish-kebab, but the forming lamellae grow into each other, and no singular lamella is observed along the nanotube axis. Both types affect the nucleating density in semicrystalline polymers. At a lower scale of unit cells, nanotubes can cause polymorphism in polymers, as do other nucleating agents, by promoting one crystal type over others (Huang & Wang, 2011; Huang, Edenzon, Fernandez, Razmpour, Woodburn & Cebe, 2010; Kang, Pal, Bang & Kim, 2011; Li, Sparks & Bonning, 2008; Li, Fang, Tong, Gu & Liu, 2006; Logakis et al., 2009; Sarno, Gorrasi, Sannino, Sorrentino, Ciambelli & Vittoria, 2004; Shieh, Liu, Twu, Wang & Yang, 2010). In the scale of spherulite, although conventional fillers might impede/restrict the spherulite growth, nanotubes may not demonstrate this effect due to their small size; however, the spherolites may extend over and around the nanotubes. Thus, the addition of nanotubes to semicrystalline polymers affects both crystallization temperature and growth rate. Due to the nucleating effects, they are expected to increase the crystallization temperatures. Also, they change the enthalpy of crystallization and may broaden the crystallization peak. However, there are two factors acting that may counteract this: the nucleating effect increasing nucleation density, and the decreased chain mobility that decreases growth rate. Thus the enthalpy of crystallization (or % crystallinity) is a compromise between these two effects. In some works, two different crystallization temperatures, high and low, were observed (Brosse, Tencé-Girault, Piccione & Leibler, 2008; Phang, Ma, Shen, Liu & Zhang, 2006; Saeed & Park, 2007).

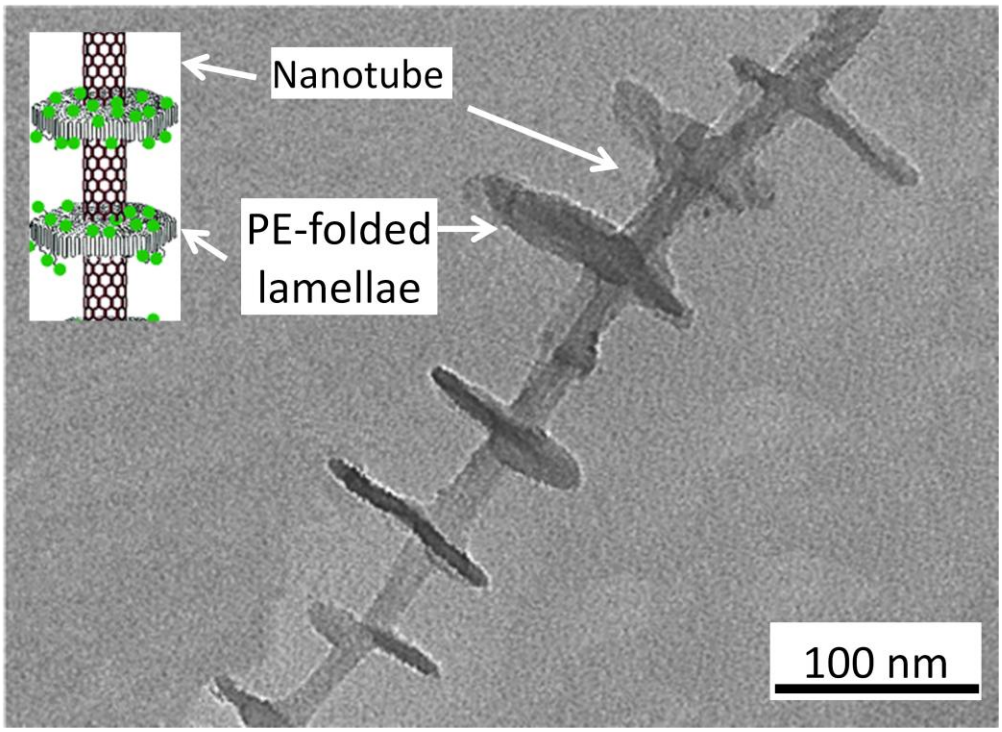

Figure 2-47 TEM and schematic representation of shish-kebab morphology in PE-CNT composites (Li, Li & Ni, 2006).

Similar to the glass transition changes observed in the amorphous parts of polymers, the crystallization temperature, T_c, levels off gradually by increasing the nanotube content (Tzavalas, Mouzakis, Drakonakis & Gregoriou, 2008).

2.4.3.5.2 Blends Morphology

The most basic issue in the incorporation of the nanotubes in polymer blends is the localization of the nanotubes, by which all other effects are defined. The majority of polymer pairs are immiscible due to differences in surface energies. This, as well as kinetic effects, will affect the localization of the nanotubes, as discussed earlier. Using nanomaterials in polymer blends for controlling the domain size seems to be a relatively new idea, though they have been shown to variously affect domain size (Buffa, Abraham, Grady & Resasco, 2007; Li, Li, Xu & Lu, 2007; Maglio, Migliozzi, Palumbo, Immirzi & Volpe, 1999; Mukherjee, Das, Rajasekar, Bose, Kumar & Das, 2009; Potschke, Bhattacharyya & Janke, 2003; Wu, Zhang, Zhang & Yu, 2009). For example, Potschke et al. (Potschke, Bhattacharyya & Janke, 2004) observed a co-continuous

structure in the PC-PE blends with 2 wt% CNT in PC phase, while the composition was 30/70 wt % for PC/PE, respectively (Figure 2-48).

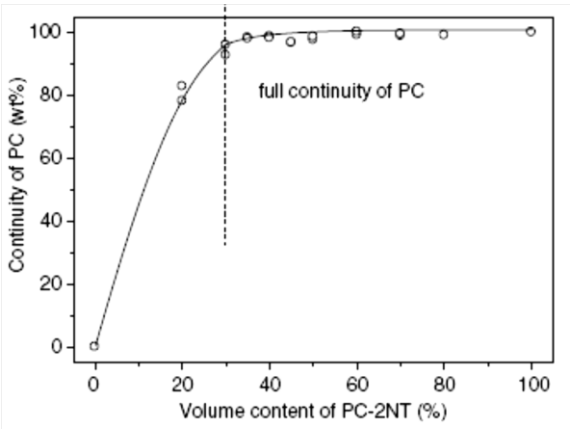

Figure 2-48 Continuity of PC in blends of PC-2NT with PE as calculated from selective extraction experiments. (Potschke, Bhattacharyya & Janke, 2004)

Li et al. (Li, Li, Xu & Lu, 2007) have studied the PC/PE and EVA/PE system. The CNTs were premixed with PC and EVA, but after blending, because of increased affinity of the CNTs with polyolefins, they migrated to the PE phase. These changes can be explained by different mechanisms: changing the viscosity of the phases; impeding the coalescence phenomenon (Elias, Fenouillot, Majeste & Cassagnau, 2007); changing the free energy of the mixing; or acting as the interfacial stabilizer (Grady, 2011). Baudouin et al. (Baudouin, Auhl, Tao, Devaux & Bailly, 2011) have schematically showed the effect of nanotubes on the morphology by impeding the coalescence of PA particles in the EA matrix (Figure 2-49).

2.4.1 TPS/Carbon nanotubes

Micro and nanofillers have been studied in the literature in order to improve the mechanical properties of starch (Alemdar & Sain, 2008; Alvarez & Vazquez, 2006; Fama, Gerschenson & Goyanes, 2009). Cao et al. (Cao, Chen, Chang & Huneault, 2007) functionalized the MWNT with an acid treatment and made a plasticized-starch/CNT composite using a solution method. SEM images of the fractured surface show a near full dispersion of CNTs, which shows that this functionalization can be a useful way to disperse CNTs in starch. This interaction was also shown

to affect the T_g of starch, increasing it from 16.5 to 25.3, in pure plasticized starch with 3 wt% CNT, respectively.

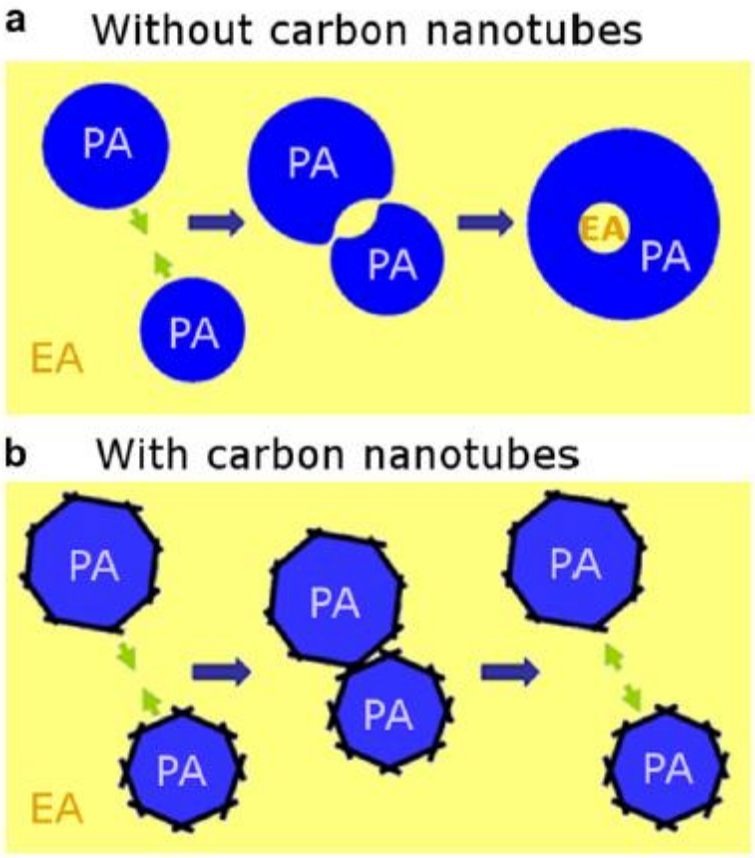

Figure 2-49 Schematic representation of coalescence hindrance by localization of nanotubes at the interface of PA particles in EA matrix (EA/PA: 90/10 wt%) (Baudouin, Auhl, Tao, Devaux & Bailly, 2011).

As expected, mechanical properties were improved, but by a very small amount: 34% with addition of 1 wt% CNT. But the interesting property here is elongation at break, which increased from 29.69% in pure plasticized starch to 41.99% in 1wt% CNT/plasticized-starch. Water uptake was another factor investigated, which was shown to decrease with addition of CNT, as shown in Figure 2-50; this seems to be because of the increasing amount of CNTs (that are less water sensitive) and hydrogen bonds of the CNT and starch blend.

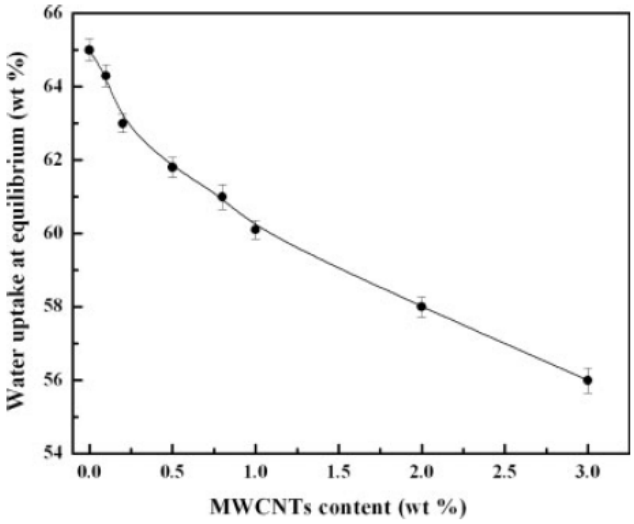

Figure 2-50 Water uptakes at equilibrium of the PS and PS/MWCNTs films conditioned at 98% RH as a function of MWCNTs content (Cao, Chen, Chang & Huneault, 2007).

In another study, amylose and amylopectin inclusions of starch have been separately blended with SWNTs (Bonnet, Albertini, Bizot, Bernard & Chauvet, 2007; Stobinski et al., 2003b). It was shown that there are some interactions between the SWNT's surface and α-D-glucose hydrophobic sites of amylopectin. The amylose portion of starch has been used in the separation of SWNTs from impurities, which have made some complexes with the CNTs. There is another interesting study done recently by Ma et al. (Ma, Yu & Wang, 2008) where they used unfunctionalized CNT, but dispersed it using a surfactant in the water through the use of sonication. They conclude that the distribution of the CNTs is homogeneous, but we could not totally verify this from the vague SEM images. In terms of mechanical properties, we again see an increase in stiffness, showing a kind of interfacial interaction similar to the functionalized nanotubes. But as usual, this comes at the expense of a deteriorating elongation at break, which is natural because of the restrictions made by CNTs on the starch modulus slippage (Figure 2-51). Famá et al. (Famá, Pettarin, Goyanes & Bernal, 2011) investigated TPS/CNT nanocomposites, finding that starch molecules could effectively wrap around the nanotubes and disrupt inter-tubular van der Waals forces and high level of dispersion could be achieved; this is a corroboration of earlier work done by Star et al. (Star, Steuerman, Heath & Stoddart, 2002).

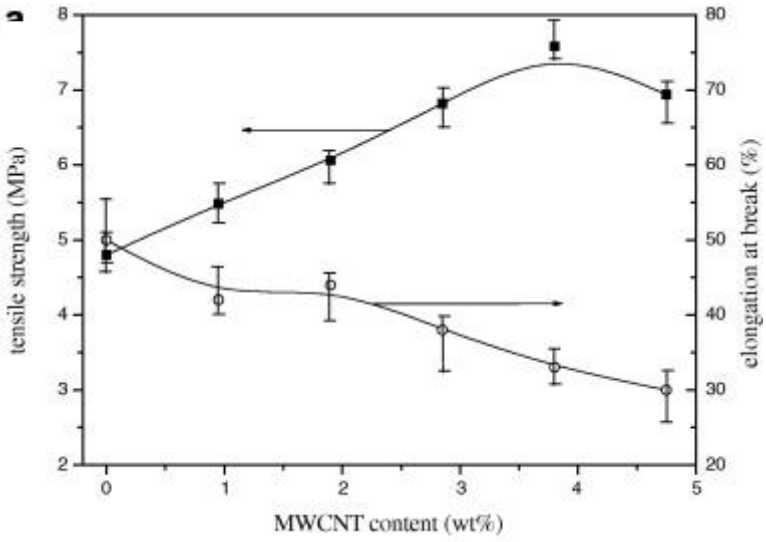

Figure 2-51 Mechanical properties of TPS/MWNT nanocomposites (Ma, Yu & Wang, 2008).

Several biodegradable polyesters like PCL, PLA or PHAs have also been investigated in composite forms. It has been shown that modified or unmodified carbon nanotubes can effectively act as a nucleating agent in different crystalline polymers (Bonnet, Albertini, Bizot, Bernard & Chauvet, 2007; Cao, Chen, Chang & Huneault, 2007; Ma, Yu & Wang, 2008; Mitchell, Bahr, Arepalli, Tour & Krishnamoorti, 2002; Moniruzzaman & Winey, 2006). But in SAXS and WAXS data, no change can be seen in the crystalline pattern of the polymers. Also, crystallinity percentage variation is a kind of dilemma. For example, in polypropylene it increases, but in PVA it decreases. So we expect the similar results with crystalline polyesters. Il Yun et al. (Il Yun, Gadd, Latella, Lo, Russell & Holden, 2008) recently investigated the incorporation of SWNTs in polyhydroxybutyrate (PHB) using the solution method. They observed that with 1 wt% SWNT, the crystalline size effectively decreased. Although the crystalline size of the polymers decreased in the nanocomposites, because the CNTs had not been completely dispersed, the nano-agglomerates acted as stress concentrators and increased the brittleness of the material. In this paper, no report of agglomeration size in the sample was given, nor any SEM images of CNT distribution.

Thomassin et al. (Thomassin et al., 2007) created MWNT/Polycaprolactone (PCL) composites using melt blending and coprecipitation and achieved a near uniformly dispersed CNT in PCL. They also showed that the thicker the CNTs, the more defects occur on the nanotube walls, so they are easily broken up in the melt blending process. In a recent work (Wu, Zhang, Zhang &

Yu, 2009), MWNTs were incorporated with PLA/PCL, and it was found that nanotubes could remarkably decrease the phase size of PLA when PCL was used as matrix (PCL/PLA 70/30 wt%). Acid functionalization of nanotubes could make them move partially to the interface while virgin nanotubes were preferentially located in the PCL matrix. In a follow-up study, Wu et al. (Wu et al., 2011) investigated the effect of the viscosity ratio on localization and observed that by reducing PCL viscosity, nanotubes migrated to their thermodynamically preferred phase (PLA).

2.5 **Literature review conclusion**

It is observed that starch can be efficiently gelatinized by means of a plasticizer in the presence of heat/shear. The extent of gelatinization and final thermoplastic starch structure is related to several factors such as starch source; plasticizers type; composition or applied heat/shear. A complex and ambiguous combination of these parameters determines the gelatinization temperatures. Some authors believe that water is the main plasticizer for starch, but some others would believe in the independent gelatinization mechanism for both water and the other plasticizers. It is always mentioned in the literature that gelatinization takes place by applying heat/shear on starch and plasticizer slurry. However, the pure effect of shear is never disintegrated from heat. So it is not known if in TPS processing we need high shears to be applied on the slurry or if it does not have an effect on gelatinization temperature and the way it proceeds. Hence there are two issues still ambiguous on the gelatinization phenomenon:

- The effect of the molecular structure/molecular weight/water solubility of the plasticizer on gelatinization phenomenon;
- The absolute effect of pure shear on the gelatinization phenomenon independent of heat or plasticizer type.

Thermoplastic starch, as a mixture of a plasticizer with starch, is now processable with conventional polymer processing equipments such as extruders or injection molding machines. This is a very interesting material to be used in plastics industry because of several advantages such as high availability, renewability and biodegradability. But due to its highly hygroscopic nature and very weak mechanical properties, it can not be used in pure form and hence, it should be blended with other polymers. Additionally, pure starch is thermally stable up to 265 ˚C, but a plasticizer like glycerol which is the mostly used plasticizer in TPS materials, is not as stable as

starch so the maximum processing temperature is limited by the stability of the glycerol. For example, at processing temperature of HDPE (180 ˚C), TPS would already lose 10% of glycerol. Moreover, in processes such as film blowing a significant amount of plasticizer surface migration is observed. The moisture sensitivity of the plasticizer is another problem adding up to the drawbacks of thermoplastic starch. Hence, the use of thermally stable and less hygroscopic plasticizers will improve the processing properties as well as their shelf life. So there is certainly a need to introduce new TPS structures which can also result in acceptable morphology and mechanical properties in its blends with other polymers, compared with glycerol-TPS.

It was observed that the incorporation of carbon nanotubes in polymers may result in significantly improved properties such as mechanical, optical, electrical and thermal properties. In polymer blends, they can influence the morphology of the blends by changing the viscosity ratio, acting as interfacial stabilizers or suppressing the coalescence. But all of these effects are directly related to the localization of the carbon nanotubes. This issue has been the subject of numerous studies. Depending on the structure of polymers, surface properties of nanotubes and the applied process, it is shown that the localization can be quite different. Hence, this phenomenon is still too complex to be able to predict in all cases. It is more a compromise between several parameters that determine the nanofillers localization. Normally the comparisons in the localizations are done by different methods such as solution or melt processing. Meanwhile, within the melt processing techniques, up to the knowledge of the author, there is not a comprehensive study on the effect of different shear fields on the localization and morphology of filled polymer blends. This is an important issue since in the polymer science and industry there are several melt processing machines that are used to prepare blends and composites which although they are in the category of the melt processing, they have different shear fields. Since the viscoelastic properties of the majority of the polymers are subjected to change in different shear fields, the localization might be significantly altered in each equipment. But the most important issue here will be finding the stable localization of the nanofillers in a polymer blend. So it will be very interesting and informative to reveal the effects of kinetics and thermodynamics on the localization and morphology of the blends and develop the skill to control this localization and morphology.

The physics of the polymers are also greatly affected by incorporation of the nanotubes. Due to the nano size and molecular level interactions between nanotubes surface and polymer chains, the

supramolecular structure of the polymers can be altered more profoundly compared to the case of conventional micron size filler counterparts. Again in this issue a lot of discrepancies are observed in the literature. Depending on the type of the nanotubes, their content and processing conditions, different and sometimes opposite effects are observed. Since the polymers supramolecular structure controls the properties of the polymers and there is no method to virtually predict the extent of this effect, it is necessary to study these effects on the filled polymer blends.

Chapitre 3 **ORGANIZATION OF THE ARTICLES**

The first part of this thesis is dedicated to study the structure of thermoplastic starch. The first article is entitled: “Effect of High Molecular Weight Plasticizers on the Gelatinization of Starch under Static and Shear Conditions”. Due to the mentioned drawbacks of glycerol in TPS blends as well as to understand the combinational effect of plasticizer structure on the gelatinization phenomenon, two new plasticizers are introduced to the family of starch plasticizers. Diglycerol and polyglycerol from the polyol polyethers family have been studied along with sorbitol and glycerol. These experiments were conducted in the presence of water under static and dynamic conditions; static meaning only a temperature ramp was applied on the slurry and the required thermal energy for gelatinization was measured calorimetrically. It was followed by optical microscopy to confirm the occurrence of gelatinization by loss of birefringence. In dynamic methods a constant shear was also applied during the temperature ramp. This rheological technique was particularly developed to track the effect of pure shear on starch gelatinization. A large number of experiments were conducted on several starch/water/plasticizer ratios in order to understand the mechanism of gelatinization and determine the effective parameters. Having studied the structural effect, three plasticizers namely glycerol, sorbitol and diglycerol were tested via the dynamic method. This reveals the pure effect of shear on the gelatinization. This article is published in the journal of “Carbohydrate Polymers” (Taghizadeh & Favis, 2012b).

Obtaining the knowledge on the internal structure of thermoplastic starch(TPS) with different plasticizers, and the effect of shear on the gelatinization phenomenon, now we are ready to tackle the performance of TPS in the blends via conventional polymer processing equipments (twin screw extruder). This was conducted according to the patented method in this laboratory (Favis, 2003, 2005). The second paper entitled “High Molecular Weight Plasticizers in Thermoplastic Starch/Polyethylene Blends” addresses the structure-morphology-property relationships of the four types of thermoplastic starch in the blends with HDPE. Due to the immiscible nature of majority of polymer pairs, the use of limited amounts of interfacial modifiers is quite common in polymer blends. So an interfacial modifier, polyethylene-grafted-maleic anhydride, was incorporated in PE/TPS blends (PE/TPS:80/20 wt%). TPS was prepared in a twin screw extruder and PE and compatibilizer was fed into the flow by a side feeding mid-way single screw extruder.

The morphology of as produced strands of the blends were microscopically investigated in SEM. The emulsification curves were made based on the number and volume average droplet size of TPS in PE vs. copolymer content. The critical concentrations were determined for all the plasticizers. Two different behaviours were observed in the emulsification curves for sorbitol and glycerol in one category and diglycerol and polyglycerol in the other category. Further analysis of the structure of TPS and the resulted morphologies led us to decode this difference in morphologies. Mechanical properties were then conducted to evaluate the practical values of the new plasticizers. This paper is published in the "Journal of Materials Science" (Taghizadeh, Sarazin & Favis, 2012).

Due to the outstanding potential of incorporation of nanotubes in the performance of the polymers, carbon nanotubes were added to the TPS blends. The masterbatch of PCL/carbon nanotubes were prepared via solution method. This was then diluted and blended with TPS (PCL/TPS:80/20 wt%) through the same patented process in this laboratory (Favis, Rodriguez & Ramsay, 2003; Favis, Rodriguez & Ramsay, 2005). The most basic step is to determine the stable localization of the nanotubes in the binary blends of PCL/TPS as well as their dispersion level. This was carried out by the application of scanning electron microscopy (SEM) and transmission electron microscopy (TEM). Then their effect on the droplet-matrix morphology of our blends was studied. Due to the importance of kinetics effect on the localization of the nanofillers in polymer blends, the same procedure was carried out via an internal mixer and the results were compared with the former method to determine the thermodynamics and kinetics contributions on the CNT localization. The crystalline structure and transition temperatures of the polymer components were then investigated. These characteristics were investigated by differential scanning calorimetry (DSC) and dynamic mechanical analyses (DMA), respectively. The results of this part have formed the body of the third paper entitled "Carbon Nanotubes in Biodegradable Blends of Polycaprolactone/ Thermoplastic Starch" which is submitted to the journal of "Biomacromolecles" and is under review (Taghizadeh & Favis, 2012a) .

Chapitre 4 EFFECT OF HIGH MOLECULAR WEIGHT PLASTICIZERS ON THE GELATINIZATION OF STARCH UNDER STATIC AND SHEAR CONDITIONS

Ata Taghizadeh, Basil D. Favis*

CREPEC, Department of Chemical Engineering, École Polytechnique de Montréal,

2900 Édouard Montpetit, P.O.Box 6079, Station Centre-Ville, Montréal, Québec,

Canada H3C 3A7

4.1 Abstract

Starch gelatinization in the presence of high molecular weight polyol plasticizers and water was studied under static and dynamic conditions and was compared to a glycerol reference. For static gelatinization, glycerol, sorbitol, diglycerol and polyglycerol were examined using polarized light microscopy and differential scanning calorimetry. A wide range of starch/water/plasticizer compositions were prepared to explore the gelatinization regime for each plasticizer. The plasticizers show that the onset and conclusion temperatures for sorbitol and glycerol are in the same range and are lower than the other two plasticizers. On the other hand, polyglycerol shows a higher gelatinization temperature than diglycerol because of its higher molecular weight and viscosity. The results indicate that in the case of all plasticizers, increasing the water content tends to decrease the gelatinization temperature and, except for polyglycerol, increasing the plasticizer content increases the gelatinization temperature. In the case of polyglycerol, however, increasing the plasticizer content had the opposite effect and this was found to be related to the borderline solubility of polyglycerol in water. When the polyglycerol/water solubility was

increased by increasing the temperature of the water/plasticizer/starch slurry, the gelatinization temperature dependence was found to be similar to the other polyols.

A rheological technique was developed to study the dynamic gelatinization process by tracking the influence of shear on the complex viscosity in a couette flow system. Glycerol, diglycerol and sorbitol were subjected to different dynamic gelatinization treatments and the results were compared with static gelatinization. It is quantitatively shown that shear has a major effect on the gelatinization process. The conclusion temperature of gelatinization is significantly diminished (up to 21˚C) in the presence of shear whereas the onset temperature of gelatinization remains virtually unchanged as compared to static conditions. By comparing glycerol, diglycerol and sorbitol data, it is shown that the molecular weight or structure did not qualitatively affect the changes shear imposed on dynamic gelatinization. Shear had a relatively more pronounced effect on diglycerol as the plasticizer with less hydrogen bonding ability.

Keywords: Thermoplastic Starch; Dynamic Rheological Properties; Shear; Wheat Starch; Gelatinization

4.2 **Introduction**

Starch is a natural homopolymer of two different structural units of α-D-glucose: amylose and amylopectine. These two subcategories are responsible for the crystalline structure of starch which, along with their high molecular weight (~10^6-10^7 Da) (Angles & Dufresne, 2000), cause starch to decompose before reaching its melting point. Due to this characteristic, starch has been used as a filler in the polymer industry for many years (Avella, Errico, Laurienzo, Martuscelli, Raimo & Rimedio, 2000; Averous, 2004; Averous, Moro, Dole & Fringant, 2000; Lawrence, Walia, Felker & Willett, 2004).

The crystalline starch structure is lost when it is subjected to heat at temperatures greater than 70–90 ˚C in presence of plasticizers such as water or glycerol. This process is called gelatinization (Otey, Westhoff & Doane, 1980a). Gelatinization is associated with the loss of

double helices together with the loss of lamellar and long range crystalline structure. In the gelatinization of starch by heat and shear three different phenomena occur successively: fragmentation of starch granules, hydrogen bond cleavage between starch molecules leading to loss of crystallinity, and partial depolymerisation of the starch molecules. Gelatinization requires sufficient chain mobility that can be provided by heat and mechanical energy in the presence of a plasticizer. The compositional mixture of starch and glycerol after gelatinization leads to the so-called "thermoplastic starch (TPS)" (Li, Luo, Wei & Huang, 2006). The more difficult it is for the plasticizer to penetrate the starch amorphous regions -which is affected by plasticizer size and type- the greater the thermal and/or mechanical energy required for the starch chains to gain the sufficient mobility to break down the crystalline structure. The degree of disruption and melting of the crystalline structure of a certain type of starch depends on the plasticizer type, content level and the processing parameters (shear stress, melt viscosity and temperature) (Kim & Kim, 2006). Thus, in order to gelatinize starch a plasticizer is required that is able to reduce the T_g of amorphous parts of starch molecules to be able to undergo decrystallization rather than degradation in the presence of heat (Jacobs & Delcour, 1998; Waigh, Kato, Donald, Gidley, Clarke & Riekel, 2000). By using water as the plasticizer for starch, the granules will absorb water, swell, lose crystallinity and will arrive at an irreversible state of gelatinized starch. Starch will stay in this condition up until the point that plasticizer is exuded from the physical network of starch molecules. When water is solely used for the plasticization, the material becomes brittle with time at room temperature due to water evaporation (plasticizer exudation) that leads to the so called retrogradation phenomenon. Additionally when water is used as the plasticizer, thermoplastic starch properties are highly affected by the ambient humidity conditions (vanSoest, Benes, deWit & Vliegenthart, 1996) . In order to produce a durable thermoplastic starch, it is necessary to use another plasticizer to hinder starch molecular retrogradation and decrease the humidity dependence. Many different kinds of plasticizers have been studied such as glycerol, glucose, sorbitol, ethylene glycol and amides (Adeodato Vieira, da Silva, dos Santos & Beppu, 2011; Nashed, Rutgers & Sopade, 2003; Poutanen & Forssell, 1996). Most of these studies have been carried out for starch prepared films in the food industry. The focus of those articles was mainly the moisture sensitivity and mechanical properties of the films e.g. sorbitol shows superior humidity resistance as compared to glycerol. Glycerol has been the most widely used plasticizer in the industry due to its availability and the final thermoplastic starch mechanical

properties (Averous, 2004) . Nashad et al (Nashed, Rutgers & Sopade, 2003) has reported that glycerol shows strong hydrogen bonding with water which results in its higher water uptake level compared with pure starch. Thus, it might act as an anti-plasticizer in the gelatinization process and increase the water content required for complete gelatinization since it actually decreases the level of available water molecules to penetrate amongst starch chains. Gang et al (Li, Sarazin & Favis, 2008) have shown that the addition of excess water is necessary to reach the gelatinization in the time frame of conventional melt processing. It is believed that water is the main plasticizing agent (Li & Favis, 2010; Li, Sarazin & Favis, 2008) and the accompanying plasticizer integration with starch molecules is preceded by its water solvation and transfer to starch rich areas. So since water is the most active plasticizer in the gelatinization process due to its low molecular weight and high affinity with starch, the affinity of a second plasticizer with water will influence the gelatinization phenomenon. In literature there is one detailed report on the effect of water/plasticizer ratio on gelatinization and only glycerol has been studied there (G. Li, et al., 2008). They have shown that a high water/plasticizer ratio is required to complete the gelatinization process in the time frame of polymer melt processing. Incorporation of higher molecular weight plasticizers have been shown to increase the gelatinization temperatures (Habeych, Guo, van Soest, der Goot & Boom, 2009; Perry & Donald, 2002; Tan, Wee, Sopade & Halley, 2004; van Soest, Bezemer, de Wit & Vliegenthart, 1996). No matter which plasticizer be used to plasticize starch, it should be able to penetrate into amorphous growth regions of starch and by the plasticizing effect (hydrogen bonding, increasing free volume), increases the molecular mobility. This mobility then allows enthalpically driven transitions happen in the starch and gelatinization begins. It is shown that in this process, aside from starch type, the solvent properties are directly influencing the gelatinization temperature. These propertires include viscosity, diffusion rate, molecular weight and hydrogen bonding ability (Tan, Wee, Sopade & Halley, 2004). In fact the major bonding element for starch granules is hydrogen bonding between them (Perry & Donald, 2000),so as the plasticizer is more efficient in hydrogen bonding, the gelatinization will need less thermal energy uptake and the onset temperature will diminish. On the other hand the availability of the plasticizer i.e. the composition, solution concentration and viscosity which determines the diffusion rate is another factor which is determined by viscosity and molecular weight (Sopade, Halley & Junming, 2004; Tan, Wee, Sopade & Halley, 2004).

It has been shown that the gelatinization of starch is facilitated in the presence of mechanical shear during the process through decreasing the required water content (Xue, Yu, Xie, Chen & Li, 2008) . A recent approach developed to study the effect of shear in the gelatinization of starch used a combination of microscopy and a rheoscope rheometer (Yu, Kealy & Chen, 2006). They were able to successfully study some aspects of the gelatinization phenomenon under shear (Chen, Yu, Kealy, Chen & Li, 2007). Some authors have also used the evolution of torque in an internal mixer to show the occurrence of gelatinization (Xue, Yu, Xie, Chen & Li, 2008). These authors have shown the influence of shear rate on the final equilibrium temperature and torque (after gelatinization) in an internal mixer. In a recent study, Teyssandier et al (Teyssandier, Cassagnau, Gerard & Mignard, 2011) studied the gelatinization of wheat starch in a parallel plate geometry and showed the increase in elastic and loss moduli during the process.

The objective of this study is to determine the mechanism and efficacy of gelatinization in presence of high molecular weight polyols in static and dynamic conditions. This will lead to develop a novel approach to analyse the impact of heat and shear separately on the gelatinization process. The effect of plasticizer molecular weight and structure on the gelatinization phenomenon will be revealed by studying different water/plasticizer ratios for four plasticizer systems in static environments (DSC and optical microscopy). Among them are two new plasticizers from polyols family (diglycerol and polyglycerol-3) which are for the first time applied for gelatinization of starch. The investigation of the dynamic gelatinization process by the help of a rheological method for selected plasticizers will determine the effect of shear on gelatinization temperatures. Comparison of static and dynamic methods will differentiate the effect of heat and shear on the gelatinization process which to our knowledge it is for the first time that these effects are being studied separately. This comparison will give us a useful tool to optimize the processing parameters in thermoplastic starch preparation procedure.

4.3 **Experimental**

4.3.1 Materials

The native wheat starch obtained from ADM is composed of 25% amylose and 75% amylopectine. Thermogravmetric analyses showed that the water content of starch granules is around 10%. The glycerol was provided by Labmat with a purity of 99.5% and contained 0.5%

water. D-Sorbitol was purchased from Labmat as pure powder. Diglycerol and Polyglycerol-3 were produced by Solvay Chemicals. Diglycerol having a min 90% purity was mainly composed of α,α′-diglycerol (84%) and α, β-diglycerol isomers. Polyglycerol-3 mainly includes 35-55% triglycerol, 15-30% of diglycerol and the rest is higher molecular weight polyglycerols resulting in a minimum of 85% of diglycerol, triglycerol and tetraglycerol. The physical properties of the plasticizers are shown in Table 4-1.

Table 4-1 Physical properties of the pure plasticizers.

Property	Unit	Glycerol	Sorbitol	Diglycerol	Polyglycerol	Water
Density	gr/cm^3	1.25	1.48	1.27	1.27	1
Glass Transition Temp.	˚C	-65	-9	-54	-45	---
Melting point.	˚C	17	95	----[a]	----[a]	0
Boiling point.	˚C	290	296	205	240	100
Solubility Parameter (δ_x)	$MPa^{1/2}$	35.76	40.33	29.98	26.9	47.9
$(\delta_{plasticizer} - \delta_{water})^2$	MPa	144	57	289	400	---

[a] no melting point was detected in the range of -150˚C to 25 ˚C

4.3.2 Sample Preparation

To study the gelatinization phenomenon in starch, different mixtures of starch/water/plasticizer were mixed in a mixer and kept at room temperature overnight. The day after, they were again mixed in a mixer for 1-2 minutes to homogenize the mixture and do the further analyses. Even though water acts as a plasticizer in starch gelatinization in order to differentiate between water and other plasticizers, plasticizer in this article will refer to glycerol, sorbitol, diglycerol and polyglycerol. The slurry compositions are shown in Table 4-2. As the slurries are composed of starch/water/plasticizer, the abbreviations for the slurries are the following: SWG# for glycerol, SWSo# for sorbitol, SWD# for diglycerol and SWP# for polyglycerol systems.

Table 4-2 Starch/water/plasticizer mixtures in weight ratio. SWG: glycerol, SWSo: sorbitol, SWD: diglycerol and SWP: polyglycerol system.

	Starch	Water	Plasticizer
SW**G1**	100	30	65
SW**G2**	100	50	65
SW**G3**	100	70	65
SW**G4**	100	100	65
SW**G5**	100	65	30
SW**G6**	100	65	50
SW**G7**	100	65	70
SW**G8**	100	65	100

4.3.3 Polarized-Light Microscopy

In order to visualize the gelatinization phenomenon under static conditions, a Nikon OPTIPHO-2 polarized-light microscope with a Mettler FP82-HT hot stage was used. Using the birefringence properties of anisotropic (crystalline) materials under crossed polarized light, the morphology of starch granules was recorded. In order to provide the same processing conditions for gelatinization as the DSC tests, the samples were heated from 30 to 150 ˚C at a heating rate of 5 ˚C .min^{-1}. The onset temperature (T_o) was the temperature at which the granules began losing their birefringence and, accordingly the conclusion temperature (T_c) was the point where the birefringence was completely lost.

4.3.4 Differential Scanning Calorimetry

In order to obtain the gelatinization temperature of the samples, DSC tests have been conducted on the samples using a differential scanning calorimetry instrument (*DSC Q1000, TA instruments*) at a heating rate of 5˚C.min^{-1} from 30 to 150 ˚C with an empty sample pan as the reference. Hermetic pans were used with a sample (starch mixtures) mass of (10-15 mg) and were then sealed using a volatile sample sealer accessory. Universal Analysis™ software was used to determine the onset (T_o), peak (T_p), and conclusion (T_c) temperatures associated with the

gelatinization of wheat starch. Onset and conclusion temperatures were the onset and completion of endothermic peaks in DSC curves, respectively, determined by TA Universal Analyses software.

4.3.5 Rheometry

Rheological characterizations of the slurries were performed in oscillation mode using an AR-2000 stress controlled rheometer from *TA instruments.* The experiments were performed in couette flow geometry with a serrated surface. A stress sweep test was run to define the region of linear viscoelasticity. Then at a shear rate of 6.283 rad/s, a temperature ramp of 5˚C.min^{-1} from 30 to 150˚C was conducted on the samples with a controlled oscillating stress. The temperature where the complex viscosity started increasing is defined as the onset temperature and the temperature where it reaches the plateau is considered as the conclusion temperature.

In order to measure the viscosities of the slurries a couette flow geometry of MCR301 rheometer from *Anton Paar* was used. The procedure was a constant shear rate with temperature ramp of 5˚C.min^{-1} from 25˚C to 70˚C.

4.3.6 Surface Tension Measurements

For glycerol and sorbitol, the surface tension values can be found in the literature. The literature does not provide this data for the other two plasticizers, diglycerol and polyglycerol. Since they are viscous liquids; the Wilhelmy Plate technique was used. In order to verify the reliability of the results, the surface tension of glycerol was also measured by this method and compared with data reported in the literature.

The surface tension of the above three plasticizers was measured using a Tensiometer (DCAT 21) from Future Digital Sci. Corp. equipped with Wilhelmy plate. In this method a vertical platinum plate, which is roughened to ensure complete wetting, is attached to a tensiometer. Prior to the test the plate was completely wetted by respective sample. The plate was first immersed in the liquid and then pulled upward. At this point the liquid tends to contract the surface area, as it was expanded by the plate, by pulling down the plate. The counteracting force (F) is then measured by the instrument. Surface tension was further calculated through Wilhelmy equation. The surface tension is then related to the solubility parameter by the following equation (Shacklette & Han, 1994):

$$\delta = (14 \ \sigma . \nu^{-1/3})^{1/2} \quad (1)$$

where δ,σ and ν are the solubility parameter, surface tension and molar volume, respectively. The results are shown in section 4.4.2.

4.4 Results and Discussion

4.4.1 Optical Microscopy

Starch is composed of crystalline parts of amylose and amylopectine and under crossed polarized light the birefringence due to this crystallinity results in a Maltese cross pattern for virgin wheat starch. The gelatinization process disrupts this crystalline structure and leaves an amorphous structure behind which does not show any pattern under polarized light. This method

Table 4-3 Optical microscopy visualized gelatinization results.

STARCH MIXTURE	T_o ˚C	T_c ˚C
SWG2 (S/W/G: 100/**50**/65)	71	93
SWSo2 (S/W/So: 100/**50**/65)	75	95
SWD2 (S/W/D: 100/**50**/65)	85	120
SWP2 (S/W/P: 100/**50**/65)	97	130

has already been used to study the gelatinization of starch in starch/water/glycerol systems (Derby, Miller, Miller & Trimbo, 1975; Li, Sarazin & Favis, 2008; Liu, Charlet, Yelle & Arul, 2002; Palav & Seetharaman, 2006). In this work we examine the loss of birefringence with temperature for a range of different plasticizers and use this optical microscope technique as evidence for the occurrence of static gelatinization. Figure 4-1 and 4-2 demonstrate this gradual loss at different temperatures for glycerol, and polyglycerol at the same water/plasticizer ratios. The onset and conclusion of gelatinization can be clearly observed visually in Figure 4-1 and 4-2. For example in Figure 4-2 the birefringence begins to disappear at around 100 ˚C and finishes at 130 ˚C which corresponds to the onset and conclusion temperatures obtained by DSC below. For the 100/50/65 (dry starch/water/plasticizer) samples it can be seen that glycerol and sorbitol show an almost identical behaviour and have the lowest onset and conclusion temperatures, followed by diglycerol and then polyglycerol (Table 4-3).

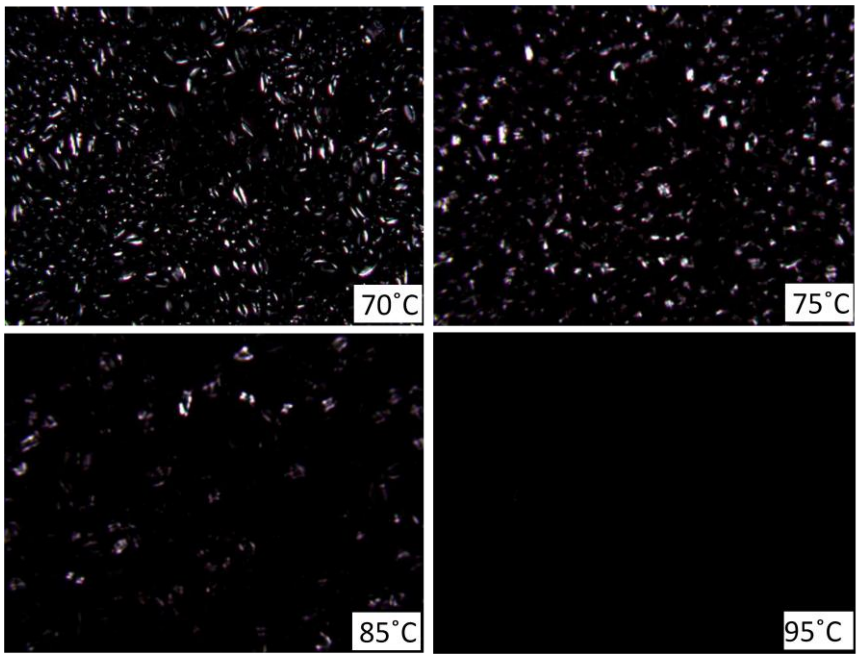

Figure 4-1 Optical microscope observation of starch gelatinization when plasticized by water and glycerol (starch/water/glycerol:100g/50g/65g).

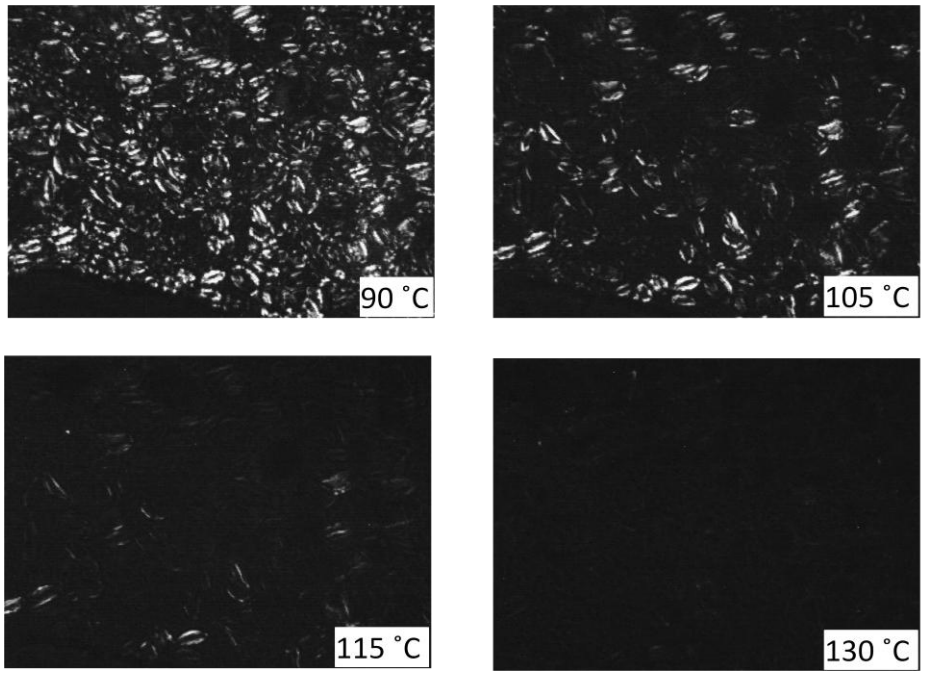

Figure 4-2 Optical microscope observation of starch gelatinization when plasticized by water and polyglycerol (starch/water/polyglycerol:100g/50g/65g).

4.4.2 Differential Scanning Calorimetry (DSC)

Gelatinization phenomenon is a first order transition in starch (Zanoni, Schiraldi & Simonetta, 1995) which produces an endothermic enthalpy peak in DSC thermograms. This DSC analysis allows for the study of samples over a wide range of water/glycerol/dry starch contents. The onset temperature for gelatinization (T_o), the peak temperature (T_P) and the conclusion temperatures (T_c) for the different plasticizers are listed in Table 4-4 and are shown graphically in 4-3 to 4-6. The DSC experiments were controlled in two ways which allowed for the observation of increased water and plasticizer content on the gelatinization process. Firstly, the water content in the water/glycerol/starch mixture was modified and the glycerol and starch content was held constant at 65/100 wt%. In the second series of tests the plasticizer content was varied and the water and starch content was held constant at 65/100 wt%.

Table 4-4 DSC characteristics of starch/water/plasticizer mixtures at various compositions: (a) sorbitol; (b) diglycerol.

STARCH MIXTURE	T_o ˚C	T_P ˚C	T_c ˚C
SWSo1 (S/W/So[a]: 100/**30**/65)	81	85	96
SWSo2 (S/W/So: 100/**50**/65)	76	80	90
SWSo3 (S/W/So: 100/**70**/65)	71	75	86
SWSo4 (S/W/So: 100/**100**/65)	68	72	81
SWSo5 (S/W/So: 100/65/**30**)	62	68	78
SWSo6 (S/W/So: 100/65/**50**)	69	74	85
SWSo7 (S/W/So: 100/65/**70**)	66	71	89
SWSo8 (S/W/So: 100/65/**100**)	73	78	92

[a]S/W/So : Starch/Water/Sorbitol wt%

(a)

Table 4-4 Cont'd.

STARCH MIXTURE	T_o ˚C	T_P ˚C	T_c ˚C
SWD1 (S/W/D[a]: 100/**30**/65)	93	98	123
SWD2 (S/W/D: 100/**50**/65)	87	91	115
SWD3 (S/W/D: 100/**70**/65)	81	86	105
SWD4 (S/W/D: 100/**100**/65)	76	79	97
SWD5 (S/W/D: 100/65/**30**)	71	76	87
SWD6 (S/W/D: 100/65/**50**)	77	83	107
SWD7 (S/W/D: 100/65/**70**)	83	88	109
SWD8 (S/W/D: 100/65/**100**)	90	95	115

[a]S/W/D : Starch/Water/Diglycerol wt%

(b)

Table 4-4 and Figures 4-3 to 4-4 clearly show that over a wide range of starch/plasticizer/water compositions, the gelatinization temperatures increase in the following manner: from glycerol and sorbitol, which show similar behaviours, to diglycerol and finally polyglycerol. The latter two show a considerable increase in gelatinization temperatures. It should be noted that in going from glycerol to diglycerol and polyglycerol there is an important increase in the viscosity of the slurry solution (see Figure 4-5).

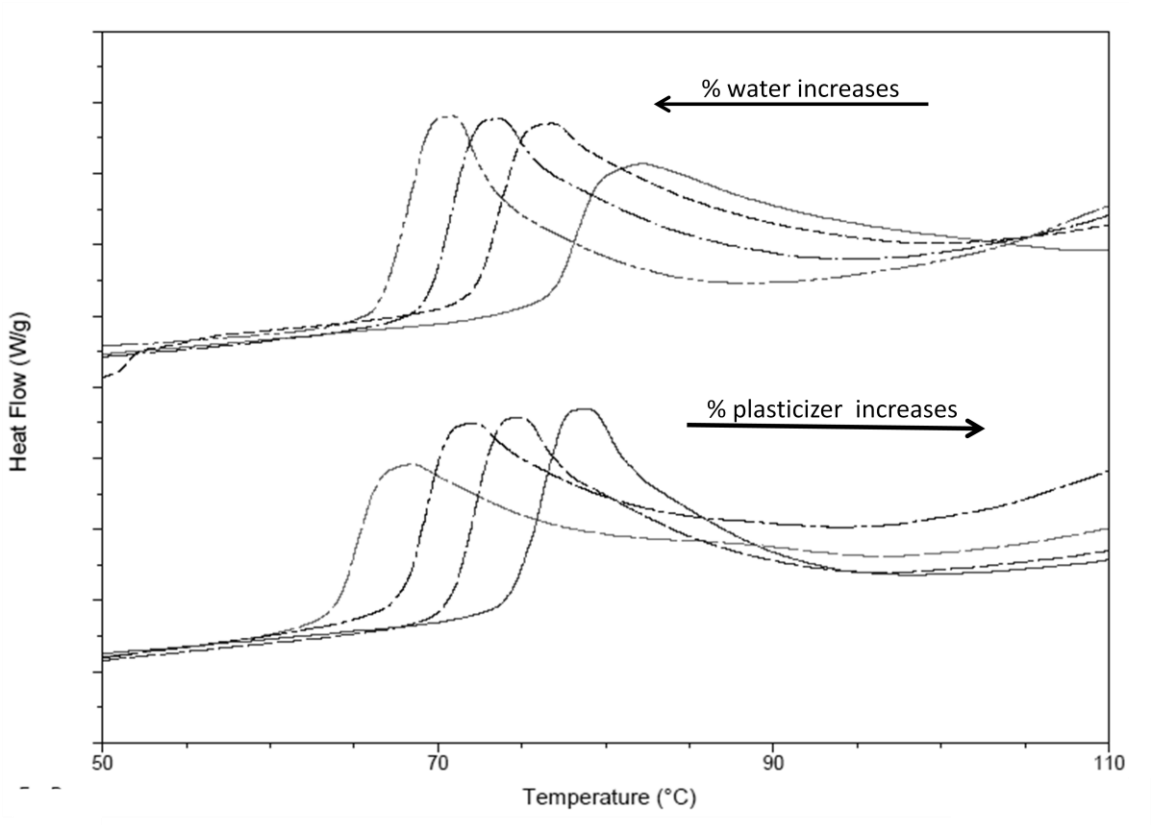

Figure 4-3 DSC traces of gelatinization for starch/water/glycerol systems after isothermal treatment at room temperature for 12 hrs. Upper set, constant starch/glycerol: 100g/65g, with increasing water: 30g(SWG1), 50g(SWG2), 70g(SWG3), 100g(SWG4). Lower row, constant starch/water: 100g/65g, with increasing glycerol: 30g(SWG5), 50g(SWG6), 70g(SWG7), 100g(SWG8).

It is believed that the crystallinity of starch is disrupted in two distinct steps independent of the type of plasticizer used (Perry & Donald, 2000, 2002). First is the plasticization which is mainly controlled by the ingress and diffusion of plasticizer into the amorphous parts of the complex starch granule structure (Antonio J.F, 2008). Independent of the type of plasticizer used, this plasticization step has been shown to be an essential precondition for the onset of gelatinization (Perry & Donald, 2002; Tan, Wee, Sopade & Halley, 2004). During that step the amorphous parts of starch gain a certain degree of freedom and molecular activity. In the second step, this mobility ascends to a level such that helix-coil irreversible transition initiates and the crystalline structure begins to disrupt; that is called gelatinization (second step). During gelatinization, starch-starch

hydrogen bonds should be disrupted and at the same time starch-solvent hydrogen bonding should be built (Antonio J.F, 2008; Tan, Wee, Sopade & Halley, 2004).

The dynamics of the plasticization process discussed above will have an influence on the gelatinization temperature. Considering that the most important structural element building the starch crystalline structure is the starch-starch hydrogen bonding (Antonio J.F, 2008), by increasing the hydrogen bonding capacity of the plasticizers, the lamellar plasticization can be reached at lower temperatures (Perry & Donald, 2000; Waigh, Gidley, Komanshek & Donald, 2000).

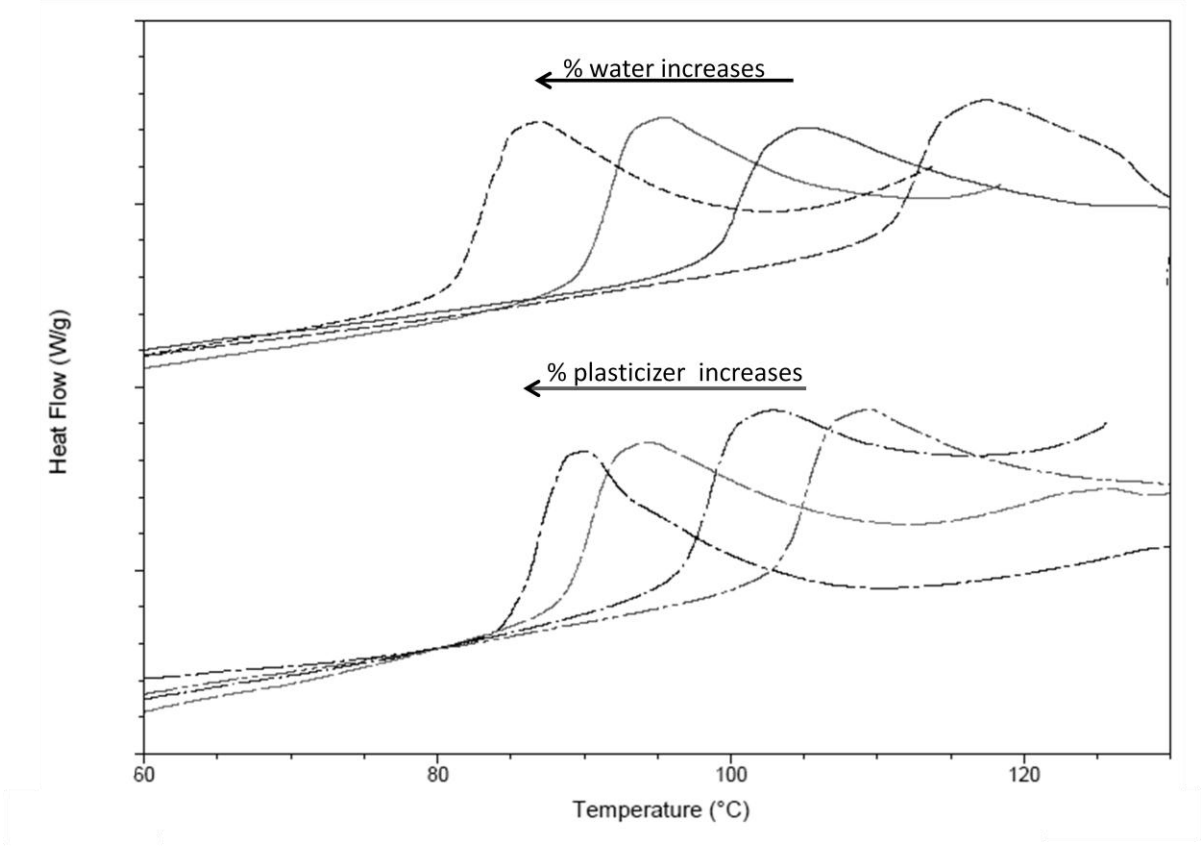

Figure 4-4 DSC traces of gelatinization for starch/water/polyglycerol systems after isothermal treatment at room temperature for 12 hrs. Upper set, constant starch/polyglycerol: 100g/65g, with increasing water: 30g(SWP1), 50g(SWP2), 70g(SWP3), 100g(SWP4). Lower row, constant starch/water: 100g/65g, with increasing polyglycerol: 30g(SWP5), 50g(SWP6), 70g(SWP7), 100g(SWP8).

Tan et al (Tan, Wee, Sopade & Halley, 2004) recently showed that in addition to the hydrogen bonding ability of plasticizers, the solvent transport ability in granules of starch is of great importance in determining the gelatinization temperature. This ability is determined by parameters like molecular weight, viscosity and diffusion rate (Perry & Donald, 2000; Tan, Wee, Sopade & Halley, 2004; Ternstrom, Sjostrand, Aly & Jernqvist, 1996). The amount of energy or molecular mobility which a certain type of plasticizer can provide to starch is another factor. It is shown that polyols cannot introduce the same level of degree of freedom that water can give to polysaccharides (Kilburn, Claude, Schweizer, Alam & Ubbink, 2005). Thus even if the ingression has reached higher levels (e.g. by long time solution conditioning), the amount of energy that is needed for the amorphous parts to reach the max level of mobility is increased in presence of polyol plasticizers as compared to water (Perry & Donald, 2002).

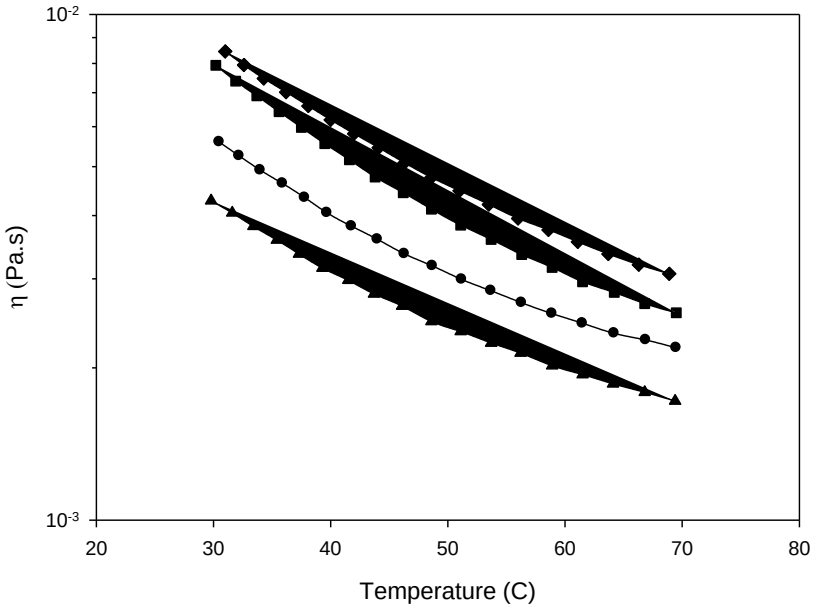

Figure 4-5 Viscosity evolution by temperature for plasticizer/water (50/50 wt%) solutions: (▲) Glycerol, (●) Diglycerol, (■) Sorbitol, (♦) Polyglycerol.

On the other hand water activity can be retarded in the presence of polyols due to their high affinity with water in such a way that over a certain ratio of plasticizer/water, the plasticizers compete with starch in bonding with water molecules (Godbillot, Dole, Joly, Roge & Mathlouthi, 2006; Mali, Sakanaka, Yamashita & Grossmann, 2005). It is also shown that the ingress rate of plasticizers in polysaccharides is greatly dependent upon the molecular weight of plasticizers

(Smits, Kruiskamp, van Soest & Vliegenthart, 2003) and the water concentration in water/polyol mixtures (Ternstrom, Sjostrand, Aly & Jernqvist, 1996). It is interesting to note that despite the higher viscosity of sorbitol as compared to glycerol, these two plasticizers show a virtually identical set of gelatinization temperatures. It has been already shown that a higher molecular weight of plasticizer would have a tendency to increase the gelatinization temperature according

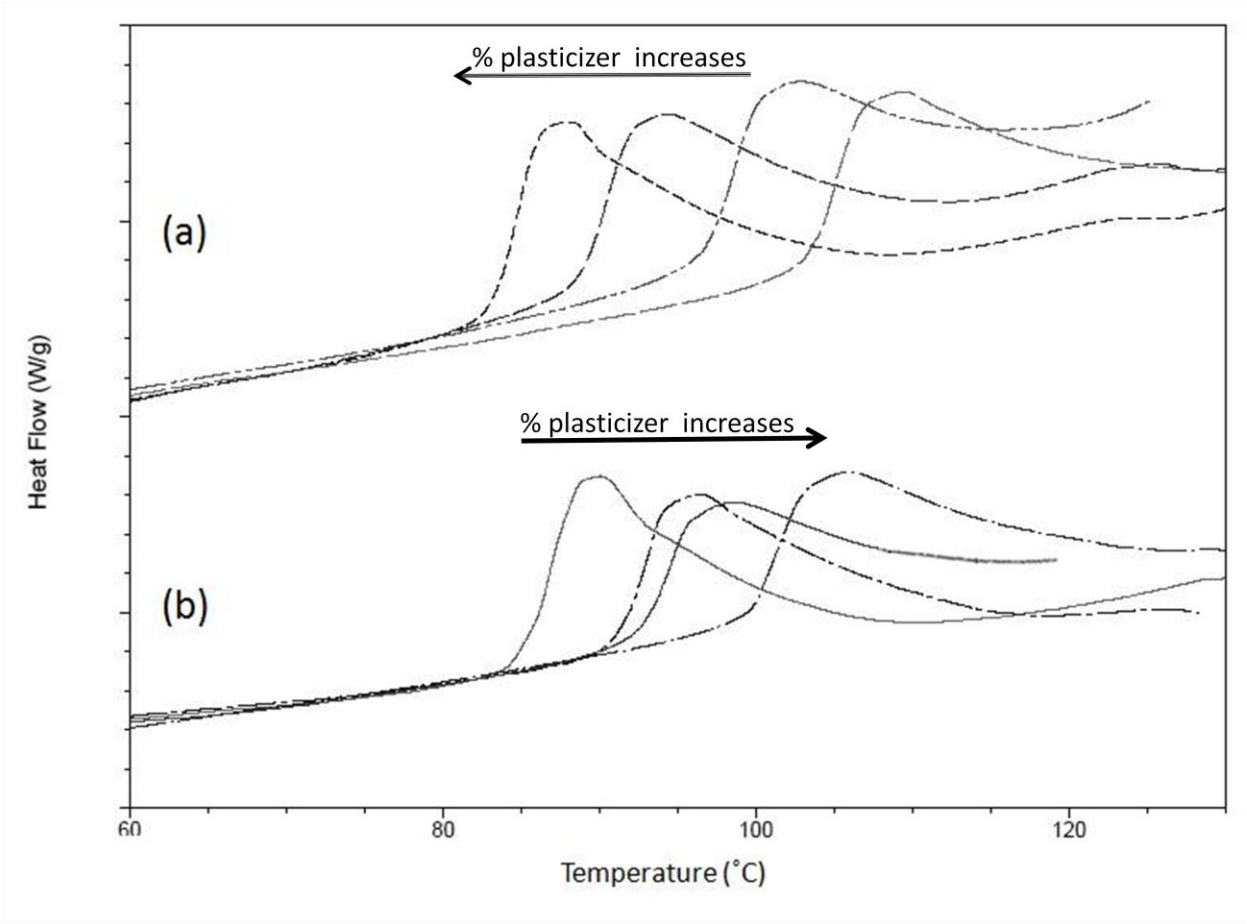

Figure 4-6 DSC traces of gelatinization for wheat starch/water/polyglycerol systems after isothermal treatment: (a) at room temperature for 12 hrs, (b) at 50˚C for 12 hrs. Constant starch/water: 100g/65g, with increasing polyglycerol: 30g(SWP5), 50g(SWP6), 70g(SWP7), 100g(SWP8).

to free-volume theory (Shacklette & Han, 1994). On the other hand the density of hydroxyl groups can also affect the hydrogen bonding ability of the plasticizers (Perry & Donald, 2000). For example in the case of sorbitol (M_w: 182 g.mol^{-1}) and glycerol (M_w: 92 g.mol^{-1}), although

sorbitol has a higher molecular weight, it has the same hydroxyl group density as glycerol. Due to the various conformational structures (Lerbret et al., 2009) that sorbitol can adopt, it has been shown to have a higher level of interaction with starch than glycerol (Garcia, Martino & Zaritzky, 2000; Mali, Sakanaka, Yamashita & Grossmann, 2005). This high level of interaction likely counterbalances any plasticization retarding effect due to the higher viscosity or molecular weight of the sorbitol and it demonstrates onset and conclusion gelatinization temperatures similar to glycerol.

In the case of diglycerol (M_w: 166 g.mol^{-1}) it has a similar molecular weight to sorbitol and, despite its lower slurry viscosity than sorbitol (Figure 4-5), it shows higher onset gelatinization temperatures. This can be attributed to the lower density of hydroxyl bonds which affects its plasticizing ability, hence the gelatinisation temperature increases (Perry & Donald, 2000). For the case of polyglycerol, the molecular weight ($M_w \approx$250 g.mol^{-1}) as well as the slurry viscosity is high and it has a hydroxyl group density which is low as compared to the other plasticizers. All these factors combined contribute to the significantly higher gelatinization temperatures observed for polyglycerol.

For glycerol, sorbitol, diglycerol and polyglycerol, when the plasticizer/starch content is held constant at 65/100 wt% and the water content is increased, the gelatinization peaks shift to lower temperatures (Table 4-4). This is quite expected because of the increasing water content and the better efficacy of water as a plasticizer of starch. It is also supported by the fact that increased water content decreases the slurry viscosity and improves the diffusion rate into the starch granules. Conversely, when the water mass is held constant and the plasticizer content is increased, the gelatinization temperature increases for glycerol, sorbitol and diglycerol as expected. Polyglycerol, however, provides a very different behaviour. Figure 4-4 shows that when the water/starch ratio is held constant and the polyglycerol plasticizer content is increased, the gelatinization temperatures for this plasticizer are moved to lower temperatures.

In order to further understand this anomalous behavior of polyglycerol, we estimated the solubility parameters and the main enthalpic term for water and the various plasticizers (Table 4-1). It can be seen that the enthalpic tendency for mixing for polyglycerol is the least amongst the various plasticizers. Thus, polyglycerol has the least tendency for solubilisation in water and sorbitol has the highest. As already mentioned, water is a key factor in plasticizing starch. In

order to test this hypothesis, the slurry temperature was increased for the polyglycerol sample and under those conditions, the normal trend of onset temperature augmentation is observed (Figure 4-6) thus confirming the solubility issue with polyglycerol.

Irrespective of the type of the plasticizer, initiation of gelatinization requires a certain level of plasticization of starch molecules. Any parameter influencing a) the efficacy of plasticizer penetration into starch granules and disruption of the existing crystalline structure, b) the water/plasticizer-starch hydrogen bonding or water/plasticizer availability for starch and c) the water/plasticizer ingress rate will affect the required thermal energy required to disrupt the crystalline structure and consequently will effect gelatinization temperatures. It should be noted that a number of these factors determining the gelatinization temperature are interrelated and it is difficult to isolate the clear role of each.

4.4.3 Effect of Shear on Gelatinization

The gelatinization of starch results in the transformation of the plasticizer/water/starch mixture from a suspension of starch particles in low molecular weight fluids to a gel-like fluid whose characteristics are dominated by the high molecular weight starch molecules. Gelatinized starch shows a pronounced shear thinning behaviour over the whole frequency sweep range (Li & Favis, 2010). This behaviour is attributed to the existence of a hydrogen bonding network between plasticizer and starch molecules as well as the physical network of starch molecules (macromolecular entanglements) or remaining crystallinity in starch molecules (Rodriguez-Gonzalez, Ramsay & Favis, 2004).

As mentioned earlier, gelatinization can proceed under static conditions in the presence of heat and a plasticizer, but in conventional polymer processing equipment such as extrusion, the gelatinization is conducted under dynamic conditions where different shear fields are engaged (Huneault & Li, 2007; Rodriguez-Gonzalez, Ramsay & Favis, 2003; Taguet, Huneault & Favis, 2009; Willett & Shogren, 2002). This part examines the potential of tracking the real effect of shear in the gelatinization process using a controlled rheological technique outlined in the experimental section.

Table 4-5 Comparison of onset and conclusion gelatinization temperatures from DSC and rheology for glycerol.

	T_o (DSC) (˚C)	T_o (Rheology) (˚C)	T_c (DSC) (˚C)	T_c (Rheology) (˚C)
SWG1 (S/W/G: 100/30/65)[a,b]	77	77	101	83
SWG2 (S/W/G: 100/50/65) [b]	72.4	74	91	82.9
SWG3 (S/W/G: 100/70/65) [b]	69.4	70	88	79
SWG4 (S/W/G: 100/100/65) [b]	66.7	67.4	83	74
SWG5 (S/W/G: 100/65/30) [c]	64.1	64.8	80.9	76
SWG6 (S/W/G: 100/65/50) [c]	68	68.3	85.6	77
SWG7 (S/W/G: 100/65/70) [c]	70.9	71	89.5	79
SWG8 (S/W/G: 100/65/100) [c]	74.7	76	91.5	84

[a] S/W/G : Starch/Water/Glycerol weights in g; [b] Plasticizer weight constant; [c] Water weight constant.

Figures 4-7 and 4-8 show the rheological curves of viscosity evolution with temperature for different wheat starch/water/plasticizer ratios. The same approach was used as in the static work reported above: in one case the composition of plasticizer/starch is held constant and water content is increased (Figures 4-7(a) and 4-8(a)); and in the other case the composition of starch/water is held constant and plasticizer content is increased (Figures 4-7(b) and 4-8(b)). The curves demonstrate a sharp increase in complex viscosity of the mixture during gelatinization. Both increasing the water content series and increasing the plasticizer content series show similar trends as that observed in the static DSC tests (Figure 4-3) and the polarized

light microscope observations i.e. the gelatinization temperature decreases when increasing the water/starch ratio and the gelatinization temperature increases when the plasticizer/starch ratio increases.

Table 4-6 Comparison of onset and conclusion gelatinization temperatures from DSC and rheology for sorbitol.

	T_o (DSC) (˚C)	T_o (Rheology) (˚C)	T_c (DSC) (˚C)	T_c (Rheology) (˚C)
SWSo1 (S/W/So: 100/30/65) [a, b]	81	80	96	88
SWSo2 (S/W/So: 100/50/65) [b]	76	77	90	79
SWSo3 (S/W/So: 100/70/65) [b]	71	70	86	75
SWS4 (S/W/So: 100/100/65) [b]	68	67	81	72
SWSo5 (S/W/So: 100/65/30) [c]	62	60	78	68
SWSo6 (S/W/So: 100/65/50) [c]	69	70	85	76
SWSo7 (S/W/So: 100/65/70) [c]	66	68	89	79
SWSo8 (S/W/So: 100/65/100) [c]	73	74	92	81

[a] S/W/So : Starch/Water/Sorbitol weights in g; [b] Plasticizer weight constant; [c] Water weight constant.

It is important to note that some very important differences are observed under shear as compared to static conditions. Table 4-5 to 4-7 shows the comparison between the onset and conclusion temperatures of the different compositions obtained by rheometry and the corresponding temperatures from the DSC for each plasticizer. It is observed that the initiation temperatures for gelatinization from both static (DSC) and dynamic (rheological) techniques closely correspond to each other and shear has virtually no effect on the onset temperature of gelatinization. However, the conclusion temperatures drop considerably under shear conditions as compared to the static DSC results.

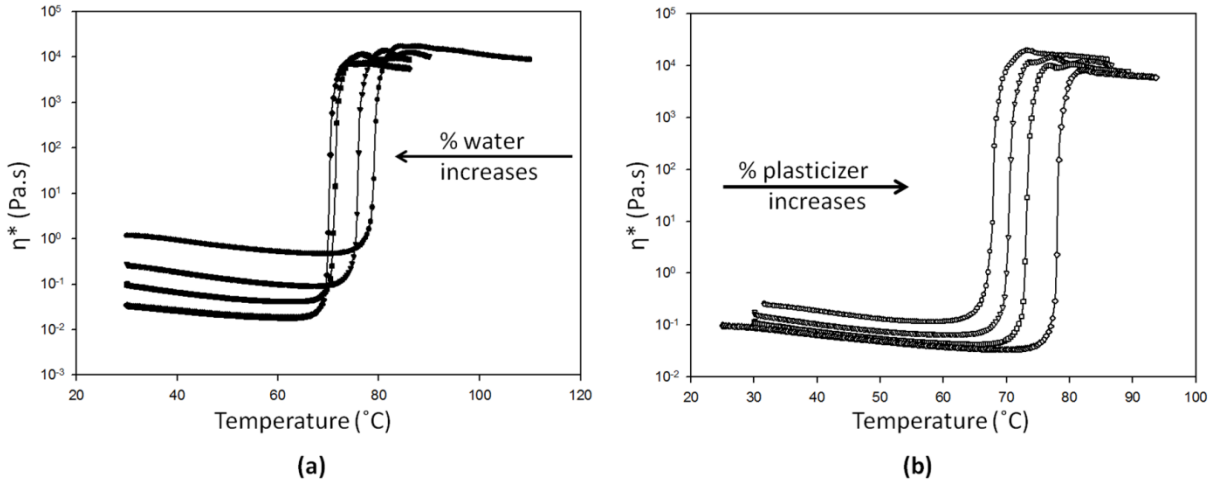

Figure 4-7 Rheological traces of gelatinization for starch/water/glycerol (S/W/G) systems at different compositions: (a) Constant starch/glycerol: 100g/65g, with increasing water: 30g(SWG1), 50g(SWG2), 70g(SWG3), 100g(SWG4), (b) Constant starch/water: 100g/65g, with increasing glycerol: 30g(SWG5), 50g(SWG6), 70g(SWG7), 100g(SWG8).

As discussed in the previous section, in order for gelatinization to occur, the amorphous parts of starch requires a certain level of energy in order to gain enough mobility to be able to begin disruption of helix-helix interactions in crystalline parts. This energy is partly obtained by plasticizer ingress into starch structure and completed afterwards by thermal energy input. Shear would be expected to have a particular influence on plasticizer ingress rates. Note however that the onset temperature for gelatinization is likely related to the onset of gelatinization of the most

accessible layer of starch granule. Following that, plasticization-gelatinization takes place in other parts of the starch granule. The plasticizer ingression to the amorphous parts continues up until the peak gelatinization temperatures (Donald, Kato, Perry & Weigh, 2001). These results suggest that ingress rates have little influence on the onset temperature, but are critical in determining the conclusion temperature.

Table 4-7 Comparison of onset and conclusion gelatinization temperatures from DSC and rheology for diglycerol.

	T_o (DSC) (˚C)	T_o (Rheology) (˚C)	T_c (DSC) (˚C)	T_c (Rheology) (˚C)
SWD1 (S/W/D: 100/30/65) [a, b]	93	92	123	102
SWD2 (S/W/D: 100/50/65) [b]	87	88	115	103
SWD3 (S/W/D: 100/70/65) [b]	81	82	105	91
SWD4 (S/W/D: 100/100/65) [b]	76	77	97	88
SWD5 (S/W/D: 100/65/30) [c]	71	71	87	81
SWD6 (S/W/D: 100/65/50) [c]	77	78	107	88
SWD7 (S/W/D: 100/65/70) [c]	83	84	109	94
SWD8 (S/W/D: 100/65/100) [c]	90	92	115	102

[a] S/W/D : Starch/Water/Diglycerol weights in g; [b] Plasticizer weight constant; [c] Water weight constant.

These results highlight the important consideration that will need to be given to the effect of residence time on gelatinization in extrusion processes where the residence time is normally very limited (<2min). The conclusion temperature of gelatinization can be significantly influenced by mixing conditions. Consequently, the initiation temperature for gelatinization of starch appears to be controlled by the efficacy of the plasticizer in plasticizing the amorphous parts of starch and shear has virtually no effect on it. The conclusion temperature, on the other hand, demonstrates the characteristics of a parameter which is more kinetically controlled. Improvements to the mixing efficacy (i.e. plasticizer ingress into starch granules) will assist the disintegration of starch crystals and the principal effect will be a drop in the conclusion temperature.

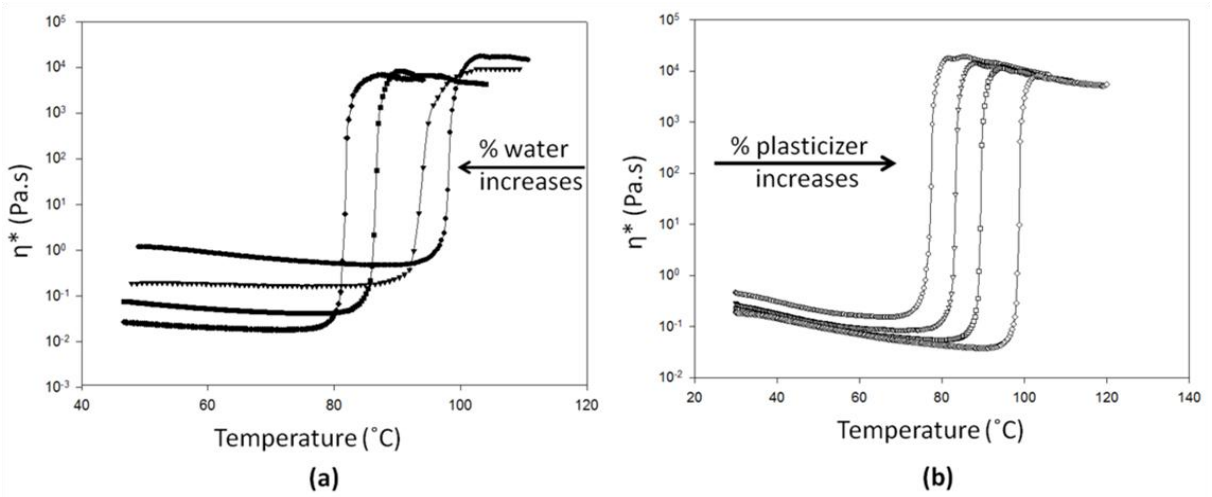

Figure 4-8 Rheological traces of gelatinization for wheat starch/water/diglycerol (S/W/D) systems at different compositions: (a) Constant starch/diglycerol: 100g/65g, with increasing water: 30g(SWD1), 50g(SWD2), 70g(SWD3), 100g(SWD4), (b) Constant starch/water: 100g/65g, with increasing diglycerol: 30g(SWD5), 50g(SWD6), 70g(SWD7), 100g(SWD8).

4.5 **Conclusions**

In this work a detailed study of the gelatinization regime at various starch/water/plasticizer ratios has been conducted for four different plasticizers. Optical microscopy is used to confirm the occurrence of gelatinization for all the plasticizers during which the starch granules lose their birefringence. Static gelatinization has also been investigated with DSC tests. The onset and

conclusion gelatinization temperatures for the different plasticizers increase in the following order:

Glycerol ≈ Sorbitol << Diglycerol < Polyglycerol

Glycerol and sorbitol have very similar gelatinization temperatures. The ascending gelatinization temperature from glycerol to diglycerol and polyglycerol was attributed to the viscosity and molecular weight increase and hydroxyl bond density diminution of the latter two plasticizers. Comparing the gelatinization temperatures of sorbitol and diglycerol, with similar molecular weights, the former is shown to have a higher efficacy in starch gelatinization than diglycerol. This is most likely due to the higher hydroxyl group density of sorbitol and its higher level of interaction with water. All of the above plasticizers demonstrate a lower gelatinization temperature when the water/starch ratio is increased, due to the efficacy of water in plasticizing starch. Conversely, when the plasticizer/starch ratio is increased, the gelatinization temperature increases for glycerol, sorbitol and diglycerol. Polyglycerol shows an anomalous behavior and the gelatinization temperature is found to drop when increasing the plasticizer/starch ratio. This was found to be the result of the limited water solubility of polyglycerol. When the slurry temperature for the polyglcerol suspension is increased, the trend of increasing gelatinization temperature with increasing plasticizer/starch ratio is observed.

The effect of shear on gelatinization is examined through a detailed rheological investigation conducted on the glycerol, diglycerol and sorbitol slurries. It is found that the onset gelatinization temperatures for glycerol, sorbitol and diglycerol are independent of the applied shear and are identical to that observed under static conditions. The conclusion temperature, on the other hand, drops considerably upon application of shear as compared to the static data. It demonstrates the characteristics of a parameter which is more kinetically controlled and which could be significantly influenced by mixing conditions.

Acknowlegments

The authors would like to thank the Teknor Apex Company for supporting this work and Dr. Pierre Sarazin of Cerestech Inc. for helpful discussions.

4.6 References

[1] M. N. Angles, A. Dufresne, *Macromolecules* **2000**, *33*, 8344.

[2] M. Avella, M. E. Errico, P. Laurienzo, E. Martuscelli, M. Raimo, R. Rimedio, *Polymer* **2000**, *41*, 3875.

[3] L. Averous, *Journal of Macromolecular Science-Polymer Reviews* **2004**, *C44*, 231.

[4] L. Averous, L. Moro, P. Dole, C. Fringant, *Polymer* **2000**, *41*, 4157.

[5] S. S. Lawrence, P. S. Walia, F. Felker, J. L. Willett, *Polymer Engineering and Science* **2004**, *44*, 1839.

[6] F. H. Otey, R. P. Westhoff, W. M. Doane, *Ind. Eng. Chem. Prod. Res. Dev* **1980**, *19*, 4.

[7] Z. F. Li, G. H. Luo, F. Wei, Y. Huang, *Composites Science and Technology* **2006**, *66*, 1022.

[8] J. Y. Kim, S. H. Kim, *Journal of Polymer Science Part B-Polymer Physics* **2006**, *44*, 1062.

[9] T. A. Waigh, K. L. Kato, A. M. Donald, M. J. Gidley, C. J. Clarke, C. Riekel, *Starch-Starke* **2000**, *52*, 450.

[10] H. Jacobs, J. A. Delcour, *J. Agric. Food Chem.* **1998**, *46*, 2895.

[11] J. J. G. vanSoest, K. Benes, D. deWit, J. F. G. Vliegenthart, *Polymer* **1996**, *37*, 3543.

[12] M. G. Adeodato Vieira, M. A. da Silva, L. O. dos Santos, M. M. Beppu, *European Polymer Journal* **2011**, *47*, 254.

[13] G. Nashed, P. P. G. Rutgers, P. A. Sopade, *Starch-Starke* **2003**, *55*, 131.

[14] K. Poutanen, P. Forssell, *Trends in Polymer Science* **1996**, *4*, 128.

[15] G. Li, P. Sarazin, B. D. Favis, *Macromolecular Chemistry and Physics* **2008**, *209*, 991.

[16] G. Li, B. D. Favis, *Macromolecular Chemistry and Physics* **2010**, *211*, 321.

[17] E. Habeych, X. Guo, J. van Soest, A. J. v. der Goot, R. Boom, *Carbohydrate Polymers* **2009**, *77*, 703.

[18] P. A. Perry, A. M. Donald, *Carbohydrate Polymers* **2002**, *49*, 155.

[19] I. Tan, C. C. Wee, P. A. Sopade, P. J. Halley, *Carbohydrate Polymers* **2004**, *58*, 191.

[20] J. J. G. van Soest, R. C. Bezemer, D. de Wit, J. F. G. Vliegenthart, *Industrial Crops and Products* **1996**, *5*, 1.

[21] P. A. Perry, A. M. Donald, *Biomacromolecules* **2000**, *1*, 424.

[22] P. A. Sopade, P. J. Halley, L. L. Junming, *Carbohydrate Polymers* **2004**, *58*, 311.

[23] T. Xue, L. Yu, F. Xie, L. Chen, L. Li, *Food Hydrocolloids* **2008**, *22*, 973.

[24] L. Yu, T. Kealy, P. Chen, *International Polymer Processing* **2006**, *21*, 283.

[25] P. Chen, L. Yu, T. Kealy, L. Chen, L. Li, *Carbohydrate Polymers* **2007**, *68*, 495.

[26] F. Teyssandier, P. Cassagnau, J. F. Gerard, N. Mignard, *Carbohydrate Polymers* **2011**, *83*, 400.

[27] L. W. Shacklette, C. C. Han, "Solubility And Dispersion Characteristics Of Polyaniline", in *Electrical, Optical, and Magnetic Properties of Organic Solid State Materials*, A.F. Garito, A.K.Y. Jen, C.Y.C. Lee, and L.R. Dalton, Eds., 1994, p. 157.

[28] T. Palav, K. Seetharaman, *Carbohydrate Polymers* **2006**, *65*, 364.

[29] Q. Liu, G. Charlet, S. Yelle, J. Arul, *Food Research International* **2002**, *35*, 397.

[30] R. I. Derby, B. S. Miller, B. F. Miller, H. B. Trimbo, *Cereal Chem* **1975**, *52*, 11.

[31] B. Zanoni, A. Schiraldi, R. Simonetta, *Journal of Food Engineering* **1995**, *24*, 25.

[32] C. Antonio J.F, "Chapter 15 - Starch: Major Sources, Properties and Applications as Thermoplastic Materials", in *Monomers, Polymers and Composites from Renewable Resources*, B. Mohamed Naceur and G. Alessandro, Eds., Elsevier, Amsterdam, 2008, p. 321.

[33] T. A. Waigh, M. J. Gidley, B. U. Komanshek, A. M. Donald, *Carbohydrate Research* **2000**, *328*, 165.

[34] G. Ternstrom, A. Sjostrand, G. Aly, A. Jernqvist, *Journal of Chemical and Engineering Data* **1996**, *41*, 876.

[35] D. Kilburn, J. Claude, T. Schweizer, A. Alam, J. Ubbink, *Biomacromolecules* **2005**, *6*, 864.

[36] L. Godbillot, P. Dole, C. Joly, B. Roge, M. Mathlouthi, *Food Chemistry* **2006**, *96*, 380.

[37] S. Mali, L. S. Sakanaka, F. Yamashita, M. V. E. Grossmann, *Carbohydrate Polymers* **2005**, *60*, 283.

[38] A. L. M. Smits, P. H. Kruiskamp, J. J. G. van Soest, J. F. G. Vliegenthart, *Carbohydrate Polymers* **2003**, *53*, 409.

[39] A. Lerbret, P. E. Mason, R. M. Venable, A. Cesàro, M. L. Saboungi, R. W. Pastor, J. W. Brady, *Carbohydrate Research* **2009**, *344*, 2229.

[40] M. A. Garcia, M. N. Martino, N. E. Zaritzky, *Starch-Starke* **2000**, *52*, 118.

[41] F. J. Rodriguez-Gonzalez, B. A. Ramsay, B. D. Favis, *Carbohydrate Polymers* **2004**, *58*, 139.

[42] F. J. Rodriguez-Gonzalez, B. A. Ramsay, B. D. Favis, *Polymer* **2003**, *44*, 1517.

[43] A. Taguet, M. A. Huneault, B. D. Favis, *Polymer* **2009**, *50*, 5733.

[44] M. A. Huneault, H. Li, *Polymer* **2007**, *48*, 270.

[45] J. L. Willett, R. L. Shogren, *Polymer* **2002**, *43*, 5935.

[46] A. M. Donald, K. L. Kato, P. A. Perry, T. A. Weigh, *Starch-Starke* **2001**, *53*, 504.

Chapitre 5 HIGH MOLECULAR WEIGHT PLASTICIZERS IN THERMOPLASTIC STARCH/POLYETHYLENE BLENDS

Ata Taghizadeh[a], Pierre Sarazin[b], Basil D. Favis[a]*

[a] *CREPEC, Dept. of Chemical Engineering, Ecole Polytechnique de Montréal, Montréal, QC, H3C 3A7, CANADA*

[b] *Cerestech Inc., Pavillon J.-A. Bombardier, 5155 Ave. Decelles, Montréal, QC, H3T 2B1, CANADA*

5.1 Abstract

In this study thermoplastic starch (TPS) was prepared with four different molecular weight polyol plasticizers: glycerol, sorbitol, diglycerol and polyglycerol. Diglycerol-TPS and polyglycerol-TPS show significantly lower moisture uptake and a higher temperature stability when compared to conventional glycerol-TPS. TPS formulations were blended with HDPE at a concentration of 20 TPS/80 HDPE wt% and a range of interfacial modifier contents via a one-step extrusion process. The emulsification curves of the blends, which track the volume and number average diameter of the dispersed TPS domains with percent interfacial modifier, show significantly different profiles and a non-correspondence between the d_n and d_v values at the critical concentration for interfacial saturation. The addition of small amounts of interfacial modifier to the blends prepared with diglycerol and polyglycerol result in TPS dispersed phases of wide polydispersity with droplets in the order of 200-300 nanometers coexisting with droplets of 5-7 microns. This wide polydispersity of TPS phase size can give insight into the mechanism of droplet formation in these systems with interfacial modifier and is indicative of an erosion type mechanism where small portions of the TPS droplet break off at the outer part of the droplet. Blends prepared with glycerol-TPS and sorbitol-TPS do not display this behavior and show a more classic correspondence of d_n and d_v at the critical concentration. Dynamic mechanical analysis shows miscible behavior for diglycerol-TPS and polyglycerol-TPS and partially miscible behavior for glycerol-TPS. This phenomenon was attributed to the presence of ether bonds in the chemical structure of diglycerol and polyglycerol. The increased chain flexibility and lower cohesive energy forces of diglycerol and polyglycerol lead to a more homogeneous TPS phase and consequently an erosion type compatibilzation at the interface. The mechanical properties of blends prepared with polyglycerol and diglycerol show a similar overall behavior to glycerol.

Keywords

polyol plasticizers, thermoplastic starch, polyethylene, morphology, emulsification, mechanical properties.

5.2 Introduction

Polymers from renewable resources are receiving increasing attention as alternatives to fossil fuel based commodity polymers. Among these, starch is the most widely produced renewable resource used in plastics (Burrell, 2003). Starch has a semicrystalline structure and is composed of two types of molecules, amylose, a linear polymer and amylopectine, a branched one. Starch from different sources like maize, rice and wheat have been used in the polymer industry for years as a solid filler (Evangelista, Nikolov, Wei, Jane & Gelina, 1991; Willett, 1994). The main purpose in that case is to reduce the cost, but its use is severely limited due to its poor mechanical performance, poor processability and high water uptake levels. Otey (Otey, Westhoff & Doane, 1980a) reported that starch granules can be gelatinized in the presence of a plasticizer (like water) and heat during which the crystalline structure is disrupted. This allows the starch to flow at high temperatures allowing it to be processed by conventional polymer processing equipment. This plasticized starch is also called thermoplastic starch (TPS).

One of the main disadvantages of thermoplastic starch is its hydrophilic structure which results in a very high moisture dependent material (Chandra & Rustgi, 1997). A way to overcome this problem is to blend TPS with hydrophobic materials such as polyolefins (Averous, 2004). St. Pierre et al. (StPierre, Favis, Ramsay, Ramsay & Verhoogt, 1997) investigated blends of TPS and polyethylene in which they demonstrated the characteristics of a fully immiscible polymer blend with a matrix-dispersed phase morphology. Rodriguez et al. (Rodriguez-Gonzalez, Ramsay & Favis, 2003, 2004; Rodriguez Gonzalez, 2002) developed a one step process with an effective control on the morphology and found that high loadings of TPS could still result in polyethylene/TPS blends of outstanding elongation at break. In order to overcome the incompatibility issue between TPS and PE, different interfacial modifiers have been used in the literature (Bikiaris & Panayiotou, 1998; Girija & Sailaja, 2006; Sailaja, 2005; Sailaja & Chanda, 2001, 2002; Shujun, Jiugao & Jinglin, 2005; Wang, Yu & Yu, 2004). Among them PE-grafted-maleic anhydride is one of the most widely used and it shows reasonable improvements in morphology and mechanical properties (Sailaja, Reddy & Chanda, 2001; Shujun, Jiugao &

Jinglin, 2005; Wang, Yu & Yu, 2005a). The maleation of other polymers has also been reported to have an effect on the morphology in polymer blends (Bikiaris & Panayiotou, 1998; Huneault & Li, 2007; Sailaja & Chanda, 2000; Zhang & Sun, 2004). As in all classical compatibilized systems, these compatibilizers have been used to decrease the interfacial tension in TPS/PE blends and, as a consequence, reduce the phase size. It has been shown that the maleic group of PE-g-MA reacts with the hydroxyl group of starch, hence, improving the morphology and mechanical properties of the blends (Wang, Yu & Yu, 2005a). Taguet et al (Taguet, Huneault & Favis, 2009) studied the morphology-mechanical properties relationship in TPS/PE blends in the presence of a compatibilizer. Based on the DMA data, emulsification curves and mechanical properties, they confirmed (Averous, Moro, Dole & Fringant, 2000; Lourdin, Bizot & Colonna, 1997) the heterogeneous nature of TPS. TPS, when plasticized by glycerol, is a partially miscible mixture of plasticizer rich and starch rich phases. Due to the low molecular weight of the glycerol plasticizer used in that work, Taguet et al. suggested that some of the glycerol would migrate to the interface and form a glycerol layer in order to reduce the interfacial tension. This layer acts as a shear transfer medium between PE and starch. In that work it was shown that an optimal combination of interfacial modifier and a glycerol rich outer TPS layer combine to improve the mechanical properties of PE/TPS blends.

The structure and miscibility of thermoplastic starch and plasticizer is one of the promising parameters in controlling the properties of TPS blends. Various plasticizers have been used in TPS such as glycerol, glucose, sorbitol, ethylene glycol and formamide (Adeodato Vieira, da Silva, dos Santos & Beppu, 2011; Nashed, Rutgers & Sopade, 2003; Poutanen & Forssell, 1996; Wang, Shogren & Carriere, 2000). From the mechanical properties standpoint, different plasticizers can show a superior range of properties based on the process, starch source and starch/plasticizer ratio (Talja, Helen, Roos & Jouppila, 2007). It is observed that a number of plasticizers or low molecular weight sugars (Kalichevsky, Jaroszkiewicz & Blanshard, 1993), fail to stay bonded to starch molecules and show clear phase separation (Mathew & Dufresne, 2002). Due to its high availability, low cost and acceptable final mechanical properties, glycerol has been one of the mostly used plasticizers for plasticizing starch (Averous, 2004; Kaseem, Hamad & Deri, 2012). The main issue with glycerol is its high hydrophilicity, low thermal stability, as well as its surface migration with time in products like thin films (Huneault & Li, 2007). Sorbitol is another plasticizer which has been frequently used in TPS (Gaudin, Lourdin, Le Botlan, Ilari &

Colonna, 1999; Li & Huneault, 2011a). The main advantage of sorbitol in addition to its effective plasticization of starch is its higher thermal stability compared to glycerol. However, high surface migration and demixing along with its re-crystallisation over time are among the major disadvantages of sorbitol (Li & Huneault, 2011a).

In a recent work from this laboratory (Taghizadeh & Favis, 2012b) two higher molecular weight plasticizers (diglycerol and polyglycerol) were used for starch gelatinization and it was shown that the gelatinization temperature and mechanism is significantly affected by the molecular weight, functional groups and water solubility of these plasticizers. Moreover, these plasticizers were shown to effectively gelatinize starch under dynamic and static conditions. Their high molecular weight and conformational structure, in addition to higher thermal stability, could be of significant advantage in polymer blends. Diglycerol and polyglycerol plasticized starch in polymer blends have not been previously studied and their efficacy to plasticize starch in a polymer processing time-frame as well as their morphology and mechanical property outcomes are unknown. More interestingly, as mentioned above, in the case of incorporating graft copolymers, the architecture, molecular weight and chemical composition of the in situ formed copolymer will mostly determine the emulsification trend (Aravind, Albert, Ranganathaiah, Kurian & Thomas, 2004; Bikiaris & Panayiotou, 1998; Kim & Lee, 1996; Macosko, 2000; Macosko, Jeon & Hoye, 2005). If the copolymer can stay at the interface, it will reduce the droplet size effectively, but in the case of a molecular weight or viscosity increase of the copolymer at the interface, small moieties can be eroded off the interface and the presence of small sized droplets will be observed at low compatibilizer contents along with large droplets(Bhadane, Tsou, Cheng & Favis, 2008; Pan, Chiba & Inoue, 2001; Pan, Inoue, Hayami & Nishikawa, 2002). The incorporation of plasticizers, which have a different molecular structure and show significantly different gelatinization temperatures, can potentially influence the state of the interface in dispersed TPS and consequently the morphology of the compatibilized TPS/PE blend.

The objective of this work is to study polymer blends comprised of high density polyethylene and thermoplastic starch plasticized with high molecular weight polyols such as diglycerol and polyglycerol. The detailed influence of interfacial modification on the morphology and properties of these systems will be examined. The moisture pickup and the thermal stability of these materials will also be demonstrated.

5.3 Experimental

5.3.1 Materials

The native wheat starch and glycerol were obtained from ADM and Labmat, respectively. The wheat starch was composed of 25% amylose and 75% amylopectin and glycerol was received with a purity of >99.5%. D-sorbitol was purchased from Labmat as a pure powder. Diglycerol and Polyglycerol-3 were obtained from Solvay Chemicals. The diglycerol has a minimum 90% purity and is mainly composed of α,α′-diglycerol (84%) and α, β-diglycerol isomers. The polyglycerol-3 mainly includes 35-55% triglycerol, 15-30% of diglycerol and the rest is higher molecular weight polyglycerols resulting in a minimum 85% of diglycerol, triglycerol and tetraglycerol. The chemical structure of the plasticizers is shown in Figure 5-1. High density polyethylene (HDPE) was supplied by Nova Chemicals, and was a Sclair HDPE2710. The PE grafted with maleic anhydride (PE-g-MA) had a molecular weight of (Mn; Mw: 31200; 112500) and MA concentration equal to 3.9% as measured by elemental analysis which corresponds to ≈ 40 MA groups per PE chain based on Mw.

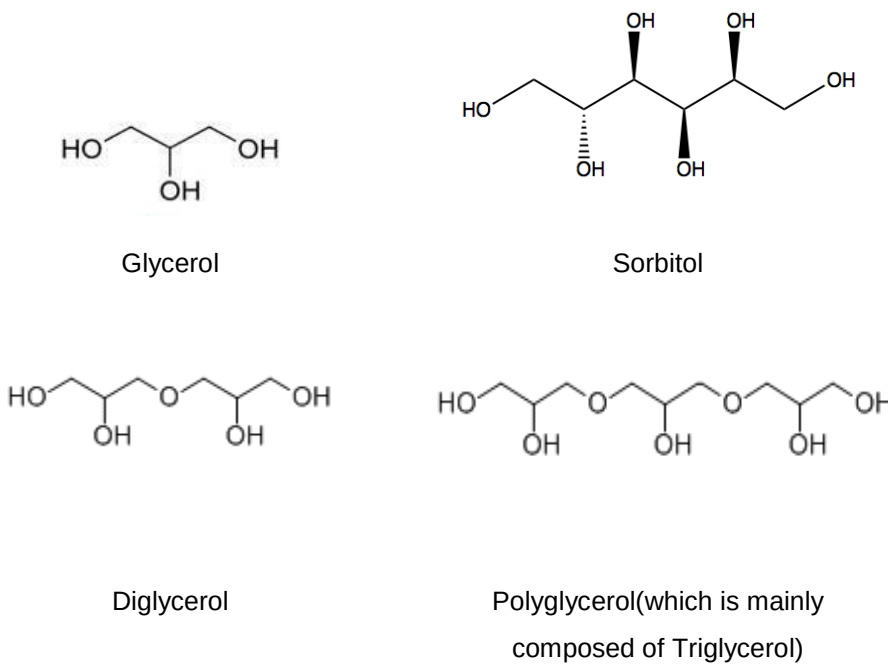

Figure 5-1 Chemical structure of different plasticizers used.

5.3.2 Blends Preparation

Starch granules were mixed with water and plasticizer and blended with HDPE and compatibilizer in a one-step extrusion process developed in this laboratory (Favis, Rodriguez & Ramsay, 2003; Favis, Rodriguez & Ramsay, 2005). The extrusion system was a single screw extruder (SSE) connected midway to a co-rotating twin screw extruder (TSE). The starch/glycerol/water suspension was fed to the TSE. In this section native starch was gelatinized and plasticized and the water was extracted before the mixing with HDPE. Molten HDPE (T= 160˚C) and copolymer were fed from the SSE to midway on the TSE. The TSE screw speed was 100 rpm for all blends. A three-hole strand die (diameter 3 mm) was used and strands were water cooled, followed by air cooling and then pelletized. All of the thermoplastic starch (TPS) compositions contain 36 wt% plasticizer based on the slurry composition. Blends were prepared containing 20 wt% of TPS and 80 wt% of HDPE and the compatibilizer was added with the HDPE at various contents. All compatibilizer concentrations are based on the TPS content. Samples for each extrusion batch were moulded in a dumbbell shape according to ASTM-D638 (type I) sample size using an injection moulding machine at 160˚C. The same conditions were used to mold the DMTA samples of rectangular shape (12.5x2.5x70mm). In order to obtain pure TPS with different plasticizers, the SSE was removed and TPS was collected using the strand or ribbon dies of the TSE.

5.3.3 Moisture treatment

Pure TPS samples of 50x20x3 mm were dried in 45˚C oven of circulating hot air for 3 weeks. The samples were then weighed and placed in a humidity chamber with 80% humidity at 30 ˚C for one week. The samples were weighed regularly and the moisture pick up was calculated as follows:

$$\Delta = \frac{W_t - W_0}{W_0} \times 100$$

Where Δ, W_t and W_0 represent moisture uptake percentage, sample mass at time t and initial dry sample mass, respectively.

5.3.4 Thermogravimetric Analyses (TGA)

TGA analyses were conducted (TGA Q500, TA Instruments) on TPS samples with different plasticizers from 25 ˚C to 500 ˚C under a nitrogen environment at 10˚C/min to study the thermal stability of the samples. The analyses were done using Universal Analysis™ software.

5.3.5 Scanning Electron Microscopy and Image Analysis

Samples were microtomed at -150 ˚C under liquid nitrogen using a glass knife, perpendicular to the machine direction. The instrument was a Leica-Jung RM 2165 equipped with a Leica LN 21 type cryochamber. TPS was then extracted at room temperature with HCl (6N) for 3 hrs. The samples were then coated with a gold-palladium alloy to be observed in scanning electron microscopy. The microscope was a Jeol JSM 840 Scanning Electron Microscope (SEM) operated at a voltage of 2 kV. For each composition two to three different samples were examined. The digitizing table and a in-house developed software (Favis & Chalifoux, 1987) were used to measure the average droplet diameters. Depending on the composition, each average diameter was based on 300-600 droplets. Number average (d_n) and volume average (d_v) diameters were obtained followed by a correction procedure developed by Saltikov (SA, 1967). The correction was applied due to the fact that microtoming knife does not normally cut the droplets at the equator and to account for polydispersity efects. The emulsification curves were then built, showing the average droplet size (d_v or d_n) vs. copolymer wt% for different plasticizers. The point after which the droplet diameter experienced only very marginal changes, was recognised as the critical concentration where interfacial saturation is achieved. Each composition point in the emulsification curve represents a separately prepared mixture. The extent of variation has been reported extensively by our group in the morphology and image analysis of polymer blend systems in previous works (Cigana & Favis, 1998; Cigana, Favis & Jerome, 1996; Favis, 1994) and does not exceed ±10% of the reported value.

5.3.6 Dynamic Mechanical Analysis (DMA)

Dynamic mechanical properties were measured using a TA dynamic mechanical analyzer (TA Instruments Model DMA 2980). The temperature was increased from -100 to 100 ˚C, with a heating rate of 3˚C/min. The frequency was 1 Hz, and the oscillation amplitude was 30 microns. The measurements were carried out using the dual cantilever clamp mode.

5.3.7 Rheology

Rheological characterizations of the as prepared thermoplastic starch and polyethylene were performed in oscillation mode using an MCR-301 strain controlled rheometer from *Anton Paar*. The experiments were performed in parallel plate geometry. A stress sweep test was run to define the region of linear viscoelasticity. Then a frequency sweep test was conducted on the samples from 0.1 to 200 rad/s at 160˚C.

5.3.8 Differential Scanning Calorimetry (DSC)

In order to obtain the glass transition temperatures of the pure plasticizers, DSC tests have been conducted on the samples using a differential scanning calorimetry instrument (*DSC Q1000, TA instruments*) at a heating rate of 3˚C.min^{-1} from -100 to 50 ˚C with an empty sample pan as the reference. The samples were loaded in Hermetic pans to a mass of (10-15 mg) and then were sealed using a volatile sample sealer accessory. Universal Analysis™ software was used to determine the glass transition temperatures.

5.3.9 Tensile Properties

Injection moulded dumbbell shaped specimens were conditioned for 48 h at 23 ˚C and 50% humidity. Tensile measurements were performed according to ASTM D638 with an Instron 4400R universal testing machine at a crosshead speed of 50 mm/min. At least eight specimens of each sample were tested and their average value was reported with error bars including the minimum and the maximum obtained values.

5.4 Results

5.4.1 Moisture Uptake and Thermal Stability of TPS with Different Plasticizers

Moisture sensitivity is one of the most serious drawbacks of TPS since the level of moisture in TPS can result in significant mechanical property fluctuations with ambient humidity. Figure 5-2 shows the moisture uptake levels in different TPS samples. It is observed that glycerol-TPS

(GTPS) shows the highest value with an almost 40 wt% water uptake level based on the TPS initial mass. Diglycerol-TPS (DTPS) and sorbitol-TPS (STPS) show similar behaviour with ~28 wt% and polyglycerol-TPS (PTPS) is the least with ~18 wt% final water uptake. This clearly shows the superior moisture resistance of PTPS.

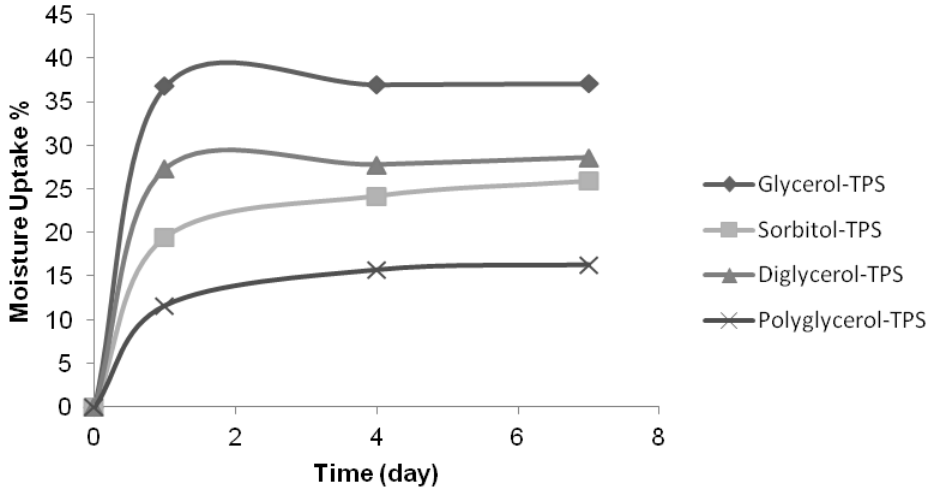

Figure 5-2 Moisture pick-up of different formulations of TPS at 80% RH and 30˚C.

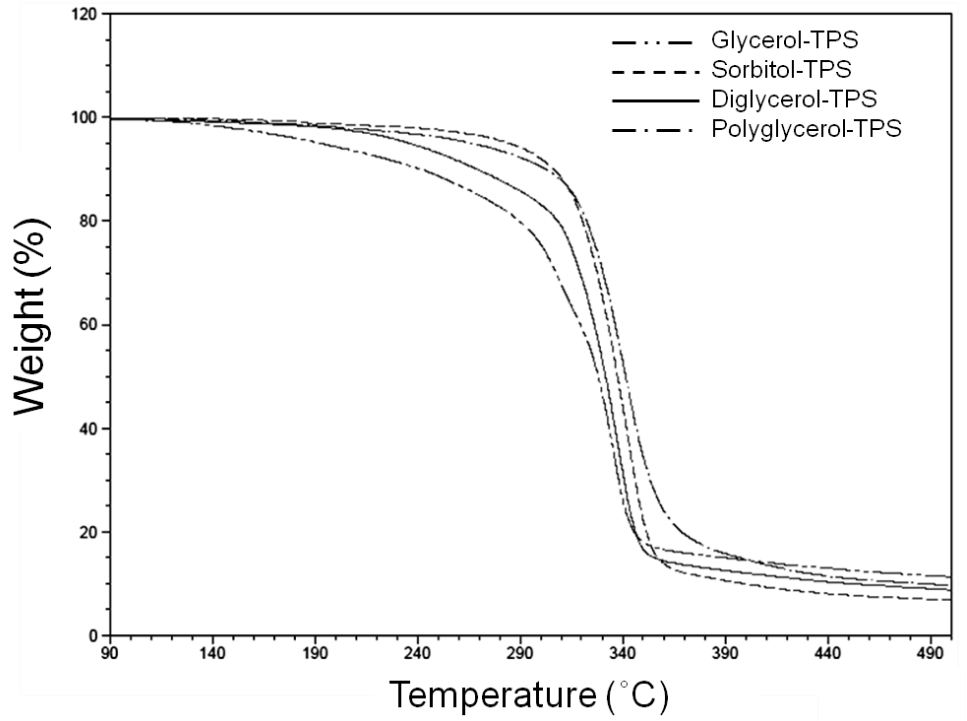

Figure 5-3 Thermogravimetric analyses of formulations of TPS with different plasticizers.

The temperature stability of TPS is another important factor in its processing. A thermoplastic starch with higher temperature stability facilitates its blending with high melting temperature polymers and reduces plasticizer evaporation during processes such as film extrusion. Figure 5-3 shows the TGA curves for TPS plasticized with various plasticizers. The results in Table 5-1 reveal the high temperature stability of STPS, PTPS and DTPS with 5% plasticizer weight loss temperatures of 235˚C, 225˚C and 203˚C respectively. By way of comparison, glycerol has a value of 156˚C.

5.4.2 Morphology of TPS/PE Blends

The morphologies of different TPS/PE blends are shown in Figure 5-4. A droplet-matrix morphology is observed for all four plasticizer types. Morphology evolution by compatibilizer addition is demonstrated for DTPS and GTPS in Figure 5-5. The effect of the compatibilizer in reducing the droplet size is clearly observed for both plasticizers. The emulsification curves (Figure 5-6) show the quantitative data for all the plasticizers. Comparing the morphology of blends, in the case where there is no added compatibilizer, it is observed that DTPS results in similar TPS droplet sizes as GTPS and STPS, but PTPS shows a slightly smaller droplet size. By incorporation of the copolymer, the droplet size decreases for all plasticizers and finally reaches a plateau at around 1.5-2μm for all except for GTPS which reaches a slightly lower value of 0.8μm due to its lower viscosity (Figure 5-7).

Table 5-1 Thermal stability of various TPS formulations.

	5 wt% plasticizer loss temp. (˚C)	10 wt% plasticizer loss temp. (˚C)
Glycerol-TPS	156	180
Diglycerol-TPS	203	230
Sorbitol-TPS	235	270
Polyglycerol-TPS	225	258

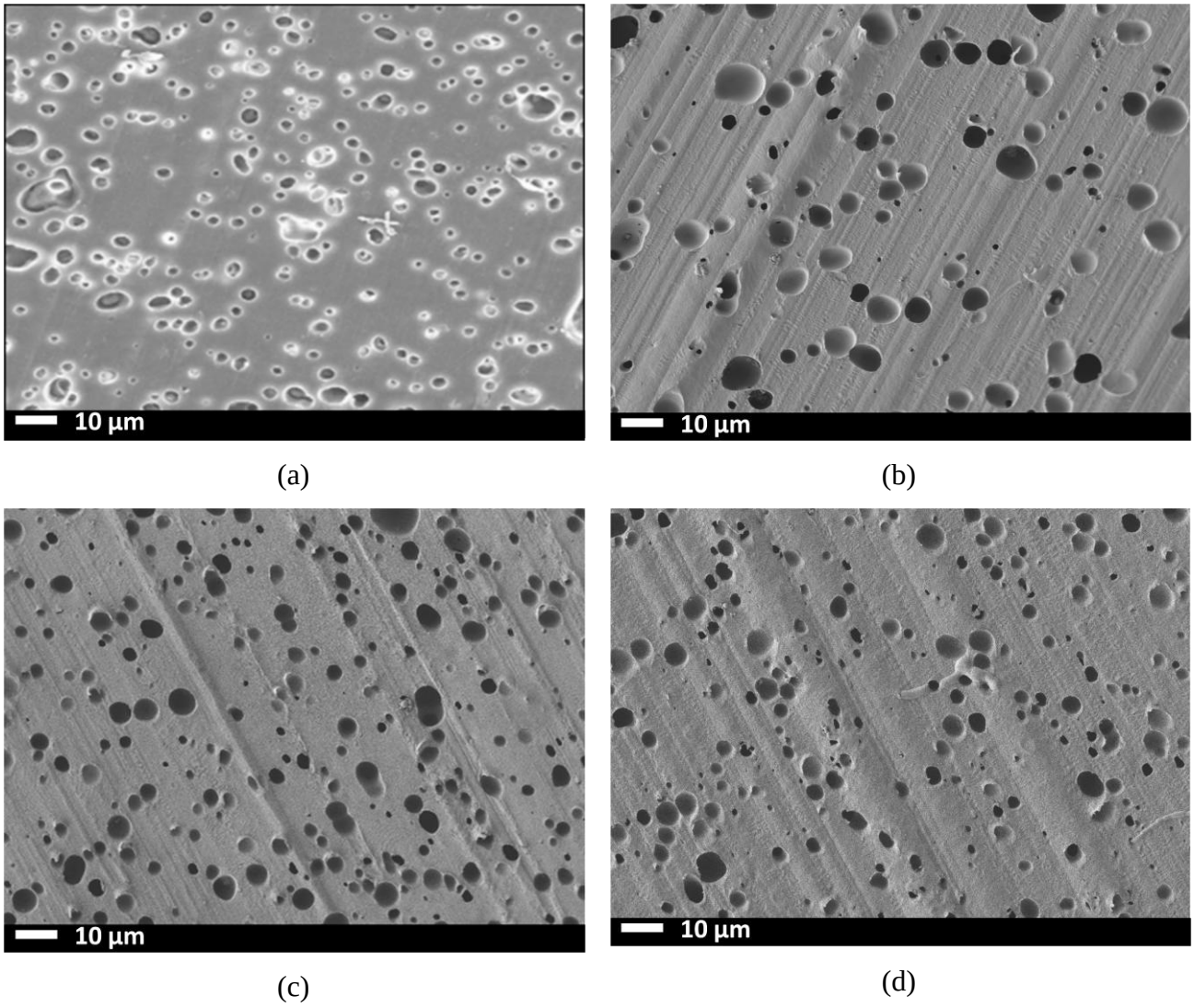

(a) (b)

(c) (d)

Figure 5-4 SEM images of TPS/PE 20/80 wt% without compatibilizer after TPS extraction: a) glycerol-TPS/PE; b) sorbitol-TPS/PE; c) diglycerol-TPS/PE; d) polyglycerol-TPS/PE.

The reduction of the number average (d_n) and volume average (d_v) diameters with increasing copolymer concentration, is a demonstration of the typical emulsification effect of compatibilizers in a polymer blend (Taguet, Huneault & Favis, 2009). In a high interfacial tension system such as TPS/PE, a copolymer reduces the interfacial tension between the phases leading to a reduction in the phase size up until the point that interfacial saturation of the copolymer is reached. The compatibilization in the case of TPS/PE compatibilized with PE-g-MA is believed to be through the formation of an ester resulting from the reaction of maleic anhydride in the copolymer with the hydroxyl groups of the TPS phase (Bikiaris & Panayiotou, 1998; Taguet, Huneault & Favis, 2009).

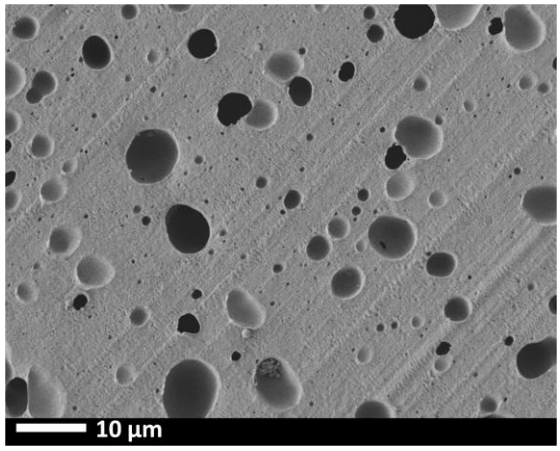

(a)

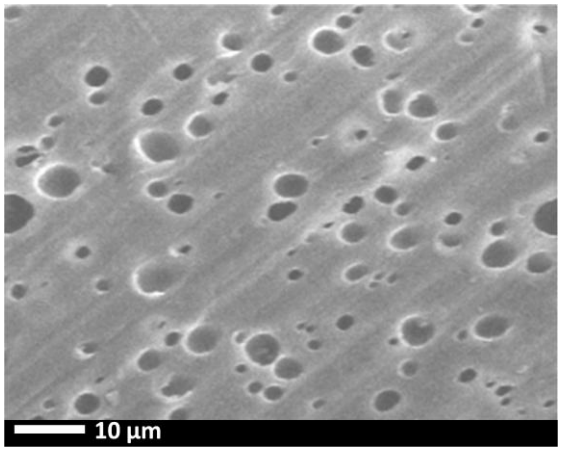

(d)

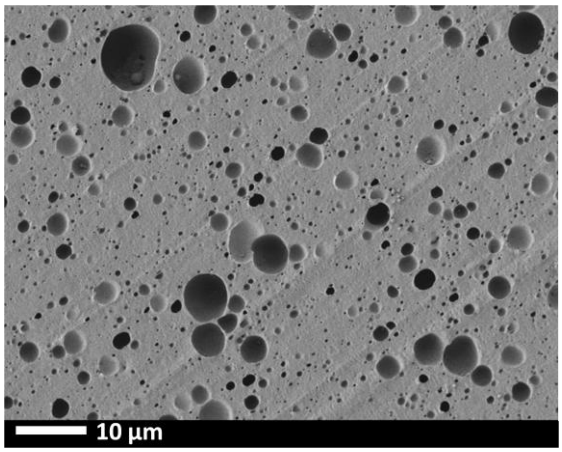

(b)

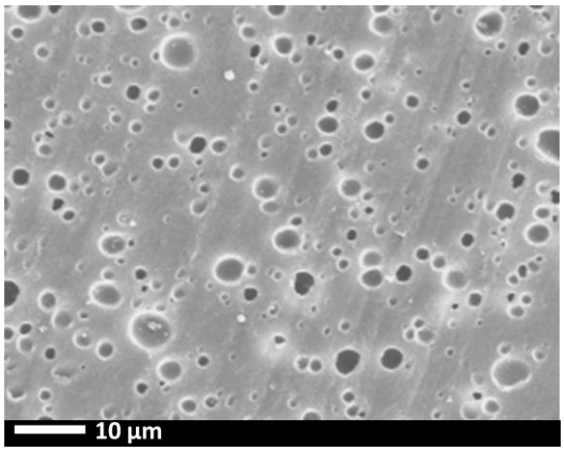

(e)

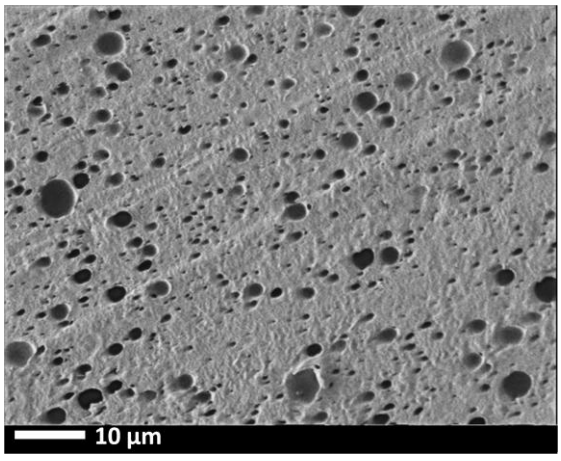

(c)

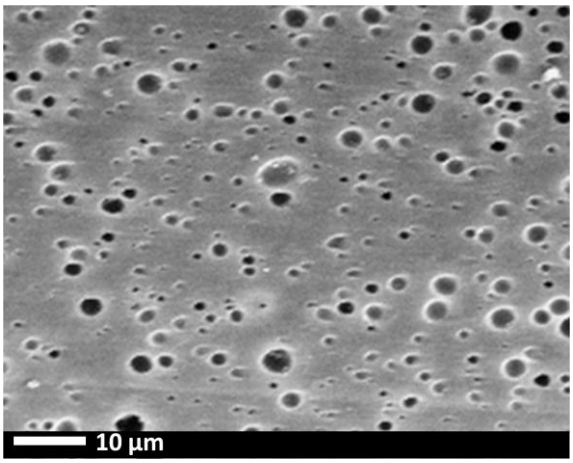

(f)

Figure 5-5 Diglycerol-TPS/PE blends (20/80 wt%) with different copolymer compatibilizer contents: (a) 1% , (b) 6% , (c) 9 %; and glycerol-TPS/PE blends (20/80 wt%) with different copolymer compatibilizer contents:(d) 1% , (e) 6% , (f) 9 % .

In all four plasticizer systems, the same trend is observed in d_v i.e. a gradual drop to reach a plateau at higher copolymer concentrations. The critical concentration of the copolymer represents the point of interfacial saturation of copolymer at the PE/TPS interface and at that point the droplet diameter experiences no further size reduction (Favis, 1994; Lomellini, Matos & Favis, 1996; Taguet, Huneault & Favis, 2009). Based on the volume average diameter, d_v, the critical concentration is the same for all of the plasticizers and occurs at approximately 9 wt% copolymer. However, the trend in the reduction of the number average diameter, d_n, in the emulsification curves of Figure 5-6 show a different behavior.

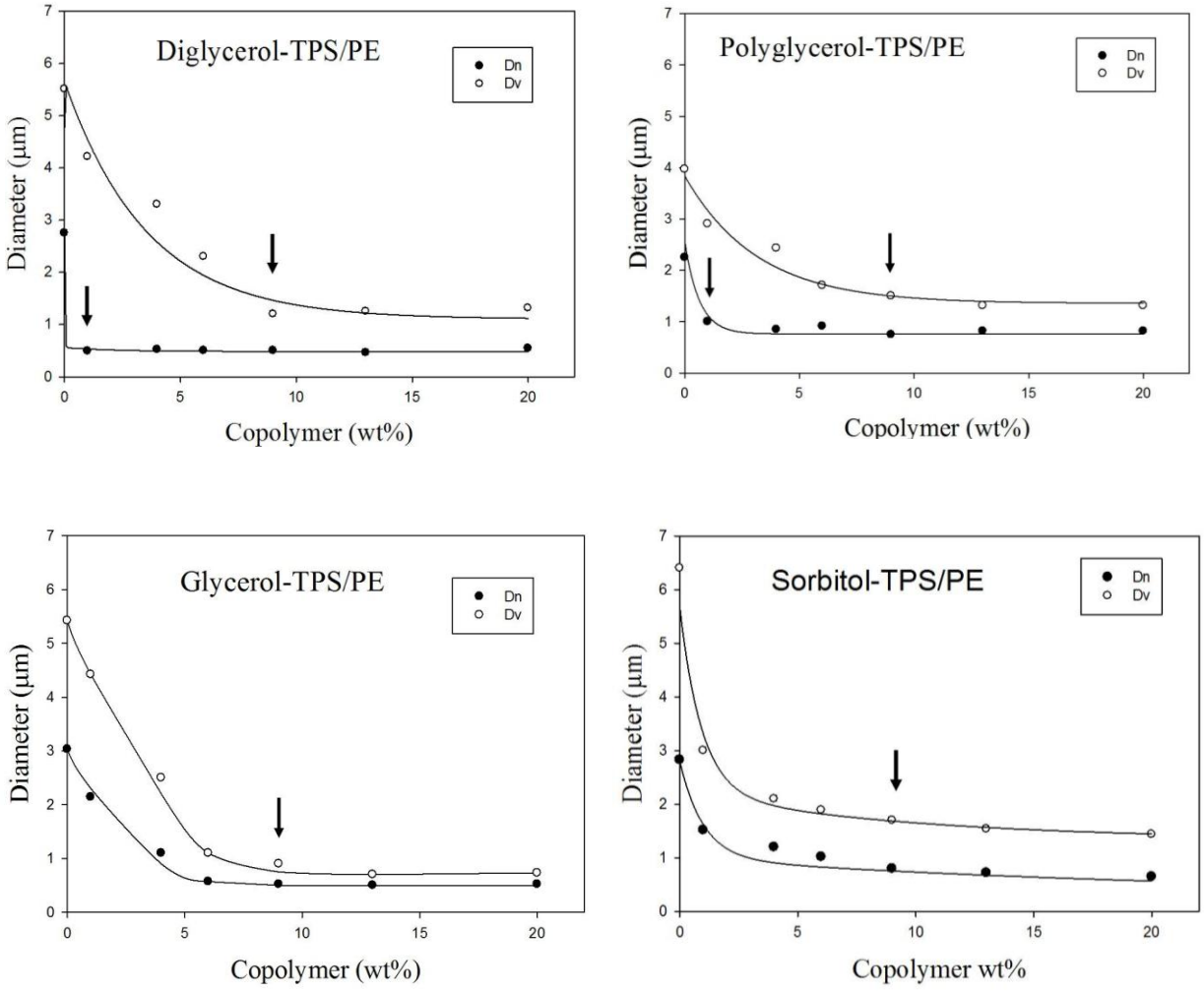

Figure 5-6 Emulsification curves showing the TPS droplet size reduction as a function of copolymer interfacial modifier concentration in various TPS/PE blends (20/80 wt%).

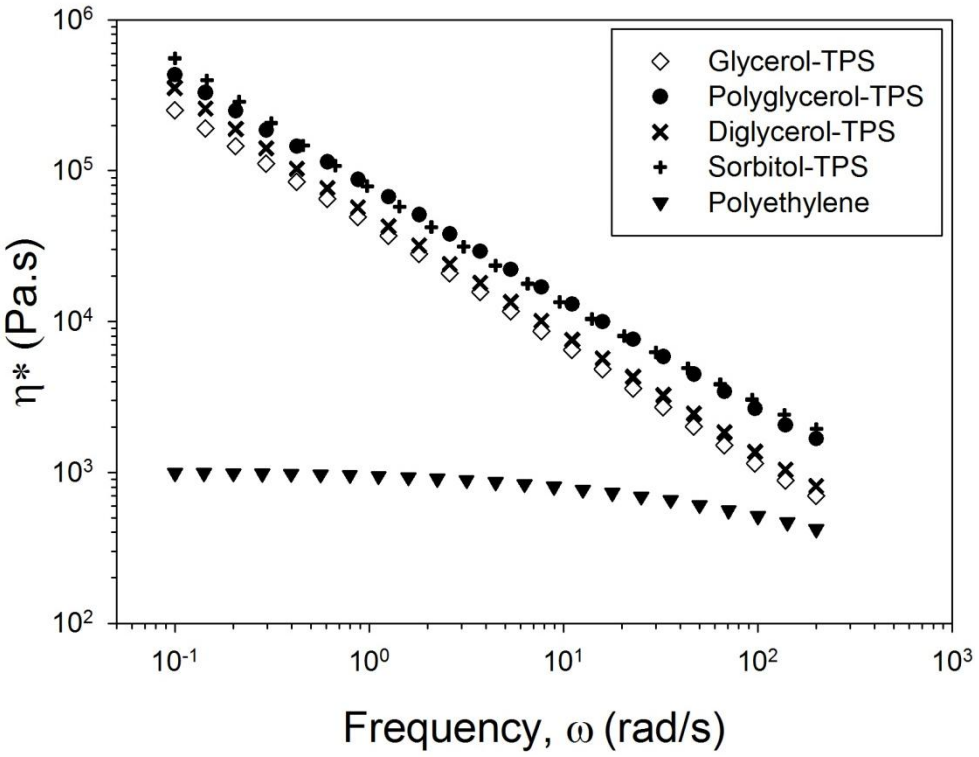

Figure 5-7 Complex viscosities of thermoplastic starch prepared with various plasticizers and polyethylene.

The blends prepared with GTPS and STPS, show a typical behaviour of compatibilized systems, in which the number and volume average diameters of the dispersed phase drop and demonstrate a close correspondence in the critical copolymer concentration for interfacial saturation (indicated by an arrow). The blends prepared with DTPS and PTPS, on the other hand, show two significantly different and unambiguous critical concentrations for the number average and volume average diameters. For the blends prepared with DTPS and PTPS, the d_n shows an abrupt drop at 1 wt% copolymer and remains at virtually the same value as a function of copolymer concentration. The volume average diameter, d_v, on the other hand descends gradually and reaches the critical concentration at 9% copolymer as was observed for the glycerol and sorbitol plasticized systems.

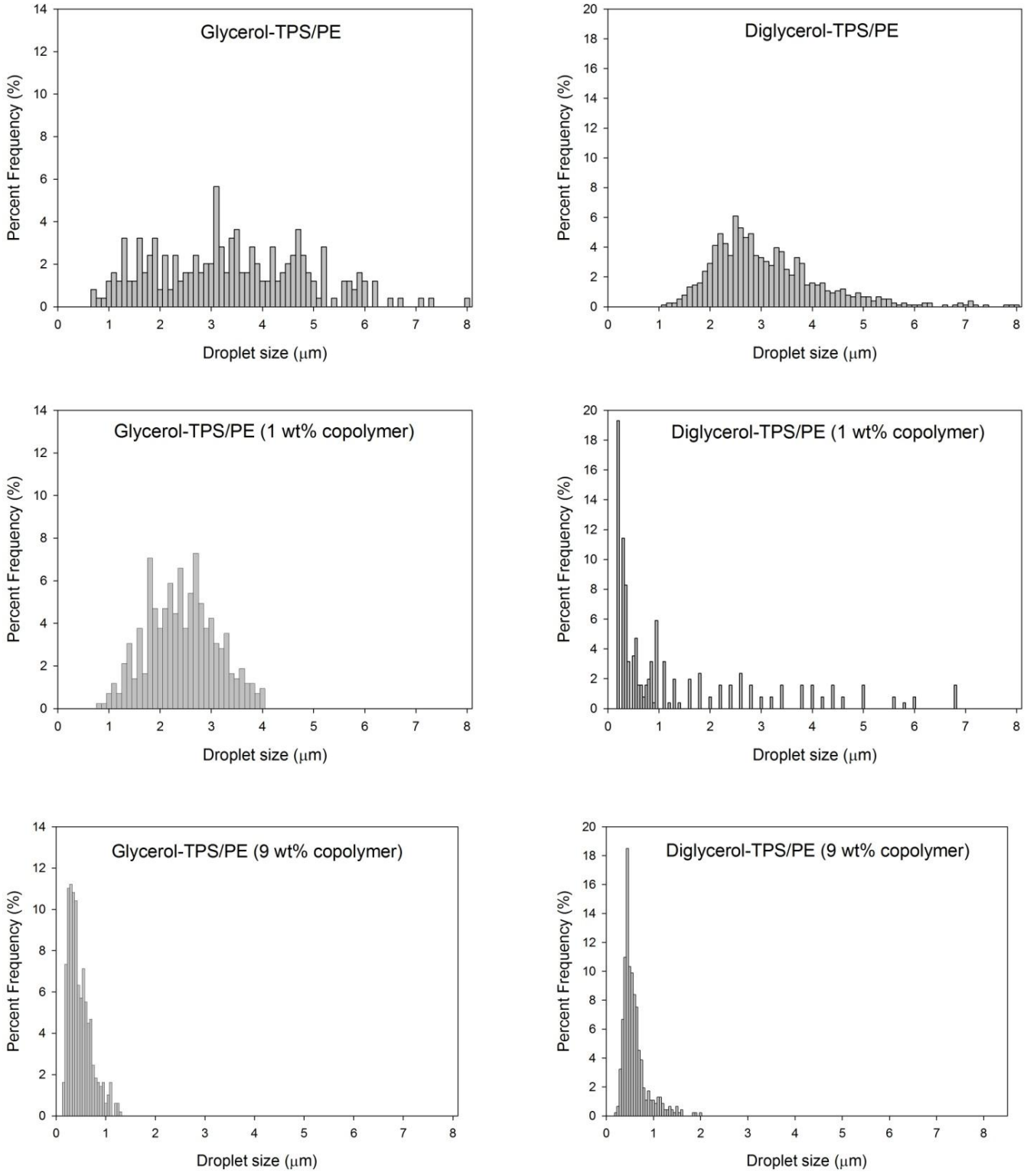

Figure 5-8 TPS droplet size distribution frequency at various compatibilizer contents for glycerol-TPS/PE and diglycerol-TPS/PE (20/80 wt%).

Since the number average value diameter is an indication of the size of the smallest droplets in a polydisperse system and the volume average diameter is a measure which weights the largest droplets in the system, these results clearly indicate that at lower copolymer concentration there is a co-existence of very small droplets with very large ones. This effect is more clearly reflected in the particle size histograms at different interfacial modifier contents for blends prepared with glycerol and diglycerol (Figure 5-8). Prior to the addition of interfacial modifier both blend systems show a classic gaussian type distribution with a long tail for the TPS particles. With the addition of 1% copolymer, the particle size distributions for the DTPS and GTPS blends differ significantly. GTPS maintains the gaussian type distribution while a very high percent frequency of small droplets is formed in the DTPS system and 200-300 nm droplets co-exist with 5-7 micron droplets. This is a very unusual behavior and it will be shown in the Discussion below that this can give insight into the droplet formation mechanism of dispersed TPS particles in polymer blends. As high concentrations of copolymer at the critical concentration are reached (9%), the particle size histograms of the DTPS and GTPS become similar.

5.4.3 Dynamic-Mechanical Analyses (DMA)

The dynamic mechanical curves of glycerol plasticized starch and its blends have already been reviewed in the literature by different authors (Angellier, Molina-Boisseau, Dole & Dufresne, 2006; Averous, Fauconnier, Moro & Fringant, 2000; Averous, Moro, Dole & Fringant, 2000; Martin & Averous, 2001; Taguet, Huneault & Favis, 2009). Starch in its pure state, demonstrates only one transition peak at ~ 100˚C (Bizot, LeBail, Leroux, Davy, Roger & Buleon, 1997; Lourdin, Bizot & Colonna, 1997) which is attributed to the β relaxation of amylose in the presence of 12-14 % water. However, after gelatinization and in the presence of a plasticizer such as glycerol, two transition peaks are observed which is an indication of the partial miscibility of starch and plasticizer (Sarazin, Li, Orts & Favis, 2008). The transition at lower temperatures (β relaxation) is attributed to the plasticizer-rich phase and the higher temperature transition is caused by the α relaxation of high molecular weight starch molecules in a starch-rich phase (Figure 5-9). The glass transition of glycerol in thermoplastic starch is shifted to higher temperatures due to its partial miscibility with starch, however, the existence of two peaks reveals the heterogeneous and partially miscible structure of thermoplastic starch. The plasticizer-rich area can even be interconnected throughout the TPS phase (Chivrac, Angellier-Coussy, Guillard,

Pollet & Averous, 2010) and result in a complete phase separation. One of the signs of miscibility in mixtures is the shift of transition peaks of two components towards each other (Martin & Averous, 2001). In thermoplastic starch the more de-mixing that occurs between starch rich and plasticizer rich domains, the more distinct the peaks are observed in DMA curves i.e. less shift in transition temperatures compared with T_g for the pure components. However, if de-mixing is restrained, the shift of glass transition of the plasticizer towards the α relaxation of starch in the blended state will be more significant.

Table 5-2 Loss modulus peak values for different plasticizers.

	T_β ˚C	T_g of pure plasticizer, ˚C	Temp. Shift
Glycerol-TPS	-28	-60	32
Diglycerol-TPS	-9	-54	45
Polyglycerol-TPS	1	-45	46

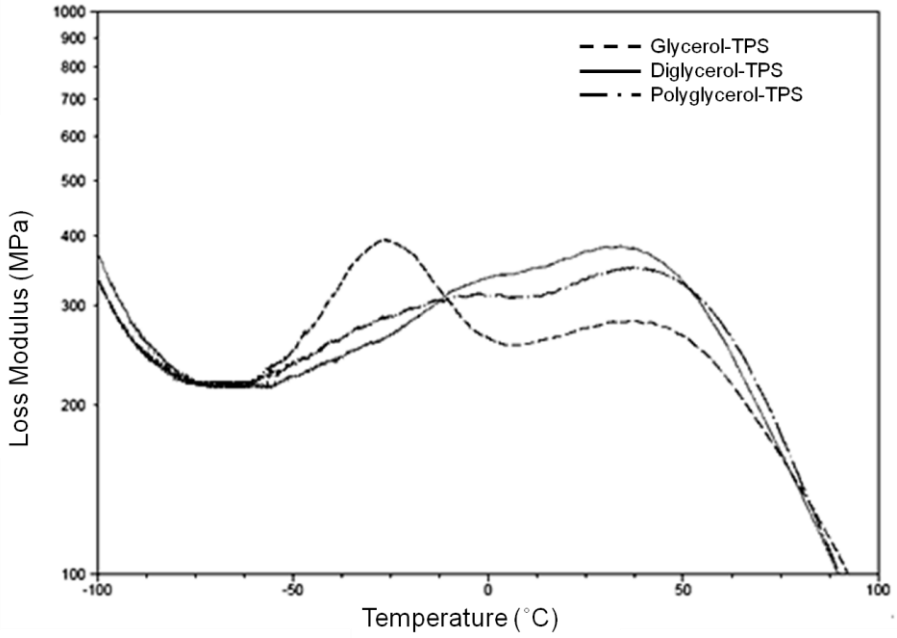

Figure 5-9 Loss modulus versus temperature for TPS/PE blends (20/80 wt%) prepared with glycerol, diglycerol and polyglycerol.

Table 5-2 compares the glass transitions of the pure plasticizers in the current work with the ones observed in their TPS/PE blend states. It is clearly seen that all the plasticizers show a shift in T_g towards higher temperatures, but in progressing from GTPS to DTPS and PTPS, this shift becomes more pronounced, in a way that in PTPS a 46˚C shift is observed. This indicates a much lower level of de-mixing (higher miscibility) in the PTPS and DTPS structure. In the case of STPS, it is not possible to clearly evaluate the DMA curves since the glass transition of pure sorbitol is already is around -10˚C and even a small shift of T_g will cause an overlap of the two peaks. On the other hand, in other studies, sorbitol has been shown to exhibit a considerable amount of de-mixing and surface migration similar to glycerol (Gaudin, Lourdin, Le Botlan, Ilari & Colonna, 1999; Krogars, Heinämäki, Karjalainen, Niskanen, Leskelä & Yliruusi, 2003; Li & Huneault, 2011a). Consequently, the level of miscibility in PTPS and DTPS appears to be superior to STPS and GTPS.

5.4.4 Tensile Properties

Figures 5-10 to 5-13 show the elongation at break, maximum tensile stress and modulus as a function of interfacial modifier concentration for the TPS/PE blends prepared with the four different plasticizers used in this study. It is observed that with 0% compatibilizer, PTPS demonstrates the highest values of elongation at break (~ 400%). Incorporation of the compatibilizer improves the interfacial adhesion and the elongation at break is improved for PTPS, DTPS and GTPS. The elongation at break for STPS remains the same over the entire copolymer composition range due to its intrinsic rigidity caused by recrystallization of sorbitol at room temperature (Li & Huneault, 2011b). Both the modulus and tensile strength curves (Figures 5-12 and 5-13) reveal that the STPS/PE blend is more rigid and shows a higher modulus and strength; while the other three plasticizers fall almost in the same range. These are the first reported results for polymer blends with thermoplastic starch plasticized with diglycerol and polyglycerol and the overall mechanical property results indicate that their performance is entirely in the range of that of glycerol.

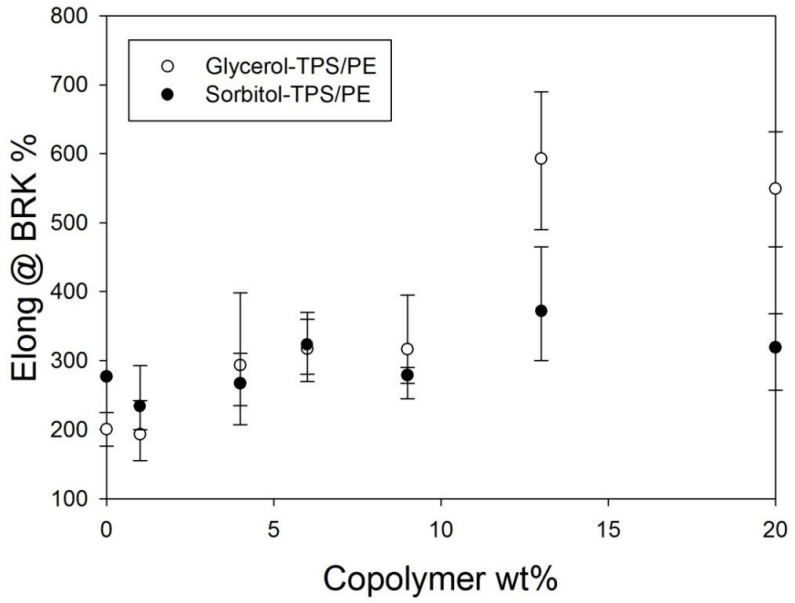

Figure 5-10 Elongation at break as a function of copolymer interfacial modifier concentration for TPS/PE (20/80 wt%) blends with glycerol-TPS and sorbitol-TPS.

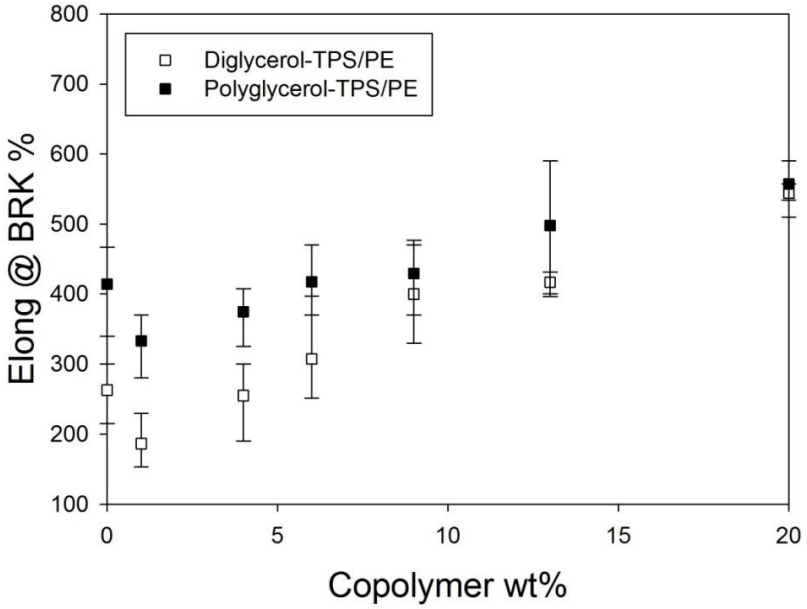

Figure 5-11 Elongation at break as a function of copolymer interfacial modifier concentration for TPS/PE (20/80 wt%) blends with diglycerol-TPS and polyglycerol-TPS.

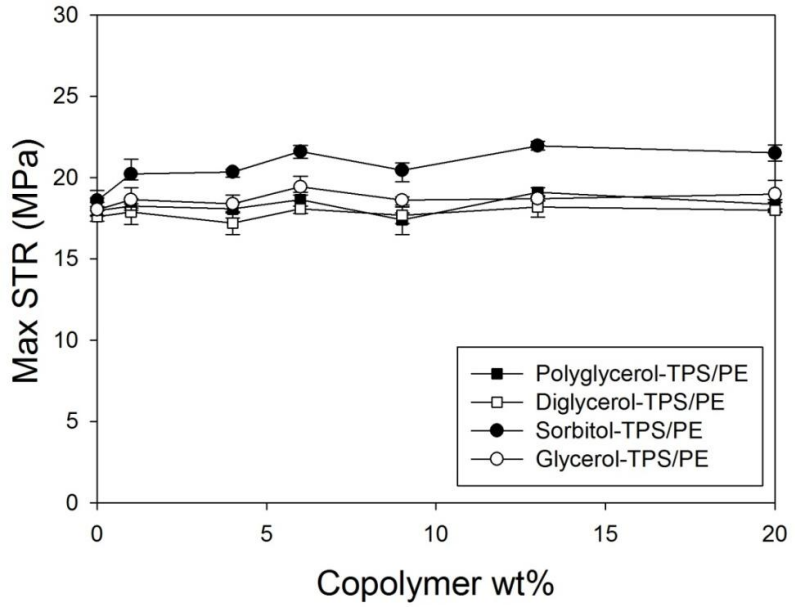

Figure 5-12 Maximum strength as a function of copolymer interfacial modifier concentration for TPS/PE (20/80 wt%) blends for different plasticizers.

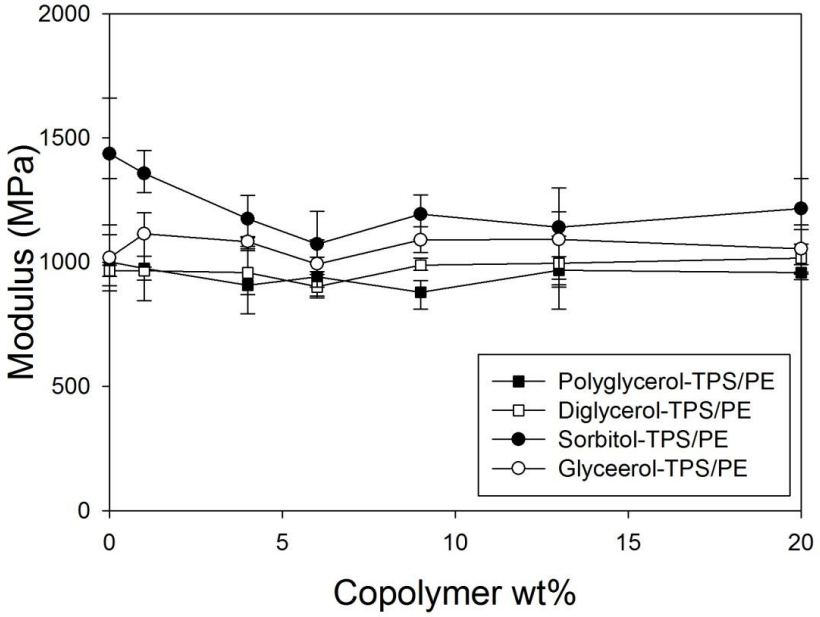

Figure 5-13 Young's Modulus as a function of copolymer interfacial modifier concentration for TPS/PE (20/80 wt%) blends for different plasticizers.

5.5 **Discussion**

As shown above in Figure 5-6, the emulsification curves for DPTS and PTPS show a different behavior from the typical GTPS type curve. It is observed that there are two different critical concentrations for the number and volume average diameters. For both DPTS and PTPS, the d_n shows an abrupt drop at 1 wt% copolymer and remains at almost the same value for the whole composition range. The volume average diameter, d_v, on the other hand, descends gradually and reaches the critical concentration at 9% copolymer for both plasticizers. GTPS and STPS, on the other hand, show the classical emulsification curves in which d_n and d_v diminish and attain critical concentrations at similar values. This non-correspondence of the critical concentration for d_n and d_v is very unusual and can provide some insights into the droplet breakup mechanism for these types of systems which will be discussed below.

Another important and related feature of this work was the observation by DMA (Figure 5-9) of shifts and a flattening of the plasticizer domain corresponding to the T_α peaks for DTPS and PTPS. This can be interpreted as revealing a higher extent of miscibility for polyglycerol and diglycerol with starch as compared to glycerol. The chemical structures of polyglycerol, diglycerol, sorbitol and glycerol reveal some important differences (Figure 5-1). The only functional group in glycerol and sorbitol is the hydroxyl group with a (hydroxyl group)/(carbon backbone) ratio of one. Diglycerol and polyglycerol have a number of hydroxyl groups which are replaced with ether bonds. Ether bonds decrease the (hydroxyl group)/(carbon backbone) ratio to lower than one for these plasticizers. Internal hydrogen bonding is the intermolecular interaction which principally influences the extent of miscibility in hydroxyl containing mixtures. The cohesive energy density as a measure of the total strength of intermolecular plasticizer-plasticizer forces (Reichardt & Welton, 2011) has been reported in another article from this laboratory (Taghizadeh & Favis, 2012b) and can serve as a quantification of this effect (Table 5-3). In addition, the existence of ether bonds in the structure of diglycerol and polyglycerol, enhances the chain conformational flexibility and molecular mobility as compared to the same backbone with only C-C bonds(Ionescu, 2005). This conformational flexibility increases the number of ways these molecules may interact with adjacent molecules under mixing conditions. All of the above explanations would support increased miscibility for polyglycerol and diglycerol with starch as compared to glycerol.

Table 5-3 Physical properties of different pure plasticizers.

Property	Unit	Glycerol	Sorbitol	Diglycerol	Polyglycerol
Density	gr/cm^3	1.25	1.48	1.27	1.27
Glass Transition Temp.	˚C	-65	-9	-54	-45
Melting point.	˚C	17	95	----*	----*
Boiling point.	˚C	290	296	205	240
Cohesive Energy Density	MPa	1278	1626	898	723

* No melting point was detected in the range of -150˚C to 25 ˚C.

In a partially miscible mixture of thermoplastic starch comprised of glycerol-rich and starch-rich regions, it is expected that the low molecular weight glycerol will tend to migrate to the interface. The migration of a low molecular weight species in the blend to the interface would reduce the PE-TPS interfacial tension and hence the surface free energy of the system. The spreading of such a glycerol-rich layer between the polyethylene and the starch would be dictated by Harkins equation (Ravati & Favis, 2010; Virgilio, Desjardins, L'Esperance & Favis, 2010) and has already been reported as a mechanism for these systems in other publications(Broseta, Fredrickson, Helfand & Leibler, 1990; Sivaniah, Jones & Higgins, 2009). In fact, in a previous paper(Taguet, Huneault & Favis, 2009) it has been reported that the polyethylene-co-maleic anhydride copolymer tends to react with the glycerol layer initially in polyethylene-TPS blends. In the case of polyglycerol and diglycerol however, the higher miscibility between plasticizer and starch would impede and probably prevent the formation of such a plasticizer layer at the PE-TPS interface. In this case and even at low concentrations of modifier, the PE-g-MA will have a high tendency to react with starch molecules. When PE-g-MA reacts with starch, it is reacting with a polymer of very high molecular weight. It has been shown that although the very high molecular weight amylopectin molecules of starch (Yoo & Jane, 2002) undergo significant molecular degradation in the extrusion process (unlike the amylose portion that shows high process

stability) their molecular weight still remains very high (in the order of 10^6) (Bindzus, Livings, Gloria-Hernandez, Fayard, van Lengerich & Meuser, 2002; Liu, Halley & Gilbert, 2010) and they have a large radius of gyration (0.2-0.3 μm) (Bao, Ao & Jane, 2005). In addition, it is known (Hameed, Quinlan, Potter & Takacs, 2012; Jeon & Kim, 1998; Lu, Macosko & Horrion, 2003) that a PE-g-MA copolymer of even lower maleic anhydride levels than those used in the present work can experience multiple grafting reactions. The resulting copolymer formed in the reaction between PE-g-MA and starch would thus tend to be of extremely high molecular weight hence causing a very high local viscosity and molecular weight gradient at the interface. These conditions result in an erosion type mechanism of droplet formation where very fine droplets are broken off the ends of much larger ones (Figure 5-14). Such erosion or pull-out of the in-situ formed graft copolymer have been reported for other systems (Bhadane, Tsou, Cheng, Ellul & Favis, 2011; Bhadane, Tsou, Cheng & Favis, 2008; Kim, Jeong & Kim, 2003; Pan, Chiba & Inoue, 2001; Pan, Inoue, Hayami & Nishikawa, 2002) and they show a similar co-existence of extremely small and very large droplets as reported in this work. The results shown here indicate that the TPS droplet formation for polyglycerol and diglycerol is an erosion mechanism. In the case of glycerol, it has already been reported that, due to the plasticizer migration to the interface, at low concentration of copolymer the PE-MA interfacial modifier tends to react with glycerol as opposed to starch (Taguet, Huneault & Favis, 2009). This erosion mechanism is also likely occurring in the glycerol plasticized blend, but the presence of a glycerol layer inhibits the effect at low copolymer concentration . This latter point is reinforced by the fact that the final states of emulsification of the TPS phases at high copolymer concentration (9%), as shown in Figure 5-6, is quite similar for all four plasticizers.

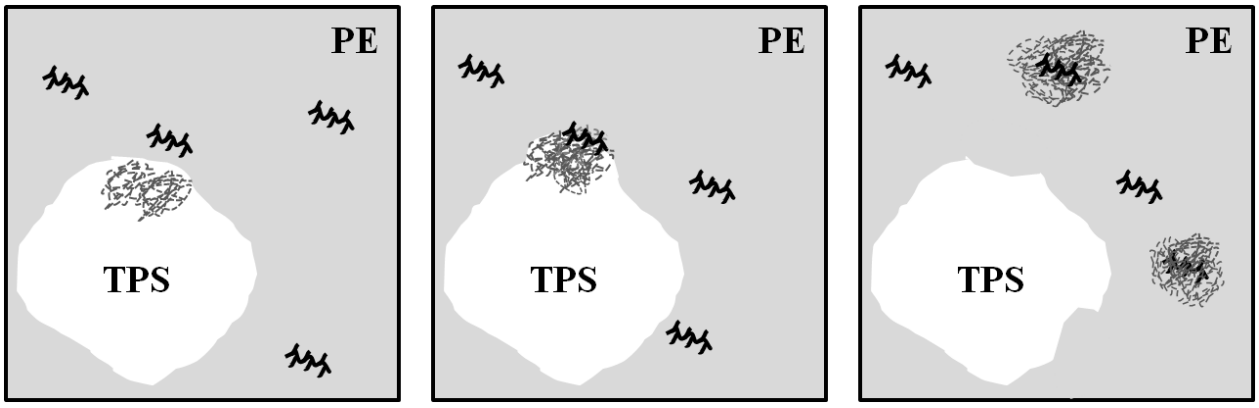

Figure 5-14 Schematic of TPS erosion for DTPS and PTPS in presence of PE-g-MA.

5.6 **Conclusions**

The effect of higher molecular weight plasticizers on the morphology development and mechanical properties of compatibilized 20TPS/80PE blends has been investigated. All of the plasticizers were chosen from the polyol family namely glycerol, sorbitol, diglycerol and polyglycerol. These latter three plasticizers were shown to have improved thermal stability and lower moisture uptake as compared to glycerol. Comparing the morphology of the blends, in the absence of compatibilizer, it is observed that DTPS, STPS and GTPS result in a similar TPS droplet size and PTPS shows a slightly smaller size. The emulsification curves, in the presence of a copolymer interfacial modifier, for DTPS and PTPS show a highly unusual non-correspondence in the diminution of the number and volume average diameters at low quantities of added copolymer. The droplet size histograms of TPS droplets for DTPS/PE blends showed that with the addition of 1 wt% copolymer a very high percent frequency of small droplets is formed i.e. 200-300 nm droplets co-exist with 5-7 micron droplets. This effect is not observed in the glycerol plasticized GTPS/PE histograms. Interestingly at higher compatibilizer contents (9 wt% copolymer) the DTPS and GTPS particle size distributions approach each other and are very similar. This unusual behavior for DTPS and PTPS provides insight into their TPS droplet formation mechanism and it is indicative of an erosion-type mechanism where fragments of TPS break off the outer envelope of the droplet.

DMA experiments show that both diglycerol and polyglycerol have significantly higher levels of miscibility with starch than glycerol. The T_g of diglycerol and polyglycerol showed a significant shift towards T_α of starch (~45 ˚C) in the blends which was 50% more than the same shift for glycerol. This indicates a more homogeneous TPS structure for DTPS and PTPS than GTPS which is known to exhibit demixing and is a partially miscible mixture of starch-rich and plasticizer-rich regions. This improved miscibility for diglycerol and polyglycerol with thermoplastic starch was attributed to the ether bonds in their structure which provide lower cohesive energies and enhanced flexibility for those plasticizers. This enhanced miscibility allows the erosion process for DTPS/PE and PTPS/PE to be observed at low interfacial modifier concentrations. The effect is likely masked in GTPS/PE due to the formation of a glycerol interlayer at the outer boundary of the droplet.

The mechanical properties indicate an overall similar performance for diglycerol, polyglycerol and sorbitol as compared to glycerol.

Acknowledgments

The authors would like to thank the Teknor Apex Company for supporting this work.

5.7 References

1. Burrell MM (2003) Starch: the need for improved quality or quantity - an overview. Journal of Experimental Botany 54 (382):451-456. doi:10.1093/jxb/erg049

2. Evangelista RL, Nikolov ZL, Wei S, Jane JL, Gelina RJ (1991) Effect Of Compounding And Starch Modification On Properties Of Starch-Filled Low-Density Polyethylene. Industrial & Engineering Chemistry Research 30 (8):1841-1846. doi:10.1021/ie00056a025

3. Willett JL (1994) Mechanical-Properties Of Ldpe Granular Starch Composites. Journal of Applied Polymer Science 54 (11):1685-1695. doi:10.1002/app.1994.070541112

4. Otey FH, Westhoff RP, Doane WM (1980) Starch-Based Blown Films. Ind Eng Chem Prod Res Dev 19 (4):4

5. Chandra R, Rustgi R (1997) Biodegradation of maleated linear low-density polyethylene and starch blends. Polymer Degradation and Stability 56 (2):185-202. doi:10.1016/s0141-3910(96)00212-1

6. Averous L (2004) Biodegradable multiphase systems based on plasticized starch: A review. Journal of Macromolecular Science-Polymer Reviews C44 (3):231-274. doi:10.1081/mc-200029326

7. StPierre N, Favis BD, Ramsay BA, Ramsay JA, Verhoogt H (1997) Processing and characterization of thermoplastic starch/polyethylene blends. Polymer 38 (3):647-655. doi:10.1016/s0032-3861(97)81176-7

8. Rodriguez-Gonzalez FJ, Ramsay BA, Favis BD (2004) Rheological and thermal properties of thermoplastic starch with high glycerol content. Carbohydrate Polymers 58 (2):139-147. doi:10.1016/j.carbpol.2004.06.002

9. Rodriguez-Gonzalez FJ, Ramsay BA, Favis BD (2003) High performance LDPE/thermoplastic starch blends: a sustainable alternative to pure polyethylene. Polymer 44 (5):1517-1526. doi:Pii s0032-3861(02)00907-210.1016/s0032-3861(02)00907-2

10. Rodriguez Gonzalez FJ (2002) Low density polyethylene/thermoplastic starch blends. NQ73435, Ecole Polytechnique, Montreal (Canada), Canada

11. Bikiaris D, Panayiotou C (1998) LDPE/starch blends compatibilized with PE-g-MA copolymers. Journal of Applied Polymer Science 70 (8):1503-1521. doi:10.1002/(sici)1097-4628(19981121)70:8<1503::aid-app9>3.0.co;2-#

12. Girija BG, Sailaja RRN (2006) Low-density polyethylene/plasticized tapioca starch blends with the low-density polyethylene functionalized with maleate ester: Mechanical and thermal properties. Journal of Applied Polymer Science 101 (2):1109-1120. doi:10.1002/app.24025

13. Sailaja RRN (2005) Mechanical properties of esterified tapioca starch-LDPE blends using LDPE-co-glycidyl methacrylate as compatibilizer. Polymer International 54 (2):286-296. doi:10.1002/pi.1669

14. Sailaja RRN, Chanda M (2001) Use of maleic anhydride-grafted polyethylene as compatibilizer for HDPE-tapioca starch blends: Effects on mechanical properties. Journal of Applied Polymer Science 80 (6):863-872. doi:10.1002/1097-4628(20010509)80:6<863::aid-app1164>3.0.co;2-r

15. Sailaja RRN, Chanda M (2002) Use of poly(ethylene-co-vinyl alcohol) as compatibilizer in LDPE/thermoplastic tapioca starch blends. Journal of Applied Polymer Science 86 (12):3126-3134. doi:10.1002/app.11340

16. Wang SJ, Yu JG, Yu JL (2004) Influence of maleic anhydride on the compatibility of thermal plasticized starch and linear low-density polyethylene. Journal of Applied Polymer Science 93 (2):686-695. doi:10.1002/app.20416

17. Shujun W, Jiugao Y, Jinglin Y (2005) Preparation and characterization of compatible thermoplastic starch/polyethylene blends. Polymer Degradation and Stability 87 (3):395-401. doi:10.1016/j.polymdegradstab.2004.08.012

18. Sailaja RRN, Reddy AP, Chanda M (2001) Effect of epoxy functionalized compatibilizer on the mechanical properties of low-density polyethylene/plasticized tapioca starch blends. Polymer International 50 (12):1352-1359. doi:10.1002/pi.787

19. Wang SJ, Yu JG, Yu JL (2005) Compatible thermoplastic starch/polyethylene blends by one-step reactive extrusion. Polymer International 54 (2):279-285. doi:10.1002/pi.1668

20. Huneault MA, Li H (2007) Morphology and properties of compatibilized polylactide/thermoplastic starch blends. Polymer 48 (1):270-280. doi:10.1016/j.polymer.2006.11.023

21. Zhang JF, Sun XZ (2004) Mechanical properties of poly(lactic acid)/starch composites compatibilized by maleic anhydride. Biomacromolecules 5 (4):1446-1451. doi:10.1021/bm0400022

22. Sailaja RRN, Chanda M (2000) Use of maleic anhydride-grafted polyethylene as compatibilizer for polyethylene-starch blends: Effects on mechanical properties. Journal of Polymer Materials 17 (2):165-176

23. Taguet A, Huneault MA, Favis BD (2009) Interface/morphology relationships in polymer blends with thermoplastic starch. Polymer 50 (24):5733-5743. doi:10.1016/j.polymer.2009.09.055

24. Averous L, Moro L, Dole P, Fringant C (2000) Properties of thermoplastic blends: starch-polycaprolactone. Polymer 41 (11):4157-4167. doi:10.1016/s0032-3861(99)00636-9

25. Lourdin D, Bizot H, Colonna P (1997) "Antiplasticization" in starch-glycerol films? Journal of Applied Polymer Science 63 (8):1047-1053. doi:10.1002/(sici)1097-4628(19970222)63:8<1047::aid-app11>3.0.co;2-3

26. Adeodato Vieira MG, da Silva MA, dos Santos LO, Beppu MM (2011) Natural-based plasticizers and biopolymer films: A review. European Polymer Journal 47 (3):254-263. doi:10.1016/j.eurpolymj.2010.12.011

27. Nashed G, Rutgers PPG, Sopade PA (2003) The plasticisation effect of glycerol and water on the gelatinisation of wheat starch. Starch-Starke 55 (3-4):131-137. doi:10.1002/star.200390027

28. Poutanen K, Forssell P (1996) Modification of starch properties with plasticizers. Trends in Polymer Science 4 (4):128-132

29. Wang L, Shogren RL, Carriere C (2000) Preparation and properties of thermoplastic starch-polyester laminate sheets by coextrusion. Polymer Engineering and Science 40 (2):499-506. doi:10.1002/pen.11182

30. Talja RA, Helen H, Roos YH, Jouppila K (2007) Effect of various polyols and polyol contents on physical and mechanical properties of potato starch-based films. Carbohydrate Polymers 67 (3):288-295. doi:10.1016/j.carbpol.2006.05.019

31. Kalichevsky MT, Jaroszkiewicz EM, Blanshard JMV (1993) A STUDY OF THE GLASS-TRANSITION OF AMYLOPECTIN SUGAR MIXTURES. Polymer 34 (2):346-358. doi:10.1016/0032-3861(93)90088-r

32. Mathew AP, Dufresne A (2002) Plasticized waxy maize starch: Effect of polyols and relative humidity on material properties. Biomacromolecules 3 (5):1101-1108. doi:10.1021/bm020065p

33. Kaseem M, Hamad K, Deri F (2012) Thermoplastic starch blends: A review of recent works. Polymer Science Series A 54 (2):165-176. doi:10.1134/s0965545x1202006x

34. Gaudin S, Lourdin D, Le Botlan D, Ilari JL, Colonna P (1999) Plasticisation and mobility in starch-sorbitol films. Journal of Cereal Science 29 (3):273-284. doi:10.1006/jcrs.1999.0236

35. Li H, Huneault MA (2011) Comparison of Sorbitol and Glycerol as Plasticizers for Thermoplastic Starch in TPS/PLA Blends. Journal of Applied Polymer Science 119 (4):2439-2448. doi:10.1002/app.32956

36. Taghizadeh A, Favis BD (2012) Effect of High Molecular Weight Plasticizers on the Gelatinization of Starch under Static and Shear Conditions. Manuscript submitted for publication.

37. Macosko CW (2000) Morphology development and control in immiscible polymer blends. Macromolecular Symposia 149:171-184. doi:10.1002/1521-3900(200001)149:1<171::aid-masy171>3.0.co;2-8

38. Aravind I, Albert P, Ranganathaiah C, Kurian JV, Thomas S (2004) Compatibilizing effect of EPM-g-MA in EPDM/poly(trimethylene terephthalate) incompatible blends. Polymer 45 (14):4925-4937. doi:10.1016/j.polymer.2004.04.063

39. Kim JK, Lee H (1996) The effect of PS-GMA as an in situ compatibilizer on the morphology and rheological properties of the immiscible PBT/PS blend. Polymer 37 (2):305-311. doi:10.1016/0032-3861(96)81103-7

40. Macosko CW, Jeon HK, Hoye TR (2005) Reactions at polymer-polymer interfaces for blend compatibilization. Progress in Polymer Science 30 (8-9):939-947. doi:10.1016/j.progpolymsci.2005.06.003

41. Bhadane PA, Tsou AH, Cheng J, Favis BD (2008) Morphology Development and Interfacial Erosion in Reactive Polymer Blending. Macromolecules 41 (20):7549-7559. doi:10.1021/ma801390s

42. Pan L, Chiba T, Inoue T (2001) Reactive blending of polyamide with polyethylene: pull-out of in situ-formed graft copolymer. Polymer 42 (21):8825-8831. doi:10.1016/s0032-3861(01)00441-4

43. Pan L, Inoue T, Hayami H, Nishikawa S (2002) Reactive blending of polyamide with polyethylene: pull-out of in situ-formed graft copolymers and its application for high-temperature materials. Polymer 43 (2):337-343. doi:10.1016/s0032-3861(01)00616-4

44. Favis BD, Rodriguez F, Ramsay BA (2003) Polymer compositions containing thermoplastic starch United States Patent 6,605,657,

45. Favis BD, Rodriguez F, Ramsay BA (2005) Method of making polymer compositions containing thermoplastic starch United States Patent 6,844,380,

46. Favis BD, Chalifoux JP (1987) The effect of viscosity ratio on the morphology of polypropylene/polycarbonate blends during processing. Polymer Engineering & Science 27 (21):1591-1600. doi:10.1002/pen.760272105

47. SA S (1967) The determination of the size distribution of particles in an opaque material from a measurement of the size distributions of their sections. In: Elias H (ed) Proceedings of Second International Congress for Stereology. Springer–Verlag, Berlin pp 163-173

48. Favis BD (1994) PHASE SIZE INTERFACE RELATIONSHIPS IN POLYMER BLENDS - THE EMULSIFICATION CURVE. Polymer 35 (7):1552-1555. doi:10.1016/0032-3861(94)90358-1

49. Cigana P, Favis BD (1998) The relative efficacy of diblock and triblock copolymers for a polystyrene/ethylene-propylene rubber interface. Polymer 39 (15):3373-3378. doi:10.1016/s0032-3861(97)10041-6

50. Cigana P, Favis BD, Jerome R (1996) Diblock copolymers as emulsifying agents in polymer blends: Influence of molecular weight, architecture, and chemical composition. Journal of Polymer Science Part B-Polymer Physics 34 (9):1691-1700. doi:10.1002/(sici)1099-0488(19960715)34:9<1691::aid-polb18>3.0.co;2-2

51. Lomellini P, Matos M, Favis BD (1996) Interfacial modification of polymer blends - The emulsification curve .2. Predicting the critical concentration of interfacial modifier from geometrical considerations. Polymer 37 (25):5689-5694. doi:10.1016/s0032-3861(96)00432-6

52. Angellier H, Molina-Boisseau S, Dole P, Dufresne A (2006) Thermoplastic starch-waxy maize starch nanocrystals nanocomposites. Biomacromolecules 7 (2):531-539. doi:10.1021/bm050797s

53. Averous L, Fauconnier N, Moro L, Fringant C (2000) Blends of thermoplastic starch and polyesteramide: Processing and properties. Journal of Applied Polymer Science 76 (7):1117-1128. doi:10.1002/(sici)1097-4628(20000516)76:7<1117::aid-app16>3.0.co;2-w

54. Martin O, Averous L (2001) Poly(lactic acid): plasticization and properties of biodegradable multiphase systems. Polymer 42 (14):6209-6219. doi:10.1016/s0032-3861(01)00086-6

55. Bizot H, LeBail P, Leroux B, Davy J, Roger P, Buleon A (1997) Calorimetric evaluation of the glass transition in hydrated, linear and branched polyanhydroglucose compounds. Carbohydrate Polymers 32 (1):33-50. doi:10.1016/s0144-8617(96)00146-4

56. Sarazin P, Li G, Orts WJ, Favis BD (2008) Binary and ternary blends of polylactide, polycaprolactone and thermoplastic starch. Polymer 49 (2):599-609. doi:10.1016/j.polymer.2007.11.029

57. Chivrac F, Angellier-Coussy H, Guillard V, Pollet E, Averous L (2010) How does water diffuse in starch/montmorillonite nano-biocomposite materials? Carbohydrate Polymers 82 (1):128-135. doi:10.1016/j.carbpol.2010.04.036

58. Krogars K, Heinämäki J, Karjalainen M, Niskanen A, Leskelä M, Yliruusi J (2003) Enhanced stability of rubbery amylose-rich maize starch films plasticized with a combination of sorbitol

and glycerol. International Journal of Pharmaceutics 251 (1–2):205-208. doi:10.1016/s0378-5173(02)00585-9

59. Li HB, Huneault MA (2011) Comparison of Sorbitol and Glycerol as Plasticizers for Thermoplastic Starch in TPS/PLA Blends. Journal of Applied Polymer Science 119 (4):2439-2448. doi:10.1002/app.32956

60. Reichardt C, Welton T (2011) Solvents and Solvent Effects in Organic Chemistry. 4 edn. John Wiley & Sons, Weinheim, Germany

61. Ionescu M (2005) Chemistry and Technology of Polyols for Polyurethanes. Smithers Rapra Technology, Shropshire, United Kingdom

62. Ravati S, Favis BD (2010) Low percolation threshold conductive device derived from a five-component polymer blend. Polymer 51 (16):3669-3684. doi:10.1016/j.polymer.2010.06.015

63. Virgilio N, Desjardins P, L'Esperance G, Favis BD (2010) Modified interfacial tensions measured in situ in ternary polymer blends demonstrating partial wetting. Polymer 51 (6):1472-1484. doi:10.1016/j.polymer.2010.01.017

64. Sivaniah E, Jones RAL, Higgins D (2009) Small Molecule Segregation at Polymer Interfaces. Macromolecules 42 (22):8844-8850. doi:10.1021/ma9017394

65. Broseta D, Fredrickson GH, Helfand E, Leibler L (1990) MOLECULAR-WEIGHT AND POLYDISPERSITY EFFECTS AT POLYMER POLYMER INTERFACES. Macromolecules 23 (1):132-139. doi:10.1021/ma00203a023

66. Yoo S-H, Jane J-l (2002) Molecular weights and gyration radii of amylopectins determined by high-performance size-exclusion chromatography equipped with multi-angle laser-light scattering and refractive index detectors. Carbohydrate Polymers 49 (3):307-314. doi:10.1016/s0144-8617(01)00339-3

67. Bindzus W, Livings SJ, Gloria-Hernandez H, Fayard G, van Lengerich B, Meuser F (2002) Glass transition of extruded wheat, corn and rice starch. Starch-Starke 54 (9):393-400. doi:10.1002/1521-379x(200209)54:9<393::aid-star393>3.0.co;2-w

68. Liu W-C, Halley PJ, Gilbert RG (2010) Mechanism of Degradation of Starch, a Highly Branched Polymer, during Extrusion. Macromolecules 43 (6):2855-2864. doi:10.1021/ma100067x

69. Bao JS, Ao ZH, Jane JI (2005) Characterization of physical properties of flour and starch obtained from gamma-irradiated white rice. Starch-Starke 57 (10):480-487. doi:10.1002/star.200500422

70. Lu QW, Macosko CW, Horrion J (2003) Compatibilized blends of thermoplastic polyurethane (TPU) and polypropylene. Macromolecular Symposia 198:221-232. doi:10.1002/masy.200350819

71. Jeon HK, Kim JK (1998) The effect of the amount of in situ formed copolymers on the final morphology of reactive polymer blends with an in situ compatibilizer. Macromolecules 31 (26):9273-9280. doi:10.1021/ma971002f

72. Hameed T, Quinlan PJ, Potter DK, Takacs E (2012) Study of Reaction Between a Low Molecular Weight, Highly Functionalized Polyethylene and Hexamethylenediamine. Macromolecular Materials and Engineering 297 (1):39-50. doi:10.1002/mame.201100117

73. Bhadane PA, Tsou AH, Cheng J, Ellul M, Favis BD (2011) Morphology and continuity development in highly reactive nanoscale polymer blends. Polymer 52 (22):5107-5117. doi:10.1016/j.polymer.2011.08.049

74. Kim HY, Jeong U, Kim JK (2003) Reaction Kinetics and Morphological Changes of Reactive Polymer−Polymer Interface. Macromolecules 36 (5):1594-1602. doi:10.1021/ma0257907

Chapitre 6 CARBON NANOTUBES IN BIODEGRADABLE BLENDS OF POLYCAPROLACTONE/ THERMOPLASTIC STARCH

*Ata Taghizadeh and Basil D. Favis**

CREPEC, Department of Chemical Engineering, École Polytechnique de Montréal,

2900 Édouard Montpetit, P.O.Box 6079, Station Centre-Ville, Montréal, Québec,

Canada H3C 3A7

6.1 Abstract

The stable localization of solid nanoinclusions in a multiphase polymer system is central to the control of its mechanical, thermal and electrical properties. Despite the importance of polymer-polymer multiphase systems, very little work has been carried out on the preferred localization of solid inclusions in such multiphase systems. In this work, carbon nanotubes (CNT) are dispersed with polycaprolactone (PCL) and thermoplastic starch (TPS) at several CNT contents via a combined solution/twin-screw extrusion melt mixing method. A PCL/CNT masterbatch was first prepared and then blended with 20 wt% TPS. Transmission electron microscopy, as well as high resolution scanning electron microscopy, images reveal a CNT localization majorly in the TPS phase and partly at the PCL/TPS interface. Clearly, during dynamic mixing, a significant proportion of the CNTs have migrated from the PCL phase to the TPS phase indicating a strong driving force for the CNTs with TPS. Annealing of the nanocomposites does not further influence this localization indicating a high stability for this morphological state. Based on the dispersive and polar surface tensions of the components, the Young's model predicts that the nanotubes should be located at the interface. Selective extraction of the system, followed by X-

ray photoelectron spectroscopy (XPS) quantitatively confirms an encapsulation by TPS and reveals a covalent bonding of carbon nanotubes with thermoplastic starch. It appears likely that the nanotubes migrate to the interface, react with TPS and then are subsequently drawn into the low viscosity TPS phase. It is interesting to note that when the same approach is incorporated in a low shear rate/low shear stress internal mixer the nanotubes are found both in the PCL phase and at the PCL/TPS interface and have not completed the transit to the TPS phase. This latter result indicates the importance of choosing appropriate processing conditions in order to minimize kinetic effects. The addition of carbon nanotubes to PCL results in an increase in the crystallization temperature and a decrease in the percent crystallinity confirming the heterogeneous nucleating effect of the nanotubes. Finally, DMA analyses reveals a dramatic decrease in the starch rich phase glass transition temperature (~26˚C), for the system with nanotubes located in the TPS phase.

.

KEYWORDS: Polycaprolactone (PCL), Thermoplastic Starch (TPS), Carbon Nanotubes, Localization, Morphology, Interface, Crystallinity,

6.2 Introduction

Bioplastics include polymers that are biodegradable e.g. polycaprolactone (PCL), or biobased such as biobased polyethylene, or both such as thermoplastic starch (TPS) and PHAs(Queiroz & Collares-Queiroz, 2009). Despite their high annual growth rates, most bioplastics suffer from their inability to cover a broad range of mechanical properties in comparison with the commodity plastics; e.g. PLA or PHB show high modulus, but very low elongation at breaks; PCL demonstrates excellent ductility but suffers from low modulus. Among them, thermoplastic starch (TPS), a widely available biobased material with reasonable cost and excellent biodegradation properties, has been significantly studied(Averous, 2004; Bocchini, Battegazzore & Frache, 2010; Chaleat, Halley & Truss, 2008; Sarazin, Li, Orts & Favis, 2008). Thermoplastic starch can easily flow at high temperatures and be melt processed in a similar fashion to other thermoplastic polymers. The major drawback of TPS, however, is its susceptibility to humidity and weak mechanical properties which generally limits its use in pure form and requires it to be blended with other polymers.

PCL has been used in soft compostable packaging (Averous, 2004) as well as in tissue engineering applications (Bajgai, Aryal, Bhattarai, Bahadur, Kim & Kim, 2008; Bendix, 1998). It has hydrophobic characteristics and shows excellent ductility. However, it is a petroleum based polymer with a low degradation rate and several copolymers such as DL-lactide or glycolide have been incorporated in the structure of PCL to improve its degradation properties(Nair & Laurencin, 2007). Additionally, the degradation rate of polycaprolactone has been shown to be significantly improved in presence of starch (Bastioli, Cerutti, Guanella, Romano & Tosin, 1995; Shin, Lee, Shin, Balakrishnan & Narayan, 2004b). The blending of PCL with thermoplastic starch will increase the biobased portion/biodegradation rate of the PCL products. Several groups have already studied blends of PCL/TPS and have reported a complete immiscibility between the two polymers(Averous, Moro, Dole & Fringant, 2000; Ishiaku, Pang, Lee & Ishak, 2002; Li & Favis, 2010; Shin, Narayan, Lee & Lee, 2008a). Averous et al(Averous, Moro, Dole & Fringant, 2000) have shown complete incompatibility of the two pairs based on T_g curves, however, significant improvements in the mechanical properties of TPS was observed. In a recent work in this laboratory(Li & Favis, 2010), the incorporation of TPS in a PCL matrix was shown to result in very fine and stable morphologies. These TPS/PCL blends demonstrated a high ductility at

values as high as 50 wt% TPS and a corresponding drop in the modulus compared to neat PCL. This level of morphology control can be used as a starting point to evaluate the effect of the incorporation of solid nanoinclusions as a route towards higher performance materials. Owing to the superior mechanical, electrical, magnetic, optical and thermal properties of carbon nanotubes (CNT), they offer the potential to generate novel materials when properly dispersed in a polymer resin(Moniruzzaman & Winey, 2006). In recent years carbon nanotubes have been successfully added to polymer blends improving the morphology and/or mechanical properties(Buffa, Abraham, Grady & Resasco, 2007; Maglio, Migliozzi, Palumbo, Immirzi & Volpe, 1999; Potschke, Bhattacharyya & Janke, 2003; Wu, Zhang, Zhang & Yu, 2009). However, any possible improvement introduced to the polymer blends is highly dependent on the level of dispersion and their localization(Baudouin, Devaux & Bailly, 2010; Hong, Kim, Ahn & Lee, 2008; Meincke, Kaempfer, Weickmann, Friedrich, Vathauer & Warth, 2004). There are two factors influencing the nanoparticles localization: thermodynamics and kinetic effects(Goeldel, Marmur, Kasaliwal, Poetschke & Heinrich, 2011). Ideally, CNTs will migrate to the phase with which they have the lowest interfacial tension in order to minimize the free energy of the system (thermodynamic effect)(Fenouillot, Cassagnau & Majeste, 2009; Goeldel, Kasaliwal & Poetschke, 2009; Potschke, Pegel, Claes & Bonduel, 2008; Wu, Wu, Zhang, Zhou & Zhang, 2008). This will lead to a stable dispersion which is expected to remain unchanged even by further processing. Goeldel et al(Goeldel, Kasaliwal & Poetschke, 2009) showed that nanotubes can migrate to their thermodynamically favorable phase (i.e. PC in PC/SAN blends), irrespective of the mixing strategy. Several authors have tried to predict the localization of nanoparticles in polymer blends by calculating the interfacial tensions between the blend components(Elias, Fenouillot, Majeste & Cassagnau, 2007; Katada, Buys, Tominaga, Asai & Sumita, 2005; Sumita, Sakata, Asai, Miyasaka & Nakagawa, 1991b). However, the evaluation of the interfacial tensions of polymers/solid inclusions is complex and has not been examined significantly in the literature. A rough estimation of the interfacial tensions can limit the ability to predict the localization in all cases(Wu et al., 2011).

Another determining factor related to the localization of nanofillers in polymeric systems is kinetics. Kinetics include the processing parameters such as mixing sequence and shear rate as well as the viscosity, temperature effects, or even the shape of the nanofiller(Baudouin, Devaux & Bailly, 2010; Fenouillot, Cassagnau & Majeste, 2009; Goeldel, Kasaliwal, Poetschke &

Heinrich, 2012; Goeldel, Marmur, Kasaliwal, Poetschke & Heinrich, 2011; Tao et al., 2011). Each of these may suppress the migration of the nanofillers to the thermodynamically stable state of dispersion, for example, an increased viscosity of PCL in PCL/PLA blends(Wu et al., 2011) or PMMA in PMMA/PP blends (Feng, Chan & Li, 2003).

There are several methods for the dispersion of nanotubes in polymer matrix. Generally, the solvent dissolution method is shown to be one of the most efficient methods to disperse nanotubes in polymers but is mostly applicable at the laboratory scale (Grady, 2010). Melt mixing is the preferred method in spite of its lower comparative efficacy(Bose, Bhattacharyya, Bondre, Kulkarni & Potschke, 2008; Goeldel, Kasaliwal, Poetschke & Heinrich, 2012; Grady, 2010; Valentini, Biagiotti, Kenny & Manchado, 2003). A combination of these methods may result in a high level of dispersion without damaging the nanotubes as is observed in masterbatch-type processes(Abbasi, Carreau & Derdouri, 2010). It is expected that kinetic effects will be different depending on the type of mixing equipment with their different flow fields and intensity or processing times and hence, the localization of the nanoparticles may be potentially different in different mixing equipments (Ansari, Ismail & Zein, 2009; Breuer & Sundararaj, 2004; Das & Maiti, 2008; Ma, Siddiqui, Marom & Kim, 2010).

The objective of this work is to investigate the localization of carbon nanotubes in blends of thermoplastic starch/polycaprolactone. Two melt blending operations will be examined. The observed localization of carbon nanotubes in the multiphase system will be compared to predictive models and the relative role of thermodynamic and kinetic effects will be addressed. The influence of carbon nanotubes on the morphology of the blend will be studied. Finally, the influence of carbon nanotubes on the physical properties of the material will be assessed.

6.3 Experimental Section

6.3.1 Materials

The native wheat starch and glycerol were obtained from ADM and Labmat, respectively. The wheat starch was composed of 25% amylose and 75% amylopectin. The glycerol was pure at 99.5% and contained 0.5% water. Polycaprolactone (PCL), CAPA 6500, was supplied by Solvay Chemicals. Capa6500 has a molecular weight of 50,000 $g.mol^{-1}$ and a MFI of 7.0 (g per min, 160˚C). Surface modified multiwall carbon nanotubes (NC3101) were purchased from Nanocyl

Co. The average diameter and length of CNTs were 9.5 nm and 1.5 μm, respectively with a carbon purity of greater than 95%. The carboxylic acid surface modification was evaluated by XPS to be ~ 4%.

6.3.2 PCL/CNT Preparation

A PCL-CNT masterbatch was first prepared at high CNT loadings (9-11 wt%) through a solution casting method at room temperature. Nanotubes were dispersed in THF for 1 hr via ultrasonication. Then the PCL/THF solution was added to CNT solution and ultrasonication continued for 1 hr more. An antisolvent was added to the solution at the end and precipitated PCL and CNT were dried in the vacuum oven at 35˚C for a week. The nanotubes wt% in the masterbatches was determined by TGA (TGA Q500, TA Universal).

6.3.3 Blend Preparation

6.3.3.1 Twin-Screw

The PCL/CNT masterbatch then went through two different methods of preparation. In method one, TPS/PCL blends were prepared in a twin screw extruder via an established method in this laboratory (Favis, Rodriguez-Gonzalez & Ramsay, 2003; Favis, Rodriguez-Gonzalez & Ramsay, 2005) which consists of a single screw extruder (SSE) connected midway to a co-rotating twin screw extruder (TSE). The starch/glycerol/water suspension was fed to TSE in which native starch was gelatinized and plasticized and the water was extracted before molten PCL/CNT are fed from the SSE to midway on the TSE. The TPS slurry was formulated in a way that the final TPS consists of 36 wt% glycerol. The compositions were all constant at PCL/TPS: 80/20 wt%. The screw speed was set at 100 rpm and the mixing zone temperatures were fixed at 145˚C. In order to obtain the CNT content of the blends, in each step thermogravimetric analyses (TGA) tests were conducted. CNT contents were 0.5 and 1 wt% based on the whole blend.

6.3.3.2 Brabender

In a second blending method, pure TPS was obtained via the above method in a twin screw extruder(Favis, Rodriguez-Gonzalez & Ramsay, 2003; Favis, Rodriguez-Gonzalez & Ramsay, 2005). The blend with PCL was then prepared via an internal mixer (Brabender Plasticorder). The rotor speed was set at 100 rpm and the processing temperature was at 145˚C. The master

batch and neat PCL were then first fed to an internal mixer and after reaching plateau of the torque, thermoplastic starch (TPS) was added to the chamber. The compositions were all constant in PCL/TPS: 80/20 wt%. CNT contents were 0.5,1 and 2 wt% based on the whole blend.

In order to prepare the samples for further characterization tests, the samples of both methods were compression molded at 145˚C. In order to be able to easily remove the samples, two Teflon sheets were inserted between metal plaques and molds. The total molding process time took 8min under a nitrogen atmosphere after which it was quenched in a cold press to freeze-in the morphology.

Quiescent annealing was further conducted on some selected samples of both methods at 145˚C for up to 60 min.

6.3.4 Rheological Characteristics

Rheological characterizations of the thermoplastic starch and PCL were performed in oscillation mode using a MCR-301 strain controlled rheometer from *Anton Paar*. The experiments were conducted in parallel plate geometry. First a stress sweep test was run to define the region of linear viscoelasticity. Then a frequency sweep test was conducted on the samples from 0.1 to 200 rad/s at 145˚C and 165˚C. Another stress sweep test was run in a constant shear rate of 52 rad/s.

6.3.5 SEM and TEM

In order to observe the localization of the nanotubes, SEM and TEM imaging were conducted on the samples. Microtoming, followed by platinum coating was carried out on certain samples. The prepared samples were then subjected to SEM imaging to observe the nanotubes on the surface. In order to obtain the morphology of the blends, the as-prepared samples were microtomed and then the TPS phase was extracted by HCL (6N). The prepared surfaces were gold coated for further microscopic investigations. Image analyses were performed on the sample images to obtain both number and volume average diameters. The microscope was a Jeol JSM 7600TFE Scanning Electron Microscope (SEM) operated at a voltage of 2 kV. Ultramicrotoming followed by TEM imaging (Jeol JSM 2100F, operating at 200 kV) was used on some selected samples to have a magnified view of the nanotubes in the blends on the prepared ultrathin samples. The micrographs were manually digitized using a digitizing table from Wacom and SigmaScan v.5 software.

6.3.6 Surface Tension Measurements

The surface tensions of thermoplastic starch and polycaprolactone were measured by the sessile drop method with probe liquids. The details of the contact angle measurement technique can be found elsewhere(Kwok & Neumann, 1999). The obtained data are represented in Table 6-1.

Table 6-1 Surface tension parameters of different materials used.

	γ_d (mN/m)	γ_p (mN/m)	γ (mN/m)
PCL: @ 23 ˚C	42	10.2	52.3
@145˚C	36.4[a]	8.8	45.2
TPS : @ 23 ˚C	25.4	7.61	33.01
@ 145˚C	19.9	6	25.9
CNT @ 145˚C	18.4	26.9	45.3

[a]Surface tensions calculated at 145 ˚C (dσ/dT: - 0.058 mN/(m K))[87].

Comparing the obtained values with other reported data, it is found that the surface tensions obtained for TPS and PCL are in agreement with the literature(Averous & Boquillon, 2004; Wu et al., 2011). The surface tension data for carbon nanotubes are obtained from the work of Nuriel et al.(Nuriel, Liu, Barber & Wagner, 2005) which reports the highest polarity values (Goeldel, Marmur, Kasaliwal, Poetschke & Heinrich, 2011) and has been frequently used in the literature for carbon nanotubes of similar size and structure(Ozdilek, Bose, Leys, Seo, Wubbenhorst & Moldenaers, 2011; Potschke, Pegel, Claes & Bonduel, 2008; Wu et al., 2011; Xiang et al., 2011; Yuan, Yao, Sylvestre & Bai, 2012). Interfacial tension was calculated based on geometric-mean:

$$\gamma_{xy} = \gamma_x + \gamma_y - 2\left[\left(\gamma_x^d \gamma_y^d\right)^{1/2} + \left(\gamma_x^p \gamma_y^p\right)^{1/2}\right] \quad (1)$$

and harmonic-mean equations(Wu, 1987b):

$$\gamma_{xy} = \gamma_x + \gamma_y - 4\left[\frac{\gamma_x^d \gamma_y^d}{\gamma_x^d + \gamma_y^d} + \frac{\gamma_x^p \gamma_y^p}{\gamma_x^p + \gamma_y^p}\right] \quad (2)$$

Where γ_x is the surface tension of material x and its two components, are dispersive γ_x^d and polar γ_x^p, and γ_{xy} is the interfacial tension between phase x and phase y (Table 6-2).

Table 6-2 Interfacial energies for all possible different interfaces.

	Interfacial Energy according to harmonic mean equation, mN/m	Interfacial Energy according to geometric mean equation, mN/m
PCL/TPS	5.4	2.7
PCL/CNT	15.1	8
TPS/CNT	13.3	7.5

6.3.7 X-ray Photoelectron Spectroscopy (XPS)

XPS was used in order to quantitatively verify the nature of the encapsulating polymer and its interaction on the carbon nanotube surface. In order to run the XPS test on the nanotubes surface, PCL was removed by THF for one week, followed by TPS extraction by 6N HCL for the same time period. This procedure was repeated twice in order to extract any polymer left on the surface of the nanotubes. The nanotubes were then separated centrifugally from the solution. The dried extracted nanotubes along with pure nanotubes were scanned by XPS. X-ray Photoelectron Spectroscopy (XPS) was conducted on a (VG ESCALAB 3 MKII) spectrometer with Mg-Kα ray source. Survey scans of 100 eV. pass energy was used to identify initially all components followed by a high resolution individual scans using a pass energy of 20 eV. The surface elemental stoichiometry was obtained from the ratios of peak areas corrected with the Wagner sensitivity factors and Shirley background subtraction.

6.3.8 Differential Scanning Calorimetry (DSC)

In order to obtain the effect of nanofillers on the crystallinity of PCL, a differential scanning calorimetry instrument (DSC Q1000, TA instruments) was used at a heating-cooling rate of ±10 $^{\circ}C.min^{-1}$ between -30 to 80 ˚C with an empty sample pan as the reference. The blends were weighed (10–15 mg) and then sealed. The calorimetric data extracted from these tests was determined using Universal Analysis® software.

6.3.9 Dynamic Mechanical Analyses (DMA)

Dynamic mechanical properties were measured using a TA dynamic mechanical analyzer (TA Instruments, DMA 2980). The temperature was increased from -100 to 40 ˚C, with a heating rate

of 3˚C/min. The frequency was 1 Hz, and the oscillation amplitude was 30 microns. The measurements were carried out using the dual cantilever clamp mode.

6.4 Results and Discussions

6.4.1 Morphology and Localization of Carbon Nanotubes in TPS/PCL Blends Prepared by Twin-Screw Extrusion

SEM images of PCL/TPS blends prepared by twin-screw extrusion are shown in Figure 6-1. The carbon nanotubes can be clearly identified as white spots and it can be seen that the nanotubes are located in the TPS phase and at the interface. TEM microscopy was also conducted on selected samples and Figure 6-2 confirms the localization of the nanotubes mainly in the bulk of the TPS phase and a small portion at the interface. Annealing selected samples was carried out in order to determine the morphological stability. The samples after annealing demonstrated the same morphological state as seen in Figures 6-1 and 6-2.

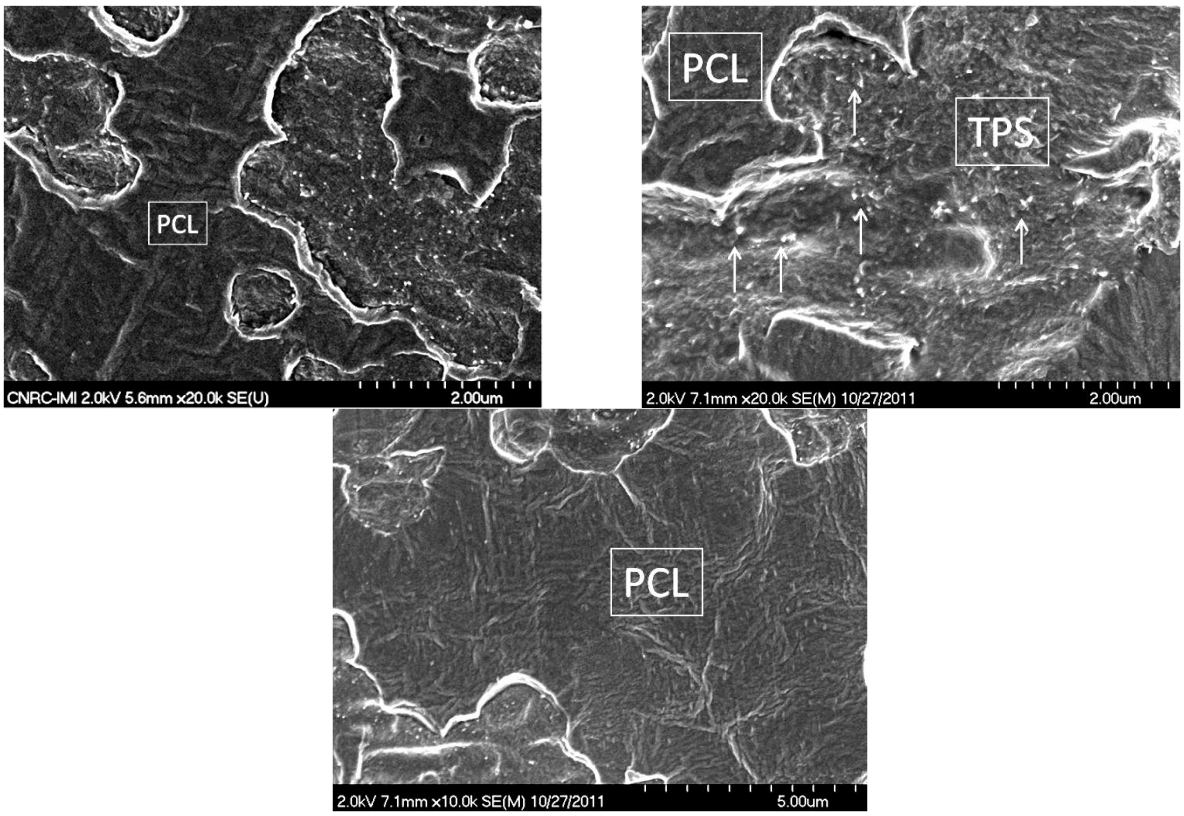

Figure 6-1 SEM images of blends of PCL/TPS 80/20 wt% with 1wt% CNT prepared by twin screw extrusion.

The strong driving force of the nanotubes for TPS is considered to be even more dramatic when it is considered that, in the blending process, the nanotubes were first introduced into the PCL phase. During the blending process the nanotubes clearly migrate from the PCL phase to the interface with a significant proportion penetrating into the TPS phase. From a thermodynamic standpoint, the localization of solid inclusions is controlled by the minimization of the free energy of the system(Goeldel, Kasaliwal & Poetschke, 2009; Poetschke, Pegel, Claes & Bonduel, 2008; Wu & Shaw, 2004; Zhang, Wan & Zhang, 2009). The thermodynamic tendency of a filler localization in the thermodynamic equilibrium state can be calculated by the Young's equation (Equation 3)(Sumita, Sakata, Asai, Miyasaka & Nakagawa, 1991a):

$$\omega = \frac{\gamma_{cnt-B} - \gamma_{cnt-A}}{\gamma_{A-B}} \quad (3)$$

where γ_{x-y} is the interfacial tension between component x and y and ω is the wetting coefficient.

If ω>1, then the CNT will migrate to phase A, if ω < -1 it will be dispersed in B, but if -1< ω <1, the CNT will mainly go to the interface. Assigning A as PCL and B as TPS and calculating the wetting coefficient based on the data obtained in Table 6-2, result in -0.33 and 0.18 for harmonic-mean and geometric-mean equations, respectively. Consequently, both the harmonic and geometric mean approaches to estimate interfacial tension and subsequently the wetting coefficient results in the prediction that the nanotubes should be located at the interface. However, the data above for twin-screw extrusion shows that the nanotubes are not only at the interface but also majorly in the bulk of the TPS phase.

The morphology and mechanical properties of PCL/TPS blends have been studied previously in this laboratory and it has been shown that PCL and TPS have a certain level of compatibility(Li & Favis, 2010). In this work, adding nanotubes to the blend did not result in any change in the TPS phase size or morphology as shown in Figure 6-3 and quantitatively reported in Table 6-3. Typically solid inclusions may affect the morphology of blends by changing the phase viscosity and/or the nature of the interface(Fenouillot, Cassagnau & Majeste, 2009). In this work, it appears that the high level of compatibility between PCL and TPS dominates the morphology and any change to the viscosity of the TPS phase through the addition of nanotubes appears to be a minor effect. It should also be noted that the elongational flow component of twin-screw

extrusion mixing is particularly effective at reducing the dispersed phase size and tends to demonstrate a reduced dependence on viscosity ratio(Favis, 2000a).

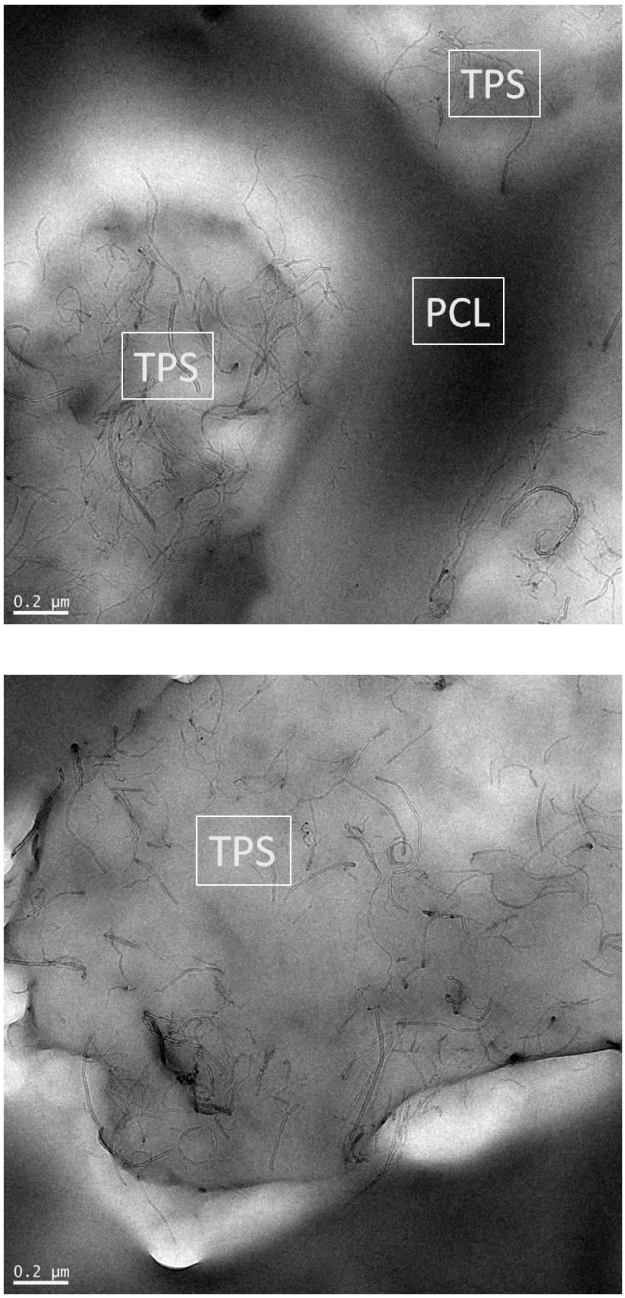

Figure 6-2 TEM images of blends of PCL/TPS 80/20 wt% with 1wt% CNT prepared by twin screw extrusion.

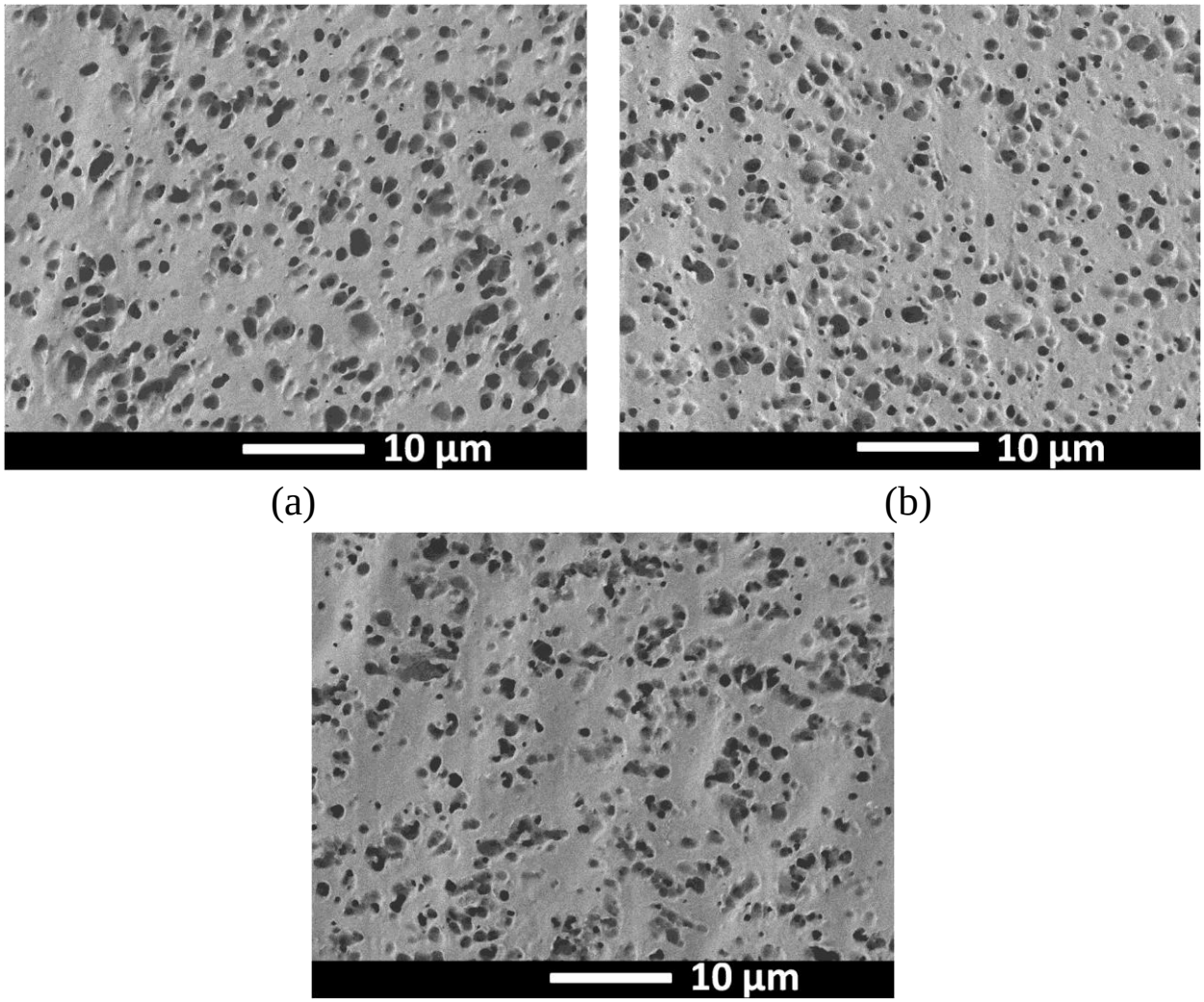

(a) (b)

(c)

Figure 6-3 SEM images of PCL/TPS 80/20 wt% with different CNT wt% prepared with twin screw extrusion: (a) 0 wt% CNT; (b) 0.5 wt% CNT; (c) 1 wt% CNT.

6.4.2 XPS Analysis of Carbon Nanotube Surface

XPS analyses were conducted on samples that had been selective extracted for both PCL and TPS in order to quantitatively confirm the encapsulating phase around the nanotubes and also evaluate the type of interaction occurring at the nanotube surface. The surface compositions of the nanotubes before and after blending in the twin-screw extruder were examined. The survey spectra overlay of pure and extracted carbon nanotubes surfaces are shown in Figure 6-4. The significant increase of atomic oxygen from 8% to 23% is clearly observed on this overlay

indicating the clear preferential encapsulation of nanotubes by one of the phases. The high resolution spectra of the carbon region for pure and extracted nanotubes are shown in Figure 6-5.

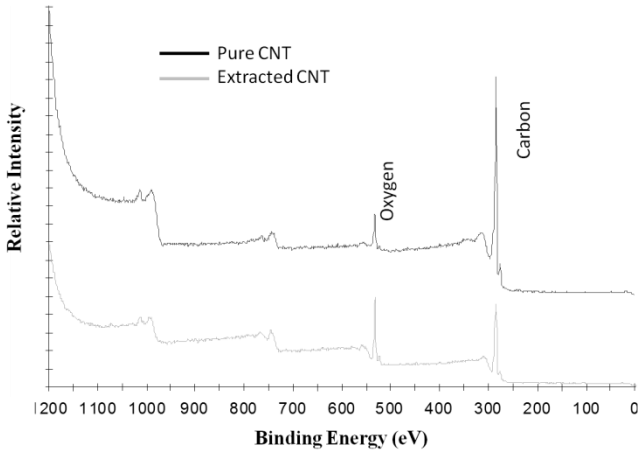

Figure 6-4 XPS survey spectra of fresh and extracted (after 2 weeks of solvent extraction) nanotubes. The curves were offset for clarity.

The carbon region curves were fitted with six symmetric components identifying the different carbon functional groups present on the surface of the nanotubes. Components C1 and C2 at a binding energy (B.E.) of 284.4 eV and 285.3 eV, respectively, indicate sp^2 graphitic carbon, and sp^3 carbon plus sp^2 carbon defects. C3 at a B.E. of 286.5 eV indicates C-O and C-O-C groups, while C4 at 288.4 eV indicates the presence of O-C-O groups(Luong et al., 2005). The relative intensity of the carbon functional groups found on the surface of the CNT in the extracted samples is significantly different from that observed on the pure nanotubes. A comparative decrease in intensity of sp^2 graphitic carbon and simultaneous increase of carbon-oxygen functional groups on the surface of extracted nanotubes compared to the pure ones allows for the identification of the encapsulating phase. By considering the ratios of C3 (C-O) and C4 (O-C-O) over C2 (sp^3 C-C and sp^2 carbon defects) on the extracted samples, C3/C2 is increased compared to that on the pure CNT by a factor of 114% while C4/C2 is increased by a factor of 24%. In other words, the increase of C-O functions is close to five times the increase of O-C-O functions (Table 6-4). Since the ratio of C-O to O-C-O functions in a model starch molecule is 5 to 1, this confirms the encapsulation of nanotubes by starch chains. The ability of starch to remain on the carbon nanotube surface even after multiple extractions and two weeks of solubilization is

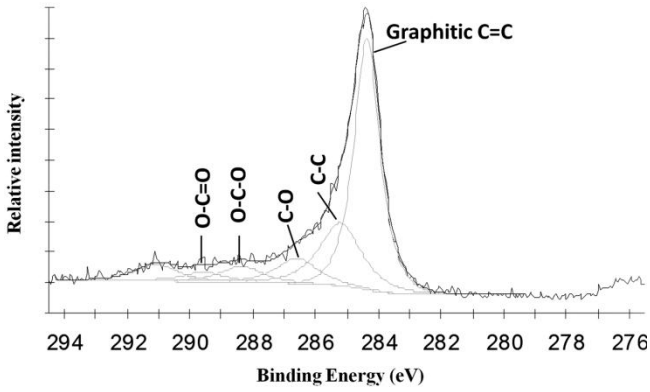

(a)

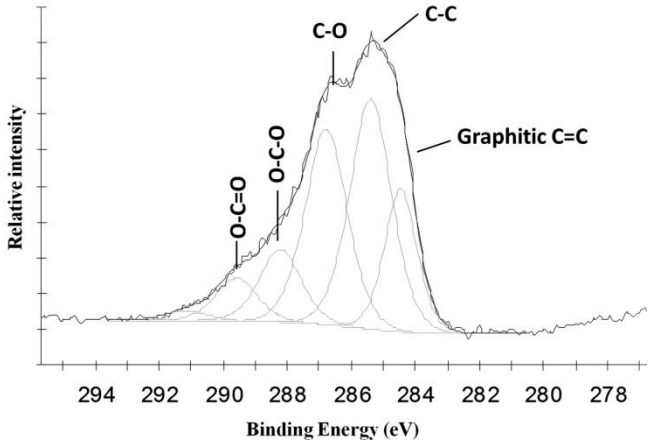

(b)

Figure 6-5 Narrow scan spectra of carbon region for: (a) fresh nanotubes; (b) extracted nanotubes.

strongly indicative of the formation of a covalent bond between the carboxylic acid groups on the nanotube surface and the TPS. Such interactions between starch and carbon nanotubes have been shown by other authors as well (Angellier, Molina-Boisseau, Dole & Dufresne, 2006; Ma, Yu & Wang, 2008; Stobinski et al., 2003a) .

Table 6-3 Relative functional groups increase on the carbon nanotube walls before and after extrusion process.

	C3/C2 (C-O/C-C)	C4/C2 (O-C-O/C-C)
pure CNT	0.399	0.255
Extracted CNT	0.854	0.318
Total increase	114%	24%

6.4.2.1 Physical Model

Dynamic mixing allows for the nanotubes to move through the PCL phase. Once in contact with the interface, the nanotubes localize there in a stable fashion in order to minimize the overall surface free energy. At the interface a reaction occurs between the carboxylic acid groups of the nanotube and the alcohol groups of the starch. Following this reaction and the formation of a TPS encapsulating layer around the nanotube, the carbon nanotubes are drawn into the thermoplastic starch dispersed phase.

6.4.3 TPS/PCL/Carbon Nanotubes localization in an alternative process (Internal Mixer)

The twin screw extrusion led to the localization of the carbon nanotubes majorly in the TPS phase. However, as explained earlier this localization may be impeded in some processes due to kinetic effects. In order to assess the influence of a different processing technique on carbon nanotube localization, an internal mixer was used. Since the internal mixer imposes a predominantly shear flow field, its influence on the localization process will be interesting to examine. In order to evaluate the performance of the internal mixer in preparing this nanocomposite, we repeated the same procedure in an internal mixer.

Although the sequence of CNT addition remains constant i.e. CNT is fed to the system through the PCL phase, it is observed that localization of CNTs in the internal mixer is totally different from the previous method In the internal mixer, the nanotubes do not migrate to the TPS phase but rather remain in the PCL phase and at the PCL/TPS interface(Figures 6-6 and 6-7). Annealing the samples makes the nanotubes move more towards the interface while TPS phase remains completely CNT-free.

Table 6-4 Number and volume average diameter sizes of the PCL/TPS 80/20 wt% blends with different carbon nanotube contents prepared by extrusion and internal mixing.

	d_n (μm)	d_v (μm)
PCl/TPS [a]	1.4	1.9
PCl/TPS + 0.5 wt% cnt [a]	1.2	1.6
PCl/TPS + 1 wt%cnt [a]	1.3	1.7
PCl/TPS [b]	3	3.6
PCl/TPS + 0.5 wt% cnt [b]	1.1	1.7
PCl/TPS + 1 wt% cnt [b]	0.7	1.6
PCl/TPS + 2 wt% cnt [b]	0.7	1.7

[a] Prepared by extrusion.

[b] Prepared by internal mixing.

In twin screw extruder and internal mixer, two different shear fields exist. Internal mixer has been majorly assumed to have simple shear flows between the rotors and the walls(Adragna, Couenne, Cassagnau & Jallut, 2007; Bousmina, Ait-Kadi & Faisant, 1999). But in twin screw extruders in addition to shear flow, strong elongational fields exist as well (Favis, 2000a; Harrats, Thomas & Groeninckx, 2006). Viscosity-shear rate variation for TPS denotes a completely shear thinning behaviour (Figure 6-9). Comparing the apparent shear rates in the two mixing procedures; it is observed that with 100 rpm in twin screw extruder, the apparent shear rate in the last zone of screws, where due to the die, the pressure increases and filling factor is ~1, is around 88 /s (Clark, Geramita & Baker, 1999; Shahbikian, 2010), while with the 100 rpm of the internal mixer the apparent shear rate is ~52 /s (Bousmina, Ait-Kadi & Faisant, 1999; Shahbikian et al., 2012). TPS viscosity is expected to increase dramatically in the internal mixer shear field. In addition to shear viscosity, TPS has shown to have a very shear thinning nature in elongational flow fields as well(Della Valle, Vergnes & Lourdin, 2007), which will act as another factor for further reducing the viscosity of TPS in twin screw extrusion process. The applied shear stress is also expected to vary and increase to very high amounts in the extruder due to the pressure variation as a result of different kneading elements.

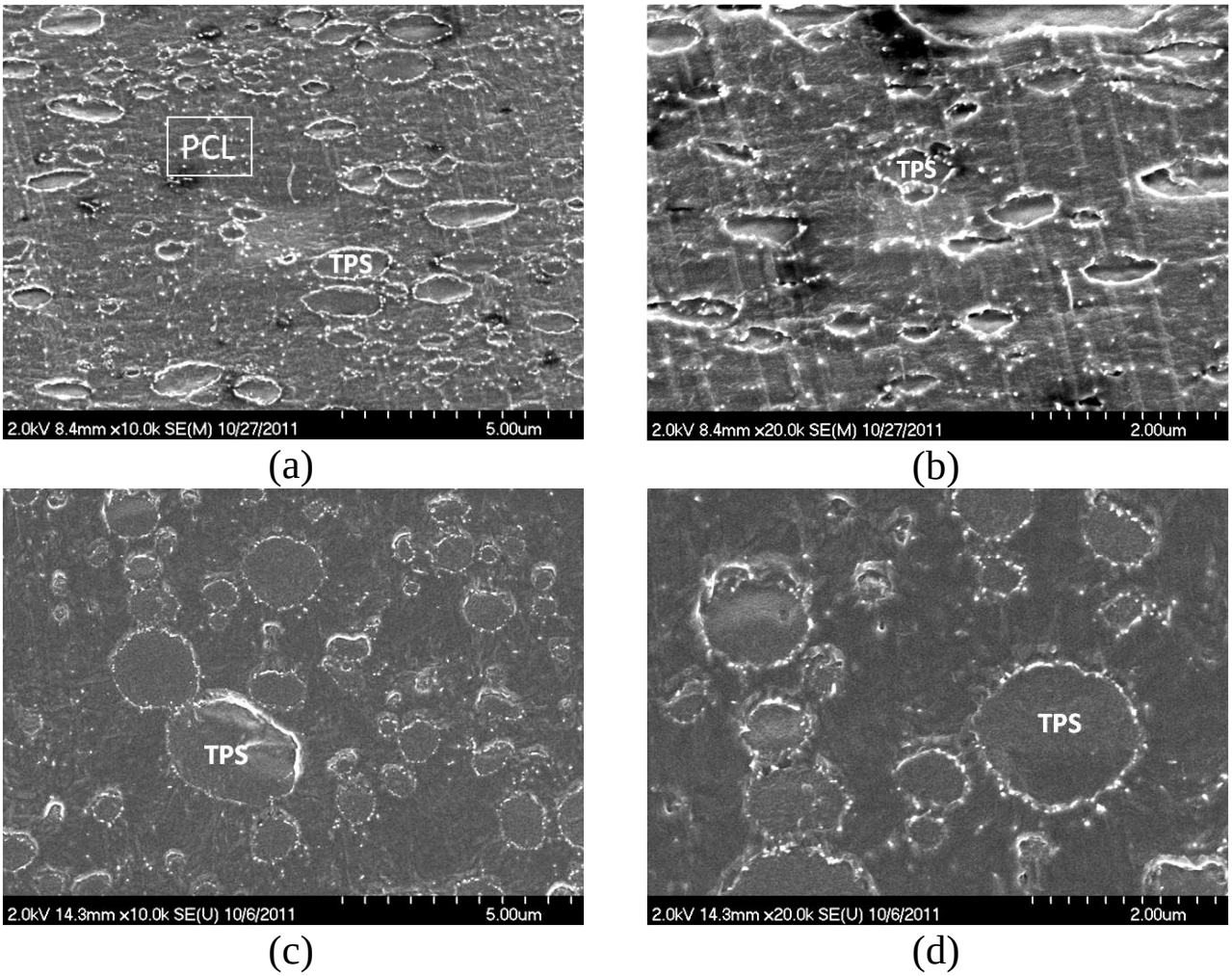

Figure 6-6 SEM images of blends of PCL/TPS 80/20 wt% with 2 wt% carbon nanotube prepared by internal mixer: (a) and (b) frozen morphology after process; (c) and (d) Annealed samples for 1 hr at 145˚C.

As it can be seen in Figure 6-10, contrary to PCL, TPS is very sensitive to shear stress. Hence, it is expected for TPS to have much lower actual viscosity in extruder than internal mixer. So it is believed that this is the increase of TPS viscosity which does not allow the reacted nanotubes to penetrate to the TPS phase and they remain at the interface. So by moderate decrease in TPS viscosity (higher temperature processing, Figure 6-9) the nanofillers should be able to at least partly locate themselves in the dispersed phase. Figure 6-11 clearly shows this change in localization in higher temperature process in a way that nanotubes have been able to partly penetrate into TPS phase in case of moderate decrease in TPS viscosity.

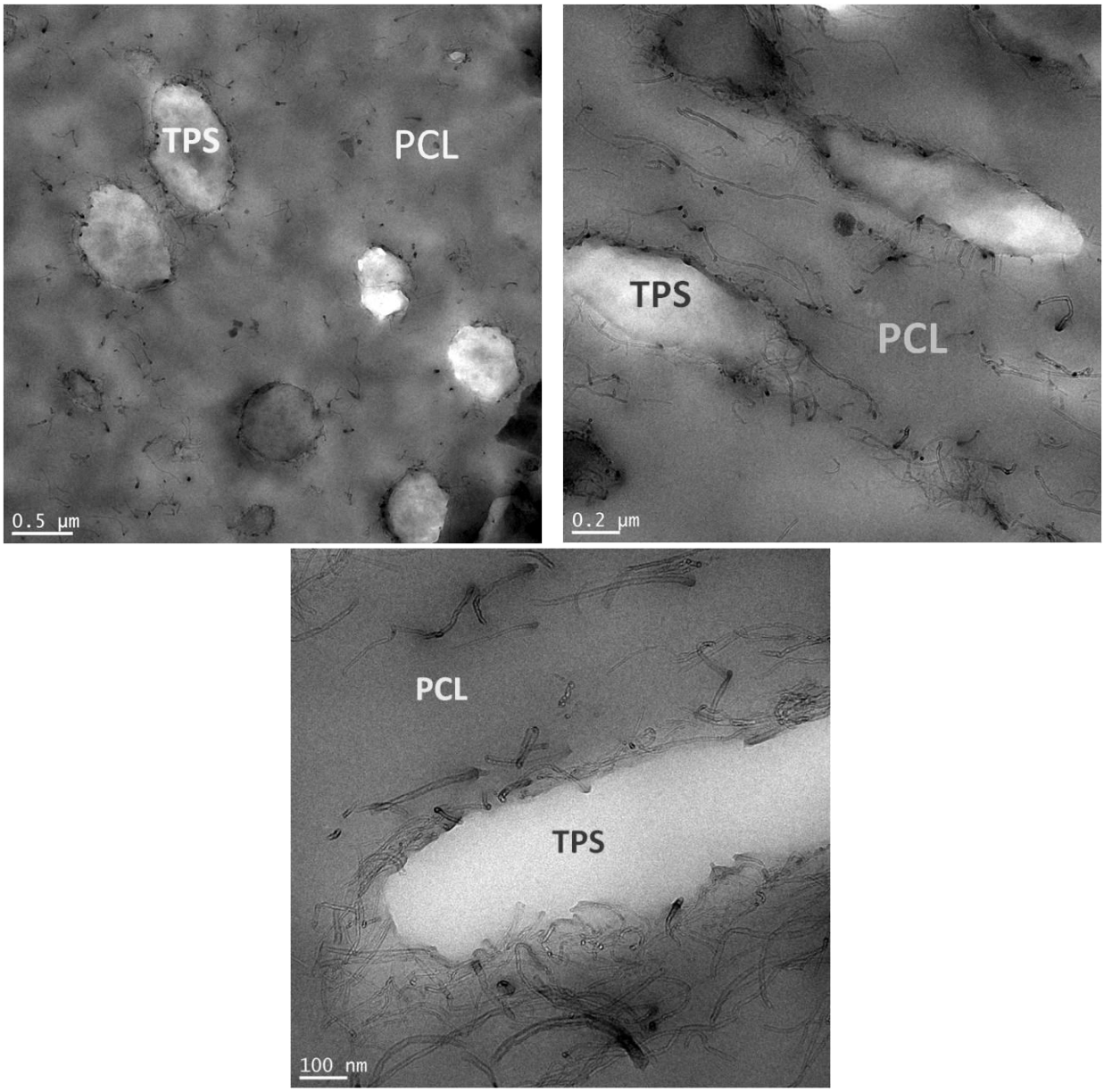

Figure 6-7 TEM images of blends of PCL/TPS 80/20 wt% with 2 wt% carbon nanotube prepared by internal mixer.

Thus, in shear sensitive materials such as TPS which the melt viscosity can be significantly changed by processing parameters, the localization of the nanofillers can be subjected to change in different shear fields. Consequently, various mixing equipments e.g. internal mixers or

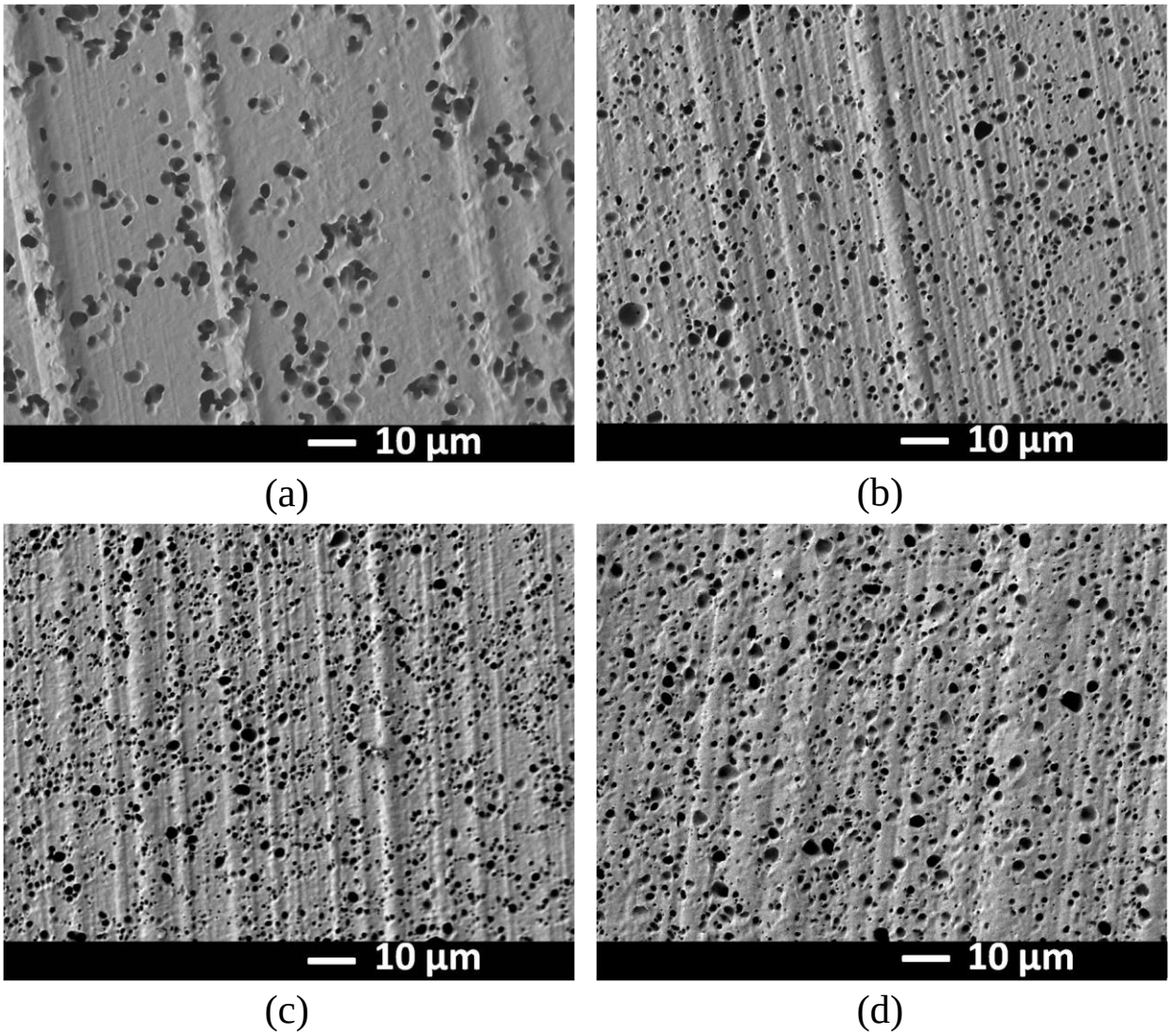

Figure 6-8 SEM images of PCL/TPS 80/20 wt% with different carbon nanotube wt% prepared with internal mixer: (a) 0 wt%; (b) 0.5 wt%; (c) 1 wt%; (d) 2 wt%.

extruders exerting different shear fields in the process can be used to govern the localization of nanofillers, however this localization may not be necessarily the thermodynamically favourable state of dispersion and therefore the nanofillers localization may be subjected to change by further processing under different processing conditions in order to reach the equilibrium state of dispersion.

The TPS dispersed phase size, in this case, is significantly improved by this concentration of nanotubes at the PCL/TPS interface. This effect is clearly observed in the Figure 6-8. With the incorporation of 0.5 wt% nanotubes, the TPS droplet size reduces by half (Table 6-3). This decrease continues for d_n up to 1 wt% CNT after which it reaches a plateau.

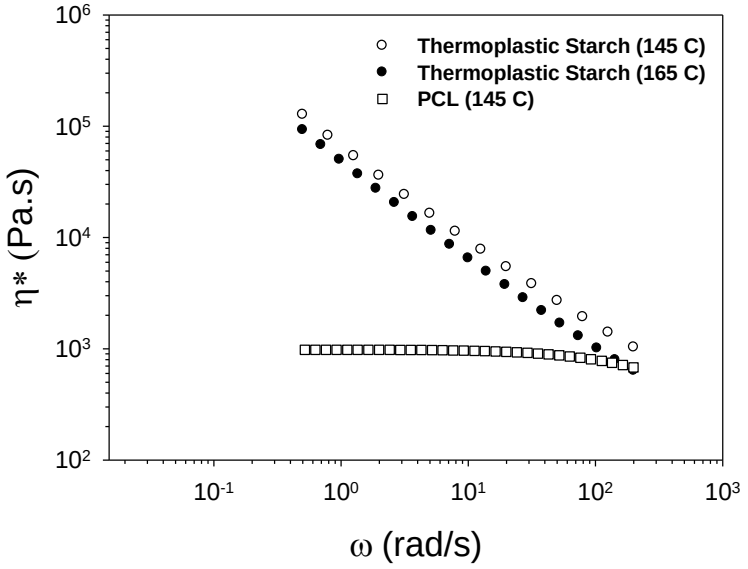

Figure 6-9 Variation of complex viscosity with frequency for TPS and PCL at different processing temperatures.

It appears in the case of the internal mixer that the localization of the nanotubes at the PCL/TPS interface generates a physical barrier for the dispersed TPS phase coalescence, thus resulting in a significant reduction of phase size. On the other hand, increasing the viscosity of the matrix will increase the capillary number resulting in a smaller droplet size(Favis, 2000a).

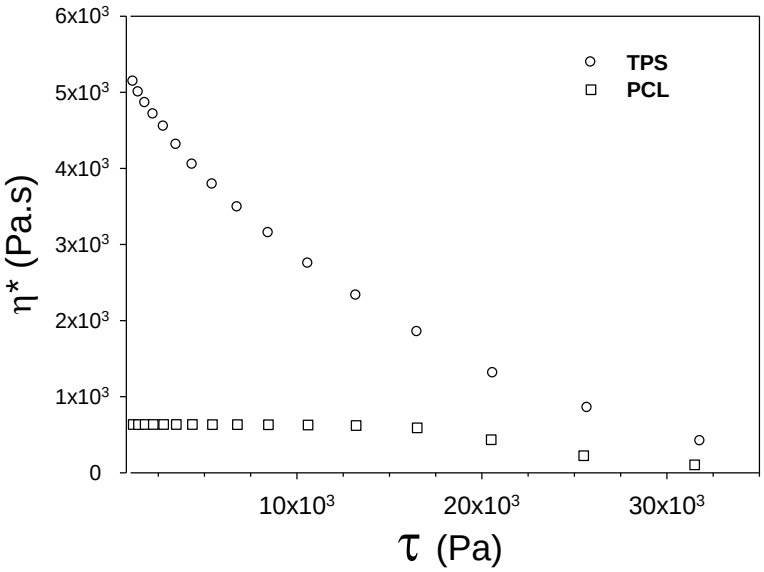

Figure 6-10 Variation of complex viscosity with shear stress for TPS and PCL at 145 ˚C.

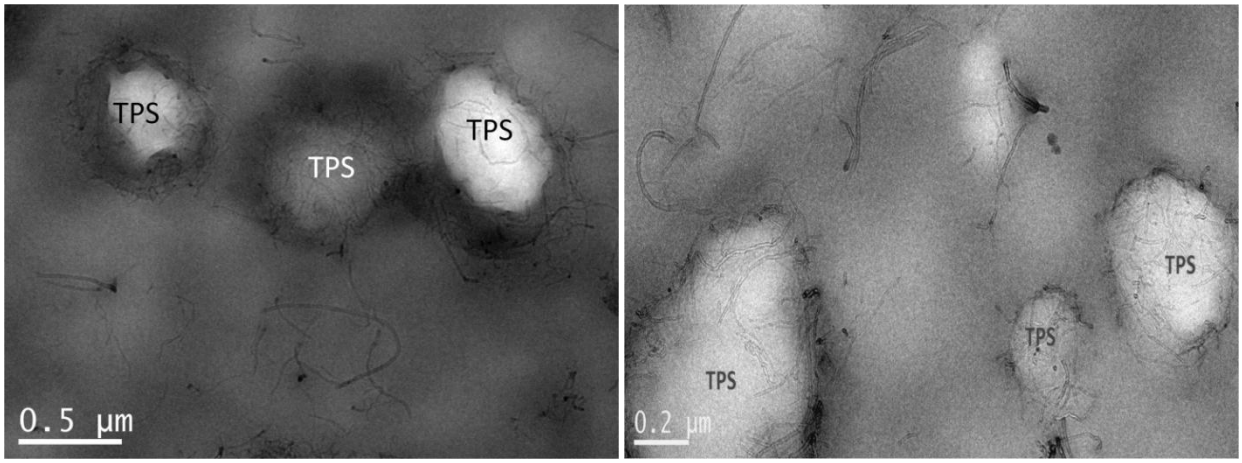

Figure 6-11 TEM images of blend of PCL/TPS 80/20 wt% with 2 wt% carbon nanotube prepared by internal mixer at 165˚C.

6.4.4 Differential Scanning Calorimetry (DSC)

Polycaprolactone (PCL) is a semicrystalline polymer with a crystallinity of around 40%. As shown in Table 6-5, the addition of TPS results in the increase of the PCL crystallisation temperature which is believed to be due to the heterogeneous nucleating effect of TPS, however, the percent crystallinity remains almost unchanged. It is shown that natural polymers such as starch can act as nucleating substrate and promote crystallization kinetics but the final small size of crystals and their low degree of perfection might decrease the enthalpy of melting and consequently the crystallinity percentage(Ciardelli et al., 2005). Nanotubes are also materials which can act as strong nucleating agents in polymers and change the crystallization type and structure(Grady, 2012). The nonisothermal crystallization exothermic peaks are shown in Figure 6-12 for extrusion and internal mixing samples. It is observed that all of the CNT-incorporated blends of PCL/TPS show a higher T_c than for the neat blend of PCL/TPS which is due to the heterogeneous nucleating effect of carbon nanotubes(Chun, Kyung, Jung & Kim, 2000; Wu, Wu, Sun & Zhang, 2007). The percent crystallinity, however, decreases by incorporating nanotubes for both processes. Like other heterogeneous nucleating agents, the presence of nanofillers has two effects, one is facilitating the crystallization due to their nucleating role and the opposite effect due to slower growth and lamellar defects in the crystalline structure(Grady, 2012; Sanchez-Garcia, Lagaron & Hoa, 2010; Wu, Wu, Sun & Zhang, 2007; Wu & Chen, 2006). In the case of nanotubes due to their size and molecular level interactions they can interfere more

effectively in the growth and forming of spherulites and impose some defects in the crystalline structure.

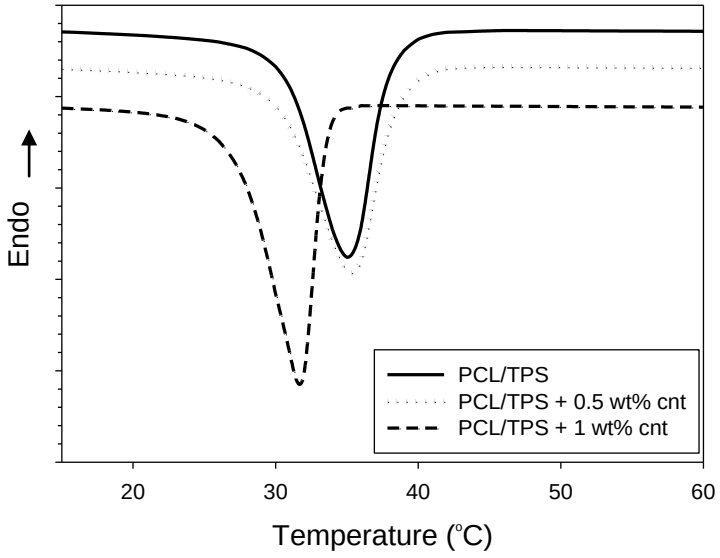

(a)

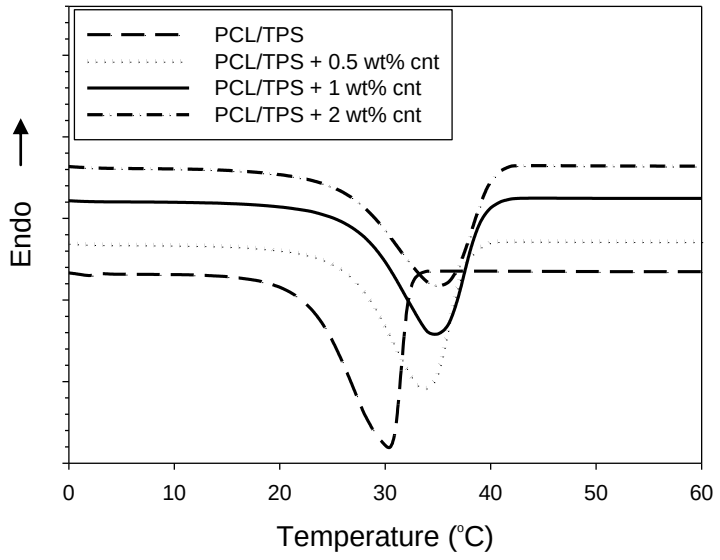

(b)

Figure 6-12 DSC thermograms of PCL/TPS 80/20 wt% with different carbon nanotube contents prepared via: (a) Extrusion; (b) Internal mixer. The curves were offset for clarity.

In a binary blend such as PCL/TPS, the localization of nanotubes determines the extent of nanotube impact on the crystallization. In the extrusion samples of PCL/TPS/nanotubes, the

addition of nanotubes decreases the percent crystallinity of PCL and increases crystallization temperature (Table 6-5), but this change remains at the same level independent of the CNT loading. This is due to the fact that the effect of carbon nanotubes on the crystallization in these samples is limited by its localization at the PCL/TPS interface. Furthermore, as mentioned previously, the droplet size and distribution and consequently the interfacial area remains almost unchanged in the extrusion samples. On the other hand, in the samples prepared by internal mixing where nanotubes were localized in both PCL and at the interface, a significant shift is observed in crystallization temperature from 0.5 wt% to 1 wt% CNT following a plateau afterwards (Table 6-5).

Table 6-5 DSC characteristics of PCL/TPS 80/20 wt% blends with different CNT contents prepared by extruder and internal mixer.

	T_c ˚C	ΔH_c [a] J/g	X_c [b] %
PCL	26	55.6	40
PCl/TPS [c]	32	56	40
PCl/TPS + 0.5 wt% cnt [c]	35	52	37
PCl/TPS + 1 wt%cnt [c]	35	53	38
PCl/TPS [d]	30	57	41
PCl/TPS + 0.5 wt% cnt [d]	34	52	37
PCl/TPS + 1 wt% cnt [d]	37	51	36
PCl/TPS + 2 wt% cnt [d]	38	51	36

[a] Normalised to PCL unit mass; [b] $Xc = \Delta Hc/ \Delta H^0c$, $\Delta H^0c = 139$ J/g [88]; [c]Prepared by extrusion; [d] Prepared by internal mixing.

6.4.5 Dynamic Mechanical Analyses (DMA)

Thermoplastic starch exists as a partially miscible mixture of starch and plasticizer and typically shows two transition peaks in DMA curves. The lower temperature alpha transition, T_α, is attributed to the low molecular weight plasticizer and the higher temperature beta transition, T_β, is for the starch rich domains in TPS (Averous, Moro, Dole & Fringant, 2000; Taguet, Huneault & Favis, 2009). The addition of carbon nanotubes results in a dramatic temperature reduction (~ 26˚C) of the starch rich phase transition, $T_{\beta,}$ for the samples prepared by extrusion (Figure 6-13a). On the other hand, the samples prepared in the internal mixer show no such change (Figure 6-

13b). In the latter case the nanotubes are localized in the PCL and at the interface, whereas in the case of extrusion a predominant number of the nanotubes are located in the TPS phase.

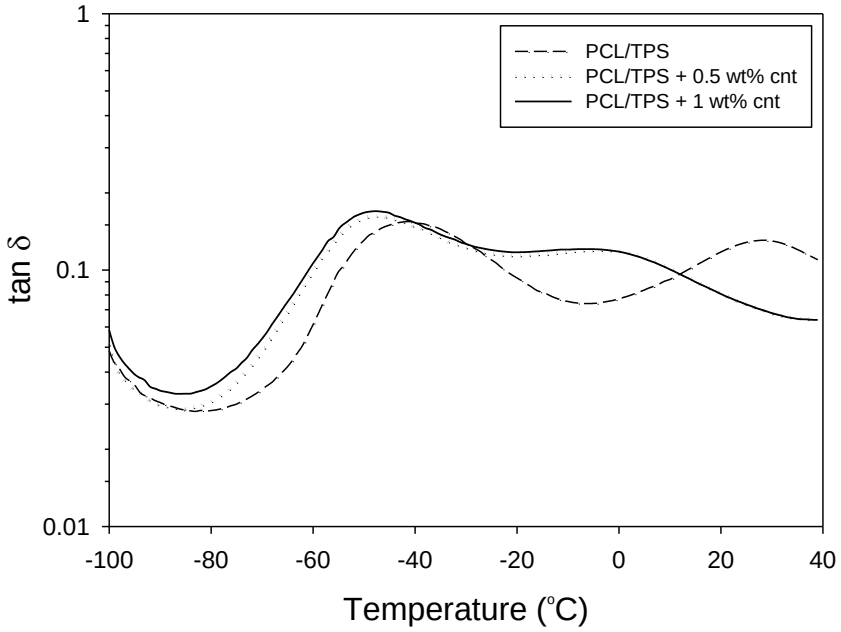

(a)

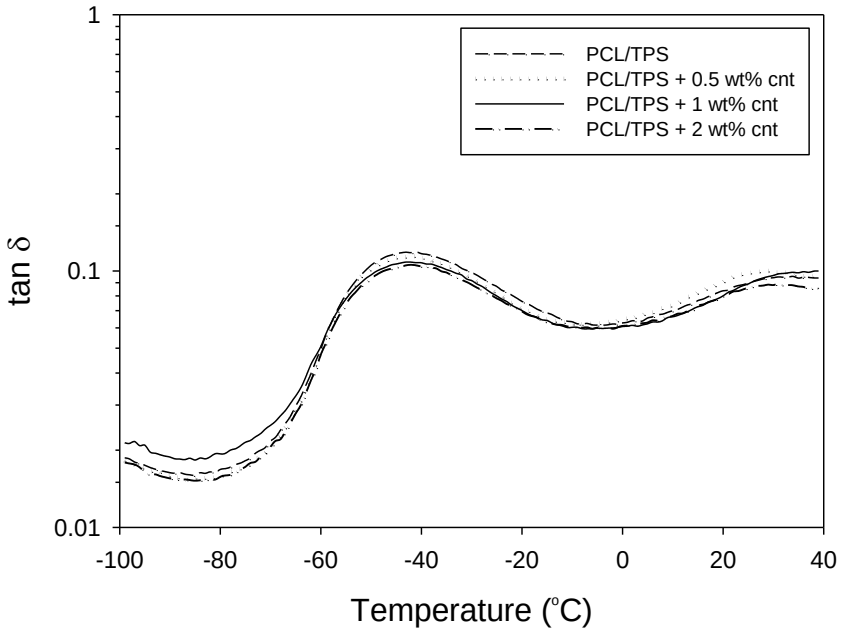

(b)

Figure 6-13 DMA curves of PCL/TPS 80/20 wt% with different carbon nanotube contents prepared via: (a) Extrusion; (b) Internal mixer.

Some authors have reported an increase in T_g by incorporation of CNTs due to the filler-polymer interaction and a lower degree of chain freedom(Choi et al., 2005; Cui, Tarte & Woo, 2009; Huang et al., 2011; Wu & Liao, 2007). However, the opposite effect, i.e. a T_g decrease, has also been frequently reported in the literature(Castillo et al., 2011; Gao, Dong, Hou & Zhang, 2012; Hsieh et al., 2004; Park, Li, Jin, Park, Cho & Ha, 2002; Potschke, Bhattacharyya, Janke & Goering, 2003; Schartel et al., 2008; Schmitt, Prashantha, Soulestin, Lacrampe & Krawczak, 2012). The latter effect was mostly attributed to the easier sliding of the polymer chains on the solid surface due to the increased alignment and lower entanglements density in the vicinity of the nanotube surface(Grady, 2011). In case of carbon nanotubes which are chemically bonded to the starch, pinned starch chains impose orientation and subsequent disentanglement on the starch molecules around them. Some authors have reported that in starch-nanocomposites, nanofillers

facilitate starch chain mobility by imposed orientation, decreased entanglement density and interruption of inter-molecular interactions(Gao, Dong, Hou & Zhang, 2012; Mbey, Hoppe & Thomas, 2012). Consequently, a lower glass transition temperature is expected. Also, some other authors have proposed that the slight degradation of polymer matrix in presence of nanofillers due to the increased viscosity and shear forces might also explain the drop in the transition temperature for starch (Castillo et al., 2011; Potschke, Bhattacharyya, Janke & Goering, 2003).

6.5 **Conclusions**

All of the properties of filled polymer blends directly depends on the localization of nanofillers. In twin screw extruder, although the nanotubes were first dispersed in low viscosity PCL phase, they were located majorly in the TPS phase and partly at the interface. Further static annealing the blends did not make any change in the localization of the nanotubes indicating a very stable state of dispersion. Wetting coefficient calculations suggested that the nanotubes will thermodynamically tend to migrate to the PCL/TPS interface. Further investigations via XPS were strongly indicative of the formation of a covalent bond between the carboxylic acid groups on the nanotube surface and the TPS. It was concluded that during dynamic mixing, the nanotube first moved to the interface to minimize the free energy of the system. At the interface a reaction occurs between the carboxylic acid groups of the nanotube and the alcohol groups of the starch and, following this reaction and the formation of a TPS encapsulating layer around the nanotube,

the carbon nanotubes are drawn into the thermoplastic starch dispersed phase. But if the nanotubes encounter kinetic barriers to their transfer, a completely different localization might be observed. Interestingly in the internal mixer, this phenomenon was completely inversed and the nanotubes remained in the PCL phase or at the interface but would not enter the TPS phase. This led to the attribution of CNT localization to kinetic effects in the internal mixer. Subsequent investigation of the shear fields, demonstrated a significant increase in the viscosity of shear thinning TPS in the internal mixer. It was concluded that the high viscosity of TPS in internal mixer inhibited the CNT penetration to the starch droplets. Localization of nanotubes may be an influential factor on morphology of polymer blends. In internal mixer the localization of nanotubes in PCL phase remarkably enhanced the morphology of PCL/TPS blends by decreasing the droplet size to the half by 0.5 wt% CNT. It appears that in the case of the internal mixer, the major localization of the nanotubes at the PCL/TPS interface and in PCL phase generates a physical barrier for the dispersed TPS phase coalescence.

Carbon nanotubes were found to effectively influence the crystallinity of PCL. It is observed that all of the CNT-incorporated blends of PCL/TPS show a higher T_c than for the neat blend of PCL/TPS which is due to the heterogeneous nucleating effect of carbon nanotubes. The percent crystallinity, however, decreases by incorporating nanotubes for both processes. Like other heterogeneous nucleating agents, the presence of nanofillers has two effects, one is facilitating the crystallization due to their nucleating role and the opposite effect due to slower growth and lamellar defects in the crystalline structure. DMA analyses were used to investigate the structural changes in TPS phase. TPS located CNTs were shown to dramatically decrease the starch glass transition temperature (~ 26˚C) that was most likely due to the easier sliding of the polymer chains on the solid surface due to the increased alignment and lower entanglements density in the vicinity of the nanotube surface(Grady, 2011).

Acknowledgments

The authors would like to express their gratitude to TeknorApex Co. for funding this research. The authors would also like to thank Dr. Sepehr Ravati and the polymer blend group for useful discussions. In addition, we would like to thank Ms. Melina Hamdine, Dr. Weawkamol

Leelapornpisit and Dr. Josianne Lefebvre at Ecole Polytechnique de Montreal for their effective support in the rheology, TEM and XPS experiments.

6.6 References

1. Queiroz, A. U. B.; Collares-Queiroz, F. P., Innovation and Industrial Trends in Bioplastics. *Polymer Reviews* 2009, 49, (2), 65-78.

2. Averous, L., Biodegradable multiphase systems based on plasticized starch: A review. *Journal of Macromolecular Science-Polymer Reviews* 2004, C44, (3), 231-274.

3. Bocchini, S.; Battegazzore, D.; Frache, A., Poly (butylensuccinate co-adipate)-thermoplastic starch nanocomposite blends. *Carbohydrate Polymers* 2010, 82, (3), 802-808.

4. Chaleat, C. M.; Halley, P. J.; Truss, R. W., Properties of a plasticised starch blend. Part 1: Influence of moisture content on fracture properties. *Carbohydrate Polymers* 2008, 71, (4), 535-543.

5. Sarazin, P.; Li, G.; Orts, W. J.; Favis, B. D., Binary and ternary blends of polylactide, polycaprolactone and thermoplastic starch. *Polymer* 2008, 49, (2), 599-609.

6. Bajgai, M. P.; Aryal, S.; Bhattarai, S. R.; Bahadur, K. C. R.; Kim, K. W.; Kim, H. Y., Poly(epsilon-caprolactone) grafted dextran biodegradable electrospun matrix: A novel scaffold for tissue engineering. *Journal of Applied Polymer Science* 2008, 108, (3), 1447-1454.

7. Bendix, D., Chemical synthesis of polylactide and its copolymers for medical applications. *Polymer Degradation and Stability* 1998, 59, (1–3), 129-135.

8. Nair, L. S.; Laurencin, C. T., Biodegradable polymers as biomaterials. *Progress in Polymer Science* 2007, 32, (8–9), 762-798.

9. Bastioli, C.; Cerutti, A.; Guanella, I.; Romano, G. C.; Tosin, M., PHYSICAL STATE AND BIODEGRADATION BEHAVIOR OF STARCH-POLYCAPROLACTONE SYSTEMS. *Journal of Environmental Polymer Degradation* 1995, 3, (2), 81-95.

10. Averous, L.; Moro, L.; Dole, P.; Fringant, C., Properties of thermoplastic blends: starch-polycaprolactone. *Polymer* 2000, 41, (11), 4157-4167.

11. Li, G.; Favis, B. D., Morphology Development and Interfacial Interactions in Polycaprolactone/Thermoplastic-Starch Blends. *Macromolecular Chemistry and Physics* 2010, 211, (3), 321-333.

12. Shin, B. Y.; Narayan, R.; Lee, S. I.; Lee, T. J., Morphology and Rheological Properties of Blends of Chemically Modified Thermoplastic Starch and Polycaprolactone. *Polymer Engineering and Science* 2008, 48, (11), 2126-2133.

13. Ishiaku, U. S.; Pang, K. W.; Lee, W. S.; Ishak, Z. A. M., Mechanical properties and enzymic degradation of thermoplastic and granular sago starch filled poly(ε-caprolactone). *European Polymer Journal* 2002, 38, (2), 393-401.

14. Moniruzzaman, M.; Winey, K. I., Polymer nanocomposites containing carbon nanotubes. *Macromolecules* 2006, 39, (16), 5194-5205.

15. Buffa, F.; Abraham, G. A.; Grady, B. P.; Resasco, D., Effect of nanotube functionalization on the properties of single-walled carbon nanotube/polyurethane composites. *Journal of Polymer Science Part B-Polymer Physics* 2007, 45, (4), 490-501.

16. Potschke, P.; Bhattacharyya, A. R.; Janke, A., Morphology and electrical resistivity of melt mixed blends of polyethylene and carbon nanotube filled polycarbonate. *Polymer* 2003, 44, (26), 8061-8069.

17. Wu, D.; Zhang, Y.; Zhang, M.; Yu, W., Selective Localization of Multiwalled Carbon Nanotubes in Poly(epsilon-caprolactone)/Polylactide Blend. *Biomacromolecules* 2009, 10, (2), 417-424.

18. Maglio, G.; Migliozzi, A.; Palumbo, R.; Immirzi, B.; Volpe, M. G., Compatibilized poly(epsilon-caprolactone)/poly(L-lactide) blends for biomedical uses. *Macromolecular Rapid Communications* 1999, 20, (4), 236-238.

19. Baudouin, A. C.; Devaux, J.; Bailly, C., Localization of carbon nanotubes at the interface in blends of polyamide and ethylene-acrylate copolymer. *Polymer* 2010, 51, (6), 1341-1354.

20. Meincke, O.; Kaempfer, D.; Weickmann, H.; Friedrich, C.; Vathauer, M.; Warth, H., Mechanical properties and electrical conductivity of carbon-nanotube filled polyamide-6 and its blends with acrylonitrile/butadiene/styrene. *Polymer* 2004, 45, (3), 739-748.

21. Hong, J. S.; Kim, Y. K.; Ahn, K. H.; Lee, S. J., Shear-induced migration of nanoclay during morphology evolution of PBT/PS blend. *Journal of Applied Polymer Science* 2008, 108, (1), 565-575.

22. Goeldel, A.; Marmur, A.; Kasaliwal, G. R.; Poetschke, P.; Heinrich, G., Shape-Dependent Localization of Carbon Nanotubes and Carbon Black in an Immiscible Polymer Blend during Melt Mixing. *Macromolecules* 2011, 44, (15), 6094-6102.

23. Wu, D. F.; Wu, L. F.; Zhang, M.; Zhou, W. D.; Zhang, Y. S., Morphology evolution of nanocomposites based on poly(phenylene sulfide)/poly(butylene terephthalate) blend. *Journal of Polymer Science Part B-Polymer Physics* 2008, 46, (12), 1265-1279.

24. Fenouillot, F.; Cassagnau, P.; Majeste, J. C., Uneven distribution of nanoparticles in immiscible fluids: Morphology development in polymer blends. *Polymer* 2009, 50, (6), 1333-1350.

25. Potschke, P.; Pegel, S.; Claes, M.; Bonduel, D., A novel strategy to incorporate carbon nanotubes into thermoplastic matrices. *Macromolecular Rapid Communications* 2008, 29, (3), 244-251.

26. Goeldel, A.; Kasaliwal, G.; Poetschke, P., Selective Localization and Migration of Multiwalled Carbon Nanotubes in Blends of Polycarbonate and Poly(styrene-acrylonitrile). *Macromolecular Rapid Communications* 2009, 30, (6), 423-429.

27. Sumita, M.; Sakata, K.; Asai, S.; Miyasaka, K.; Nakagawa, H., Dispersion of fillers and the electrical conductivity of polymer blends filled with carbon black. *Polymer Bulletin* 1991, 25, (2), 265-271.

28. Elias, L.; Fenouillot, F.; Majeste, J. C.; Cassagnau, P., Morphology and rheology of immiscible polymer blends filled with silica nanoparticles. *Polymer* 2007, 48, (20), 6029-6040.

29. Katada, A.; Buys, Y.; Tominaga, Y.; Asai, S.; Sumita, M., Relationship between electrical resistivity and particle dispersion state for carbon black filled poly (ethylene-<i>co</i>-vinyl acetate)/poly (<small>L</small> -lactic acid) blend. *Colloid & Polymer Science* 2005, 284, (2), 134-141.

30. Wu, D.; Lin, D.; Zhang, J.; Zhou, W.; Zhang, M.; Zhang, Y.; Wang, D.; Lin, B., Selective Localization of Nanofillers: Effect on Morphology and Crystallization of PLA/PCL Blends. *Macromolecular Chemistry and Physics* 2011, 212, (6), 613-626.

31. Goeldel, A.; Kasaliwal, G. R.; Poetschke, P.; Heinrich, G., The kinetics of CNT transfer between immiscible blend phases during melt mixing. *Polymer* 2012, 53, (2), 411-421.

32. Tao, F.; Nysten, B.; Baudouin, A.-C.; Thomassin, J.-M.; Vuluga, D.; Detrembleur, C.; Bailly, C., Influence of nanoparticle–polymer interactions on the apparent migration behaviour of carbon nanotubes in an immiscible polymer blend. *Polymer* 2011, 52, (21), 4798-4805.

33. Feng, J.; Chan, C.-m.; Li, J.-x., A method to control the dispersion of carbon black in an immiscible polymer blend. *Polymer Engineering & Science* 2003, 43, (5), 1058-1063.

34. Grady, B. P., Recent Developments Concerning the Dispersion of Carbon Nanotubes in Polymers. *Macromolecular Rapid Communications* 2010, 31, (3), 247-257.

35. Valentini, L.; Biagiotti, J.; Kenny, J. M.; Manchado, M. A. L., Physical and mechanical behavior of single-walled carbon nanotube/polypropylene/ethylene-propylene-diene rubber nanocomposites. *Journal of Applied Polymer Science* 2003, 89, (10), 2657-2663.

36. Bose, S.; Bhattacharyya, A. R.; Bondre, A. P.; Kulkarni, A. R.; Potschke, P., Rheology, electrical conductivity, and the phase behavior of cocontinuous PA6/ABS blends with MWNT: Correlating the aspect ratio of MWNT with the percolation threshold. *Journal of Polymer Science Part B-Polymer Physics* 2008, 46, (15), 1619-1631.

37. Abbasi, S.; Carreau, P. J.; Derdouri, A., Flow induced orientation of multiwalled carbon nanotubes in polycarbonate nanocomposites: Rheology, conductivity and mechanical properties. *Polymer* 2010, 51, (4), 922-935.

38. Ansari, M. N. M.; Ismail, H.; Zein, S. H. S., Effect of Multi-walled Carbon Nanotubes on Mechanical Properties of Feldspar Filled Polypropylene Composites. *Journal of Reinforced Plastics and Composites* 2009, 28, (20), 2473-2485.

39. Breuer, O.; Sundararaj, U., Big returns from small fibers: A review of polymer/carbon nanotube composites. *Polymer Composites* 2004, 25, (6), 630-645.

40. Das, N. C.; Maiti, S., Electromagnetic interference shielding of carbon nanotube/ethylene vinyl acetate composites. *Journal of Materials Science* 2008, 43, (6), 1920-1925.

41. Ma, P.-C.; Siddiqui, N. A.; Marom, G.; Kim, J.-K., Dispersion and functionalization of carbon nanotubes for polymer-based nanocomposites: A review. *Composites Part A: Applied Science and Manufacturing* 2010, 41, (10), 1345-1367.

42. Favis, B. D.; Rodriguez-Gonzalez, F. J.; Ramsay, B. A. Polymer compositions containing thermoplastic starch. 6,605,657, Aug 12, 2003.

43. Favis, B. D.; Rodriguez-Gonzalez, F. J.; Ramsay, B. A. Method of making polymer compositions containing thermoplastic starch. 6,844,380, Jan 18, 2005.

44. Kwok, D. Y.; Neumann, A. W., Contact angle measurement and contact angle interpretation. *Advances in Colloid and Interface Science* 1999, 81, (3), 167-249.

45. Averous, L.; Boquillon, N., Biocomposites based on plasticized starch: thermal and mechanical behaviours. *Carbohydrate Polymers* 2004, 56, (2), 111-122.

46. Nuriel, S.; Liu, L.; Barber, A. H.; Wagner, H. D., Direct measurement of multiwall nanotube surface tension. *Chemical Physics Letters* 2005, 404, (4-6), 263-266.

47. Yuan, J. K.; Yao, S. H.; Sylvestre, A.; Bai, J. B., Biphasic Polymer Blends Containing Carbon Nanotubes: Heterogeneous Nanotube Distribution and Its Influence on the Dielectric Properties. *Journal of Physical Chemistry C* 2012, 116, (2), 2051-2058.

48. Xiang, F. M.; Wu, J.; Liu, L.; Huang, T.; Wang, Y.; Chen, C.; Peng, Y.; Jiang, C. X.; Zhou, Z. W., Largely enhanced ductility of immiscible high density polyethylene/polyamide 6 blends via nano-bridge effect of functionalized multiwalled carbon nanotubes. *Polymers for Advanced Technologies* 2011, 22, (12), 2533-2542.

49. Ozdilek, C.; Bose, S.; Leys, J.; Seo, J. W.; Wubbenhorst, M.; Moldenaers, P., Thermally induced phase separation in P alpha MSAN/PMMA blends in presence of functionalized multiwall carbon nanotubes: Rheology, morphology and electrical conductivity. *Polymer* 2011, 52, (20), 4480-4489.

50. Wu, S., Interfacial energy, structure and adhesion between polymers. In *Polymer Blends* Paul, D. R.; Newman, S., Eds. Academic Press: New York, 1987; Vol. 1, pp 244-248.

51. Poetschke, P.; Pegel, S.; Claes, M.; Bonduel, D., A novel strategy to incorporate carbon nanotubes into thermoplastic matrices. *Macromolecular Rapid Communications* 2008, 29, (3), 244-251.

52. Wu, M.; Shaw, L. L., On the improved properties of injection-molded, carbon nanotube-filled PET/PVDF blends. *Journal of Power Sources* 2004, 136, (1), 37-44.

53. Zhang, L.; Wan, C.; Zhang, Y., Investigation on the Multiwalled Carbon Nanotubes Reinforced Polyamide 6/Polypropylene Composites. *Polymer Engineering and Science* 2009, 49, (10), 1909-1917.

54. Sumita, M.; Sakata, K.; Asai, S.; Miyasaka, K.; Nakagawa, H., DISPERSION OF FILLERS AND THE ELECTRICAL-CONDUCTIVITY OF POLYMER BLENDS FILLED WITH CARBON-BLACK. *Polymer Bulletin* 1991, 25, (2), 265-271.

55. Favis, B. D., Factors Influencing the Morphology of Immiscible Polymer Blends in Melt Processing. In *POLYMER BLENDS V. 1: Formulation*, Paul, D. R.; Bucknall, C. B., Eds. John Wiley & Sons Inc.: Toronto, ON, 2000.

56. Luong, J. H. T.; Hrapovic, S.; Liu, Y. L.; Yang, D. Q.; Sacher, E.; Wang, D. S.; Kingston, C. T.; Enright, G. D., Oxidation, deformation, and destruction of carbon nanotubes in aqueous ceric sulfate. *Journal of Physical Chemistry B* 2005, 109, (4), 1400-1407.

57. Stobinski, L.; Tomasik, P.; Lii, C. Y.; Chan, H. H.; Lin, H. M.; Liu, H. L.; Kao, C. T.; Lu, K. S., Single-walled carbon nanotube - amylopectin complexes. *Carbohydrate Polymers* 2003, 51, (3), 311-316.

58. Angellier, H.; Molina-Boisseau, S.; Dole, P.; Dufresne, A., Thermoplastic starch-waxy maize starch nanocrystals nanocomposites. *Biomacromolecules* 2006, 7, (2), 531-539.

59. Ma, X. F.; Yu, J. G.; Wang, N., Glycerol plasticized-starch/multiwall carbon nanotube composites for electroactive polymers. *Composites Science and Technology* 2008, 68, (1), 268-273.

60. Bousmina, M.; Ait-Kadi, A.; Faisant, J. B., Determination of shear rate and viscosity from batch mixer data. *Journal of Rheology* 1999, 43, (2), 415-433.

61. Adragna, L.; Couenne, F.; Cassagnau, P.; Jallut, C., Modeling of the complex mixing process in internal mixers. *Industrial & Engineering Chemistry Research* 2007, 46, (22), 7328-7339.

62. Harrats, C.; Thomas, S.; Groeninckx, G., *Micro- and nanostructured polymer blend systems: phase morphology and interfaces*. CRC/Taylor & Francis: Boca Raton, FL, 2006.

63. Clark, D. C.; Geramita, K.; Baker, W. E., Investigation of the shear stresses experienced during melting using novel microencapsulated dye sensors. *Journal of Reinforced Plastics and Composites* 1999, 18, (3), 271-278.

64. Shahbikian, S. Phase morphology development and rheological behavior of non-plasticized and plasticized thermoplastic elastomer blends. NR70467, Ecole Polytechnique, Montreal (Canada), Canada, 2010.

65. Shahbikian, S.; Carreau, P. J.; Heuzey, M. C.; Ellul, M. D.; Cheng, J.; Shirodkar, P.; Nadella, H. P., Morphology development of EPDM/PP uncross-linked/dynamically cross-linked blends. *Polymer Engineering and Science* 2012, 52, (2), 309-322.

66. Della Valle, G.; Vergnes, B.; Lourdin, D., Viscous properties of thermoplastic starches from different botanical origin. *International Polymer Processing* 2007, 22, (5), 471-479.

67. Ciardelli, G.; Chiono, V.; Vozzi, G.; Pracella, M.; Ahluwalia, A.; Barbani, N.; Cristallini, C.; Giusti, P., Blends of poly-(epsilon-caprolactone) and polysaccharides in tissue engineering applications. *Biomacromolecules* 2005, 6, (4), 1961-1976.

68. Grady, B. P., Effects of carbon nanotubes on polymer physics. *Journal of Polymer Science Part B-Polymer Physics* 2012, 50, (9), 591-623.

69. Chun, Y. S.; Kyung, Y. J.; Jung, H. C.; Kim, W. N., Thermal and rheological properties of poly(epsilon-caprolactone) and polystyrene blends. *Polymer* 2000, 41, (24), 8729-8733.

70. Wu, D.; Wu, L.; Sun, Y.; Zhang, M., Rheological properties and crystallization behavior of multi-walled carbon Nanotube/Poly(epsilon-caprolactone) composites. *Journal of Polymer Science Part B-Polymer Physics* 2007, 45, (23), 3137-3147.

71. Sanchez-Garcia, M. D.; Lagaron, J. M.; Hoa, S. V., Effect of addition of carbon nanofibers and carbon nanotubes on properties of thermoplastic biopolymers. *Composites Science and Technology* 2010, 70, (7), 1095-1105.

72. Wu, T. M.; Chen, E. C., Crystallization behavior of poly(epsilon-caprolactone)/multiwalled carbon nanotube composites. *Journal of Polymer Science Part B-Polymer Physics* 2006, 44, (3), 598-606.

73. Taguet, A.; Huneault, M. A.; Favis, B. D., Interface/morphology relationships in polymer blends with thermoplastic starch. *Polymer* 2009, 50, (24), 5733-5743.

74. Choi, Y. J.; Hwang, S. H.; Hong, Y. S.; Kim, J. Y.; Ok, C. Y.; Huh, W.; Lee, S. W., Preparation and characterization of PS/multi-walled carbon nanotube nanocomposites. *Polymer Bulletin* 2005, 53, (5-6), 393-400.

75. Cui, L.; Tarte, N. H.; Woo, S. I., Synthesis and Characterization of PMMA/MWNT Nanocomposites Prepared by in Situ Polymerization with Ni(acac)(2) Catalyst. *Macromolecules* 2009, 42, (22), 8649-8654.

76. Huang, Y.-L.; Ma, C.-C. M.; Yuen, S.-M.; Chuang, C.-Y.; Kuan, H.-C.; Chiang, C.-L.; Wu, S.-Y., Effect of maleic anhydride modified MWCNTs on the morphology and dynamic mechanical properties of its PMMA composites. *Materials Chemistry and Physics* 2011, 129, (3), 1214-1220.

77. Wu, C.-S.; Liao, H.-T., Study on the preparation and characterization of biodegradable polylactide/multi-walled carbon nanotubes nanocomposites. *Polymer* 2007, 48, (15), 4449-4458.

78. Schartel, B.; Braun, U.; Knoll, U.; Bartholmai, M.; Goering, H.; Neubert, D.; Potschke, P., Mechanical, thermal, and fire behavior of bisphenol a polycarbonate/multiwall carbon nanotube nanocomposites. *Polymer Engineering and Science* 2008, 48, (1), 149-158.

79. Potschke, P.; Bhattacharyya, A. R.; Janke, A.; Goering, H., Melt mixing of polycarbonate/multi-wall carbon nanotube composites. *Compos. Interfaces* 2003, 10, (4-5), 389-404.

80. Castillo, F. Y.; Socher, R.; Krause, B.; Headrick, R.; Grady, B. P.; Prada-Silvy, R.; Pötschke, P., Electrical, mechanical, and glass transition behavior of polycarbonate-based nanocomposites with different multi-walled carbon nanotubes. *Polymer* 2011, 52, (17), 3835-3845.

81. Hsieh, A. J.; Moy, P.; Beyer, F. L.; Madison, P.; Napadensky, E.; Ren, J.; Krishnamoorti, R., Mechanical response and rheological properties of polycarbonate layered-silicate nanocomposites. *Polymer Engineering & Science* 2004, 44, (5), 825-837.

82. Gao, W.; Dong, H.; Hou, H.; Zhang, H., Effects of clays with various hydrophilicities on properties of starch–clay nanocomposites by film blowing. *Carbohydrate Polymers* 2012, 88, (1), 321-328.

83. Park, H. M.; Li, X. C.; Jin, C. Z.; Park, C. Y.; Cho, W. J.; Ha, C. S., Preparation and properties of biodegradable thermoplastic starch/clay hybrids. *Macromolecular Materials and Engineering* 2002, 287, (8), 553-558.

84. Schmitt, H.; Prashantha, K.; Soulestin, J.; Lacrampe, M. F.; Krawczak, P., Preparation and properties of novel melt-blended halloysite nanotubes/wheat starch nanocomposites. *Carbohydrate Polymers* 2012, 89, (3), 920-927.

85. Grady, B. P., EFFECTS OF CARBON NANOTUBES ON POLYMER PHYSICS. In *CARBON NANOTUBE–POLYMER COMPOSITES,Manufacture, Properties, and Applications*, John Wiley & Sons, Inc.: Hoboken, NJ, 2011; pp 119-190.

86. Mbey, J. A.; Hoppe, S.; Thomas, F., Cassava starch–kaolinite composite film. Effect of clay content and clay modification on film properties. *Carbohydrate Polymers* 2012, 88, (1), 213-222.

87. Cava, D.; Gavara, R.; Lagarón, J. M.; Voelkel, A., Surface characterization of poly(lactic acid) and polycaprolactone by inverse gas chromatography. *Journal of Chromatography A* 2007, 1148, (1), 86-91.

88. Pitt, C. G.; Chasalow, F. I.; Hibionada, Y. M.; Klimas, D. M.; Schindler, A., Aliphatic polyesters. I. The degradation of poly(ϵ-caprolactone) in vivo. *Journal of Applied Polymer Science* 1981, 26, (11), 3779-3787.

Chapitre 7 GENERAL DISCUSSIONS AND PERSPECTIVE

In this work we first identified existing problems with thermoplastic starch (TPS) and its blends. The main issues are the highly hygroscopic nature of TPS as well as its poor mechanical properties.

The plasticizer content of TPS which is roughly between 25-35 wt% plays a major role in the hygroscopic nature of TPS. Improved water resistance of the plasticizers will result in the diminished hydrophilicity of TPS materials. Polyglycerol-TPS and diglycerol-TPS show better water resistance after exposure in a humidity chamber. Additionally, those higher molecular weight plasticizers show better heat stability as compared to glycerol-TPS. So some of the disadvantages of TPS are now improved with the new plasticizers. In evaluating their efficacy in gelatinizing starch, we tried to determine the effect of pure shear on the gelatinization phenomenon. Rheological tests in a couette flow geometry gave us the ability to study this phenomenon. There, when we mention "effect of shear" it means the difference between a static method in which no shear is involved and a method which a small shear is involved. As discussed in chapter 4, we show that in the case of higher applied shear only the conclusion temperature is affected. The onset temperature remains constant since it is a more thermodynamically controlled parameter. This work can be a route to future projects. An issue which has not been studied is the overall energy use for the processing of these new plasticizers. In other words, although they result in superior water resistance and high thermal stability their high viscosity can result in more energy required for their processing as compared to glycerol-TPS. It is possible that new semi-durable or durable applications would justify this energy consumption hike.

The high molecular weight plasticizers showed a similar performance to glycerol-TPS with respect to the morphology and the mechanical properties, a sign of high plasticization efficiency. Also, an interesting mechanism of TPS particle formation was proposed for these new plasticizers. Due to less plasticizer migration to the interface of PE/TPS and hence low plasticizer concentration at the interface, the interfacial modifier only reacts with starch molecules and erodes tiny fragments of the starch molecules off the TPS phase rather than breaking up the

droplets. This phenomenon was evidenced by the droplet size histograms based on SEM images particularly at low compatibilizer contents. Another strategy was adopted to further improve the mechanical properties of TPS. One of the ways to improve the mechanical properties of the polymeric materials is to add nanofillers. Among them, carbon nanotubes have been shown to improve multiple physico-mechanical properties of the polymers. Since there is little knowledge on the behaviour of carbon nanotube/TPS blends in the literature, we focused on the localization of acid functionalized carbon nanotubes in TPS blends with polycaprolactone. It was found that the carbon nanotubes are located preferably in the TPS phase. The nanotubes have a thermodynamic tendency to place themselves at the PCL/TPS interface, they then react with the TPS phase and are subsequently drawn into the TPS phase. Experiments carried out in different processing equipment showed that the localization could also be process dependent. It would be interesting to continue the former part (different plasticizers systems) by the incorporation of nanotubes and to show the effect of new plasticizers as well as the compatibilizers on the nanotube localization. For this part, we could not use polyethylene due to technical difficulties in the masterbatch preparations. So we shifted towards the PCL since we had an extensive knowledge on the TPS/PCL blends in this laboratory and the mutual solvent with carbon nanotubes facilitated the masterbatch preparation.

The other issue is the DMA curves of PCL/TPS/CNT systems. There we showed that in the case of TPS localization of the carbon nanotubes, the transition temperature of the starch molecules shifted significantly to lower temperatures (26 C˚). This is likely due to the immobilization of starch molecules in the region of the nanotubes, but more work would be required to understand this phenomenon. Further work should also consider examining the mechanical properties of the nanotube based blends.

CONCLUDING REMARKS AND RECOMMENDATIONS

Thermoplastic starch (TPS) is a bio-based and biodegradable material gaining a lot of attention in the bioplastics field, though it still has two major drawbacks (moisture sensitivity, weak mechanical properties) and further improvements are required to enhance in its properties. The applications of TPS products are currently limited to non-durable products, so by improving the above-mentioned drawbacks, it will be possible to incorporate TPS blends for use in semi-durable and durable applications. To achieve this, two strategies have been pursued: a change in TPS structure, and the addition of nanofillers.

Two new plasticizers were introduced for preparing TPS. But in order to be able to effectively use them in blends, it was first necessary to understand their efficacy in the gelatinization process. The gelatinization of starch is a very complicated phenomenon, and the parameters involved are so interconnected that a clear explanation of them is not available in the literature. So at first, gelatinization was studied with regard to four plasticizers: glycerol, sorbitol, diglycerol and polyglycerol under a wide range of starch/water/plasticizer ratios. It was shown that, due to its high water solubility, the gelatinization temperatures of sorbitol are in the same vicinity as glycerol. By moving towards diglycerol and polyglycerol, the gelatinization temperature experienced a further increase. In comparing the structure of these plasticizers, this was attributed to the molecular weight and viscosity increase, as well as a lower water affinity and decrease in the hydroxyl group density of the new plasticizers, which require higher temperatures to start gelatinization. Further studies on various starch/water/plasticizer ratios revealed different behaviour for the polyglycerol system. When the plasticizer content was kept constant, it was found that by increasing water content, the gelatinization temperature decreased for all the formulations. This demonstrates the high activity and efficacy of water in penetrating the heavily packed structure of starch granules. On the other hand, it was found that when the water content was kept constant and the plasticizer content increased, the glycerol, sorbitol and diglycerol systems showed an increase in gelatinization temperature. Conversely, the opposite was observed in the polyglycerol system. This was found to be due to the borderline solubility of polyglycerol in water, such that by increasing the plasticizer content in the slurry composition, water efficacy in starch gelatinization did not decrease. So it was concluded that when applying a

plasticizer with limited interaction with water, it is the total amount of water+plasticizer which determines the starch gelatinization temperatures, rather than the water/plasticizer ratio.

In order to incorporate one of the most widely used polymers, which is now in the bioplastic family too, polyethylene was used in new TPS blend formulations. The goal was to investigate the performance of the new plasticizers in polymer processing. One of the main drawbacks of the TPS is its moisture sensitivity, though it was shown that the new plasticizers demonstrate lower moisture sensitivity as moisture pick-up had decreased from 40% for glycerol-TPS to 15% for polyglycerol-TPS. This was quite interesting since the new TPS-based materials show less sensitivity to ambient humidity, and consequently they have more stable properties in various humidity conditions. Plasticizer evaporation has always been a problem in glycerol-TPS products, as, for example, 10% of glycerol would evaporate at the processing temperature of HDPE (180˚C). It was again found that the new plasticizers demonstrated higher thermal stability, which is an indication that these new thermoplastic starch formulations can be blended with a broader range of high melting point polymers such as PHB or PLA or PET.

After these preliminary studies, HDPE/TPS blends (80/20 wt% with a range of interfacial modifier contents) were prepared using a one-step method. This includes a twin screw extruder side-fed in the midway via a single screw extruder. The morphology of the blends revealed a similar droplet size for all plasticizers in absence of the interfacial modifier (d_n;d_v: 3;5μm), with a slightly smaller droplet size for polyglycerol-TPS. By adding the modifier, the volume average diameter dropped gradually to lower values. All the d_v curves reached a plateau at 9 wt% compatibilizer (based on TPS phase), which is called the critical concentration after which droplet size undergoes no further change. So the new plasticizers demonstrate high efficacy in starch plasticization during the extrusion process that is comparable with glycerol-TPS. In the emulsification curves, an interesting trend was observed for diglycerol-TPS and polyglycerol-TPS: by adding an interfacial modifier, unlike in normal emulsification curves, a highly non-correspondent behaviour was observed for d_n and d_v. It was then clearly shown for diglycerol-TPS, on the droplet size histograms, that a very large number of small (200-300 nm) droplets emerge and co-exist with larger droplets (~ 5-7 μm) by adding only 1% copolymer to the system. This behaviour was not observed in the glycerol-TPS system. At higher copolymer concentrations, the emulsification curves become similar to each other by approaching the droplet size and distribution together for both glycerol and diglycerol. This unusual behaviour gives an

insight to the difference of compatibilization mechanism between diglycerol-TPS and glycerol-TPS. Subsequently, DMA analysis demonstrates a significant shift of T_g of diglycerol and polyglycerol in TPS towards T_α of starch domains (~45 ˚C) compared with the T_g in their pure state, while this shift was 50% less in the case of glycerol. The extent of T_g convergence of the two components in a blend demonstrates more compatibility between the phases, in a way that completely miscible mixtures show only one glass transition temperature. Hence, this is an indication of more homogeneity in the partially miscible mixture of starch and plasticizer (TPS). This enhanced homogeneity is due to the lower cohesive energy density of diglycerol and polyglycerol, as well as their chemical structure that allows them to stay dispersed and prevent colonization in the TPS structure. The result was a reduction of the plasticizer-rich layer at the interface. Consequently, multiple reactions of compatibilizer and heavy starch molecules occur, leading to an erosion-type compatibilization mechanism in the blends that may be masked in the case of glycerol due to the existence of a glycerol-rich layer at the interface.

When the above-mentioned morphology and high temperature stability, as well as low humidity sensitivity of new TPS formulas, are combined with the mechanical properties of glycerol-TPS, a potentially promising new category of plasticizers has emerged in thermoplastic starch domain.

Due to the extraordinary properties that carbon nanotubes (CNT) may introduce to the polymers and expand the application field for bioplastics, the second strategy was their incorporation in TPS blends. In multiphase polymers, the localization of the fillers is one of the most determining factors on final properties. So in this part, the stable localization of CNT and their effect on the morphology and physics of the phases, are investigated. A combination of solution and melt mixing methods was used to prepare the PCL/TPS/CNT nanocomposites. A twin screw extruder (TSE) was used for this step to blend the prepared CNT/PCL masterbatch with TPS. Although the nanotubes were introduced to the system via PCL, it was interestingly shown that they were located mainly in the TPS phase and partly at the PCL/TPS interface. The Young's model was used to determine the thermodynamically driven localization of CNTs in this blend. It was shown that the nanotubes have the tendency to locate themselves at the interface. XPS tests were conducted on the extracted nanotubes to investigate the surface properties of carbon nanotubes after processing. It was observed that after multiple selective extractions, the nanotubes were still partly encapsulated by starch chains, indicating high interaction levels (covalent bonding). It was concluded that during dynamic mixing, the nanotube first moved to the interface to minimize the

free energy of the system. At the interface a reaction occurs between the carboxylic acid groups of the nanotube and the alcohol groups of the starch and, following this reaction and the formation of a TPS encapsulating layer around the nanotube, the carbon nanotubes are drawn into the thermoplastic starch dispersed phase.

Along with thermodynamic affinity, the kinetics of the mixing process has shown to be a determining parameter influencing localization. In melt mixing, different mixing equipment may provide different processing conditions and consequently different kinetic parameters are ruling the process. The same procedure was repeated using an Internal Mixer (IM). Carbon nanotubes demonstrated completely different localization in PCL/TPS blends and remained in the PCL phase and at the interface after the IM process. A subsequent investigation of the shear fields demonstrated a significant change in effective shear rate/shear stress in the extruder and internal mixer which could dramatically influence the viscosity of shear thinning TPS. It was concluded that the high viscosity of TPS in the internal mixer inhibited CNT penetration into the starch droplets. It was shown that in the case of a moderate viscosity drop in high temperature processing, the nanotubes were able to partly penetrate to the TPS phase. Thus, although melt mixing has always been studied as one single method, and the data were compared together under one category, the type of mixer and the effective shear fields present in the mixing process effectively change the viscoelastic properties of the polymers and may subsequently change the localization of nanotubes. However, the kinetically driven localization may not be as stable under different processing conditions if it does not correspond to the thermodynamic equilibrium state of the system.

The localization of nanotubes can be an influential factor on the morphology of polymer blends. In internal mixer, the nanotuebes remarkably enhanced the morphology of PCL/TPS blends by decreasing the droplet size by half with the addition of 0.5 wt% CNT. This was attributed to an improved coalescence suppression imposed by solid nanofillers and increased PCL viscosity. CNTs were also found to effectively change the crystallinity of PCL. In extrusion samples, this effect was limited to the nanotubes located at the interface, and due to the unchanged morphology of the blend, the CNT content variance did not show further changes in crystallinity. However, using the internal mixer, since the nanotubes were located in the PCL phase, the CNT content effectively altered the crystallinity up to 1 wt% CNT content. DMA analysis was used to investigate the structural changes in the TPS phase. TPS-located CNTs were shown to

dramatically decrease the starch glass transition temperature (~ 26˚C), which was most likely due to the combinational effects of the nanotubes on the starch molecules, such as the interruption of starch intermolecular interactions, as well as the ease of sliding due to a lower entanglement density around the pinned starch molecules on the nanotubes walls.

Based on the present research, the following recommendations are proposed:

1. In this work, new TPS formulae were introduced, and high levels of plasticization, as well as excellent heat stability and moisture resistance, were reported. Due to the high availability of glycerol, it will be interesting to study the new TPS structures with combined plasticizer compositions such as polyglycerol/glycerol or diglycerol/glycerol. This will lead to finding the optimal glycerol content in the TPS structure in order to optimize the cost/performance ratio.
2. One of the drawbacks of commercial glycerol-TPS is its low thermal stability, which is due to plasticizer evaporation. So it is difficult to blend TPS in high percentages at high temperatures. Because of the high temperature stability of these plasticizers, new high melting point polymers such as PHBV, PET or PLA can be easily produced without a significant loss of plasticizer content.
3. The significant drop of moisture pick-up of the new plasticizers compared with glycerol-TPS is an indication of properties stability in various environment humidity. So it will be worthwhile to perform mechanical property evaluations of the new TPS formulations in different humidities so that they can be employed in semi-durable or durable applications.
4. One of the main drawbacks of TPS products is their weak mechanical properties. Now that nanotubes have been successfully incorporated in TPS blends, their mechanical properties should be further investigated to reveal the effects of the nanotubes.
5. Finally, by combining these strategies, it will be useful to study the effect of CNTs on the highly plasticized but viscous TPS formulations with the new plasticizers (diglycerol and polyglycerol). In fact, it is possible to adjust the viscosity of TPS by mixing the new plasticizers with glycerol in order to control the localization of the nanotubes in the twin-screw extruder and subsequently control the properties.

REFERENCES

Abbasi, S., Carreau, P. J., & Derdouri, A. (2010). Flow induced orientation of multiwalled carbon nanotubes in polycarbonate nanocomposites: Rheology, conductivity and mechanical properties. *Polymer, 51*(4), 922-935.

Adeodato Vieira, M. G., da Silva, M. A., dos Santos, L. O., & Beppu, M. M. (2011). Natural-based plasticizers and biopolymer films: A review. *European Polymer Journal, 47*(3), 254-263.

Adragna, L., Couenne, F., Cassagnau, P., & Jallut, C. (2007). Modeling of the complex mixing process in internal mixers. *Industrial & Engineering Chemistry Research, 46*(22), 7328-7339.

Alemdar, A., & Sain, M. (2008). Biocomposites from wheat straw nanofibers: Morphology, thermal and mechanical properties. *Composites Science and Technology, 68*(2), 557-565.

Alvarez, V. A., & Vazquez, A. (2006). Influence of fiber chemical modification procedure on the mechanical properties and water absorption of MaterBi-Y/sisal fiber composites. *Composites Part a-Applied Science and Manufacturing, 37*(10), 1672-1680.

Anand, K. A., Agarwal, U. S., & Joseph, R. (2006). Carbon nanotubes induced crystallization of poly(ethylene terephthalate). *Polymer, 47*(11), 3976-3980.

Angellier, H., Molina-Boisseau, S., Dole, P., & Dufresne, A. (2006). Thermoplastic starch-waxy maize starch nanocrystals nanocomposites. *Biomacromolecules, 7*(2), 531-539.

Angles, M. N., & Dufresne, A. (2000). Plasticized starch/tunicin whiskers nanocomposites. 1. Structural analysis. *Macromolecules, 33*(22), 8344-8353.

Ansari, M. N. M., Ismail, H., & Zein, S. H. S. (2009). Effect of Multi-walled Carbon Nanotubes on Mechanical Properties of Feldspar Filled Polypropylene Composites. *Journal of Reinforced Plastics and Composites, 28*(20), 2473-2485.

Antonio J.F, C. (2008). Chapter 15 - Starch: Major Sources, Properties and Applications as Thermoplastic Materials. In B. Mohamed Naceur & G. Alessandro (Eds.). *Monomers, Polymers and Composites from Renewable Resources* (pp. 321-342). Amsterdam: Elsevier.

Antonoff, G. (1942). On the Validity of Antonoff's Rule. *The Journal of Physical Chemistry, 46*(4), 497-499.

Aravind, I., Albert, P., Ranganathaiah, C., Kurian, J. V., & Thomas, S. (2004). Compatibilizing effect of EPM-g-MA in EPDM/poly(trimethylene terephthalate) incompatible blends. *Polymer, 45*(14), 4925-4937.

Asai, S., Sakata, K., Sumita, M., & Miyasaka, K. (1992). Effect of interfacial free energy on the heterogeneous distribution of oxidized carbon black in polymer blends. *Polymer Journal, 24*(5), 415-420.

Avella, M., Errico, M. E., Laurienzo, P., Martuscelli, E., Raimo, M., & Rimedio, R. (2000). Preparation and characterisation of compatibilised polycaprolactone/starch composites. *Polymer, 41*(10), 3875-3881.

Averous, L. (2004). Biodegradable multiphase systems based on plasticized starch: A review. *Journal of Macromolecular Science-Polymer Reviews, C44*(3), 231-274.

Averous, L., & Boquillon, N. (2004). Biocomposites based on plasticized starch: thermal and mechanical behaviours. *Carbohydrate Polymers, 56*(2), 111-122.

Averous, L., Fauconnier, N., Moro, L., & Fringant, C. (2000). Blends of thermoplastic starch and polyesteramide: Processing and properties. *Journal of Applied Polymer Science, 76*(7), 1117-1128.

Averous, L., Moro, L., Dole, P., & Fringant, C. (2000). Properties of thermoplastic blends: starch-polycaprolactone. *Polymer, 41*(11), 4157-4167.

Bajgai, M. P., Aryal, S., Bhattarai, S. R., Bahadur, K. C. R., Kim, K. W., & Kim, H. Y. (2008). Poly(epsilon-caprolactone) grafted dextran biodegradable electrospun matrix: A novel scaffold for tissue engineering. *Journal of Applied Polymer Science, 108*(3), 1447-1454.

Baks, T., Ngene, I. S., van Soest, J. J. G., Janssen, A. E. M., & Boom, R. M. (2007). Comparison of methods to determine the degree of gelatinisation for both high and low starch concentrations. *Carbohydrate Polymers, 67*(4), 481-490.

Bao, J. S., Ao, Z. H., & Jane, J. I. (2005). Characterization of physical properties of flour and starch obtained from gamma-irradiated white rice. *Starch-Starke, 57*(10), 480-487.

Bastioli, C., Cerutti, A., Guanella, I., Romano, G. C., & Tosin, M. (1995). PHYSICAL STATE AND BIODEGRADATION BEHAVIOR OF STARCH-POLYCAPROLACTONE SYSTEMS. *Journal of Environmental Polymer Degradation, 3*(2), 81-95.

Baudouin, A.-C., Bailly, C., & Devaux, J. (2010). Interface localization of carbon nanotubes in blends of two copolymers. *Polymer Degradation and Stability, 95*(3), 389-398.

Baudouin, A. C., Auhl, D., Tao, F. F., Devaux, J., & Bailly, C. (2011). Polymer blend emulsion stabilization using carbon nanotubes interfacial confinement. *Polymer, 52*(1), 149-156.

Baudouin, A. C., Devaux, J., & Bailly, C. (2010). Localization of carbon nanotubes at the interface in blends of polyamide and ethylene-acrylate copolymer. *Polymer, 51*(6), 1341-1354.

Bayram, G., Yilmazer, U., Xanthos, M., & Patel, S. H. (2002). Rheological behavior of styrene-maleic anhydride/polyol blends obtained through reactive processing. *Journal of Applied Polymer Science, 85*(12), 2615-2623.

Bendix, D. (1998). Chemical synthesis of polylactide and its copolymers for medical applications. *Polymer Degradation and Stability, 59*(1–3), 129-135.

Bhadane, P. A., Tsou, A. H., Cheng, J., Ellul, M., & Favis, B. D. (2011). Morphology and continuity development in highly reactive nanoscale polymer blends. *Polymer, 52*(22), 5107-5117.

Bhadane, P. A., Tsou, A. H., Cheng, J., & Favis, B. D. (2008). Morphology Development and Interfacial Erosion in Reactive Polymer Blending. *Macromolecules, 41*(20), 7549-7559.

Bikiaris, D., & Panayiotou, C. (1998). LDPE/starch blends compatibilized with PE-g-MA copolymers. *Journal of Applied Polymer Science, 70*(8), 1503-1521.

Bikiaris, D., Prinos, J., Koutsopoulos, K., Vouroutzis, N., Pavlidou, E., Frangis, N., & Panayiotou, C. (1998). LDPE/plasticized starch blends containing PE-g-MA copolymer as compatibilizer. *Polymer Degradation and Stability, 59*(1-3), 287-291.

Biliaderis, C. G. (1992). STRUCTURES AND PHASE-TRANSITIONS OF STARCH IN FOOD SYSTEMS. *Food Technology, 46*(6), 98-&.

Biliaderis, C. G., Page, C. M., Maurice, T. J., & Juliano, B. O. (1986). Thermal characterization of rice starches: a polymeric approach to phase transitions of granular starch. *Journal of Agricultural and Food Chemistry, 34*(1), 6-14.

Bindzus, W., Livings, S. J., Gloria-Hernandez, H., Fayard, G., van Lengerich, B., & Meuser, F. (2002). Glass transition of extruded wheat, corn and rice starch. *Starch-Starke, 54*(9), 393-400.

Biresaw, G., & Carriere, C. (2004). Compatibility and mechanical properties of blends of polystyrene with biodegradable polyesters. *Composites Part a-Applied Science and Manufacturing, 35*(3), 313-320.

Bizot, H., LeBail, P., Leroux, B., Davy, J., Roger, P., & Buleon, A. (1997). Calorimetric evaluation of the glass transition in hydrated, linear and branched polyanhydroglucose compounds. *Carbohydrate Polymers, 32*(1), 33-50.

Bocchini, S., Battegazzore, D., & Frache, A. (2010). Poly (butylensuccinate co-adipate)-thermoplastic starch nanocomposite blends. *Carbohydrate Polymers, 82*(3), 802-808.

Bonnet, P., Albertini, D., Bizot, H., Bernard, A., & Chauvet, O. (2007). Amylose/SWNT composites: From solution to film - Synthesis, characterization and properties. *Composites Science and Technology, 67*(5), 817-821.

Bose, S., Bhattacharyya, A. R., Bondre, A. P., Kulkarni, A. R., & Potschke, P. (2008). Rheology, electrical conductivity, and the phase behavior of cocontinuous PA6/ABS blends with MWNT: Correlating the aspect ratio of MWNT with the percolation threshold. *Journal of Polymer Science Part B-Polymer Physics, 46*(15), 1619-1631.

Bose, S., Khare, R. A., & Moldenaers, P. (2010). Assessing the strengths and weaknesses of various types of pre-treatments of carbon nanotubes on the properties of polymer/carbon nanotubes composites: A critical review. *Polymer, 51*(5), 975-993.

Bousmina, M., Ait-Kadi, A., & Faisant, J. B. (1999). Determination of shear rate and viscosity from batch mixer data. *Journal of Rheology, 43*(2), 415-433.

Breuer, O., & Sundararaj, U. (2004). Big returns from small fibers: A review of polymer/carbon nanotube composites. *Polymer Composites, 25*(6), 630-645.

Broseta, D., Fredrickson, G. H., Helfand, E., & Leibler, L. (1990). MOLECULAR-WEIGHT AND POLYDISPERSITY EFFECTS AT POLYMER POLYMER INTERFACES. *Macromolecules, 23*(1), 132-139.

Brosse, A.-C., Tencé-Girault, S., Piccione, P. M., & Leibler, L. (2008). Effect of multi-walled carbon nanotubes on the lamellae morphology of polyamide-6. *Polymer, 49*(21), 4680-4686.

Broz, M. E., VanderHart, D. L., & Washburn, N. R. (2003). Structure and mechanical properties of poly(D,L-lactic acid)/poly(epsilon-caprolactone) blends. *Biomaterials, 24*(23), 4181-4190.

Buffa, F., Abraham, G. A., Grady, B. P., & Resasco, D. (2007). Effect of nanotube functionalization on the properties of single-walled carbon nanotube/polyurethane composites. *Journal of Polymer Science Part B-Polymer Physics, 45*(4), 490-501.

Buléon, A., Colonna, P., Planchot, V., & Ball, S. (1998). Starch granules: structure and biosynthesis. *International Journal of Biological Macromolecules, 23*(2), 85-112.

Burrell, M. M. (2003). Starch: the need for improved quality or quantity - an overview. *Journal of Experimental Botany, 54*(382), 451-456.

Cameron, R. E., & Donald, A. M. (1992). A SMALL-ANGLE X-RAY-SCATTERING STUDY OF THE ANNEALING AND GELATINIZATION OF STARCH. *Polymer, 33*(12), 2628-2636.

Cao, X. D., Chen, Y., Chang, P. R., & Huneault, M. A. (2007). Preparation and properties of plasticized Starch/Multiwalled carbon nanotubes composites. *Journal of Applied Polymer Science, 106*(2), 1431-1437.

Carrillo, A., Swartz, J. A., Gamba, J. M., Kane, R. S., Chakrapani, N., Wei, B. Q., & Ajayan, P. M. (2003). Noncovalent functionalization of graphite and carbon nanotubes with polymer multilayers and gold nanoparticles. *Nano Letters, 3*(10), 1437-1440.

Carvalho, A. (2008). Starch: Major Sources, Properties and Applications as Thermoplastic Materials. In M. Belgacem & A. Gandini (Eds.). *Monomers, Polymers And Composites From Renewable Resources*. Oxford, UK: Elsevier.

Castillo, F. Y., Socher, R., Krause, B., Headrick, R., Grady, B. P., Prada-Silvy, R., & Pötschke, P. (2011). Electrical, mechanical, and glass transition behavior of polycarbonate-based nanocomposites with different multi-walled carbon nanotubes. *Polymer, 52*(17), 3835-3845.

Cava, D., Gavara, R., Lagarón, J. M., & Voelkel, A. (2007). Surface characterization of poly(lactic acid) and polycaprolactone by inverse gas chromatography. *Journal of Chromatography A, 1148*(1), 86-91.

Chaleat, C. M., Halley, P. J., & Truss, R. W. (2008). Properties of a plasticised starch blend. Part 1: Influence of moisture content on fracture properties. *Carbohydrate Polymers, 71*(4), 535-543.

Chandra, R., & Rustgi, R. (1997). Biodegradation of maleated linear low-density polyethylene and starch blends. *Polymer Degradation and Stability, 56*(2), 185-202.

Chen, L., Pang, X. J., Qu, M. Z., Zhang, Q. T., Wang, B., Zhang, B. L., & Yu, Z. L. (2006). Fabrication and characterization of polycarbonate/carbon nanotubes composites. *Composites Part a-Applied Science and Manufacturing, 37*(9), 1485-1489.

Chen, P., Yu, L., Kealy, T., Chen, L., & Li, L. (2007). Phase transition of starch granules observed by microscope under shearless and shear conditions. *Carbohydrate Polymers, 68*(3), 495-501.

Chen, X. H., Hu, J., Zhou, L. P., Li, W. H., Yang, Z., & Wang, Y. G. (2008). Preparation and crystallization of carbon nanotube/maleic anhydride-grafted polypropylene composites. *Journal of Materials Science & Technology, 24*(2), 279-284.

Chivrac, F., Angellier-Coussy, H., Guillard, V., Pollet, E., & Averous, L. (2010). How does water diffuse in starch/montmorillonite nano-biocomposite materials? *Carbohydrate Polymers, 82*(1), 128-135.

Cho, C. G., Park, T. H., & Kim, Y. S. (1997). Interfacial enrichment of a compatibilizing graft copolymer in a partially miscible polymer blend. *Polymer, 38*(18), 4687-4696.

Choi, Y. J., Hwang, S. H., Hong, Y. S., Kim, J. Y., Ok, C. Y., Huh, W., & Lee, S. W. (2005). Preparation and characterization of PS/multi-walled carbon nanotube nanocomposites. *Polymer Bulletin, 53*(5-6), 393-400.

Chun, Y. S., Kyung, Y. J., Jung, H. C., & Kim, W. N. (2000). Thermal and rheological properties of poly(epsilon-caprolactone) and polystyrene blends. *Polymer, 41*(24), 8729-8733.

Ciardelli, G., Chiono, V., Vozzi, G., Pracella, M., Ahluwalia, A., Barbani, N., Cristallini, C., & Giusti, P. (2005). Blends of poly-(epsilon-caprolactone) and polysaccharides in tissue engineering applications. *Biomacromolecules, 6*(4), 1961-1976.

Cigana, P., & Favis, B. D. (1998). The relative efficacy of diblock and triblock copolymers for a polystyrene/ethylene-propylene rubber interface. *Polymer, 39*(15), 3373-3378.

Cigana, P., Favis, B. D., & Jerome, R. (1996). Diblock copolymers as emulsifying agents in polymer blends: Influence of molecular weight, architecture, and chemical composition. *Journal of Polymer Science Part B-Polymer Physics, 34*(9), 1691-1700.

Clark, D. C., Geramita, K., & Baker, W. E. (1999). Investigation of the shear stresses experienced during melting using novel microencapsulated dye sensors. *Journal of Reinforced Plastics and Composites, 18*(3), 271-278.

Clarke, J., & Harris, J. (2001). Controlled orientation of short fibre reinforcement for anisotropic performance of rubber compounds. *Plastics Rubber and Composites, 30*(9), 406-415.

Cox, R. G. (1969). The deformation of a drop in a general time-dependent fluid flow. *Journal of Fluid Mechanics, 37*(03), 601-623.

Cui, L., Tarte, N. H., & Woo, S. I. (2009). Synthesis and Characterization of PMMA/MWNT Nanocomposites Prepared by in Situ Polymerization with Ni(acac)(2) Catalyst. *Macromolecules, 42*(22), 8649-8654.

Curvelo, A. A. S., de Carvalho, A. J. F., & Agnelli, J. A. M. (2001). Thermoplastic starch-cellulosic fibers composites: preliminary results. *Carbohydrate Polymers, 45*(2), 183-188.

Das, N. C., & Maiti, S. (2008). Electromagnetic interference shielding of carbon nanotube/ethylene vinyl acetate composites. *Journal of Materials Science, 43*(6), 1920-1925.

Davis, G., & Song, J. H. (2006). Biodegradable packaging based on raw materials from crops and their impact on waste management. *Industrial Crops and Products, 23*(2), 147-161.

De Kesel, C., Lefevre, C., Nagy, J. B., & David, C. (1999). Blends of polycaprolactone with polyvinylalcohol: a DSC, optical microscopy and solid state NMR study. *Polymer, 40*(8), 1969-1978.

Della Valle, G., Buleon, A., Carreau, P. J., Lavoie, P. A., & Vergnes, B. (1998). Relationship between structure and viscoelastic behavior of plasticized starch. *Journal of Rheology, 42*(3), 507-525.

Della Valle, G., Vergnes, B., & Lourdin, D. (2007). Viscous properties of thermoplastic starches from different botanical origin. *International Polymer Processing, 22*(5), 471-479.

Derby, R. I., Miller, B. S., Miller, B. F., & Trimbo, H. B. (1975). Visual Observation of Wheat-Starch Gelatinization in Limited Water Systems. *Cereal Chem, 52*, 11.

Donald, A. M., Kato, K. L., Perry, P. A., & Weigh, T. A. (2001). Scattering studies of the internal structure of starch granules. *Starch-Starke, 53*(10), 504-512.

Dondero, W. E., & Gorga, R. E. (2006). Morphological and mechanical properties of carbon nanotube/polymer composites via melt compounding. *Journal of Polymer Science Part B-Polymer Physics, 44*(5), 864-878.

Donovan, J. W. (1979). Phase transitions of the starch–water system. *Biopolymers, 18*(2), 263-275.

Drummond, K. M., Hopewell, J. L., & Shanks, R. A. (2000). Crystallization of low-density polyethylene- and linear low-density polyethylene-rich blends. *Journal of Applied Polymer Science, 78*(5), 1009-1016.

Du, F. M., Fischer, J. E., & Winey, K. I. (2003). Coagulation method for preparing single-walled carbon nanotube/poly(methyl methacrylate) composites and their modulus, electrical conductivity, and thermal stability. *Journal of Polymer Science Part B-Polymer Physics, 41*(24), 3333-3338.

Dumitrescu, L., Wilson, N. R., & Macpherson, J. V. (2007). Functionalizing single-walled carbon nanotube networks: Effect on electrical and electrochemical properties. *Journal of Physical Chemistry C, 111*(35), 12944-12953.

Dyke, C. A., & Tour, J. M. (2004a). Covalent Functionalization of Single-Walled Carbon Nanotubes for Materials Applications. *The Journal of Physical Chemistry A, 108*(51), 11151-11159.

Dyke, C. A., & Tour, J. M. (2004b). Overcoming the insolubility of carbon nanotubes through high degrees of sidewall functionalization. *Chemistry-a European Journal, 10*(4), 813-817.

Elemans, P. H. M., Janssen, J. M. H., & Meijer, H. E. H. (1990). The measurement of interfacial tension in polymer/polymer systems: The breaking thread method. *Journal of Rheology, 34*(8), 1311-1325.

Elias, L., Fenouillot, F., Majeste, J. C., & Cassagnau, P. (2007). Morphology and rheology of immiscible polymer blends filled with silica nanoparticles. *Polymer, 48*(20), 6029-6040.

Evangelista, R. L., Nikolov, Z. L., Wei, S., Jane, J. L., & Gelina, R. J. (1991). EFFECT OF COMPOUNDING AND STARCH MODIFICATION ON PROPERTIES OF STARCH-FILLED LOW-DENSITY POLYETHYLENE. *Industrial & Engineering Chemistry Research, 30*(8), 1841-1846.

Everaert, V., Aerts, L., & Groeninckx, G. (1999). Phase morphology development in immiscible PP/(PS/PPE) blends influence of the melt-viscosity ratio and blend composition. *Polymer, 40*(24), 6627-6644.

Fama, L., Gerschenson, L., & Goyanes, S. (2009). Starch-vegetable fibre composites to protect food products. *Carbohydrate Polymers, 75*(2), 230-235.

Famá, L. M., Pettarin, V., Goyanes, S. N., & Bernal, C. R. (2011). Starch/multi-walled carbon nanotubes composites with improved mechanical properties. *Carbohydrate Polymers, 83*(3), 1226-1231.

Favis, B. D. (1990). The effect of processing parameters on the morphology of an immiscible binary blend. *Journal of Applied Polymer Science, 39*(2), 285-300.

Favis, B. D. (1994). PHASE SIZE INTERFACE RELATIONSHIPS IN POLYMER BLENDS - THE EMULSIFICATION CURVE. *Polymer, 35*(7), 1552-1555.

Favis, B. D. (2000a). Factors Influencing the Morphology of Immiscible Polymer Blends in Melt Processing. In D. R. Paul & C. B. Bucknall (Eds.). *POLYMER BLENDS V. 1: Formulation*. Toronto: John Wiley & Sons Inc.

Favis, B. D. (2000b). Factors Influensing the Morphology of Immiscible olymer Blends in Melt Processing. In D. R. Paul & C. B. Bucknall (Eds.). *Polymer Blends Volume 1. Formulation* (Vol. 1, pp. 501-538). New York: John Wiley & Sons.

Favis, B. D., & Chalifoux, J. P. (1987). The effect of viscosity ratio on the morphology of polypropylene/polycarbonate blends during processing. *Polymer Engineering & Science, 27*(21), 1591-1600.

Favis, B. D., Rodriguez-Gonzalez, F. J., & Ramsay, B. A. (2003). Polymer compositions containing thermoplastic starch. *US Patent*. United States.

Favis, B. D., Rodriguez-Gonzalez, F. J., & Ramsay, B. A. (2005). Method of making polymer compositions containing thermoplastic starch. *U.S. Patent*. United States.

Favis, B. D., Rodriguez, F., & Ramsay, B. A. (2003). Polymer compositions containing thermoplastic starch *US Patent*. United States: Polyvalor, Societe en Commandite (Quebec, CA).

Favis, B. D., Rodriguez, F., & Ramsay, B. A. (2005). Method of making polymer compositions containing thermoplastic starch *U.S. Patent*. United States: Polyvalor, Societe en Commandite (Quebec, CA).

Favis, B. D., & Therrien, D. (1991). Factors influencing structure formation and phase size in an immiscible polymer blend of polycarbonate and polypropylene prepared by twin-screw extrusion. *Polymer, 32*(8), 1474-1481.

Feng, J., Chan, C.-m., & Li, J.-x. (2003). A method to control the dispersion of carbon black in an immiscible polymer blend. *Polymer Engineering & Science, 43*(5), 1058-1063.

Fenouillot, F., Cassagnau, P., & Majeste, J. C. (2009). Uneven distribution of nanoparticles in immiscible fluids: Morphology development in polymer blends. *Polymer, 50*(6), 1333-1350.

Fisher, F. T., Eitan, A., Andrews, R., Schadler, L. S., & Brinson, L. C. (2004). Spectral response and effective viscoelastic properties of MWNT-reinforced polycarbonate. *Advanced Composites Letters, 13*(2), 105-111.

Flumerfelt, R. W. (1980). Effects of dynamic interfacial properties on drop deformation and orientation in shear and extensional flow fields. *Journal of Colloid and Interface Science, 76*(2), 330-349.

Frost & Sullivan. (2011). Potential Market for Carbon Nanomaterials' Applications. Frost & Sullivan.

Gao, W., Dong, H., Hou, H., & Zhang, H. (2012). Effects of clays with various hydrophilicities on properties of starch–clay nanocomposites by film blowing. *Carbohydrate Polymers, 88*(1), 321-328.

Garcia, M. A., Martino, M. N., & Zaritzky, N. E. (2000). Microstructural characterization of plasticized starch-based films. *Starch-Starke, 52*(4), 118-124.

Gaudin, S., Lourdin, D., Le Botlan, D., Ilari, J. L., & Colonna, P. (1999). Plasticisation and mobility in starch-sorbitol films. *Journal of Cereal Science, 29*(3), 273-284.

Girifalco, L. A., & Good, R. J. (1957). A Theory for the Estimation of Surface and Interfacial Energies. I. Derivation and Application to Interfacial Tension. *The Journal of Physical Chemistry, 61*(7), 904-909.

Girija, B. G., & Sailaja, R. R. N. (2006). Low-density polyethylene/plasticized tapioca starch blends with the low-density polyethylene functionalized with maleate ester: Mechanical and thermal properties. *Journal of Applied Polymer Science, 101*(2), 1109-1120.

Godbillot, L., Dole, P., Joly, C., Roge, B., & Mathlouthi, M. (2006). Analysis of water binding in starch plasticized films. *Food Chemistry, 96*(3), 380-386.

Goeldel, A., Kasaliwal, G., & Poetschke, P. (2009). Selective Localization and Migration of Multiwalled Carbon Nanotubes in Blends of Polycarbonate and Poly(styrene-acrylonitrile). *Macromolecular Rapid Communications, 30*(6), 423-429.

Goeldel, A., Kasaliwal, G. R., Poetschke, P., & Heinrich, G. (2012). The kinetics of CNT transfer between immiscible blend phases during melt mixing. *Polymer, 53*(2), 411-421.

Goeldel, A., Marmur, A., Kasaliwal, G. R., Poetschke, P., & Heinrich, G. (2011). Shape-Dependent Localization of Carbon Nanotubes and Carbon Black in an Immiscible Polymer Blend during Melt Mixing. *Macromolecules, 44*(15), 6094-6102.

Good, R. J., & Girifalco, L. A. (1960). A THEORY FOR ESTIMATION OF SURFACE AND INTERFACIAL ENERGIES. III. ESTIMATION OF SURFACE ENERGIES OF SOLIDS FROM CONTACT ANGLE DATA. *The Journal of Physical Chemistry, 64*(5), 561-565.

Good, R. J., Girifalco, L. A., & Kraus, G. (1958). A Theory for Estimation of Interfacial Energies. II. Application to Surface Thermodynamics of Teflon and Graphite. *The Journal of Physical Chemistry, 62*(11), 1418-1421.

Grace, H. P. (1982). DISPERSION PHENOMENA IN HIGH VISCOSITY IMMISCIBLE FLUID SYSTEMS AND APPLICATION OF STATIC MIXERS AS DISPERSION DEVICES IN SUCH SYSTEMS. *Chemical Engineering Communications, 14*(3-6), 225-277.

Grady, B. P. (2010). Recent Developments Concerning the Dispersion of Carbon Nanotubes in Polymers. *Macromolecular Rapid Communications, 31*(3), 247-257.

Grady, B. P. (2011). EFFECTS OF CARBON NANOTUBES ON POLYMER PHYSICS. *CARBON NANOTUBE–POLYMER COMPOSITES,Manufacture, Properties, and Applications* (pp. 119-190). Hoboken, NJ: John Wiley & Sons, Inc.

Grady, B. P. (2012). Effects of carbon nanotubes on polymer physics. *Journal of Polymer Science Part B-Polymer Physics, 50*(9), 591-623.

Grady, B. P., Paul, A., Peters, J. E., & Ford, W. T. (2009). Glass Transition Behavior of Single-Walled Carbon Nanotube-Polystyrene Composites. *Macromolecules, 42*(16), 6152-6158.

Grady, B. P., Pompeo, F., Shambaugh, R. L., & Resasco, D. E. (2002). Nucleation of polypropylene crystallization by single-walled carbon nanotubes. *Journal of Physical Chemistry B, 106*(23), 5852-5858.

Grohens, Y., Brogly, M., Labbe, C., David, M. O., & Schultz, J. (1998). Glass transition of stereoregular poly(methyl methacrylate) at interfaces. *Langmuir, 14*(11), 2929-2932.

Grohens, Y., Hamon, L., Reiter, G., Soldera, A., & Holl, Y. (2002). Some relevant parameters affecting the glass transition of supported ultra-thin polymer films. *European Physical Journal E, 8*(2), 217-224.

Grossiord, N., Miltner, H. E., Loos, J., Meuldijk, J., Van Mele, B., & Koning, C. E. (2007). On the crucial role of wetting in the preparation of conductive polystyrene-carbon nanotube composites. *Chemistry of Materials, 19*(15), 3787-3792.

Gubbels, F., Jerome, R., Teyssie, P., Vanlathem, E., Deltour, R., Calderone, A., Parente, V., & Bredas, J. L. (1994). Selective Localization of Carbon Black in Immiscible Polymer Blends: A Useful Tool To Design Electrical Conductive Composites. *Macromolecules, 27*(7), 1972-1974.

Gubbels, F., Jerome, R., Vanlathem, E., Deltour, R., Blacher, S., & Brouers, F. (1998). Kinetic and Thermodynamic Control of the Selective Localization of Carbon Black at the Interface of Immiscible Polymer Blends. *Chemistry of Materials, 10*(5), 1227-1235.

Habeych, E., Guo, X., van Soest, J., der Goot, A. J. v., & Boom, R. (2009). On the applicability of Flory–Huggins theory to ternary starch–water–solute systems. *Carbohydrate Polymers, 77*(4), 703-712.

Hameed, T., Quinlan, P. J., Potter, D. K., & Takacs, E. (2012). Study of Reaction Between a Low Molecular Weight, Highly Functionalized Polyethylene and Hexamethylenediamine. *Macromolecular Materials and Engineering, 297*(1), 39-50.

Harrats, C., Thomas, S., & Groeninckx, G. (2006). *Micro- and nanostructured polymer blend systems: phase morphology and interfaces*. Boca Raton, FL: CRC/Taylor & Francis.

Haugaard, V. K., Udsen, A. M., Mortensen, G., Hoegh, L., Petersen, K., & Monahan, F. (2001). Food biopackaging, in biobased packaging materials for the food industry - status and perspectives". *A European concerted action*, 13-14.

Hickman, B. E., Janaswamy, S., & Yao, Y. (2008). Properties of Starch Subjected to Partial Gelatinization and β-Amylolysis. *Journal of Agricultural and Food Chemistry, 57*(2), 666-674.

Hong, J. S., Kim, Y. K., Ahn, K. H., & Lee, S. J. (2008). Shear-induced migration of nanoclay during morphology evolution of PBT/PS blend. *Journal of Applied Polymer Science, 108*(1), 565-575.

Hoover, R. (2001). Composition, molecular structure, and physicochemical properties of tuber and root starches: a review. *Carbohydrate Polymers, 45*(3), 253-267.

Hsieh, A. J., Moy, P., Beyer, F. L., Madison, P., Napadensky, E., Ren, J., & Krishnamoorti, R. (2004). Mechanical response and rheological properties of polycarbonate layered-silicate nanocomposites. *Polymer Engineering & Science, 44*(5), 825-837.

Huang, C.-L., & Wang, C. (2011). Polymorphism and transcrystallization of syndiotactic polystyrene composites filled with carbon nanotubes. *European Polymer Journal, 47*(11), 2087-2096.

Huang, W., Edenzon, K., Fernandez, L., Razmpour, S., Woodburn, J., & Cebe, P. (2010). Nanocomposites of poly(vinylidene fluoride) with multiwalled carbon nanotubes. *Journal of Applied Polymer Science, 115*(6), 3238-3248.

Huang, Y.-L., Ma, C.-C. M., Yuen, S.-M., Chuang, C.-Y., Kuan, H.-C., Chiang, C.-L., & Wu, S.-Y. (2011). Effect of maleic anhydride modified MWCNTs on the morphology and dynamic mechanical properties of its PMMA composites. *Materials Chemistry and Physics, 129*(3), 1214-1220.

Huneault, M. A., & Li, H. (2007). Morphology and properties of compatibilized polylactide/thermoplastic starch blends. *Polymer, 48*(1), 270-280.

Huneault, M. A., Shi, Z. H., & Utracki, L. A. (1995). Development of polymer blend morphology during compounding in a twin-screw extruder. Part IV: A new computational model with coalescence. *Polymer Engineering & Science, 35*(1), 115-127.

Ibarra-Gomez, R., Marquez, A., Valle, L., & Rodriguez-Fernandez, O. S. (2003). Influence of the blend viscosity and interface energies on the preferential location of CB and conductivity of BR/EPDM blends. *Rubber Chemistry and Technology, 76*(4), 969-978.

Ijima, S. (1991). Helical microtubules of graphitic carbon. *Nature, 354*, 56-58.

Il Yun, S., Gadd, G. E., Latella, B. A., Lo, V., Russell, R. A., & Holden, P. J. (2008). Mechanical properties of biodegradable polyhydroxyalkanoates/single wall carbon nanotube nanocomposite films. *Polymer Bulletin, 61*(2), 267-275.

Ionescu, M. (2005). *Chemistry and Technology of Polyols for Polyurethanes*. Shropshire, United Kingdom: Smithers Rapra Technology.

Ishiaku, U. S., Pang, K. W., Lee, W. S., & Ishak, Z. A. M. (2002). Mechanical properties and enzymic degradation of thermoplastic and granular sago starch filled poly(ε-caprolactone). *European Polymer Journal, 38*(2), 393-401.

Jacobs, H., & Delcour, J. A. (1998). Hydrothermal modifications of granular starch, with retention of the granular structure: A review. *Journal of Agricultural and Food Chemistry, 46*(8), 2895-2905.

Jang, B. C., Huh, S. Y., Jang, J. G., & Bae, Y. C. (2001). Mechanical properties and morphology of the modified HDPE/starch reactive blend. *Journal of Applied Polymer Science, 82*(13), 3313-3320.

Janssen, J. M. H., & Meijer, H. E. H. (1993). Droplet breakup mechanisms: Stepwise equilibrium versus transient dispersion. *Journal of Rheology, 37*(4), 597-608.

Jenkins, P. J., & Donald, A. M. (1995). The influence of amylose on starch granule structure. *International Journal of Biological Macromolecules, 17*(6), 315-321.

Jenkins, P. J., & Donald, A. M. (1998). Geratinisation of starch: a combined SAXS/WAXS/DSC and SANS study. *Carbohydrate Research, 308*(1-2), 133-147.

Jeon, H. K., & Kim, J. K. (1998). The effect of the amount of in situ formed copolymers on the final morphology of reactive polymer blends with an in situ compatibilizer. *Macromolecules, 31*(26), 9273-9280.

Jiang, C. H., Filippi, S., & Magagnini, P. (2003). Reactive compatibilizer precursors for LDPE/PA6 blends. II: maleic anhydride grafted polyethylenes. *Polymer, 44*(8), 2411-2422.

Jin, S.-H., & Lee, D.-S. (2008). Preparation and Properties of the Nanocomposites Based on Poly(methyl methacrylate-co-butyl acrylate) and Multiwalled Carbon Nanotube. *Journal of Nanoscience and Nanotechnology, 8*(9), 4675-4678.

Jin, S. H., Choi, D. K., & Lee, D. S. (2008). Electrical and rheological properties of polycarbonate/multiwalled carbon nanotube nanocomposites. *Colloids and Surfaces A: Physicochemical and Engineering Aspects, 313–314*(0), 242-245.

Jin, S. H., Kang, I. H., Kim, Y. S., Park, C. Y., & Lee, D. S. (2008). Thermal and Electrical Properties of Nanocomposites Based on Acrylic Copolymers and Multiwalled Carbon Nanotube. *Journal of Nanoscience and Nanotechnology, 8*(10), 5076-5079.

Kalambur, S., & Rizvi, S. S. H. (2006). An overview of starch-based plastic blends from reactive extrusion. *Journal of Plastic Film & Sheeting, 22*(1), 39-58.

Kalichevsky, M. T., Jaroszkiewicz, E. M., & Blanshard, J. M. V. (1993). A STUDY OF THE GLASS-TRANSITION OF AMYLOPECTIN SUGAR MIXTURES. *Polymer, 34*(2), 346-358.

Kang, D. J., Pal, K., Bang, D. S., & Kim, J. K. (2011). Synergistic effect on crystalline structure of polyvinylidene fluoride nanocomposites with multiwalled carbon nanotube loading by a twin screw extruder. *Journal of Applied Polymer Science, 121*(1), 226-233.

Karam, H. J., & Bellinger, J. C. (1968). Deformation and Breakup of Liquid Droplets in a Simple Shear Field. *Industrial & Engineering Chemistry Fundamentals, 7*(4), 576-581.

Kaseem, M., Hamad, K., & Deri, F. (2012). Thermoplastic starch blends: A review of recent works. *Polymer Science Series A, 54*(2), 165-176.

Katada, A., Buys, Y., Tominaga, Y., Asai, S., & Sumita, M. (2005). Relationship between electrical resistivity and particle dispersion state for carbon black filled poly (ethylene-<i>co</i>-vinyl acetate)/poly (<small>L</small> -lactic acid) blend. *Colloid & Polymer Science, 284*(2), 134-141.

Kavan, L., & Dunsch, L. (2003). Diameter-selective electrochemical doping of HiPco single-walled carbon nanotubes. *Nano Letters, 3*(7), 969-972.

Kilburn, D., Claude, J., Schweizer, T., Alam, A., & Ubbink, J. (2005). Carbohydrate polymers in amorphous states: An integrated thermodynamic and nanostructural investigation. *Biomacromolecules, 6*(2), 864-879.

Kim, H. Y., Jeong, U., & Kim, J. K. (2003). Reaction Kinetics and Morphological Changes of Reactive Polymer−Polymer Interface. *Macromolecules, 36*(5), 1594-1602.

Kim, J. K., & Lee, H. (1996). The effect of PS-GMA as an in situ compatibilizer on the morphology and rheological properties of the immiscible PBT/PS blend. *Polymer, 37*(2), 305-311.

Kim, J. Y., & Kim, S. H. (2006). Influence of multiwall carbon nanotube on physical properties of poly(ethylene 2,6-naphthalate) nanocomposites. *Journal of Polymer Science Part B-Polymer Physics, 44*(7), 1062-1071.

Kim, M., & Lee, S.-J. (2002). Characteristics of crosslinked potato starch and starch-filled linear low-density polyethylene films. *Carbohydrate Polymers, 50*(4), 331-337.

Koulouri, E. G., Georgaki, A. X., & Kallitsis, J. K. (1997). Reactive compatibilization of aliphatic polyimides with functionalized polyethylenes. *Polymer, 38*(16), 4185-4192.

Krogars, K., Heinämäki, J., Karjalainen, M., Niskanen, A., Leskelä, M., & Yliruusi, J. (2003). Enhanced stability of rubbery amylose-rich maize starch films plasticized with a combination of sorbitol and glycerol. *International Journal of Pharmaceutics, 251*(1–2), 205-208.

Kum, C. K., Sung, Y. T., Kim, Y. S., Lee, H. G., Kim, W. N., Lee, H. S., & Yoon, H. G. (2007). Effects of compatibilizer on mechanical, morphological, and rheological properties of polypropylene/poly(acrylonitrile-butadiene-styrene) blends. *Macromolecular Research, 15*(4), 308-314.

Kwok, D. Y., & Neumann, A. W. (1999). Contact angle measurement and contact angle interpretation. *Advances in Colloid and Interface Science, 81*(3), 167-249.

Kymakis, E., & Amaratunga, G. A. J. (2006). Electrical properties of single-wall carbon nanotube-polymer composite films. *Journal of Applied Physics, 99*(8), -.

Laredo, E., Grimau, M., Bello, A., Wu, D. F., Zhang, Y. S., & Lin, D. P. (2010). AC Conductivity of Selectively Located Carbon Nanotubes in Poly(epsilon-caprolactone)/Polylactide Blend Nanocomposites. *Biomacromolecules, 11*(5), 1339-1347.

Lawal, O. S., & Adebowale, K. O. (2005). Physicochemical characteristics and thermal properties of chemically modified jack bean (Canavalia ensiformis) starch. *Carbohydrate Polymers, 60*(3), 331-341.

Lawrence, S. S., Walia, P. S., Felker, F., & Willett, J. L. (2004). Starch-filled ternary polymer composites. II: Room temperature tensile properties. *Polymer Engineering and Science, 44*(10), 1839-1847.

Lee, C. W., Ryu, S. H., & Kim, H. S. (1997). Morphological changes in nylon-6/acrylonitrile-butadiene-styrene reactive blend. *Journal of Applied Polymer Science, 64*(8), 1595-1604.

Lee, J. K., & Han, C. D. (1999). Evolution of polymer blend morphology during compounding in an internal mixer. *Polymer, 40*(23), 6277-6296.

Lee, J. K., & Han, C. D. (2000). Evolution of polymer blend morphology during compounding in a twin-screw extruder. *Polymer, 41*(5), 1799-1815.

Lehmann, U., & Robin, F. (2007). Slowly digestible starch – its structure and health implications: a review. *Trends in Food Science & Technology, 18*(7), 346-355.

Lerbret, A., Mason, P. E., Venable, R. M., Cesaro, A., Saboungi, M. L., Pastor, R. W., & Brady, J. W. (2009). Molecular dynamics studies of the conformation of sorbitol. *Carbohydrate Research, 344*(16), 2229-2235.

Li, G., & Favis, B. D. (2010). Morphology Development and Interfacial Interactions in Polycaprolactone/Thermoplastic-Starch Blends. *Macromolecular Chemistry and Physics, 211*(3), 321-333.

Li, G., Sarazin, P., & Favis, B. D. (2008). The relationship between starch gelatinization and morphology control in melt-processed polymer blends with thermoplastic starch. *Macromolecular Chemistry and Physics, 209*(10), 991-1002.

Li, H., & Huneault, M. A. (2011a). Comparison of Sorbitol and Glycerol as Plasticizers for Thermoplastic Starch in TPS/PLA Blends. *Journal of Applied Polymer Science, 119*(4), 2439-2448.

Li, H., Sparks, W., & Bonning, B. (2008). Protocols for microapplicator-assisted infection of lepidopteran larvae with baculovirus. *Journal of visualized experiments : JoVE*(18).

Li, H. B., & Huneault, M. A. (2011b). Comparison of Sorbitol and Glycerol as Plasticizers for Thermoplastic Starch in TPS/PLA Blends. *Journal of Applied Polymer Science, 119*(4), 2439-2448.

Li, J., Fang, Z., Tong, L., Gu, A., & Liu, F. (2006). Polymorphism of nylon-6 in multiwalled carbon nanotubes/nylon-6 composites. *Journal of Polymer Science Part B: Polymer Physics, 44*(10), 1499-1512.

Li, L., Li, C. Y., & Ni, C. (2006). Polymer Crystallization-Driven, Periodic Patterning on Carbon Nanotubes. *Journal of the American Chemical Society, 128*(5), 1692-1699.

Li, Z. F., Luo, G. H., Wei, F., & Huang, Y. (2006). Microstructure of carbon nanotubes/PET conductive composites fibers and their properties. *Composites Science and Technology, 66*(7-8), 1022-1029.

Li, Z. M., Li, S. N., Xu, X. B., & Lu, A. (2007). Carbon nanotubes can enhance phase dispersion in polymer blends. *Polymer-Plastics Technology and Engineering, 46*(2), 129-134.

Lim, K. Y., Kim, B. C., & Yoon, K. J. (2003). Structural and physical properties of biodegradable copolyesters from poly(ethylene terephthalate) and polycaprolactone blends. *Journal of Applied Polymer Science, 88*(1), 131-138.

Lin, B., Sundararaj, U., & Potschke, P. (2006). Melt mixing of polycarbonate with multi-walled carbon nanotubes in miniature mixers. *Macromolecular Materials and Engineering, 291*(3), 227-238.

Liu, L., Wang, Y., Xiang, F. M., Li, Y. L., Han, L., & Zhou, Z. W. (2009). Effects of Functionalized Multiwalled Carbon Nanotubes on the Morphologies and Mechanical Properties of PP/EVA Blend. *Journal of Polymer Science Part B-Polymer Physics, 47*(15), 1481-1491.

Liu, Q., Charlet, G., Yelle, S., & Arul, J. (2002). Phase transition in potato starch–water system I. Starch gelatinization at high moisture level. *Food Research International, 35*(4), 397-407.

Liu, W.-C., Halley, P. J., & Gilbert, R. G. (2010). Mechanism of Degradation of Starch, a Highly Branched Polymer, during Extrusion. *Macromolecules, 43*(6), 2855-2864.

Logakis, E., Pandis, C., Peoglos, V., Pissis, P., Stergiou, C., Pionteck, J., Pötschke, P., Mičušík, M., & Omastová, M. (2009). Structure–property relationships in polyamide 6/multi-walled carbon nanotubes nanocomposites. *Journal of Polymer Science Part B: Polymer Physics, 47*(8), 764-774.

Lomellini, P., Matos, M., & Favis, B. D. (1996). Interfacial modification of polymer blends - The emulsification curve .2. Predicting the critical concentration of interfacial modifier from geometrical considerations. *Polymer, 37*(25), 5689-5694.

Lourdin, D., Bizot, H., & Colonna, P. (1997). "Antiplasticization" in starch-glycerol films? *Journal of Applied Polymer Science, 63*(8), 1047-1053.

Lu, Q. W., Macosko, C. W., & Horrion, J. (2003). Compatibilized blends of thermoplastic polyurethane (TPU) and polypropylene. *Macromolecular Symposia, 198*, 221-232.

Luong, J. H. T., Hrapovic, S., Liu, Y. L., Yang, D. Q., Sacher, E., Wang, D. S., Kingston, C. T., & Enright, G. D. (2005). Oxidation, deformation, and destruction of carbon nanotubes in aqueous ceric sulfate. *Journal of Physical Chemistry B, 109*(4), 1400-1407.

Ma, P.-C., Siddiqui, N. A., Marom, G., & Kim, J.-K. (2010). Dispersion and functionalization of carbon nanotubes for polymer-based nanocomposites: A review. *Composites Part A: Applied Science and Manufacturing, 41*(10), 1345-1367.

Ma, P. C., Kim, J. K., & Tang, B. Z. (2007). Effects of silane functionalization on the properties of carbon nanotube/epoxy nanocomposites. *Composites Science and Technology, 67*(14), 2965-2972.

Ma, X. F., Yu, J. G., & Wang, N. (2008). Glycerol plasticized-starch/multiwall carbon nanotube composites for electroactive polymers. *Composites Science and Technology, 68*(1), 268-273.

Macosko, C. W. (2000). Morphology development and control in immiscible polymer blends. *Macromolecular Symposia, 149*, 171-184.

Macosko, C. W., Guegan, P., Khandpur, A. K., Nakayama, A., Marechal, P., & Inoue, T. (1996). Compatibilizers for melt blending: Premade block copolymers. *Macromolecules, 29*(17), 5590-5598.

Macosko, C. W., Jeon, H. K., & Hoye, T. R. (2005). Reactions at polymer-polymer interfaces for blend compatibilization. *Progress in Polymer Science, 30*(8-9), 939-947.

Maglio, G., Migliozzi, A., Palumbo, R., Immirzi, B., & Volpe, M. G. (1999). Compatibilized poly(epsilon-caprolactone)/poly(L-lactide) blends for biomedical uses. *Macromolecular Rapid Communications, 20*(4), 236-238.

Mali, S., Sakanaka, L. S., Yamashita, F., & Grossmann, M. V. E. (2005). Water sorption and mechanical properties of cassava starch films and their relation to plasticizing effect. *Carbohydrate Polymers, 60*(3), 283-289.

Mamunya, Y. (2001). Polymer blends filled with carbon black: structure and electrical properties. *Macromolecular Symposia, 170*(1), 257-264.

Martin, O., & Averous, L. (2001). Poly(lactic acid): plasticization and properties of biodegradable multiphase systems. *Polymer, 42*(14), 6209-6219.

Martinez, J. G., Benavides, R., & Guerrer, C. (2008). Compatibilization of commingled plastics with maleic anhydride modified polyethylenes and ultraviolet preirradiation. *Journal of Applied Polymer Science, 108*(4), 2597-2603.

Mathew, A. P., & Dufresne, A. (2002). Plasticized waxy maize starch: Effect of polyols and relative humidity on material properties. *Biomacromolecules, 3*(5), 1101-1108.

Matzinos, P., Tserki, V., Gianikouris, C., Pavlidou, E., & Panayiotou, C. (2002). Processing and characterization of LDPE/starch/PCL blends. *European Polymer Journal, 38*(9), 1713-1720.

Mbey, J. A., Hoppe, S., & Thomas, F. (2012). Cassava starch–kaolinite composite film. Effect of clay content and clay modification on film properties. *Carbohydrate Polymers, 88*(1), 213-222.

Meincke, O., Kaempfer, D., Weickmann, H., Friedrich, C., Vathauer, M., & Warth, H. (2004). Mechanical properties and electrical conductivity of carbon-nanotube filled polyamide-6 and its blends with acrylonitrile/butadiene/styrene. *Polymer, 45*(3), 739-748.

Meng, H., Sui, G. X., Fang, P. F., & Yang, R. (2008). Effects of acid- and diamine-modified MWNTs on the mechanical properties and crystallization behavior of polyamide 6. *Polymer, 49*(2), 610-620.

Meyyappan, M. (2005). *Carbon Nanotubes: Scinece and Applications*. Moffett Field, CA: CRC PRESS.

Mitchell, C. A., Bahr, J. L., Arepalli, S., Tour, J. M., & Krishnamoorti, R. (2002). Dispersion of functionalized carbon nanotubes in polystyrene. *Macromolecules, 35*(23), 8825-8830.

Moniruzzaman, M., & Winey, K. I. (2006). Polymer nanocomposites containing carbon nanotubes. *Macromolecules, 39*(16), 5194-5205.

Mua, J. P., & Jackson, D. S. (1997). Fine Structure of Corn Amylose and Amylopectin Fractions with Various Molecular Weights†. *Journal of Agricultural and Food Chemistry, 45*(10), 3840-3847.

Mukherjee, M., Das, T., Rajasekar, R., Bose, S., Kumar, S., & Das, C. K. (2009). Improvement of the properties of PC/LCP blends in the presence of carbon nanotubes. *Composites Part a-Applied Science and Manufacturing, 40*(8), 1291-1298.

Myllarinen, P., Buleon, A., Lahtinen, R., & Forssell, P. (2002). The crystallinity of amylose and amylopectin films. *Carbohydrate Polymers, 48*(1), 41-48.

Nair, L. S., & Laurencin, C. T. (2007). Biodegradable polymers as biomaterials. *Progress in Polymer Science, 32*(8–9), 762-798.

Nashed, G., Rutgers, P. P. G., & Sopade, P. A. (2003). The plasticisation effect of glycerol and water on the gelatinisation of wheat starch. *Starch-Starke, 55*(3-4), 131-137.

Nawang, R., Danjaji, I. D., Ishiaku, U. S., Ismail, H., & Ishak, Z. A. M. (2001). Mechanical properties of sago starch-filled linear low density polyethylene (LLDPE) composites. *Polymer Testing, 20*(2), 167-172.

Nayak, P. L. (1999). Biodegradable polymers: Opportunities and challenges. *Journal of Macromolecular Science-Reviews in Macromolecular Chemistry and Physics, C39*(3), 481-505.

Nuriel, S., Liu, L., Barber, A. H., & Wagner, H. D. (2005). Direct measurement of multiwall nanotube surface tension. *Chemical Physics Letters, 404*(4-6), 263-266.

O'Connell, M. J., Boul, P., Ericson, L. M., Huffman, C., Wang, Y. H., Haroz, E., Kuper, C., Tour, J., Ausman, K. D., & Smalley, R. E. (2001). Reversible water-solubilization of single-walled carbon nanotubes by polymer wrapping. *Chemical Physics Letters, 342*(3-4), 265-271.

Otey, F. H., Mark, A. M., Mehltretter, C. L., & Russell, C. R. (1974). Starch-Based Film for Degradable Agricultural Mulch. *Product R&D, 13*(1), 90-92.

Otey, F. H., Westhoff, R. P., & Doane, W. M. (1980a). Starch-Based Blown Films. *Ind. Eng. Chem. Prod. Res. Dev, 19*(4), 4.

Otey, F. H., Westhoff, R. P., & Doane, W. M. (1980b). Starch-Based Blown Films. *Industrial & Engineering Chemistry Product Research and Development, 19*(4), 592-595.

Ounaies, Z., Park, C., Wise, K. E., Siochi, E. J., & Harrison, J. S. (2003). Electrical properties of single wall carbon nanotube reinforced polyimide composites. *Composites Science and Technology, 63*(11), 1637-1646.

Ozdilek, C., Bose, S., Leys, J., Seo, J. W., Wubbenhorst, M., & Moldenaers, P. (2011). Thermally induced phase separation in P alpha MSAN/PMMA blends in presence of functionalized multiwall carbon nanotubes: Rheology, morphology and electrical conductivity. *Polymer, 52*(20), 4480-4489.

Palav, T., & Seetharaman, K. (2006). Mechanism of starch gelatinization and polymer leaching during microwave heating. *Carbohydrate Polymers, 65*(3), 364-370.

Pan, L., Chiba, T., & Inoue, T. (2001). Reactive blending of polyamide with polyethylene: pull-out of in situ-formed graft copolymer. *Polymer, 42*(21), 8825-8831.

Pan, L., Inoue, T., Hayami, H., & Nishikawa, S. (2002). Reactive blending of polyamide with polyethylene: pull-out of in situ-formed graft copolymers and its application for high-temperature materials. *Polymer, 43*(2), 337-343.

Park, H. M., Li, X. C., Jin, C. Z., Park, C. Y., Cho, W. J., & Ha, C. S. (2002). Preparation and properties of biodegradable thermoplastic starch/clay hybrids. *Macromolecular Materials and Engineering, 287*(8), 553-558.

Pérez, S., Baldwin, P., & Gallant, D. (2009). Structural Features ofStarch Granules I. In J. BeMiller & R. Whistler (Eds.). *Starch: Chemistry and Technology*. London, UK: Academic Press.

Perry, P. A., & Donald, A. M. (2000). The role of plasticization in starch granule assembly. *Biomacromolecules, 1*(3), 424-432.

Perry, P. A., & Donald, A. M. (2002). The effect of sugars on the gelatinisation of starch. *Carbohydrate Polymers, 49*(2), 155-165.

Persson, A. L., & Bertilsson, H. (1998). Viscosity difference as distributing factor in selective absorption of aluminium borate whiskers in immiscible polymer blends. *Polymer, 39*(23), 5633-5642.

Phang, I. Y., Ma, J., Shen, L., Liu, T., & Zhang, W.-D. (2006). Crystallization and melting behavior of multi-walled carbon nanotube-reinforced nylon-6 composites. *Polymer International, 55*(1), 71-79.

Piringer, O. G., & Baner, A. L. (2008). *Plastic Packaging: Interactions with Food and Pharmaceuticals*. Darmstadt, Germany: Wiley-VCH.

Pitt, C. G., Chasalow, F. I., Hibionada, Y. M., Klimas, D. M., & Schindler, A. (1981). Aliphatic polyesters. I. The degradation of poly(ϵ-caprolactone) in vivo. *Journal of Applied Polymer Science, 26*(11), 3779-3787.

Plochocki, A. P., Dagli, S. S., Starita, J., & Curry, J. E. (1986). Effect of Mixing History on Phase Morphology of a Polyalloy (Tentative Results for Three Mixers. *Journal of Elastomers and Plastics, 18*(4), 256-266.

Poetschke, P., Pegel, S., Claes, M., & Bonduel, D. (2008). A novel strategy to incorporate carbon nanotubes into thermoplastic matrices. *Macromolecular Rapid Communications, 29*(3), 244-251.

Potschke, P., Bhattacharyya, A. R., & Janke, A. (2003). Morphology and electrical resistivity of melt mixed blends of polyethylene and carbon nanotube filled polycarbonate. *Polymer, 44*(26), 8061-8069.

Potschke, P., Bhattacharyya, A. R., & Janke, A. (2004). Carbon nanotube-filled polycarbonate composites produced by melt mixing and their use in blends with polyethylene. *Carbon, 42*(5-6), 965-969.

Potschke, P., Bhattacharyya, A. R., Janke, A., & Goering, H. (2003). Melt mixing of polycarbonate/multi-wall carbon nanotube composites. *Composite Interfaces, 10*(4-5), 389-404.

Potschke, P., Pegel, S., Claes, M., & Bonduel, D. (2008). A novel strategy to incorporate carbon nanotubes into thermoplastic matrices. *Macromolecular Rapid Communications, 29*(3), 244-251.

Poutanen, K., & Forssell, P. (1996). Modification of starch properties with plasticizers. *Trends in Polymer Science, 4*(4), 128-132.

Queiroz, A. U. B., & Collares-Queiroz, F. P. (2009). Innovation and Industrial Trends in Bioplastics. *Polymer Reviews, 49*(2), 65-78.

Raghavan, D., & Emekalam, A. (2001). Characterization of starch/polyethylene and starch/polyethylene/poly(lactic acid) composites. *Polymer Degradation and Stability, 72*(3), 509-517.

Ravati, S. (2010). NOVEL CONDUCTIVE POLYMER BLENDS. *Chemical Engineering* (Vol. PhD). Montreal, QC: Ecole Polytechnique de Montreal.

Ravati, S., & Favis, B. D. (2010). Low percolation threshold conductive device derived from a five-component polymer blend. *Polymer, 51*(16), 3669-3684.

Redl, A., Morel, M. H., Bonicel, J., Guilbert, S., & Vergnes, B. (1999). Rheological properties of gluten plasticized with glycerol: dependence on temperature, glycerol content and mixing conditions. *Rheologica Acta, 38*(4), 311-320.

Reichardt, C., & Welton, T. (2011). *Solvents and Solvent Effects in Organic Chemistry*. Weinheim, Germany: John Wiley & Sons.

Reignier, J., & Favis, B. D. (2000). Control of the subinclusion microstructure in HDPE/PS/PMMA ternary blends. *Macromolecules, 33*(19), 6998-7008.

Ring, S. G., L'Anson, K., & Morris, V. J. (1985). Static and dynamic light scattering studies of amylose solutions. *Macromolecules, 18*(2), 182-188.

Rodriguez-Gonzalez, F. J., Ramsay, B. A., & Favis, B. D. (2003). High performance LDPE/thermoplastic starch blends: a sustainable alternative to pure polyethylene. *Polymer, 44*(5), 1517-1526.

Rodriguez-Gonzalez, F. J., Ramsay, B. A., & Favis, B. D. (2004). Rheological and thermal properties of thermoplastic starch with high glycerol content. *Carbohydrate Polymers, 58*(2), 139-147.

Rodriguez-Gonzalez, F. J., Virgilio, N., Ramsay, B. A., & Favis, B. D. (2003). Influence of melt drawing on the morphology of one- and two-step processed LDPE/thermoplastic starch blends. *Advances in Polymer Technology, 22*(4), 297-305.

Rodriguez Gonzalez, F. J. (2002). Low density polyethylene/thermoplastic starch blends. (Vol. Ph.D., p. 181 p.). Canada: Ecole Polytechnique, Montreal (Canada).

Rumscheidt, F. D., & Mason, S. G. (1961). Particle motions in sheared suspensions XII. Deformation and burst of fluid drops in shear and hyperbolic flow. *Journal of Colloid Science, 16*(3), 238-261.

SA, S. (1967). The determination of the size distribution of particles in an opaque material from a measurement of the size distributions of their sections. In H. Elias (Ed.). *Proceedings of Second International Congress for Stereology* (pp. 163-173). Berlin Springer–Verlag.

Saeed, K., & Park, S.-Y. (2007). Preparation of multiwalled carbon nanotube/nylon-6 nanocomposites by in situ polymerization. *Journal of Applied Polymer Science, 106*(6), 3729-3735.

Sailaja, R. R. N. (2005). Mechanical properties of esterified tapioca starch-LDPE blends using LDPE-co-glycidyl methacrylate as compatibilizer. *Polymer International, 54*(2), 286-296.

Sailaja, R. R. N., & Chanda, M. (2000). Use of maleic anhydride-grafted polyethylene as compatibilizer for polyethylene-starch blends: Effects on mechanical properties. *Journal of Polymer Materials, 17*(2), 165-176.

Sailaja, R. R. N., & Chanda, M. (2001). Use of maleic anhydride-grafted polyethylene as compatibilizer for HDPE-tapioca starch blends: Effects on mechanical properties. *Journal of Applied Polymer Science, 80*(6), 863-872.

Sailaja, R. R. N., & Chanda, M. (2002). Use of poly(ethylene-co-vinyl alcohol) as compatibilizer in LDPE/thermoplastic tapioca starch blends. *Journal of Applied Polymer Science, 86*(12), 3126-3134.

Sailaja, R. R. N., Reddy, A. P., & Chanda, M. (2001). Effect of epoxy functionalized compatibilizer on the mechanical properties of low-density polyethylene/plasticized tapioca starch blends. *Polymer International, 50*(12), 1352-1359.

Saito, R., Dresselhaus, G., & Dresselhaus, M. S. (1998). *PHYSICAL PROPERTIES OF CARBON NANOTUBES*. London, UK: Imperial College Press.

Sanchez-Garcia, M. D., Lagaron, J. M., & Hoa, S. V. (2010). Effect of addition of carbon nanofibers and carbon nanotubes on properties of thermoplastic biopolymers. *Composites Science and Technology, 70*(7), 1095-1105.

Sarazin, P., Li, G., Orts, W. J., & Favis, B. D. (2008). Binary and ternary blends of polylactide, polycaprolactone and thermoplastic starch. *Polymer, 49*(2), 599-609.

Sarno, M., Gorrasi, G., Sannino, D., Sorrentino, A., Ciambelli, P., & Vittoria, V. (2004). Polymorphism and Thermal Behaviour of Syndiotactic Poly(propylene)/Carbon Nanotube Composites. *Macromolecular Rapid Communications, 25*(23), 1963-1967.

Schartel, B., Braun, U., Knoll, U., Bartholmai, M., Goering, H., Neubert, D., & Potschke, P. (2008). Mechanical, thermal, and fire behavior of bisphenol a polycarbonate/multiwall carbon nanotube nanocomposites. *Polymer Engineering and Science, 48*(1), 149-158.

Schmitt, H., Prashantha, K., Soulestin, J., Lacrampe, M. F., & Krawczak, P. (2012). Preparation and properties of novel melt-blended halloysite nanotubes/wheat starch nanocomposites. *Carbohydrate Polymers, 89*(3), 920-927.

Senna, M. M., Yossef, A. M., Hossam, F. M., & El-Naggar, A. W. M. (2007). Biodegradation of low-density polyethylene/thermoplastic starch foams before and after electron beam irradiation. *Journal of Applied Polymer Science, 106*(5), 3273-3281.

Serpe, G., Jarrin, J., & Dawans, F. (1990). MORPHOLOGY-PROCESSING RELATIONSHIPS IN POLYETHYLENE-POLYAMIDE BLENDS. *Polymer Engineering and Science, 30*(9), 553-565.

Shacklette, L. W., & Han, C. C. (1994). SOLUBILITY AND DISPERSION CHARACTERISTICS OF POLYANILINE. In A. F. Garito, A. K. Y. Jen, C. Y. C. Lee & L. R. Dalton (Eds.). *Electrical, Optical, and Magnetic Properties of Organic Solid State Materials* (Vol. 328, pp. 157-166).

Shaffer, M. S. P., Fan, X., & Windle, A. H. (1998). Dispersion and packing of carbon nanotubes. *Carbon, 36*(11), 1603-1612.

Shaffer, M. S. P., & Windle, A. H. (1999). Analogies between polymer solutions and carbon nanotube dispersions. *Macromolecules, 32*(20), 6864-6866.

Shah, P. B., Bandopadhyay, S., & Bellare, J. R. (1995). ENVIRONMENTALLY DEGRADABLE STARCH FILLED LOW-DENSITY POLYETHYLENE. *Polymer Degradation and Stability, 47*(2), 165-173.

Shahbikian, S. (2010). Phase morphology development and rheological behavior of non-plasticized and plasticized thermoplastic elastomer blends. (Vol. Ph.D.). Canada: Ecole Polytechnique, Montreal (Canada).

Shahbikian, S., Carreau, P. J., Heuzey, M. C., Ellul, M. D., Cheng, J., Shirodkar, P., & Nadella, H. P. (2012). Morphology development of EPDM/PP uncross-linked/dynamically cross-linked blends. *Polymer Engineering and Science, 52*(2), 309-322.

Shi, X. F., Hudson, J. L., Spicer, P. P., Tour, J. M., Krishnamoorti, R., & Mikos, A. G. (2005). Rheological behaviour and mechanical characterization of injectable poly(propylene fumarate)/single-walled carbon nanotube composites for bone tissue engineering. *Nanotechnology, 16*(7), S531-S538.

Shi, Z. H., & Utracki, L. A. (1992). Development of polymer blend morphology during compounding in a twin-screw extruder. Part II: Theoretical derivations. *Polymer Engineering & Science, 32*(24), 1834-1845.

Shieh, Y.-T., Liu, G.-L., Twu, Y.-K., Wang, T.-L., & Yang, C.-H. (2010). Effects of carbon nanotubes on dynamic mechanical property, thermal property, and crystal structure of poly(L-lactic acid). *Journal of Polymer Science Part B: Polymer Physics, 48*(2), 145-152.

Shin, B.-Y., Lee, S., II, Shin, Y.-S., Balakrishnan, S., & Narayan, R. (2004a). Rheological, mechanical and biodegradation studies on blends of thermoplastic starch and polycaprolactone. *Polymer Engineering & Science, 44*(8), 1429-1438.

Shin, B. Y., Lee, S. I., Shin, Y. S., Balakrishnan, S., & Narayan, R. (2004b). Rheological, mechanical and biodegradation studies on blends of thermoplastic starch and polycaprolactone. *Polymer Engineering and Science, 44*(8), 1429-1438.

Shin, B. Y., Narayan, R., Lee, S. I., & Lee, T. J. (2008a). Morphology and Rheological Properties of Blends of Chemically Modified Thermoplastic Starch and Polycaprolactone. *Polymer Engineering and Science, 48*(11), 2126-2133.

Shin, B. Y., Narayan, R., Lee, S. I., & Lee, T. J. (2008b). Morphology and rheological properties of blends of chemically modified thermoplastic starch and polycaprolactone. *Polymer Engineering & Science, 48*(11), 2126-2133.

Shujun, W., Jiugao, Y., & Jinglin, Y. (2005). Preparation and characterization of compatible thermoplastic starch/polyethylene blends. *Polymer Degradation and Stability, 87*(3), 395-401.

Singh, R. P., Pandey, J. K., Rutot, D., Degee, P., & Dubois, P. (2003). Biodegradation of poly(epsilon-caprolactone)/starch blends and composites in composting and culture environments: the effect of compatibilization on the inherent biodegradability of the host polymer. *Carbohydrate Research, 338*(17), 1759-1769.

Sivaniah, E., Jones, R. A. L., & Higgins, D. (2009). Small Molecule Segregation at Polymer Interfaces. *Macromolecules, 42*(22), 8844-8850.

Smits, A. L. M., Kruiskamp, P. H., van Soest, J. J. G., & Vliegenthart, J. F. G. (2003). Interaction between dry starch and plasticisers glycerol or ethylene glycol, measured by differential scanning calorimetry and solid state NMR spectroscopy. *Carbohydrate Polymers, 53*(4), 409-416.

Song, Y. S. (2006). Effect of surface treatment for carbon nanotubes on morphological and rheological properties of poly(ethylene oxide) nanocomposites. *Polymer Engineering and Science, 46*(10), 1350-1357.

Sopade, P. A., Halley, P. J., & Junming, L. L. (2004). Gelatinisation of starch in mixtures of sugars. II. Application of differential scanning calorimetry. *Carbohydrate Polymers, 58*(3), 311-321.

Sperling, L. H. (2006). Dilute Solution Thermodynamics, Molecular Weights, and Sizes. *INTRODUCTION TO PHYSICAL POLYMER SCIENCE*. Hoboken, New Jersey: John Wiley & Sons, Inc.

Srivastava, R., Banerjee, S., Jehnichen, D., Voit, B., & Boehme, F. (2009). In situ Preparation of Polyimide Composites Based on Functionalized Carbon Nanotubes. *Macromolecular Materials and Engineering, 294*(2), 96-102.

Star, A., Steuerman, D. W., Heath, J. R., & Stoddart, J. F. (2002). Starched carbon nanotubes. *Angewandte Chemie-International Edition, 41*(14), 2508-+.

Stobinski, L., Tomasik, P., Lii, C. Y., Chan, H. H., Lin, H. M., Liu, H. L., Kao, C. T., & Lu, K. S. (2003a). Single-walled carbon nanotube - amylopectin complexes. *Carbohydrate Polymers, 51*(3), 311-316.

Stobinski, L., Tomasikc, P., Liid, C.-Y., Chand, H.-H., Lina, H.-M., Liue, H.-L., Kaoe, C.-T., & Lu, K.-S. (2003b). Single-walled carbon nanotube–amylopectin complexes. *Carbohydrate Polymers*

51(3), 311-316.

Stoddard, F. L. (1999). Survey of starch particle-size distribution in wheat and related species. *Cereal Chemistry, 76*(1), 145-149.

StPierre, N., Favis, B. D., Ramsay, B. A., Ramsay, J. A., & Verhoogt, H. (1997). Processing and characterization of thermoplastic starch/polyethylene blends. *Polymer, 38*(3), 647-655.

Sumita, M., Sakata, K., Asai, S., Miyasaka, K., & Nakagawa, H. (1991a). DISPERSION OF FILLERS AND THE ELECTRICAL-CONDUCTIVITY OF POLYMER BLENDS FILLED WITH CARBON-BLACK. *Polymer Bulletin, 25*(2), 265-271.

Sumita, M., Sakata, K., Asai, S., Miyasaka, K., & Nakagawa, H. (1991b). Dispersion of fillers and the electrical conductivity of polymer blends filled with carbon black. *Polymer Bulletin, 25*(2), 265-271.

Sun, Y., Guo, Z.-X., & Yu, J. (2010). Effect of ABS Rubber Content on the Localization of MWCNTs in PC/ABS Blends and Electrical Resistivity of the Composites. *Macromolecular Materials and Engineering, 295*(3), 263-268.

Sundararaj, U., & Macosko, C. W. (1995). DROP BREAKUP AND COALESCENCE IN POLYMER BLENDS - THE EFFECTS OF CONCENTRATION AND COMPATIBILIZATION. *Macromolecules, 28*(8), 2647-2657.

Swatloski, R. P., Spear, S. K., Holbrey, J. D., & Rogers, R. D. (2002). Dissolution of cellose with ionic liquids. *Journal of the American Chemical Society, 124*(18), 4974-4975.

Taghizadeh, A., & Favis, B. D. (2012a). Carbon Nanotubes in Biodegradable Blends of Polycaprolactone/ Thermoplastic Starch. Manuscript Submitted. *Biomacromolecules*.

Taghizadeh, A., & Favis, B. D. (2012b). Effect of High Molecular Weight Plasticizers on the Gelatinization of Starch under Static and Shear Conditions. *Carbohydrate Polymers*.

Taghizadeh, A., Sarazin, P., & Favis, B. D. (2012). High Molecular Weight Plasticizers in Thermoplastic Starch/Polyethylene Blends. *Journal of Materials Science*.

Taguet, A., Huneault, M. A., & Favis, B. D. (2009). Interface/morphology relationships in polymer blends with thermoplastic starch. *Polymer, 50*(24), 5733-5743.

Talja, R. A., Helen, H., Roos, Y. H., & Jouppila, K. (2007). Effect of various polyols and polyol contents on physical and mechanical properties of potato starch-based films. *Carbohydrate Polymers, 67*(3), 288-295.

Tan, I., Wee, C. C., Sopade, P. A., & Halley, P. J. (2004). Investigation of the starch gelatinisation phenomena in water–glycerol systems: application of modulated temperature differential scanning calorimetry. *Carbohydrate Polymers, 58*(2), 191-204.

Tao, F., Nysten, B., Baudouin, A.-C., Thomassin, J.-M., Vuluga, D., Detrembleur, C., & Bailly, C. (2011). Influence of nanoparticle–polymer interactions on the apparent migration behaviour of carbon nanotubes in an immiscible polymer blend. *Polymer, 52*(21), 4798-4805.

Taylor, G. I. (1932). The Viscosity of a Fluid Containing Small Drops of Another Fluid. *Proceedings of the Royal Society of London. Series A, 138*(834), 41-48.

Taylor, G. I. (1934). The Formation of Emulsions in Definable Fields of Flow. *Proceedings of the Royal Society of London. Series A, 146*(858), 501-523.

Tchomakov, K. P., Favis, B. D., Huneault, M. A., Champagne, M. F., & Tofan, F. (2005). Mechanical properties and morphology of ternary PP/EPDM/PE blends. *Canadian Journal of Chemical Engineering, 83*(2), 300-309.

Tchoul, M. N., Ford, W. T., Ha, M. L. P., Chavez-Sumarriva, I., Grady, B. P., Lolli, G. L., Resasco, D. E., & Arepalli, S. (2008). Composites of single-walled carbon nanotubes and polystyrene: Preparation and electrical conductivity. *Chemistry of Materials, 20*(9), 3120-3126.

Ternstrom, G., Sjostrand, A., Aly, G., & Jernqvist, A. (1996). Mutual diffusion coefficients of water plus ethylene glycol and water plus glycerol mixtures. *Journal of Chemical and Engineering Data, 41*(4), 876-879.

Tester, R. F., Karkalas, J., & Qi, X. (2004). Starch—composition, fine structure and architecture. *Journal of Cereal Science, 39*(2), 151-165.

Teyssandier, F., Cassagnau, P., Gerard, J. F., & Mignard, N. (2011). Sol-gel transition and gelatinization kinetics of wheat starch. *Carbohydrate Polymers, 83*(2), 400-406.

Thomassin, J. M., Lou, X., Pagnoulle, C., Saib, A., Bednarz, L., Huynen, I., Jerome, R., & Detrembleur, C. (2007). Multiwalled carbon Nanotube/Poly(epsilon-caprolactone) nanocomposites with exceptional electromagnetic interference shielding properties. *Journal of Physical Chemistry C, 111*(30), 11186-11192.

Torres, N., Robin, J. J., & Boutevin, B. (2001). Study of compatibilization of HDPE-PET blends by adding grafted or statistical copolymers. *Journal of Applied Polymer Science, 81*(10), 2377-2386.

Tsuji, H., & Ishizaka, T. (2001). Blends of aliphatic polyesters. VI. Lipase-catalyzed hydrolysis and visualized phase structure of biodegradable blends from poly(epsilon-caprolactone) and poly(L-lactide). *International Journal of Biological Macromolecules, 29*(2), 83-89.

Tzavalas, S., Mouzakis, D. E., Drakonakis, V., & Gregoriou, V. G. (2008). Polyethylene terephthalate–multiwall nanotubes nanocomposites: Effect of nanotubes on the conformations, crystallinity and crystallization behavior of PET. *Journal of Polymer Science Part B: Polymer Physics, 46*(7), 668-676.

Utracki, L. A., & Shi, G. Z.-H. (2002). Compounding Polymer Blends. In L. A. Utracki (Ed.). *POLYMER BLENDS HANDBOOK* (Vol. 1). Dordrecht, The Netherlands: KLUWER ACADEMIC PUBLISHERS.

Valentini, L., Biagiotti, J., Kenny, J. M., & Manchado, M. A. L. (2003). Physical and mechanical behavior of single-walled carbon nanotube/polypropylene/ethylene-propylene-diene rubber nanocomposites. *Journal of Applied Polymer Science, 89*(10), 2657-2663.

Van Soest, J. J. G., Bezemer, R. C., de Wit, D., & Vliegenthart, J. F. G. (1996). Influence of glycerol on the melting of potato starch. *Industrial Crops and Products, 5*(1), 1-9.

Van Soest, J. J. G., De Wit, D., & Vliegenthart, J. F. G. (1996). Mechanical properties of thermoplastic waxy maize starch. *Journal of Applied Polymer Science, 61*(11), 1927-1937.

Vandeputte, G. E., & Delcour, J. A. (2004). From sucrose to starch granule to starch physical behaviour: a focus on rice starch. *Carbohydrate Polymers, 58*(3), 245-266.

vanSoest, J. J. G., Benes, K., deWit, D., & Vliegenthart, J. F. G. (1996). The influence of starch molecular mass on the properties of extruded thermoplastic starch. *Polymer, 37*(16), 3543-3552.

Velasco-Santos, C., Martinez-Hernandez, A. L., Fisher, F., Ruoff, R., & Castano, V. M. (2003). Dynamical-mechanical and thermal analysis of carbon nanotube-methyl-ethyl methacrylate nanocomposites. *Journal of Physics D-Applied Physics, 36*(12), 1423-1428.

Vikman, M., Hulleman, S. H. D., Van der Zee, M., Myllarinen, P., & Feil, H. (1999). Morphology and enzymatic degradation of thermoplastic starch-polycaprolactone blends. *Journal of Applied Polymer Science, 74*(11), 2594-2604.

Virgilio, N., Desjardins, P., L'Esperance, G., & Favis, B. D. (2010). Modified interfacial tensions measured in situ in ternary polymer blends demonstrating partial wetting. *Polymer, 51*(6), 1472-1484.

Virgilio, N., & Favis, B. D. (2011). Self-Assembly of Janus Composite Droplets at the Interface in Quaternary Immiscible Polymer Blends. *Macromolecules, 44*(15), 5850-5856.

Waigh, T. A., Gidley, M. J., Komanshek, B. U., & Donald, A. M. (2000). The phase transformations in starch during gelatinisation: a liquid crystalline approach. *Carbohydrate Research, 328*(2), 165-176.

Waigh, T. A., Kato, K. L., Donald, A. M., Gidley, M. J., Clarke, C. J., & Riekel, C. (2000). Side-chain liquid-crystalline model for starch. *Starch-Starke, 52*(12), 450-460.

Wang, L., Shogren, R. L., & Carriere, C. (2000). Preparation and properties of thermoplastic starch-polyester laminate sheets by coextrusion. *Polymer Engineering and Science, 40*(2), 499-506.

Wang, S., Jiugao, Y., & Jinglin, Y. (2005). Preparation and characterization of compatible thermoplastic starch/polyethylene blends. *Polymer Degradation and Stability, 87*(3), 395-401.

Wang, S. J., Yu, J. G., & Yu, J. L. (2004). Influence of maleic anhydride on the compatibility of thermal plasticized starch and linear low-density polyethylene. *Journal of Applied Polymer Science, 93*(2), 686-695.

Wang, S. J., Yu, J. G., & Yu, J. L. (2005a). Compatible thermoplastic starch/polyethylene blends by one-step reactive extrusion. *Polymer International, 54*(2), 279-285.

Wang, S. J., Yu, J. G., & Yu, J. L. (2005b). Preparation and characterization of compatible thermoplastic starch/polyethylene blends. *Polymer Degradation and Stability, 87*(3), 395-401.

Wang, S. J., Yu, J. G., & Yu, J. L. (2006). Preparation and characterization of compatible and degradable thermoplastic starch/polyethylene film. *Journal of Polymers and the Environment, 14*(1), 65-70.

Wang, Z. Z., Qu, B. J., Fan, W. C., Hu, Y. A., & Shen, X. F. (2002). Effects of PE-g-DBM as a compatiblizer on mechanical properties and crystallization behaviors of magnesium hydroxide-based LLDPE blends. *Polymer Degradation and Stability, 76*(1), 123-128.

Wildes, G., Keskkula, H., & Paul, D. R. (1999). Morphology of PC/SAN blends: Effect of reactive compatibilization, SAN concentration, processing, and viscosity ratio. *Journal of Polymer Science Part B-Polymer Physics, 37*(1), 71-82.

Willett, J. L. (1994). MECHANICAL-PROPERTIES OF LDPE GRANULAR STARCH COMPOSITES. *Journal of Applied Polymer Science, 54*(11), 1685-1695.

Willett, J. L., Jasberg, B. K., & Swanson, C. L. (1995). RHEOLOGY OF THERMOPLASTIC STARCH - EFFECTS OF TEMPERATURE, MOISTURE-CONTENT, AND ADDITIVES ON MELT VISCOSITY. *Polymer Engineering and Science, 35*(2), 202-210.

Willett, J. L., Millard, M. M., & Jasberg, B. K. (1997). Extrusion of waxy maize starch: melt rheology and molecular weight degradation of amylopectin. *Polymer, 38*(24), 5983-5989.

Willett, J. L., & Shogren, R. L. (2002). Processing and properties of extruded starch/polymer foams. *Polymer, 43*(22), 5935-5947.

Williams, J. M., Adewunmi, A., Schek, R. M., Flanagan, C. L., Krebsbach, P. H., Feinberg, S. E., Hollister, S. J., & Das, S. (2005). Bone tissue engineering using polycaprolactone scaffolds fabricated via selective laser sintering. *Biomaterials, 26*(23), 4817-4827.

Willis, J. M., Caldas, V., & Favis, B. D. (1991). Processing morphology relationships of compatibilized polyolefin polyamide blends .2. the emulsifying effect of an ionomer compatibilizer as a function of blend composition and viscosity ratio. *Journal of Materials Science, 26*(17), 4742-4750.

Wu, C.-S., & Liao, H.-T. (2007). Study on the preparation and characterization of biodegradable polylactide/multi-walled carbon nanotubes nanocomposites. *Polymer, 48*(15), 4449-4458.

Wu, C. S. (2003). Physical properties and biodegradability of maleated-polycaprolactone/starch composite. *Polymer Degradation and Stability, 80*(1), 127-134.

Wu, D., Lin, D., Zhang, J., Zhou, W., Zhang, M., Zhang, Y., Wang, D., & Lin, B. (2011). Selective Localization of Nanofillers: Effect on Morphology and Crystallization of PLA/PCL Blends. *Macromolecular Chemistry and Physics, 212*(6), 613-626.

Wu, D., Wu, L., Sun, Y., & Zhang, M. (2007). Rheological properties and crystallization behavior of multi-walled carbon Nanotube/Poly(epsilon-caprolactone) composites. *Journal of Polymer Science Part B-Polymer Physics, 45*(23), 3137-3147.

Wu, D., Zhang, Y., Zhang, M., & Yu, W. (2009). Selective Localization of Multiwalled Carbon Nanotubes in Poly(epsilon-caprolactone)/Polylactide Blend. *Biomacromolecules, 10*(2), 417-424.

Wu, D. F., Wu, L. F., Zhang, M., Zhou, W. D., & Zhang, Y. S. (2008). Morphology evolution of nanocomposites based on poly(phenylene sulfide)/poly(butylene terephthalate) blend. *Journal of Polymer Science Part B-Polymer Physics, 46*(12), 1265-1279.

Wu, H. L., Ma, C. C. M., Yang, Y. T., Kuan, H. C., Yang, C. C., & Chiang, C. L. (2006). Morphology, electrical resistance, electromagnetic interference shielding and mechanical properties of functionalized MWNT and poly(urea urethane) nanocomposites. *Journal of Polymer Science Part B-Polymer Physics, 44*(7), 1096-1105.

Wu, M., & Shaw, L. (2006). Electrical and mechanical behaviors of carbon nanotube-filled polymer blends. *Journal of Applied Polymer Science, 99*(2), 477-488.

Wu, M., & Shaw, L. L. (2004). On the improved properties of injection-molded, carbon nanotube-filled PET/PVDF blends. *Journal of Power Sources, 136*(1), 37-44.

Wu, S. (1971). Calculation of interfacial tension in polymer systems. *Journal of Polymer Science Part C: Polymer Symposia, 34*(1), 19-30.

Wu, S. (1978). Interfacial Energy, Structure, and Adhesion between Polymers. In D. R. Paul & S. Newman (Eds.). *Polymer Blends* (Vol. 1, pp. 244-295). New York, NY: Academic Press Inc.

Wu, S. (1982). *Polymer Interface and Adhesion*. New York, NY: Marcel Dekker Inc.

Wu, S. (1987a). Formation of dispersed phase in incompatible polymer blends: Interfacial and rheological effects. *Polymer Engineering & Science, 27*(5), 335-343.

Wu, S. (1987b). Interfacial energy, structure and adhesion between polymers. In D. R. Paul & S. Newman (Eds.). *Polymer Blends* (Vol. 1, pp. 244-248). New York: Academic Press.

Wu, T. M., & Chen, E. C. (2006). Crystallization behavior of poly(epsilon-caprolactone)/multiwalled carbon nanotube composites. *Journal of Polymer Science Part B-Polymer Physics, 44*(3), 598-606.

Xia, H. S., & Song, M. (2006). Preparation and characterisation of polyurethane grafted single-walled carbon nanotubes and derived polyurethane nanocomposites. *Journal of Materials Chemistry, 16*(19), 1843-1851.

Xiang, F. M., Wu, J., Liu, L., Huang, T., Wang, Y., Chen, C., Peng, Y., Jiang, C. X., & Zhou, Z. W. (2011). Largely enhanced ductility of immiscible high density polyethylene/polyamide 6 blends via nano-bridge effect of functionalized multiwalled carbon nanotubes. *Polymers for Advanced Technologies, 22*(12), 2533-2542.

Xie, X. L., Mai, Y. W., & Zhou, X. P. (2005). Dispersion and alignment of carbon nanotubes in polymer matrix: A review. *Materials Science & Engineering R-Reports, 49*(4), 89-112.

Xue, T., Yu, L., Xie, F., Chen, L., & Li, L. (2008). Rheological properties and phase transition of starch under shear stress. *Food Hydrocolloids, 22*(6), 973-978.

Yang, K. M., Lee, S. H., & Oh, J. M. (1999). Effects of viscosity ratio and compatibilizers on the morphology and mechanical properties of polycarbonate/acrylonitrile-butadiene-styrene blends. *Polymer Engineering and Science, 39*(9), 1667-1677.

Yoo, S.-H., & Jane, J.-l. (2002). Molecular weights and gyration radii of amylopectins determined by high-performance size-exclusion chromatography equipped with multi-angle laser-light scattering and refractive index detectors. *Carbohydrate Polymers, 49*(3), 307-314.

Yu, L., Kealy, T., & Chen, P. (2006). Study of starch gelatinization in a flow field using simultaneous rheometric data collection and microscopic observation. *International Polymer Processing, 21*(3), 283-289.

Yuan, J.-K., Yao, S.-H., Sylvestre, A., & Bai, J. (2011). Biphasic Polymer Blends Containing Carbon Nanotubes: Heterogeneous Nanotube Distribution and Its Influence on the Dielectric Properties. *The Journal of Physical Chemistry C, 116*(2), 2051-2058.

Yuan, J. K., Yao, S. H., Sylvestre, A., & Bai, J. B. (2012). Biphasic Polymer Blends Containing Carbon Nanotubes: Heterogeneous Nanotube Distribution and Its Influence on the Dielectric Properties. *Journal of Physical Chemistry C, 116*(2), 2051-2058.

Zaikin, A., Zharinova, E., & Bikmullin, R. (2007). Specifics of localization of carbon black at the interface between polymeric phases. *Polymer Science Series A, 49*(3), 328-336.

Zaikin, A. E., Karimov, R. R., & Arkhireev, V. P. (2001). A Study of the Redistribution Conditions of Carbon Black Particles from the Bulk to the Interface in Heterogeneous Polymer Blends. *Colloid Journal, 63*(1), 53-59.

Zanoni, B., Schiraldi, A., & Simonetta, R. (1995). NAIVE MODEL OF STARCH GELATINIZATION KINETICS. *Journal of Food Engineering, 24*(1), 25-33.

Zhang, C. L., Feng, L. F., Gu, X. P., Hoppe, S., & Hu, G. H. (2007). Efficiency of graft copolymers as compatibilizers for immiscible polymer blends. *Polymer, 48*(20), 5940-5949.

Zhang, D. H., Kandadai, M. A., Cech, J., Roth, S., & Curran, S. A. (2006). Poly(L-lactide) (PLLA)/multiwalled carbon nanotube (MWCNT) composite: Characterization and biocompatibility evaluation. *Journal of Physical Chemistry B, 110*(26), 12910-12915.

Zhang, J. F., & Sun, X. Z. (2004). Mechanical properties of poly(lactic acid)/starch composites compatibilized by maleic anhydride. *Biomacromolecules, 5*(4), 1446-1451.

Zhang, L., Wan, C., & Zhang, Y. (2009). Investigation on the Multiwalled Carbon Nanotubes Reinforced Polyamide 6/Polypropylene Composites. *Polymer Engineering and Science, 49*(10), 1909-1917.

Zhang, Q. H., Lippits, D. R., & Rastogi, S. (2006). Dispersion and rheological aspects of SWNTs in ultrahigh molecular weight polyethylene. *Macromolecules, 39*(2), 658-666.

Zobel, H. F. (1988). Molecules to Granules: A Comprehensive Starch Review. *Starch - Stärke, 40*(2), 44-50.

ANNEXES

ANNEXE 1 XPS ANALYSIS OF CARBON NANOTUBES

The results of the XPS and their application in this work have been explained in detail in section 6.7.3. But for more clarity, the detailed results as well as the fundamentals of this method are shown in this part.

A-1.1 XPS Fundamentals

X-ray Photoelectron Spectroscopy (XPS) is one of the techniques used to analyze the surface structure of substances (Gunther, Kaulich, Gregoratti & Kiskinova, 2002). In this technique, the surface of the sample is bombarded by photons of specific energy (X-ray) and if its energy is high enough, the atom's core electron will be emitted out of the surface. The electrons ejected from the atoms are energy filtered by a hemispherical analyser. Then the energy spectrum of the filtered electrons is determined via a high resolution electron spectrometer.

An ultra-high vacuum chamber should be used to conduct a XPS test (~10^{-10} torr) because it facilitates the transmission of the photoelectrons to the analyzer. The sampling depth of XPS is less than ~10nm due to the fact that the ejected electrons of the deeper layers have very low probability of leaving the surface without energy loss due to the collisions with other atoms. These electrons are then translated as background noise. The core electrons of each atom at the surface have a specific binding energy. So as the energy of an emitted X-ray is known, the electron binding energy of rejected electrons can be determined as well by the Einestein relation (Cederbaum & Domcke, 1977):

$$E_b = h\gamma - KE - \varphi \qquad (1.1)$$

Where, E_b is the binding energy, hγ is the X-ray photon energy, KE is the kinetic energy of the analysed electron measured by the analyser and φ is the work function of the spectrometer which is measured in calibration process.

Thus, a typical XPS graph is a plot of number of electrons detected vs. their binding energy (eV). Any specific atom has its own set of XPS peaks at certain binding energies depending on the state of their electronegativity and surrounding bonded atoms. So this is used to determine the structure of the surface (Dementjev, de Graaf, van de Sanden, Maslakov, Naumkin & Serov, 2000). By counting the number of electrons in each peak the amount of the material in that volume is determined.

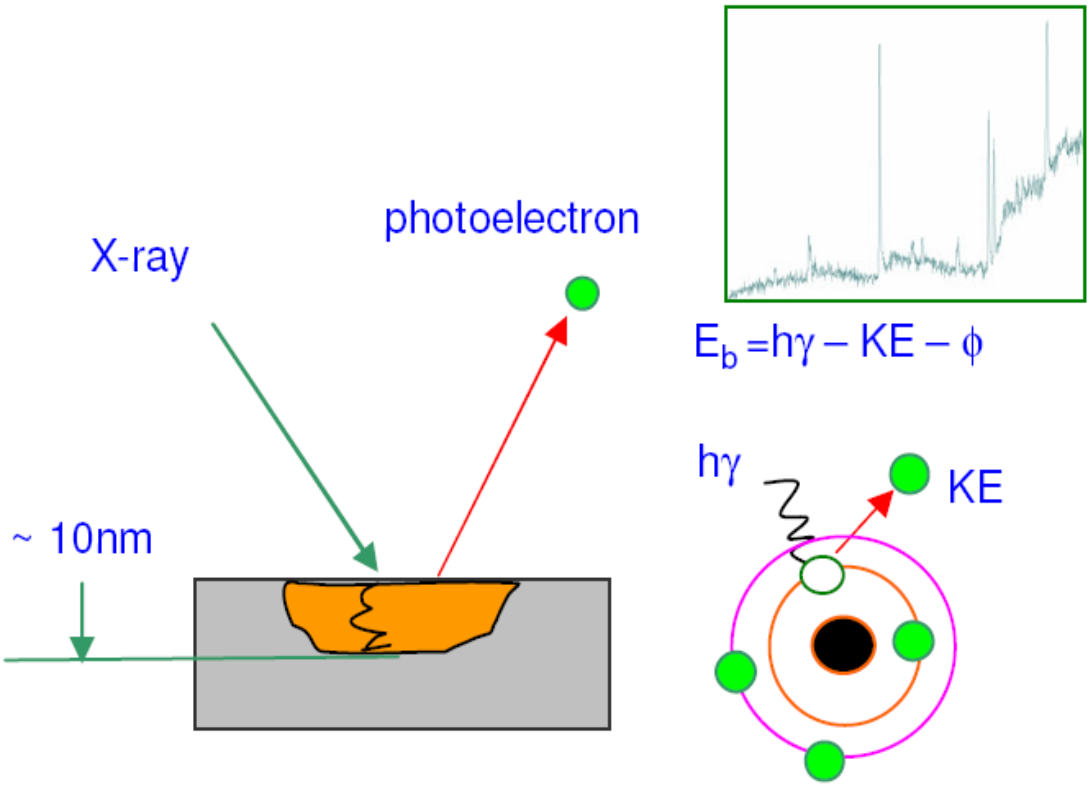

Figure A-1.1 Schematic of XPS analyser.

Typical applications of XPS include:

- Determination of elements present and the quantity of atoms present at the surface of a material (max~ 10nm),
- Determining the contaminations at the surface of a material,

- Finding the Empirical formula of substances on the material's surface,
- Measuring the thickness of one or more thin layers of less than ~8nm at the surface.

A-1.1. **Experimental Conditions**

The details of the conducted experiment can be observed in table A-1.1

Table A-1.1 The XPS analyses experimental details.

Apparatus		VG ESCALAB 3 MKII
Source		Mg Kα
Power		300W (15kV, 20mA)
Analysed surface		2mm x 3mm
Analysed depth		50-100 Å
Survey scans	Energy step size	1.0 eV
	Pass energy	100 eV
High resolution scans	Energy step size	0.05 eV
	Pass energy	20 eV
Background subtraction		Shirley method [1]
Sensitivity factor table		Wagner[2]
Charge correction with respect to C1s at		285.0eV

[1] (Shirley, 1972); [2] (Wagner, Davis, Zeller, Taylor, Raymond & Gale, 1981)

The relative atomic percent is calculated from the formula:

$$\left(rel.at.\%\right)_1 . = \frac{A_1 / SF_1}{\sum_n A_n / SF_n} \qquad (1.2)$$

where A_1 represents the area of the peak for a given element and SF_1 is the sensitivity factor for that same element. Sensitivity factors are used from the Wagner table.

A-1.2. **Results**

As shown in Table A-1.2, the amount of sp^3 to sp^2 carbon ratio (C2/C1+C6) increases on extracted CNT samples compared to that on virgin CNT samples. The concentration of other carbon-oxygen functionalities is also greatly increased on these samples. This could indicate that the surface of the nanotubes in these samples is covered with another material rich in sp^3 carbon and other carbon functionalities.

Table A-1.2 Identification of chemical bonding from high resolution scans (Datsyuk et al., 2008)

Element	**Binding Energy (eV)**	**Identification**		**Relative atomic % (Total on all identified carbon species)**	
				Virgin CNT	**Extracted CNT**
C	284.4	**C1**	C=C(sp^2 carbon) (graphitic carbon)	54.3	16.7
	285.0	**C2**	C-C sp^3		
	285.5		C-C sp^3 and sp^2 with defective alternant hydrocarbon structure	22.1	34.7
	286.7	**C3**	C-O, C-O-C	8.8	29.6
	288.1	**C4**	O-C-O		
	288.3		O-C-O and/or O-C=O	5.6	11.0
	289.0		O-C=O		
	289.6	**C5**	CO_3	3.3	6.5
	291.1	**C6**	$\pi \rightarrow \pi^*$ of C1	5.8	1.4

Table A-1.3 Table of ratios

Sample	C2/C1+C6	C3/C1+C6	C4/C1+C6	C5/C1+C6
Virgin CNT	0.368	0.146	0.093	0.055
Extracted CNT	1.917	1.635	0.608	0.359

Table A-1.2 identifies the relative atomic % of all carbon species identified in the samples. Presuming that all carbon species other than C=C (sp^2 graphitic carbon) are located on the surface of the nanotubes, we removed the contributions of C1 and C6 from Table A-1.2 and only the contributions of C2, C3, C4 and C5 is presented in Table A-1.4.

Table A-1.4 Identification of chemical bonding from high resolution scans

Element	Binding Energy (eV)	Identification		Relative atomic % (Total on C2+C3+C4+C5)	
				Virgin CNT	Extracted CNT
C	285.0	**C2**	C-C sp^3		
	285.5		C-C sp^3 and sp^2 with defective alternant hydrocarbon structure	55.4	42.4
	286.7	**C3**	C-O, C-O-C	22.1	36.2
	288.1	**C4**	O-C-O		
	288.3		O-C-O and/or O-C=O	14.1	13.5
	289.0		O-C=O		
	289.6	**C5**	CO_3	8.4	7.9

Table A-1.5 Table of ratios

Sample	C3/C2	C4/C2
Virgin CNT	0.399	0.255
Extracted CNT	0.854	0.318

The C1s components observed at a binding energy (B.E.) of 285.5 (C2), 286.7 (C3), 288.3 (C4) and 289.6eV (C5) on the virgin CNT sample indicate respectively the presence of sp^3 C-C bonds or defects in the graphene structure, C-O, O-C-O or O-C=O, and carbonates on the surface of nanotubes. The presence of more surface O-C=O is as expected.

The relative concentration of the different carbon functional groups found on the surface of the extracted CNT samples is very different from that observed on the virgin CNT samples. For instance a decrease of component C2 on the extracted samples compared to the functionalized CNT samples is obvious. This is an indication that the surface of the CNTs in the extracted samples is covered with more carbon-oxygen functionalities compared to the virgin CNT samples.

As highlighted in Table A-1.5, we observe the ratios C3/C2 and C4/C2 which are respectively the ratios of C-O functionalities, and O-C-O and/or O-C=O to sp^3 C-C and sp^2 carbon defects. On the extracted sample, C3/C2 is increased compared to that on the virgin CNTs by a factor of 2.14 while C4/C2 is increased by a factor of 1.25. In other words, the increase of C-O functions is close to five times the increase of O-C-O functions. Since the ratio of C-O to O-C-O functions in a model starch molecule is 5 to 1, this provides an indication that starch molecules remain on the surface of the CNTs in the extracted sample.

The spectra of virgin and extracted carbon nanotubes are included in the following page.

XPS Spectra of Virgin and extracted Carbon Nanotubes.

Virgin CNT

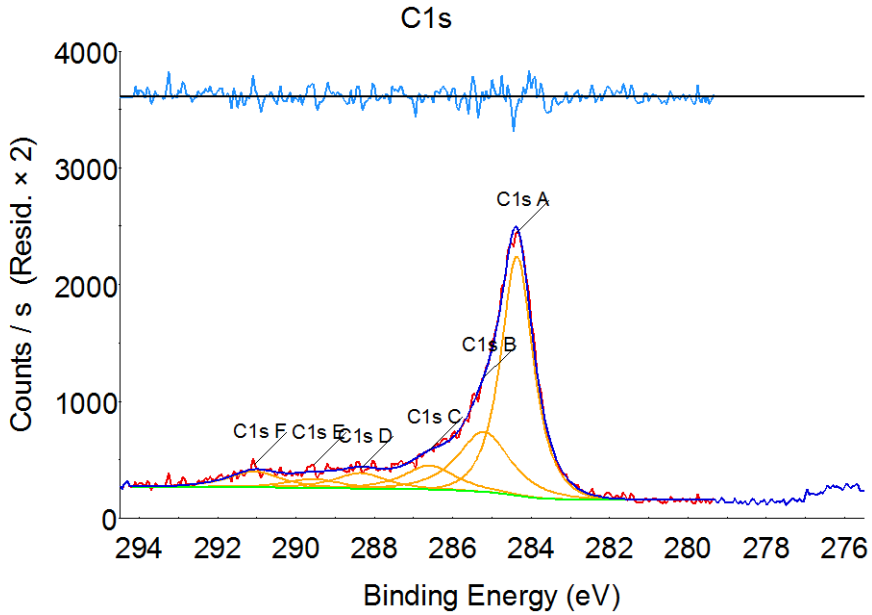

Extracted CNT

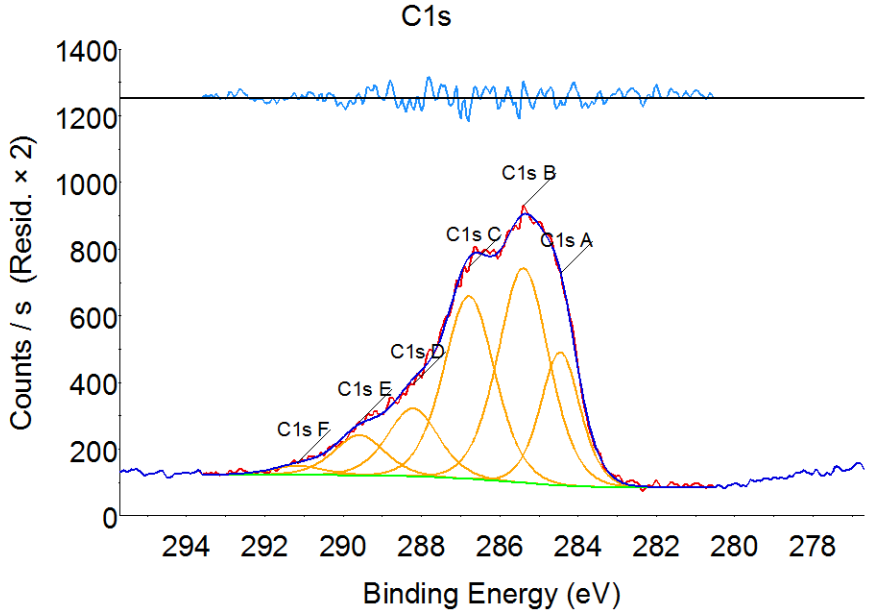

ANNEXE 2 FUNDAMENTALS OF CONTACT ANGLE MEASUREMENT

A-2.1. **Definition of Surface Free Energy**

The atoms at the surface of a material experience a very different environment than the atoms in the bulk. In the bulk, the atoms are surrounded with like atoms, so the force balance exerted on each of them is zero. But the atoms at the surface are in contact with their like atoms only from one side, however, from outside they see a different environment. Hence, they have a different energy distribution from the bulk atoms. This excess energy is called surface energy, γ. Thermodynamically speaking, surface energy is the measure of increase in the Gibb's free energy (ΔG) of the system by reversibly increasing the surface by an infinitesimal amount of ΔA at a constant temperature, pressure and composition:

$$\gamma = \left(\frac{\partial G}{\partial A}\right)_{T,P,n_i} \tag{2.1}$$

So it can be said that surface energy is an amount of reversible work required to increase the surface area.

A-2.2. **Contact Angle Measurement**

One of the most straight forward methods in determining the excess free energy of a surface is using the Contact Angle method. The basics of this method and classical calculations of contact angle is well documented in the literature. So here we do not intend to rewrite the principles but rather explaining the method used by the author to determine the surface tensions of polycaprolactone and thermoplastic starch.

Two hundred years ago, Young (Young, 1805) made a qualitative observation, shown in Figure A-2.1. It is shown that at any point along the rim of a liquid drop on a solid, three surface tension components interacted to limit the spread of a drop.

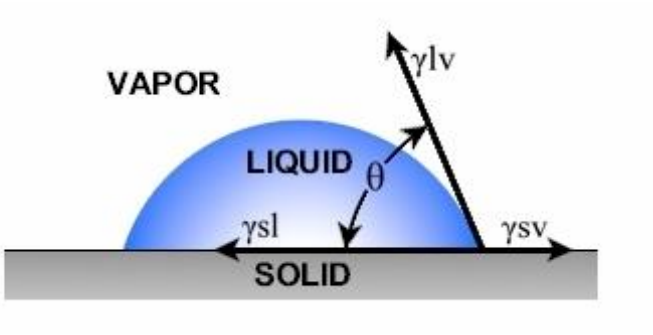

Figure A-2.1 The surface tension components in equilibrium in the plane of a substance.

At the equilibrium stage:

$$\gamma_{SV} = \gamma_{SL} + \gamma_{LV} \cos\theta \tag{2.2}$$

Where γ is the surface tension and S, L and V refer to solid, liquid and vapor, respectively and θ is the contact angle. By taking into account that the effect of the liquid vapor on the surface tension of the solid surface is negligible for low energy surfaces (Good, 1992), equation (2.2) can be re-written as:

$$\gamma_S = \gamma_{SL} + \gamma_L \cos\theta \tag{2.3}$$

Where $\gamma_S$and γ_L are the surface free energy of solid and liquid phases, respectively.

Work of adhesion is the reversible work required per unit area to separate a liquid from a solid surface, leaving an adsorbed film in equilibrium with the saturated vapour of the liquid on the surface of the solid. Dupré defined a thermodynamic work of adhesion (W_a) as below (Wu, 1978):

$$W_a = \gamma_{ij} - \gamma_i - \gamma_j \tag{2.4}$$

Where γ_i, γ_j and γ_{ij} refer to the surface tension of component i, component j and the interfacial tension of i and j, respectively.

The surface tension is separated into two components, namely dispersive,γ_i^d, and polar γ_i^p:

$$\gamma_i = \gamma_i^d + \gamma_i^p \tag{2.5}$$

Based on this concept and according to the geometric mean equation, It is assumed that the interfacial tension between two materials is (Fowkes Frederick, 1964; Wu, 1978):

$$\gamma_{ij} = \gamma_i + \gamma_j - 2\left(\gamma_i^d \gamma_j^d\right)^{1/2} - 2\left(\gamma_i^p \gamma_j^p\right)^{1/2} \quad (2.6)$$

So combining equations 2.4 and 2.6 (assuming i: S ; j: L) results in:

$$W_a = 2\left(\gamma_S^d \gamma_L^d\right)^{1/2} + 2\left(\gamma_S^p \gamma_L^p\right)^{1/2} \quad (2.7)$$

On the other hand combing equation 2.3 and 2.4 gives:

$$W_a = \gamma_L(1 + \cos\theta) \quad (2.8)$$

Thus based on equations 2.7 and 2.8 we can conclude that:

$$\gamma_L(1 + \cos\theta) = 2\left(\gamma_S^d \gamma_L^d\right)^{1/2} + 2\left(\gamma_S^p \gamma_L^p\right)^{1/2} \quad (2.9)$$

As it is observed for a specific liquid with known surface energy parameters, we have three unknown parameters in this equation. By examining at least two different liquids and measuring the contact angle (θ) for each, we can determine polar and dispersive components of solid films surface energy. There is a variety of liquids that may be used for contact angle measurements such as water, glycerol, formamide.

Technically, the equation is reshaped in the form below:

$$W_a/2\alpha_L = \alpha_S + \beta_S(\beta_L/\alpha_L) \quad (2.10)$$

Where

$$\alpha_i = (\gamma_i^d)^{1/2} \ ; \ \beta_i = (\gamma_i^p)^{1/2}$$

So a plot of $W_a/2\alpha_L$ vs. β_L/α_Lshould result in a straight line whose slope is β_S and its intercept is α_S. Although using two liquids is mathematically enough to determine the surface energy components, but by using different liquids, the off-the-trend line points will be also determined and consequently reliable data will be reported.

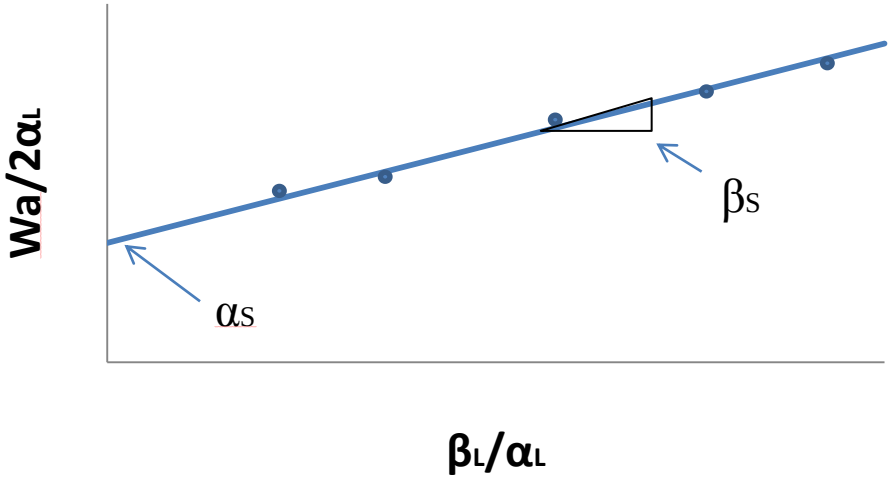

Figure A-2.2 A plot of the surface tension components of several contact liquids on a substrate.

The required parameters of some of the most used liquids are shown in Table B-1.

Table A-2.1 Surface tension calculation parameters (equation 2.10) for several contact liquids.

	γ_L	$2\alpha_L$	β_L/α_L
Water	72.8	9.34	1.54
Glycerol	64	11.66	0.94
Formamide	58.3	11.37	0.90
Ethylene glycol	48.3	10.83	0.81
Tricresyl phosphate	40.9	12.52	0.21
n-dodecane	25.4	10.08	0.00

By using the above mentioned plot and the data in the Table A-2.1 the author has determined the surface tension parameters for thermoplastic starch and polycaprolactone which are reported in Table 6-1.

References:

Cederbaum, L. S., & Domcke, W. (1977). Theoretical Aspects of Ionization Potentials and Photoelectron Spectroscopy: A Green's Function Approach. In I. Prigogine & S. A. Rice (Eds.). *Advances in Chemical Physics* (Vol. 36). New York, NY: John Wiley & Sons.

Datsyuk, V., Kalyva, M., Papagelis, K., Parthenios, J., Tasis, D., Siokou, A., Kallitsis, I., & Galiotis, C. (2008). Chemical oxidation of multiwalled carbon nanotubes. *Carbon, 46*(6), 833-840.

Dementjev, A. P., de Graaf, A., van de Sanden, M. C. M., Maslakov, K. I., Naumkin, A. V., & Serov, A. A. (2000). X-Ray photoelectron spectroscopy reference data for identification of the C3N4 phase in carbon–nitrogen films. *Diamond and Related Materials, 9*(11), 1904-1907.

Fowkes Frederick, M. (1964). Dispersion Force Contributions to Surface and Interfacial Tensions, Contact Angles, and Heats of Immersion. *Contact Angle, Wettability, and Adhesion* (Vol. 43, pp. 99-111): AMERICAN CHEMICAL SOCIETY.

Good, R. J. (1992). Contact angle, wetting, and adhesion: a critical review. *Journal of Adhesion Science and Technology, 6*(12), 1269-1302.

Gunther, S., Kaulich, B., Gregoratti, L., & Kiskinova, M. (2002). Photoelectron microscopy and applications in surface and materials science. *Progress in Surface Science, 70*(4-8), 187-260.

Shirley, D. A. (1972). High-Resolution X-Ray Photoemission Spectrum of the Valence Bands of Gold. *Physical Review B, 5*(12), 5.

Wagner, C. D., Davis, L. E., Zeller, M. V., Taylor, J. A., Raymond, R. H., & Gale, L. H. (1981). Empirical atomic sensitivity factors for quantitative analysis by electron spectroscopy for chemical analysis. *Surface and Interface Analysis, 3*(5), 211-225.

Wu, S. (1978). Interfacial Energy, Structure, and Adhesion between Polymers. In D. R. Paul & S. Newman (Eds.). *Polymer Blends* (Vol. 1, pp. 244-296). San Diego, CA: Academic Press Inc.

Young, T. (1805). An Essay on the Cohesion of Fluids. *Philosophical Transactions of the Royal Society of London, 95*(ArticleType: research-article / Full publication date: 1805 /), 65-87.